Excess Molar Volume and Isentropic Compressibility for Binary or Ternary Ionic Liquid Systems

Submitted in fulfillment of the requirements of the Degree of Doctor of Technology: Chemistry, in the Faculty of Applied Sciences at the

Durban University of Technology

Indra Bahadur

M Sc : Chemistry

July 2008

Supervisor: Prof N. Deenadayalu

PREFACE

The work described in this thesis was performed by the author under the supervision of Professor N. Deenadayalu at Durban University of Technology, Durban, South Africa, from 2008-2010. The study presents original work by the author and has not been submitted in any form to another tertiary institution or university. Where use is made of the work of others, it has been clearly stated in the text.

Signed: Date:

Indra Bahadur

Signed:

Prof. N. Deenadayalu (Supervisor) Date:

ACKNOWLEDGMENTS

I would like to express my sincere gratitude to God, who always gives me strength and knowledge.

I would like to express my sincere gratitude to the National Research Foundation (South Africa) for funding of the project.

I would like to express my sincere gratitude to Durban University of Technology, Durban, South Africa, for part of my financial support and for giving me the opportunity to undertake my research at the institution.

I deem it a great pleasure to express my deep sense of gratitude and indebtedness to my venerable supervisor **Prof. N. DEENADAYALU**, Associate Professor, Department of Chemistry, Durban University of Technology, Durban, South Africa, for introducing me to the *World of Chemical Thermodynamics*, inspiring guidance, valuable suggestions, and constant encouragement throughout the period of this research work.

My sincere thanks to the Head of Department of Chemistry, Durban University of Technology, Durban, South Africa, for providing the facilities to carry out the present work.

I express my profound respect and deep sense of gratitude to **Prof. T. Hoffman,** Warsaw University of Technology, Faculty of Chemistry, Division of Physical Chemistry, Warszawa, Poland, **Prof. N. K. Kausik,** Department of Chemistry, University of Delhi, India, **Prof M. Kidwayi,** Department of Chemistry, University of Delhi, India, **Prof. S. M. S. Chuahan,** Department of Chemistry, University of Delhi, India, **Dr. P. Venkatesu,** Assistant Professor, Department of Chemistry, University of Delhi, India, **Dr. Sailendra Kumar Singh,** Assistant Professor, Department of Chemistry, University of Delhi, India, **Dr. N. Agasthi,** Assistant

Professor, Department of Chemistry, University of Delhi, India, **Dr. Sunil Uppadhya, Dr. Sanjeev Shrama,** for their valuable suggestions and the generous help in various ways throughout the course.

I owe many thanks to my friends **Dr. Ajit Kumar Kanwal, Dr. P. Pitchaito, Mr. Akhilesh Kumar Azad, Mr. S. R. Ramphal, Mr. Nitin Kumar, Ms. Sangmitra Singh, Mr. Arun Kumar, Mrs. Saroj Bala Kanwal, Ms. T. Singh, and Ms. Zikhona Tywabi, Ms. Krishna Purohit, Mr. Tarun Purohit,** all who wished me success.

Finally, my indebtedness extends to my parents, brother, sister and family members. Special thanks to my grandfather **Mr. Mithai Lal,** grandmother **Mrs. Bhukhala Devi,** my father **Mr. Mangla Prasad,** my mother **Mrs. Rani Devi,** my brother **Mr. Sandeep Kumar,** my sister **Ms. Kumud Ben Joshi** my family members **Mr. Soti Ram, Mr. Lalji Ram, Mr. Rajendra Prasad, Mr. Jugjeevan Ram, Mr. Jagdish Prasad, Mr. Shyam Bihari Madhukar, Mr. Jitendra Kumar, Mr. Surendra Kumar, Mrs. Lachi Devi, Mrs. Sita Devi**, **Ms. Sangeeta Singh, Mrs. And Mr. Ram Singh,** for their constant encouragement and patient endurance which made this venture possible.

Indra Bahadur

ABSTRACT

The thermodynamic properties of mixtures involving ionic liquids (ILs) with alcohols or alkyl acetate or nitromethane at different temperatures were determined. The ILs used were methyl trioctylammonium bis(trifluoromethylsulfonyl)imide ($[MOA]^+[Tf_2N]^-$) and 1-butyl-3-methylimidazolium methyl sulphate $[BMIM]^+[MeSO_4]^-$.

The ternary excess molar volumes (V_{123}^{E}) for the mixtures {methyl trioctylammonium bis (trifluoromethylsulfonyl)imide + methanol or ethanol + methyl acetate or ethyl acetate}and (1-butyl-3-methylimidazolium methylsulfate + methanol or ethanol or 1-propanol + nitromethane) were calculated from experimental density values, at T = (298.15, 303.15 and 313.15) K and

T = 298.15, respectively. The Cibulka equation was used to correlate the ternary excess molar volume data using binary data from literature. The V_{123}^{E} values for both IL ternary systems were negative at each temperature. The negative contribution of V_{123}^{E} values are due to the packing effect and/or strong intermolecular interactions (ion-dipole) between the different molecules.

The density and speed of sound of the binary solutions ($[MOA]^+[Tf_2N]^-$ + methyl acetate or ethyl acetate or methanol or ethanol), (methanol + methyl acetate or ethyl acetate) and (ethanol + methyl acetate or ethyl acetate) were also measured at T = (298.15, 303.15, 308.15 and 313.15) K and at atmospheric pressure. The apparent molar volume, V_ϕ , and the apparent molar isentropic compressibility, κ_ϕ , were evaluated from the experimental density and speed of sound data. A Redlich-Mayer type equation was fitted to the apparent molar volume and apparent molar isentropic compressibility data. The results are discussed in terms of solute-solute, solute- solvent and solvent-solvent interactions. The apparent molar volume and apparent molar isentropic compressibility at infinite dilution, V_ϕ^0 and κ_ϕ^0, respectively of the binary solutions have been calculated at each temperature. The V_ϕ^0 values for the binary

systems ([MOA]$^{+}$[Tf_2N]$^{-}$ + methyl acetate or ethyl acetate or methanol or ethanol) and (methanol + methyl acetate or ethyl acetate) and (ethanol + methyl acetate or ethyl acetate) are positive and increase with an increase in temperature. For the (methanol + methyl acetate or ethyl acetate) systems V_ϕ^0 values indicate that the (ion-solvent) interactions are weaker.

The κ_ϕ^0 is both positive and negative. Positive κ_ϕ^0, for ([MOA]$^{+}$ [Tf_2N]$^{-}$ + ethyl acetate or ethanol), (methanol + ethyl acetate) and (ethanol + methyl acetate or ethyl acetate) can be attributed to the predominance of solvent intrinsic compressibility effect over the effect of penetration of ions of IL or methanol or ethanol. The positive κ_ϕ^0 values can be interpreted in terms of increase in the compressibility of the solution compared to the pure solvent methyl acetate or ethyl acetate or ethanol. The κ_ϕ^0 values increase with an increase in temperature. Negative κ_ϕ^0, for ([MOA]$^{+}$ [Tf_2N]$^{-}$ + methyl acetate or methanol), and (methanol + methyl acetate) can be attributed to the predominance of penetration effect of solvent molecules into the intra-ionic free space of IL or methanol molecules over the effect of their solvent intrinsic compressibility. Negative κ_ϕ^0 indicate that the solvent surrounding the IL or methanol would present greater resistance to compression than the bulk solvent. The κ_ϕ^0 values decrease with an increase in the temperature. The infinite dilution apparent molar expansibility, E_ϕ^0 , values for the binary systems (IL + methyl acetate or ethyl acetate or methanol or ethanol) and (methanol + methyl acetate or ethyl acetate) and (ethanol + methyl acetate or ethyl acetate) are positive and decrease with an increase in temperature due to the solution volume increasing less rapidly than the pure solvent. For (IL + methyl acetate or ethyl acetate or methanol or ethanol) systems E_ϕ^0 indicates that the interaction between (IL + methyl acetate) is stronger than that of the (IL + ethanol) or (IL + methanol) or (IL + ethyl acetate) solution. For the (methanol + methyl acetate or ethyl acetate) systems E_ϕ^0 values

indicate that the interactions are stronger than (ethanol + methyl acetate or ethyl acetate) systems.

CONTENTS Pages

Preface i

Acknowledgments ii-iii

Abstract iv-vi

List of Tables xv-xix

List of Figures xx-xxix

List of Symbols xxx-xxxi

Ionic Liquid Abbreviations xxxii-xxxiv

Chapter 1: INTRODUCTION 1-6

1.1 The importance of thermodynamic physical properties 2-3

1.2 Scope of the present work 4-5

(A) TERNARY EXCESS MOLAR VOLUMES 4

(B) APPARENT MOLAR PROPERTIES 5

Chapter 2: LITERATURE REVIEW

(A) TERNARY EXCESS MOLAR VOLUME 7-19

(B) APPARENT MOLAR PROPERTIES 20-25

Chapter 3: IONIC LIQUIDS

3.1 Properties of ionic liquids 26-27

3.2 Physical properties of ionic liquids 28-32

3.2.1 Melting Point 29

3.2.2 Density 29

3.2.3 Viscosity 29

3.2.4 Solubility 29-30

3.2.5 Conductivity and electrochemical properties 30

3.2.6 Stability 31

3.2.7 Color 31

3.2.8 Hygroscopicity 31

3.2.9 Hydrophopicity 31-32

3.3 Chemical properties 32

3.4 Structure of ionic liquids 32-37

3.5 ILs as a replacement solvent for VOCs 38-39

3.6 Applications of ionic liquids 39-43

3.6.1 Energatic application 39-40

3.6.2 The Biphosic Acid Scavenging utilising Ionic Liquids (BASIL) process 40

3.6.3 Cellulose Processing 41

3.6.4 Dimersol – Difasol 41

3.6.5 Paint additives 41

3.6.6 Air products – ILs as a transport medium for reactive gases 41

3.6.7 Hydrogen storage 42

3.6.8 Nuclear industry 42

3.6.9 Separations 42-43

Chapter 4: THEORETICAL FRAMEWORK

(A) TERNARY EXCESS MOLAR VOLUME 44-76

(i) Excess Gibbs free energy 48

(ii) Excess entropy 49

(iii) Excess enthalpy 49

(iv) Excess volume 49-50

(v) Excess energy 50

(vi) Excess heat capacity 50

4.1 A brief review of the theory of solutions 50-68

4.2 Excess molar volumes 68-72

4.3 Correlation and prediction theories for V_{123}^{E} 72-76

(i) Redlich-Kister equation 72

(ii) Kohler's equation 72-73

(iii) Tsao-Smith equation 73

(iv) Jacob-Fitzner equation 73-74

(v) Cibulka's equation 74

(a) For normal projection 74

(b) For direct projection 75

(c) For parallel projection 75-76

(B) APPARENT MOLAR PROPERTIES 76-90

4.4 Apparent molar volume and derived properties 76-77

4.5 Sound velocity 78-85

4.5.1 Theories of sound 80-85

4.5.1.1 Free length theory (FLT) 80-81

4.5.1.2 Collision Factor Theory (CFT) 82-84

4.5.1.3 Nomoto relation 84-85

4.6 Isentropic compressibility 85-89

4.7 Apparent molar isentropic compressibility and derived properties 89-90

Chapter 5: EXPERIMENTAL

(A) EXCESS MOLAR VOLUMES AND APPARENT MOLAR VOLUMES 91-114

5.1 Experimental methods for measurement of excess molar volumes 91-100

5.1.1 Direct method 92-94

5.1.1.1 Batch dilatometer 92-93

5.1.1.2 Continuous dilatometer 93-94

5.1.2 Indirect determination 95-100

5.1.2.1 Pycnometry 95-96

5.1.2.2 Magnetic float densimeter 96

5.1.2.3 Mechanical oscillating densitometer 96-100

5.2 Experimental apparatus and method used in this work 100-114

5.2.1 Vibrating tube densitomer (Anton Paar DMA 38) 100

5.2.2 Mode of operation 101-103

5.2.3 Materials 103-107

5.2.4 Preparation of mixtures 108-109

5.2.5 Experimental procedure for instrument 110-111

5.2.6 Specifications of the Anton Paar DMA 38 instrument 111

5.2.7 Validation of experimental technique 111-112

5.2.8 Systems studied in this work 112-114

Ternary V_{123}^{E} systems (an IL + an alcohol + alkyl acetate or nitromethane) 113

Binary V_{ϕ} systems (an IL + an alcohol or alkyl acetate) and (an alcohol + alkyl acetate) 113-114

(B) ISENTROPIC COMPRESSIBILITY AND APPARENT MOLAR ISENTROPIC COMPRESSIBILITY 114-119

5.3 Introduction 114-115

5.3.1 Ultrasonic interferometer 115-117

5.3.2 Working principle 118

5.3.3 Systems studied in this work 118-119

Binary κ_{ϕ} systems (an IL + an alcohol or alkyl acetate) and (an alcohol

+ alkyl acetate) 118-119

Chapter 6: RESULTS

(A) TERNARY EXCESS MOLAR VOLUME 120-179

6.1 V_{123}^{E} 120-179

6.1.1 $[MOA]^{+}[Tf_2N]^{-}$ 122

6.1.2 $[BMIM]^{+}[MeSO_4]^{-}$ 122

(B) APPARENT MOLAR PROPERTIES 180-198

6.2 Apparent molar volume and derived properties 183-198

6.2.1 Apparent molar volumes 183-195

6.2.2 Partial molar volumes at infinite dilution 196

6.2.3 Limiting apparent molar expansibility 196

6.3 Isentropic compressibility 199-217

6.3.1 Apparent molar isentropic compressibility 199-215

6.3.2 The limiting apparent molar isentropic compressibility 216

Chapter 7: DISCUSSION

7.1 TERNARY EXCESS MOLAR VOLUMES 218-236

7.1.1 ($[MOA]^{+}[Tf_2N]^{-}$ + methanol + methyl acetate) ternary system 219-223

7.1.2. ($[MOA]^{+}[Tf_2N]^{-}$ + methanol + ethyl acetate) ternary system 224-225

7.1.3 ([MOA]$^+$[Tf_2N]$^-$ + ethanol + methyl acetate) ternary system 226-230

7.1.4 ([MOA]$^+$[Tf_2N]$^-$ + ethanol + ethyl acetate) ternary system 230-231

7.1.5 ([BMIM]$^+$[$MeSO_4$]$^-$ + methanol or ethanol or 1-propanol + nitromethane) 232-236

7.2 APPARENT MOLAR PROPERTIES 237-247

7.2 .1 V_ϕ, and κ_ϕ, 237-247

7.2.1 {methyltrioctylammonium bis(trifluoromethylsulfonyl)imide + methyl acetate or methanol} and (methanol + methyl acetate) binary system 237-242

7.2.2 {methyltrioctylammonium bis(trifluoromethylsulfonyl)imide + ethyl acetate or ethanol), (methanol + ethyl acetate) and (ethanol + methyl acetate or ethyl acetate) binary system 242-247

Chapter 8: CONCLUSIONS

8.1 TERNARY EXCESS MOLAR VOLUMES 248-249

8.1.1 ([MOA]$^+$[Tf_2N]$^-$ + methanol or ethanol + methyl acetate or ethyl acetate) 248-249

8.1.2 ([BMIM]$^+$[$MeSO_4$]$^-$ + methanol or ethanol or 1-propanol + nitromethane) 249

8.2 APPARENT MOLAR PROPERTIES 250-251

REFERENCES 252-273

APPENDICES 274-277

APPENDIX 1 276-275

APPENDIX 2 276-277

List of Tables

Table 2.1 Summary of the binary systems from literature used for the ternary systems.

Table 2.2 Binary systems with common cation or anion or an alcohols or nitromethane from literature (used in this work) is given below

Table 2.3 V_{123}^{E} from literature for ternary systems for all the same temperature

Table 5.1 Chemicals, their suppliers and mass % purity

Table 5.2 Densities, ρ, of pure chemicals at T = (298.15, 303.15, and 313.15) K

Table 5.3 Speed of sound, u, of pure chemicals at T = (298.15, 303.15, 308.15 and 313.15) K

Table 6.1 Density, ρ, and ternary excess molar volume, V_{123}^{E} ,, for {$[MOA]^+[Tf_2N]^-$ + methanol + methyl acetate} at T = (298.15, 303.15, and 313.15) K

Table 6.2 Density, ρ, and ternary excess molar volume, V_{123}^{E} ,, for {$[MOA]^+[Tf_2N]^-$ + methanol + ethyl acetate} at T = (298.15, 303.15, and 313.15) K

Table 6.3 Density, ρ, and ternary excess molar volume, V_{123}^{E} ,, for {$[MOA]^+[Tf_2N]^-$ + ethanol + methyl acetate} at T = (298.15, 303.15, and 313.15) K

Table 6.4 Density, ρ, and ternary excess molar volume, V_{123}^{E} ,, for {$[MOA]^+[Tf_2N]^-$ + ethanol + methyl acetate} at T = (298.15, 303.15, and 313.15) K

Table 6.5 Density, ρ, and ternary excess molar volume, V_{123}^{E} , for {$[BMIM]^+[MeSO4]^-$ + methanol + nitromethane} at T = 298.15K

Table 6.6 Density, ρ, and ternary excess molar volume, V_{123}^{E} , for {$[BMIM]^+[MeSO4]^-$ + ethanol + nitromethane} at T = 298.15K

Table 6.7 Density, ρ, and ternary excess molar volume, V_{123}^{E} , for {[BMIM]$^{+}$[MeSO4]$^{-}$ + 1-propanol + nitromethane} at T = 298.15K

Table 6.8 Smoothing Coefficients b_n, and Standard Deviation σ_S , for the Cibulka Equation at T = (298.15, 303.15 and 313.15) K

Table 6.9 Smoothing Coefficients b_n, and Standard Deviation σ_S , for the Cibulka Equation at T = 298.15 K

Table 6.10 Molality, m, densities, ρ, apparent molar volumes, V_ϕ, for ([MOA]$^{+}$ [Tf$_2$N]$^{-}$ + methyl acetate) at T = (298.15, 303.15, 308.15 and 313.15) K

Table 6.11 Molality, m, densities, ρ, apparent molar volumes, V_ϕ, for ([MOA]$^{+}$ [Tf$_2$N]$^{-}$ + ethyl acetate) at T = (298.15, 303.15, 308.15 and 313.15) K

Table 6.12 Molality, m, densities, ρ, apparent molar volumes, V_ϕ, for ([MOA]$^{+}$ [Tf$_2$N]$^{-}$ + methanol) at T = (298.15, 303.15, 308.15) and 313.15 K

Table 6.13 Molality, m, densities, ρ, apparent molar volumes, V_ϕ, for ([MOA]$^{+}$ [Tf$_2$N]$^{-}$ + ethanol) at T = (298.15, 303.15, 308.15 and 313.15) K

Table 6.14 Molality, m, densities, ρ, apparent molar volumes, V_ϕ, for (methanol + methyl acetate) at T = (298.15, 303.15, 308.15 and 313.15) K

Table 6.15 Molality, m, densities, ρ, apparent molar volumes, V_ϕ, for (methanol + ethyl acetate) at T = (298.15, 303.15, 308.15 and 313.15) K

Table 6.16 Molality, m, densities, ρ, apparent molar volumes, V_ϕ , for (ethanol + methyl acetate) at T = (298.15, 303.15, 308.15 and 313.15) K

Table 6.17 Molality, m, densities, ρ, apparent molar volumes, V_ϕ, for (ethanol + ethyl acetate) at T = (298.15, 303.15, 308.15 and 313.15) K

Table 6.18 The values of V_ϕ^0 , S_v , B_v , and standard deviation, σ_v, obtained for each binary system at T = (298.15, 303.15, 308.15 and 313.15) K

Table 6.19 The infinite dilution apparent molar expansibility, E_ϕ^0, values for each binary system at T = (298.15, 303.15, 308.15 and 313.15) K

Table 6.20 Molality, m, densities, ρ, speed of sound, u, isentropic compressibilities, κ_s, and apparent molar isentropic compressibilities, κ_ϕ , for $(MOA)^+ [Tf_2N]^-$ + methyl acetate) at T = (298.15, 303.15, 308.15 and 313.15) K

Table 6.21 Molality, m, densities, ρ, speed of sound, u, isentropic compressibilities, κ_s, and apparent molar isentropic compressibilities, κ_ϕ , for $(MOA)^+ [Tf_2N]^-$ + ethyl acetate) at T = (298.15, 303.15, 308.15 and 313.15) K

Table 6.22 Molality, m, densities, ρ, speed of sound, u, isentropic compressibilities, κ_s, and apparent molar isentropic compressibilities, κ_ϕ , for $([MOA]^+ [Tf_2N]^-$ + methanol) at T = (298.15, 303.15, 308.15 and 313.15) K

Table 6.23 Molality, m, densities, ρ, speed of sound, u, isentropic compressibilities, κ_s, and apparent molar isentropic compressibilities, κ_ϕ , for $([MOA]^+ [Tf_2N]^-$ + ethanol) at T = (298.15, 303.15, 308.15 and 313.15) K

Table 6.24 Molality, m, densities, ρ, speed of sound, u, isentropic compressibilities, κ_s, and apparent molar isentropic compressibilities, κ_ϕ , for (methanol + methyl acetate) at T = (298.15, 303.15, 308.15 and 313.15) K

Table 6.25 Molality, m, densities, ρ, speed of sound, u, isentropic compressibilities, κ_s , and apparent molar isentropic compressibilities, κ_ϕ , for (methanol + ethyl acetate) at T = (298.15, 303.15, 308.15 and 313.15) K

Table 6.26 Molality, m, densities, ρ, speed of sound, u, isentropic compressibilities, κ_s, and apparent molar isentropic compressibilities, κ_ϕ, for (ethanol + methyl acetate) at T = (298.15, 303.15, 308.15 and 313.15) K

Table 6.27 Molality, m, densities, ρ, speed of sound, u, isentropic compressibilities, κ_s, and apparent molar isentropic compressibilities, κ_ϕ, for (ethanol + ethyl acetate) at T = (298.15, 303.15, 308.15 and 313.15) K

Table 6.28 The values of κ_ϕ^0, S_k, B_k, and standard deviation, σ_k, for each binary system at T = (298.15, 303.15, 308.15 and 313.15) K

Table 7.1 The V_{min}^E for the five binary systems at T = (298.15, 303.15, and 313.15) K from literature for the {$[MOA]^+[Tf_2N]^-$ + methanol + methyl acetate or ethyl acete} ternary systems

Table 7.2 The minimum ternary excess molar volume, $V_{123\,min}^E$ for ternary systems {$[MOA]^+[Tf_2N]^-$ + methanol + methyl acetate or ethyl acetate} at constant z values and at each temperature

Table 7.3 The V_{min}^E for the five binary systems at T = (298.15, 303.15, and 313.15) K from literature for the {$[MOA]^+[Tf_2N]^-$ + ethanol + methyl acetate or ethyl acete} ternary systems

Table 7.4 The minimum ternary excess molar volume, $V_{123\,min}^E$ for ternary systems {$[MOA]^+[Tf_2N]^-$ + ethanol + methyl acetate or ethyl acetate} at constant z values and at each temperature

Table 7.5 The V_{min}^E for the seven binary systems at T = (298.15, 303.15, and 313.15) K from literature for the ($[BMIM]^+[MeSO_4]^-$ + methanol or ethanol or 1-propanol + nitromethane) ternary systems

Table 7.6 The minimum ternary excess molar volume, $V^{E}_{123\ min}$ for ternary systems ($[BMIM]^{+}[MeSO_4]^{-}$ + methanol or ethanol or 1-propanol + nitromethane) at constant *z* values and at *T* = 298.15 K

List of Figures

Figure 1.1 Methyl trioctylammonium bis(trifluoromethylsulfonyl)imide

Figure 1.2 1-Butyl-3methylimidazolium methyl sulphate

Figure 3.1 Map of physical properties of ionic liquid

Figure 3.2 (a) 1-Alkyl-3-methylimidazolium, (b)1-alkylpyridinium, (c) N-methyl-N-alkylpyrrolidinium and (d) ammonium ions

Figure 3.3 4-*n*-Butyl-4-methylpyridinium tetrafluoroborate

Figure 3.4 1-*n*-Butyl-3-methylimidazolium tetrafluoroborate

Figure 3.5 1-*n*-Butyl-3-methylimidazolium hexafluorophosphate

Figure 3.6 1-*n*-Butyl-3-methylimidazolium chloride

Figure 3.7 1-*n*-Butyl-3-methylimidazolium bromide

Figure 3.8 1-*n*-Butyl-3-methylimidazolium dicyanamide

Figure 3.9 1-*n*-Butyl-3-methylimidazolium trifluoromethanesulfonate

Figure 3.10 1-*n*-Butyl-3-methylimidazolium bis(trifluoromethylsulfonyl)imide

Figure 3.11 1-*n*-Ethyl-3-methylimidazolium bis(trifluoromethylsulfonyl)imide

Figure 3.12 1-Ethyl-2, 3-dimethyl-imidazolium bis(trifluoromethylsulfonyl)imide

Figure 3.13 2,3-Dimethyl-1-propylimidazolium bis(trifluoromethylsulfonyl)imide

Figure 3.14 1-Butyl-2,3-dimethyl hexafluorophosphate

Figure 3.15 1-Butyl-2,3-Dimethyl tetrafluoroborate

Figure 3.16 1, 2-Dimethyl-3-Octylimidazolium bis(trifluoromethylsulfonyl)imide

Figure 3.17 Map of the applications of ionic liquids

Figure 5.1 A typical batch dilatometer

Figure 5.2 Continuous dilatometer (i) design of Bottomly and Scott, (ii) design of Kumaran and McGlashan.

Figure 5.3 The pycnometer based on the design of Wood and Bruisie

Figure 5.4 Magnetic float densitometer

Figure 5.5 DMA 38 Densitometer

Figure 5.6 Typical plots showing each z values covering the entire composition range.

Figure 5.7 Comparison of the, V_m^E, from this work with the literature results for the mixtures {$C_6H_5CH_3$(x_1) + C_6H_{14}(x_2)} at T = 298.15 K, ●, literature results; ▲, this work

Figure 5.8 Ultrasonic interferometer M-81G

Figure 5.9 Diagram of interferometer

Figure 6.1 Graph of ternary excess molar volumes, V_{123}^E , for {$[MOA]^+[Tf_2N]^-$ (x_1) + methanol (x_2) + methyl acetate (x_3)} against mole fraction of methanol at T = 298.15 K. The symbols represent experimental data at constant z = x_3/x_1: ●, z = 0.30; □, z = 0.50; ▲, z = 1.00; ◊, z = 1.50; ■, z = 4.00; ♦, z = 9.00.

Figure 6.2 Graph of ternary excess molar volumes, V_{123}^{E} , for {$[MOA]^+[Tf_2N]^-$ (x_1) + methanol (x_2) + methyl acetate (x_3)} against mole fraction of methanol at T = 303.15 K. The symbols represent experimental data at constant z = x_3/x_1: ●, z = 0.30; □, z = 0.50; ▲, z = 1.00; ◊, z = 1.50; ■, z = 4.00; ♦, z = 9.00.

Figure 6.3 Graph of ternary excess molar volumes, V_{123}^{E} , for {$[MOA]^+[Tf_2N]^-$ (x_1) + methanol (x_2) + methyl acetate (x_3)} against mole fraction of methanol at T = 313.15 K. The symbols represent experimental data at constant z = x_3/x_1: ●, z = 0.30; □, z = 0.50; ▲, z = 1.00; ◊, z = 1.50; ■, z = 4.00; ♦, z = 9.00.

Figure 6.4 Graph of ternary excess molar volumes, V_{123}^{E} , for {$[MOA]^+[Tf_2N]^-$ (x_1) + methanol (x_2) + ethyl acetate (x_3)} against mole fraction of methanol at T = 298.15 K. The symbols represent experimental data at constant z = x_3/x_1: ●, z = 7.50; □, z = 3.36; ▲, z = 1.80; ◊, z = 1.00; ■, z = 0.43; ♦, z = 0.10.

Figure 6.5 Graph of ternary excess molar volumes, V_{123}^{E} , for {$[MOA]^+[Tf_2N]^-$ (x_1) + methanol (x_2) + ethyl acetate (x_3)} against mole fraction of methanol at T = 303.15 K. The symbols represent experimental data at constant z = x_3/x_1: ●, z = 7.50; □, z = 3.36; ▲, z = 1.80; ◊, z = 1.00; ■, z = 0.43; ♦, z = 0.10.

Figure 6.6 Graph of ternary excess molar volumes, V_{123}^{E} , for {$[MOA]^+[Tf_2N]^-$ (x_1) + methanol (x_2) + ethyl acetate (x_3)} against mole fraction of methanol at T = 313.15 K. The symbols represent experimental data at constant z = x_3/x_1: ●, z = 7.50; □, z = 3.36; ▲, z = 1.80; ◊, z = 1.00; ■, z = 0.43; ♦, z = 0.10.

Figure 6.7 Graph of ternary excess molar volumes, V_{123}^{E} , for {[MOA]$^{+}$[Tf$_2$N]$^{-}$ (x_1) + ethanol (x_2) + methyl acetate (x_3)} against mole fraction of methanol at T = 298.15 K. The symbols represent experimental data at constant z = x_3/x_1: Δ, z = 0.10 □, z = 0.20; ◊, z = 0.50; ●, z = 1.00; ▲, z = 1.50; ■, z = 4.00; ♦, z = 9.00.

Figure 6.8 Graph of ternary excess molar volumes, V_{123}^{E} , for {[MOA]$^{+}$[Tf$_2$N]$^{-}$ (x_1) + ethanol (x_2) + methyl acetate (x_3)} against mole fraction of methanol at T = 303.15 K. The symbols represent experimental data at constant z = x_3/x_1: Δ, z = 0.10 □, z = 0.20; ◊, z = .50; ●, z = 1.00; ▲, z = 1.50; ■, z = 4.00; ♦, z = 9.00.

Figure 6.9 Graph of ternary excess molar volumes, V_{123}^{E} , for {[MOA]$^{+}$[Tf$_2$N]$^{-}$ (x_1) + ethanol (x_2) + methyl acetate (x_3)} against mole fraction of methanol at T = 313.15 K. The symbols represent experimental data at constant z = x_3/x_1: Δ, z = 0.10 □, z = 0.20; ◊, z = .50; ●, z = 1.00; ▲, z = 1.50; ■, z = 4.00; ♦, z = 9.00.

Figure 6.10 Graph of ternary excess molar volumes, V_{123}^{E} , for {[MOA]$^{+}$[Tf$_2$N]$^{-}$ (x_1) + ethanol (x_2) + ethyl acetate (x_3)} against mole fraction of methanol at T = 298.15 K. The symbols represent experimental data at constant z = x_3/x_1: ♦, z = 0.08; ■, z = 0.25; ▲, z = 0.40; ●, z = 0.80; ◊, z = 1.30; □, z = 4.00; Δ, z = 9.00.

Figure 6.11 Graph of ternary excess molar volumes, V_{123}^{E} , for {[MOA]$^{+}$[Tf$_2$N]$^{-}$ (x_1) + ethanol (x_2) + ethyl acetate (x_3)} against mole fraction of methanol at

T = 303.15 K. The symbols represent experimental data at constant z = x_3/x_1: ♦, z = 0.08; ■, z = 0.25; ▲, z = 0.40; ●, z = 0.80; ◊, z = 1.30; □, z = 4.00; Δ, z = 9.00.

Figure 6.12 Graph of ternary excess molar volumes, V_{123}^{E} , for {$[MOA]^+[Tf_2N]^-$ (x_1) + ethanol (x_2) + ethyl acetate (x_3)} against mole fraction of methanol at T = 313.15 K. The symbols represent experimental data at constant z = x_3/x_1: ♦, z = 0.08; ■, z = 0.25; ▲, z = 0.40; ●, z = 0.80; ◊, z = 1.30; □, z = 4.00; Δ, z = 9.00.

Figure 6.13 Graph of ternary excess molar volumes, V_{123}^{E} , for {$[BMIM]^+[MeSO_4]^-$ (x_1) + methanol (x_2) + nitromethane (x_3)} against mole fraction of methanol at T = 298.15 K. The symbols represent experimental data at constant $z = x_3/x_1$: ♦, z = 0.04; ■, z = 0.23; ▲, z = 0.72; ●, z = 1.80; ◊, z = 4.21.

Figure 6.14 Graph of ternary excess molar volumes, V_{123}^{E} , for {$[BMIM]^+[MeSO_4]^-$ (x_1) + ethanol (x_2) + nitromethane (x_3)} against mole fraction of methanol at T = 298.15 K. The symbols represent experimental data at constant $z = x_3/x_1$: ♦, z = 0.04; ■, z = 0.23; ▲, z = 0.72; ●, z = 1.80; ◊, z = 4.21.

Figure 6.15 Graph of ternary excess molar volumes, V_{123}^{E} , for {$[BMIM]^+[MeSO_4]^-$ (x_1) + 1-propanol (x_2) + nitromethane (x_3)} against mole fraction of methanol at T = 298.15 K. The symbols represent experimental data at constant $z = x_3/x_1$: ♦, z = 0.04; ■, z = 0.23; ▲, z = 0.72; ●, z = 1.80; ◊, z = 4.21.

Figure 6.16 Graph obtained from the Cibulka equation for the ternary system {$[MOA]^+[Tf_2N]^-$ (x_1) + methanol (x_2) + methyl acetate (x_3)} at T = 298.15 K.

Figure 6.17 Graph obtained from the Cibulka equation for the ternary system

{[MOA]$^+$[Tf$_2$N]$^-$ (x_1) + methanol (x_2) + methyl acetate (x_3)} at T = 303.15 K

Figure 6.18 Graph obtained from the Cibulka equation for the ternary system {[MOA]$^+$[Tf$_2$N]$^-$ (x_1) + methanol (x_2) + methyl acetate (x_3)} at T = 313.15 K.

Figure 6.19 Graph obtained from the Cibulka equation for the ternary system {[MOA]$^+$[Tf$_2$N]$^-$ (x_1) + methanol (x_2) + ethyl acetate (x_3)} at T = 298.15 K.

Figure 6.20 Graph obtained from the Cibulka equation for the ternary system {[MOA]$^+$[Tf$_2$N]$^-$ (x_1) + methanol (x_2) + ethyl acetate (x_3)} at T = 303.15 K.

Figure 6.21 Graph obtained from the Cibulka equation for the ternary system {[MOA]$^+$[Tf$_2$N]$^-$ (x_1) + methanol (x_2) + ethyl acetate (x_3)} at T = 313.15 K.

Figure 6.22 Graph obtained from the Cibulka equation for the ternary system {[MOA]$^+$[Tf$_2$N]$^-$ (x_1) + ethanol (x_2) + methyl acetate (x_3)} at T = 298.15 K.

Figure 6.23 Graph obtained from the Cibulka equation for the ternary system {[MOA]$^+$[Tf$_2$N]$^-$ (x_1) + ethanol (x_2) + methyl acetate (x_3)} at T = 303.15 K.

Figure 6.24 Graph obtained from the Cibulka equation for the ternary system {[MOA]$^+$[Tf$_2$N]$^-$ (x_1) + ethanol (x_2) + methyl acetate (x_3)} at T = 313.15 K.

Figure 6.25 Graph obtained from the Cibulka equation for the ternary system {[MOA]$^+$[Tf$_2$N]$^-$ (x_1) + ethanol (x_2) + ethyl acetate (x_3)} at T = 298.15 K.

Figure 6.26 Graph obtained from the Cibulka equation for the ternary system {[MOA]$^+$[Tf$_2$N]$^-$ (x_1) + ethanol (x_2) + ethyl acetate (x_3)} at T = 303.15 K.

Figure 6.27 Graph obtained from the Cibulka equation for the ternary system {[MOA]$^+$[Tf$_2$N]$^-$ (x_1) + ethanol (x_2) + ethyl acetate (x_3)} at T = 313.15 K.

Figure 6.28 Graph obtained from the Cibulka equation for the ternary system $[BMIM]^+[MeSO_4]^-$ (x_1) + methanol (x_2) + nitromethane (x_3) at T = 298.15 K.

Figure 6.29 Graph obtained from the Cibulka equation for the ternary system $[BMIM]^+[MeSO_4]^-$ (x_1) + ethanol (x_2) + nitromethane (x_3) at T = 298.15 K.

Figure 6.30 Graph obtained from the Cibulka equation for the ternary system $[BMIM]^+[MeSO_4]^-$ (x_1) + 1-propanol (x_2) + nitromethane (x_3) at T = 298.15 K.

Figure 6.31 Apparent molar volume (V_ϕ) versus molality $(m)^{1/2}$ of binary mixture of ($[MOA]^+[Tf_2N]^-$ + methyl acetate) at T = 298.15 K (♦), 303.15 K (■), 308.15 K (▲) and 313.15 K (•).

Figure 6.32 Apparent molar volume (V_ϕ) versus molality $(m)^{1/2}$ of binary mixture of ($[MOA]^+[Tf_2N]^-$ + ethyl acetate) at T = 298.15 K (♦), 303.15 K (■), 308.15 K (▲) and 313.15 K (•).

Figure 6.33 Apparent molar volume (V_ϕ) versus molality $(m)^{1/2}$ of binary mixture of ($[MOA]^+[Tf_2N]^-$ + methanol) at T = 298.15 K (♦), 303.15 K (■), 308.15 K (▲) and 313.15 K (•).

Figure 6.34 Apparent molar volume (V_ϕ) versus molality $(m)^{1/2}$ of binary mixture of ($[MOA]^+[Tf_2N]^-$ + ethanol) at T = 298.15 K (♦), 303.15 K (■), 308.15 K (▲) and 313.15 K (•).

Figure 6.35 Apparent molar volume (V_ϕ) versus molality $(m)^{1/2}$ of binary mixture of (methanol + methyl acetate) at T = 298.15 K (♦), 303.15 K (■), 308.15 K (▲) and 313.15 K (•).

Figure 6.36 Apparent molar volume (V_ϕ) versus molality $(m)^{1/2}$ of binary mixture of (methanol + ethyl acetate) at T = 298.15 K (♦), 303.15 K (■), 308.15 K (▲) and 313.15 K (•).

Figure 6.37 Apparent molar volume (V_ϕ) versus molality $(m)^{1/2}$ of binary mixture of (ethanol + methyl acetate) at T = 298.15 K (♦), 303.15 K (■), 308.15 K (▲) and 313.15 K (•).

Figure 6.38 Apparent molar volume (V_ϕ) versus molality $(m)^{1/2}$ of binary mixture of (ethanol + ethyl acetate) at T = 298.15 K (♦), 303.15 K (■), 308.15 K (▲) and 313.15 K (•).

Figure 6.39 Isentropic compressibility (κ_s) versus molality (m) of binary mixture of ($[MOA]^+[Tf_2N]^-$ + methyl acetate) at T = 298.15 K (♦), 303.15 K (■), 308.15 K (▲) and 313.15 K (•).

Figure 6.40 Isentropic compressibility (κ_s) versus molality (m) of binary mixture of ($[MOA]^+[Tf_2N]^-$ + ethyl acetate) at T = 298.15 K (♦), 303.15 K (■), 308.15 K (▲) and 313.15 K (•).

Figure 6.41 Isentropic compressibility (κ_s) versus molality (m) of binary mixture of ($[MOA]^+[Tf_2N]^-$ + methanol) at T = 298.15 K (♦), 303.15 K (■), 308.15 K (▲) and 313.15 K (•).

Figure 6.42 Isentropic compressibility (κ_s) versus molality (m) of binary mixture of ($[MOA]^+[Tf_2N]^-$ + ethanol) at T = 298.15 K (♦), 303.15 K (■), 308.15 K (▲) and 313.15 K (•).

Figure 6.43 Isentropic compressibility (κ_s) versus molality (m) of binary mixture of (methanol + methyl acetate) at T = 298.15 K (♦), 303.15 K (■), 308.15 K (▲) and 313.15 K (•).

Figure 6.44 Isentropic compressibility (κ_s) versus molality (m) of binary mixture of (methanol + ethyl acetate) at T = 298.15 K (♦), 303.15 K (■), 308.15 K (▲) and 313.15 K (•).

Figure 6.45 Isentropic compressibility (κ_s) versus molality (m) of binary mixture of (ethanol + methyl acetate) at T = 298.15 K (♦), 303.15 K (■), 308.15 K (▲) and 313.15 K (•).

Figure 6.46 Isentropic compressibility (κ_s) versus molality (m) of binary mixture of (ethanol + ethyl acetate) at T = 298.15 K (♦), 303.15 K (■), 308.15 K (▲) and 313.15 K (•).

Figure 6.47 Apparent molar isentropic compressibility (κ_ϕ) versus molality $(m)^{1/2}$ of binary mixture of ($[MOA]^+[Tf_2N]^-$ + methyl acetate) at T = 298.15 K (♦), 303.15 K (■), 308.15 K (▲) and 313.15 K (•).

Figure 6.48 Apparent molar isentropic compressibility (κ_ϕ) versus molality $(m)^{1/2}$ of binary mixture of ($[MOA]^+[Tf_2N]^-$ + ethyl acetate) at T = 298.15 K (♦), 303.15 K (■), 308.15 K (▲) and 313.15 K (•).

Figure 6.49 Apparent molar isentropic compressibility (κ_ϕ) versus molality $(m)^{1/2}$ of binary mixture of ($[MOA]^+[Tf_2N]^-$ + methanol) at T = 298.15 K (♦), 303.15 K (■), 308.15 K (▲) and 313.15 K (•).

Figure 6.50 Apparent molar isentropic compressibility (κ_ϕ) versus molality $(m)^{1/2}$ of binary mixture of ($[MOA]^+[Tf_2N]^-$ + ethanol) at T = 298.15 K (♦), 303.15 K (■), 308.15 K (▲) and 313.15 K (•).

Figure 6.51 Apparent molar isentropic compressibility (κ_ϕ) versus molality $(m)^{1/2}$ of binary mixture of (methanol + methyl acetate) at T = 298.15 K (♦), 303.15 K (■), 308.15 K (▲) and 313.15 K (•).

Figure 6.52 Apparent molar isentropic compressibility (κ_ϕ) versus molality $(m)^{1/2}$ of binary mixture of (methanol + ethyl acetate) at T = 298.15 K (♦), 303.15 K (■), 308.15 K (▲) and 313.15 K (•).

Figure 6.53 Apparent molar isentropic compressibility (κ_ϕ) versus molality $(m)^{1/2}$ of binary mixture of (ethanol + methyl acetate) at T = 298.15 K (♦), 303.15 K (■), 308.15 K (▲) and 313.15 K (•).

Figure 6.54 Apparent molar isentropic compressibility (κ_ϕ) versus molality $(m)^{1/2}$ of binary mixture of (ethanol + ethyl acetate) at T = 298.15 K (♦), 303.15 K (■), 308.15 K (▲) and 313.15 K (•).

List of Symbols

ρ	density
$V_{\mathrm{m}}^{\mathrm{E}}$, $V_{i,\mathrm{j}}^{\mathrm{E}}$	binary excess molar volume
$V_{\mathrm{min}}^{\mathrm{E}}$	minimum binary excess molar volume
V_{123}^{E}	ternary excess molar volume
$V_{123\,\mathrm{min}}^{\mathrm{E}}$	minimum ternary excess molar volume
z	mole fractions ratio between the 3rd and 1s component of the ternary system
(b_0, b_1, b_2)	Cibulka parameters
T	temperature
K	Kelvin
x_1	mole fraction of the 1st component
x_2	mole fraction of the 2nd component
x_3	mole fraction of the 3rd component
σ	standard deviation of ternary excess molar volume
σ_{v}	standard deviation of apparent molar volume
σ_{κ}	standard deviation of apparent molar isentropic compressibility
M_1	molar mass of ionic liquid
M_2	molar mass of alcohol

M_3	molar mass of alkyl acetate or nitromethane
A_i	polynomial coefficient
N	polynomial degree
n	number of experimental point
k	number of coefficients used in the Redlich –Kister correlation
V_ϕ	apparent molar volume
V_ϕ^0	apparent molar volume at infinite dilution
E_ϕ^0	infinite dilution apparent molar expansibility
S_v	empirical parameter for apparent molar volume
B_v	empirical parameter for apparent molar volume
u	speed of sound
κ_s	isentropic compressibility of mixture
κ_{s0}	isentropic compressibility of pure solvent
κ_ϕ	apparent molar isentropic compressibility
κ_ϕ^0	apparent molar isentropic compressibility at infinite dilution
S_k	empirical parameter for apparent molar isentropic compressibility
B_k	empirical parameter for apparent molar isentropic compressibility
m	molality

Ionic Liquid Abbreviations

$[MOA]^+[Tf_2N]^-$	methyl trioctylammonium bis(trifluoromethylsulfonyl)imide
$[BMIM]^+[MeSO_4]^-$	1-butyl-3-methylimidazolium methyl sulfate
$[BMIM]^+[BF_4]^-$	1-butyl-3-methylimidazolium tetrafluoroborate
$[BMPy]^+[BF_4]^-$	1-butyl-3-methylpyridinium tetrafluoroborate
$[BMIM]^+[PF_6]^-$	1-butyl-3-methylimidazolium hexafluorophosphate
$[MMIM]^+[MeSO_4]^-$	1,3-dimethylimidazolium methyl sulphate
$[HMIM]^+[PF_6]^-$	1-hexyl-3-methylimidazolium hexafluorophosphate
$[MOIM]^+[PF_6]^-$	1-methyl-3-octylimidazolium hexafluorophosphate
$[BMIM]^+[OcSO_4]^-$	1-butyl-3-methylimidazolium octyl sulphate
$[EMIM]^+[CH_3(OCH_2CH_2)_2OSO_3]^-$	1-ethyl-3-methylimidazolium diethyleneglycol monomethylether sulphate
$[BMIM]^+[CH_3(OCH_2CH_2)_2OSO_3]^-$	1-butyl-3-methyl-imidazolium diethyleneglycol monomethylether sulphate
$[MOIM]^+[CH_3(OCH_2CH_2)_2OSO_3]^-$	1-methyl-3-octyl-imidazolium diethyleneglycol monomethylether sulphate

$[EMIM]^+[BETI]^-$	1-ethyl-3-methylimidazolium bis(perfluoroethylsulphonyl)imide
$[EMIM]^+[EtSO_4]^-$	1-ethyl-3-methylimidazolium ethyl sulfate
$[BMIM]^+[CF_3SO_3]^-$	1-butyl-3-methylimidazolium trifluoromethanesulfonate
$[MOIM]^+[Tf_2N]^-$	1- methyl-3-octylimidazolium bis(trifluoromethylsulfonyl)imide
$[BMIM]^+[Tf_2N]^-$	1-butyl-3-methylimidazolium bis(trifluoromethylsulfonyl)imide
$[EMI]^+[GaCl_4]^-$	1-methyl-3-ethylimidazolium guanidiniumtetra chloride
$[BMIM]^+[Br]^-$	1-butyl-3-methylimidazolium bromide
$[BMIM]^+[Cl]^-$	1-butyl-3-methylimidazolium chloride
$[HMIM]^+[Cl]^-$	1-hexyl-3-methylimidazolium chloride
$[MOIM]^+[Cl]^-$	1- methyl-3-octylimidazolium chloride
$[EMI]^+[EtSO_4]^-$	1-ethyl-3-methylimidazolium ethyl sulphate
$[PMIM]^+[BF_4]^-$	1-methyl-3-pentylimidazolium tetrafluoroborate
$[HMIM]^+[Tf_2N]^-$	1-hexyl-3-methylimidazolium bis(trifluoromethylsulfonyl)imide

$[MOIM]^+[BF_4]^-$	1-methyl-3-octylimidazolium tetrafluoroborate
$[HMIM]^+[Tf_2N]^-$	1-hexyl-3-methylimidazolium bis(trifluoromethylsulfonyl)imide
$[EMIM]^+[Br]^-$	1-ethyl-3-methylimidazolium bromide
$[BMIM]^+[Cl]^-$	1-butyl-3-methylimidazolium chloride
$[RMIM]^+[Br]^-$	1-alkyl-3-methylimidazolium bromide
$[EMI]^+[Cl]^-$	1-ethyl-3-methylimidazolium chloride
$[BMIM]^+[DCA]^-$	1-*n*-Butyl-3-methylimidazolium dicyanamide
$[EMMIM]^+[Tf_2N]^-$	2, 3-Dimethyl-1-ethylimidazolium bis(trifluoromethylsulfonyl)imide
$[PMMIM]^+[Tf_2N]^-$	2, 3-Dimethyl-1-propylimidazolium bis(trifluoromethylsulfonyl)imide
$[BDMIM]^+[PF_6]^-$	1-Butyl-2, 3-dimethyl hexafluorophosphate
$[BDMIM]^+[BF_4]^-$	1-Butyl-2, 3-dimethyl tetrafluoroborate
$[BMPy]^+[BF_4]^-$	4-Butyl-4-methylpyridinium tetrafluoroborate

CHAPTER 1

INTRODUCTION

Before you start some work, always ask yourself three questions: Why am I doing it? What the results might be? and will I be successful? Only when you think deeply and find satisfactory answers to these questions, go ahead.

.. *Chanakya*

(Indian politician, strategist and writer 350 BC – 275 BC)

Thermophysical and thermodynamic properties of pure liquids and liquid mixtures are of interest to both chemists and chemical engineers. These properties are used to:

(i) interpret, correlate and predict thermodynamics properties via molecular thermodynamic considerations,

(ii) find the applicability of theories of liquids and to predict the properties of mixtures of similar nature,

(iii) design industrial equipment with better precision and

(iv) test the current theories of solutions because of their sensitivity to the difference in magnitude of intermolecular forces and geometry of the component molecules.

The excess thermodynamic properties are extensively used to study the deviation of the real liquid mixture from ideality.

Excess functions may be positive or negative, their sign and magnitude representing the deviation from ideality.

1.1 THE IMPORTANCE OF THERMOPHYSICAL AND THERMODYNAMIC PROPERTIES

During the last few years, investigations of thermophysical and thermodynamic properties have increased remarkably, but they are by no means exhausted (Marsh and Boxall 2004; Heintz 2005; Zhang *et al.* 2006; Fredlake 2004; Tokuda *et al.* 2004; Tokuda *et al.* 2005; Tokuda *et al.* 2006; Azevedo *et al.* 2005(a); Azevedo *et al.* 2005(b); Esperancia *et al.* 2006; Domanska 2005; Domanska 2006; Pereiro *et al.* 2007(a); Pereiro and Rodriguez 2007(b); Greaves *et al.* 2006). Moreover, thermophysical and thermodynamic properties of ionic liquids (ILs) are increasing rapidly.

The complexity of the molecular interactions present in the liquid phase makes the task of predicting thermodynamic quantities difficult. Thermophysical data are useful industrially, for the optimization of the design of various industrial processes (Bhujrajh and Deenadayalu 2006; Marsh and Boxal 2004; Domanska and Marciniak 2005). Knowledge of thermo physical properties of the ILs mixed with other organic solvents are useful for development of specific chemical processes (Dupont *et al.* 2002; Anastas and Warner 1998; Cann and Connelly 2000).

Thermodynamic properties, including activity coefficients at infinite dilution and excess molar volumes, $V_{\mathrm{m}}^{\mathrm{E}}$, are also useful for the development of reliable predictive models for systems containing ionic liquids. To this end, a database of IL cation, anion and thermo physical properties should be useful (Domanska and Pobudkowska 2006).

$V_{\mathrm{m}}^{\mathrm{E}}$, and partial molar volumes at infinite dilution, $V_{\mathrm{m},\ \mathrm{i}}^{\infty}$, can be used as a basis for understanding some of the molecular interactions (such as dispersion forces, hydrogen-bonding interactions) in binary and ternary mixtures (Zhong and Wang 2007). Excess molar

volume data is a helpful parameter in the design of technological processes of a reaction (Gómez and González 2006), and can be used to predict vapour liquid equilibria using appropriate equation of state (EoS) models (Sen 2007).

$V^{\infty}_{\mathrm{m,\ i}}$ data provides useful information about interactions occurring at infinitely dilution. These studies are of great help in characterizing the structure and properties of dilute solutions (Domanska and Pobudkowska 2006).

Measurement of speed of sound, *u*, in liquids provides information (e.g. the effects of small concentrations changes) on the thermophysical properties of chemical substances and their mixtures (Azevedo and Szydlowski 2004).

The objective of studying thermophysical properties of binary and ternary mixtures of ILs is to contribute to a data bank of thermodynamic properties containing ILs and to investigate the relationship between ionic structure of the IL and density of the binary and ternary mixtures, in order to establish principles for the molecular design of suitable ILs for chemical separation processes (Azevedo and Szydlowski 2004).
Thermophysical and thermodynamic properties of ionic liquids are unlimited because the number of potential ILs are large (Yang *et al.* 2005 (a), Najdanovic-Visak *et al*. 2002; Krummen *et al.* 2002; Arce *et al.* 2006; Jaquemin *et al.* 2006).

To design any process containing an IL on an industrial scale it is necessary to know the thermodynamic or physic-chemical properties such as density, speed of sound and activity coefficients at infinite dilution (Letcher *et al.* 2005). The precise numerical values of these properties are of significance in design and control of the chemical processes involving the ILs (Plechkova and Seddon 2008; Gómez and González 2006; Smith and Pagni 1989).

1.2 SCOPE OF THE PRESENT WORK

The work undertaken was composed of two parts:

(A) TERNARY EXCESS MOLAR VOLUMES

In this work the ternary excess molar volume, V_{123}^{E}, were determined for the ternary systems {methyl trioctylammonium bis (trifluoromethylsulfonyl)imide $[MOA]^{+}[Tf_2N]^{-}$ + methanol or ethanol + methyl acetate or ethyl acetate } at T = (298.15, 303.15 and 313.15) K, and (1-butyl-3-methylimidazolium methylsulfate $[BMIM]^{+}[MeSO_4]^{-}$ + methanol or ethanol or 1-propanol + nitromethane), at T = 298.15 K over the entire composition range. The V_{123}^{E} data was correlated with the Cibulka equation (Cibulka *et al.* 1982) using binary parameters. Binary Redlich-Kister parameters were obtained from the Redlich-Kister equation (Redlich and Kister 1948) applied to the binary systems obtained from literature.

The experimental and Cibulka correlated ternary excess molar volumes are used to understand the influence of the third component on the pair-wise interactions in the ternary mixtures and the change in nature and degree of interaction between pairs of molecules.

Factors that can influence interactions are:

(i) Decrease in dipolar association of the polar components

(ii) Differences in size and shapes of components

(iii) Break-up of hydrogen bonds in hydrogen bonded aggregated of alcohols

(iv) Intermolecular interaction between like and unlike molecules

(v) Interstitial accommodation of the smaller components into the larger components

(B) APPARENT MOLAR PROPERTIES

The density, ρ, speed of sound, u , at 3 MHz, apparent molar volumes, V_ϕ , isentropic compressibility,κ_S , and apparent molar isentropic compressibility, κ_ϕ , at T = (298.15, 303.15, 308.15 and 313.15) K were determined for ($[MOA]^+[Tf_2N]^-$ + methanol or ethanol or methyl acetate or ethyl acetate), (methanol + methyl acetate or ethyl acetate) and(ethanol + methyl acetate or ethyl acetate) binary systems. A Redlich-Mayer (Redlich *et al.* 1964) type equation was fitted to the apparent molar volume and apparent molar isentropic compressibility data.

The apparent molar volume at infinite dilution (V_ϕ^0), the limiting apparent molar expansibility (E_ϕ^0), and the limiting apparent molar isentropic compressibilitiy (κ_ϕ^0) of the eight binary systems at T = (298.15, 303.15, 308.15 and 313.15) K were also calculated. All derived thermodynamic properties were interpreted in terms of intermolecular interactions.

The structures of the ILs used in this work are presented in Figures 1.1 -1.2.

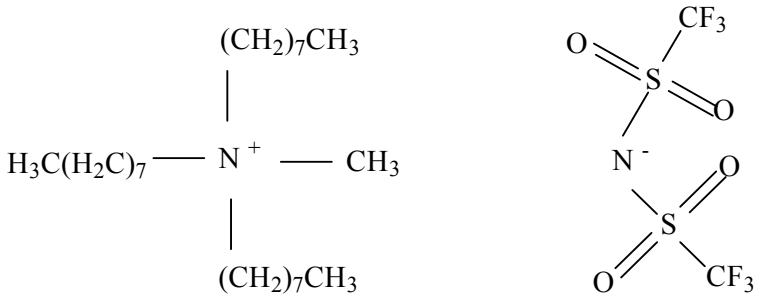

Figure 1.1 Methyl trioctylammonium bis(trifluoromethylsulfonyl)imide $[MOA]^{+}[Tf_2N]^{-}$

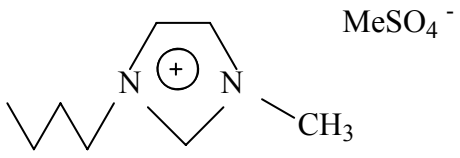

Figure 1.2 1-Butyl-3-methylimidazolium methyl sulphate $[BMIM]^{+}[MeSO_4]^{-}$

CHAPTER 2

LITERATURE REVIEW

(A) TERNARY EXCESS MOLAR VOLUME

The need for studying thermophysical properties of composite materials (or mixtures of pure substances) is often due to the deviation from ideality due to mixing, or a specific application for the required property (Blandamer 1973; Franks and Reid 1973; Millero 1971; Millero 1980; Hoiland 1986).

The composition dependence of the excess molar volume is used to understand the nature of the molecular interactions in these mixtures.

There is a large amount of binary $V_{\mathrm{m}}^{\mathrm{E}}$ and few ternary V_{123}^{E} data on ionic liquids with alcohols and other organic solvents in the literature. A summary of the literature binary $V_{\mathrm{m}}^{\mathrm{E}}$ systems are given in Table 2.1.

Table 2.1 Summary of the binary systems from literature used for the ternary systems.

Author	Systems	V_m^E/cm^3·mol^{-1}
González *et al.* 2007	(methanol or ethanol + methyl acetate or ethyl acetate)	positive and negative
Nakanishi *et al.* 1970	(methanol or ethanol + nitromethane)	positive and negative
Cerdeirina *et al.* 1999	(nitromethane + 1-propanol)	positive
Sibiya and Deenadayalu 2008	([MOA]$^+$[Tf_2N]$^-$ + methanol or ethanol or 1-propanol)	positive and negative
Deenadayalu and Bahadur 2010	{[MOA]$^+$[Tf_2N]$^-$ + methyl acetate or ethyl acetate)	negative
Sibiya and Deenadayalu 2009	([BMIM]$^+$[$MeSO_4$]$^-$ + methanol or ethanol or 1-propanol)	negative
Iglesias-Otero *et al*. 2008	([BMIM]$^+$[$MeSO_4$]$^-$ + nitromethane)	negative

González *et al.* (2007) reported the densities and dynamic viscosities for (methanol or ethanol + water or ethyl acetate or methyl acetate) at T = (293.15, 298.15, and 303.15) K. The binary excess molar volumes are both negative and positive.

Nakanishi *et al.* (1970) determined binary excess volumes at T = 298.15 K for (methanol or ethanol + nitromethane). The excess volumes are both positive and negative.

Cerdeirina *et al.* (1999) reported densities and heat capacities of binary mixtures containing (nitromethane + 1-propanol or 2-propanol) at T = (288.15, 293.15, 298.15, and 308.15) K and atmospheric pressure, over the whole composition range. The binary excess molar volumes were positive.

Sibiya and Deenadayalu (2008) evaluated densities for the binary systems ($[MOA]^+[Tf_2N]^-$ + methanol, or ethanol, or 1-propanol) at T = (298.15, 303.15, and 313.15) K. The speed of sound at T = 298.15 K for the same binary systems was also measured. The excess molar volumes and the isentropic compressibilities for the above systems were then calculated from the experimental densities and the speed of sound, respectively. The binary excess molar volumes were both negative and positive.

Deenadayalu and Bahadur (2010) reported experimental densities, and excess molar volume for the binary systems ($[MOA]^+[Tf_2N]^-$ + methyl acetate or ethyl acetate) at T = (298.15, 303.15, 313.15) K. The excess molar volume is negative over the entire composition range for both binary systems.

Sibiya and Deenadayalu (2009) reported excess molar volumes from density measurements over the entire composition range for binary systems of ($[BMIM]^+[MeSO_4]^-$ + methanol or

ethanol or 1-propanol) at T = (298.15, 303.15 and 313.15) K. Partial molar volumes were determined from the Redlich-Kister coefficients. For all the systems studied, the excess molar volumes were negative over the entire composition range at all temperatures.

Iglesias-Otero *et al*. (2008) reported correlations between volumetric properties and refractive indices of binary mixtures of room temperature ionic liquids (RTILs) + ethanol or nitromethane or 1,3-dicloropropane or diethylene glycol monoethyl ether or ethyleneglycol. The density and refractive index for a set of these systems were measured at atmospheric pressure at T = 298.15 K throughout the composition range. This data was used to calculate excess volumes and refractive index deviations by using expressions firmly based on the physical significance of each quantity that allowed for the expected relations between the two quantities to be confirmed. Based on these results, the molar refraction and free or void volume of the mixtures were calculated with a view to estimating the relative contribution of both quantities to the excess molar volume. Once molar refraction was confirmed to exhibit a near-ideal behaviour in all mixtures, a method for predicting the density and refractive index of ($[BMIM]^+[MeSO_4]^-$ or $[BMIM]^+[[BF_4]^-$ + ethanol or nitromethane or 1,3-dicloropropane or diethylene glycol monoethyl ether or ethyleneglycol) mixtures was developed; the results show that this procedure can be a highly useful alternative to the usually complex experimental methods available for the thermophysical characterization of these systems. The binary excess molar volume were negative.

Binary excess molar volumes for the same cation or anion or an alcohol or nitromethane (used in this work) from the literature is given in Table 2.2.

Table 2.2 Binary systems with common cation or anion or an alcohol or nitromethane (used in this work) from literature is given below

Author	Systems	V_m^E/cm^3·mol^{-1}
Seddon *et al.* (2000)	([BMIM]$^+$[BF_4]$^-$ + water)	positive
Heintz *et al.* (2002)	([BMPy]$^+$[BF_4]$^-$ + methanol)	negative
Wang *et al.* (2003)	([BMIM]$^+$[BF_4]$^-$ + acetonitrile or dichloromethane or 2-butanone or N, N-dimethylformamide)	negative
Rebelo *et al.* (2004)	([BMIM]$^+$[BF_4]$^-$ + water)	positive
Domańska *et al.* (2006)	([MMIM]$^+$[$MeSO_4$]$^-$ + methanol, ethanol or 1-butanol or water), ([BMIM]$^+$[$MeSO_4$]$^-$ + methanol or ethanol or 1-butanol or 1-hexanol or 1-octanol or 1-decanol or water) and ([BMIM]$^+$[$OcSO_4$]$^-$ + methanol or 1-butanol or 1-hexanol or 1-octanol or 1-decanol)	positive and negative
Pereiro and Rodriguez (2007)	(ethanol + [MMIM]$^+$[$MeSO_4$]$^-$or [BMIM]$^+$[$MeSO_4$]$^-$ or [BMIM]$^+$[PF_6]$^-$ or [HMIM]$^+$[PF_6]$^-$ or [MOIM]$^+$[PF_6]$^-$)	negative
Bhujrajh and Deenadayalu (2007)	([EMIM]$^+$[$CH_3(OCH_2CH_2)_2OSO_3$]$^-$ or [BMIM]$^+$[$CH_3(OCH_2CH_2)_2OSO_3$]$^-$ or 1-[MOIM]$^+$[$CH_3(OCH_2CH_2)_2OSO_3$]$^-$ + methanol) and ([EMIM]$^+$[$CH_3(OCH_2CH_2)_2OSO_3$]$^-$ + water)	negative
Zhong and Wang (2007)	([BMIM]$^+$ [PF_6]$^-$ + aromatic benzyl alcohol or benzaldehyde)	negative
González *et al.* (2007)	([BPYr]$^+$[BF_4]$^-$ + water or ethanol or nitromethane)	positive and negative
Ming-Lan Ge *et al.* (2008)	(H_2O + [BMIM]$^+$[CF_3SO_3]$^-$)	positive
Hofman *et al.* (2008)	([EMIM]$^+$[$EtSO_4$]$^-$ + methanol)	negative
Deenadayalu *et al.* (2009)	([EMIM]$^+$[$EtSO_4$]$^-$ + methanol or 1- propanol or 2-propanol)	negative
Feng *et al.* (2009)	([BMIM]$^+$[BF_4]$^-$ or [BMIM]$^+$[PF_6]$^-$ +*N*-methyl-2-pyrrolidinone)	

Seddon *et al.* (2000) published the excess molar volumes data for the binary system ($[BMIM]^+[BF_4]^-$ + water) at T = (313.15 and 353.15) K. The excess molar volumes are large and positive and increase with an increase in temperature.

Heintz *et al.* (2002) reported densities and viscosities for the system ($[BMPy]^+[BF_4]^-$ + methanol) at T = (298.15, 313.15 and 323.15) K and ambient pressure. V_m^E were negative.

Wang *et al.* (2003) utilized the Redlich-Kister equation with four parameters for the description of V_m^E data for ($[BMIM]^+[BF_4]^-$ + acetonitrile or dichloromethane or 2-butanone or N, N-dimethylformamide) at T = 298.15 K. The excess molar volumes are negative.

Rebelo *et al.* (2004) conducted an extensive thermodynamic analysis of the ($[BMIM]^+[BF_4]^-$ + water) for T = (278.15 – 333.15) K which included determination of V_m^E, H_m^E and C_p^m. The excess molar volumes are positive.

Domańska *et al.* (2006) determined the solubility of ($[BMIM]^+[OcSO_4]^-$ + n-hexane or n-heptane or n-octane or n-decane) and ($[BMIM]^+[OcSO_4]^-$ + methanol or 1-butanol or 1-hexanol or 1-octanol or 1-decanol) solutions. Densities and excess molar volumes were determined for ($[MMIM]^+[MeSO_4]^-$ + methanol, ethanol or 1-butanol or water), for ($[BMIM]^+[MeSO_4]^-$ + methanol or ethanol or 1-butanol or 1-hexanol or 1-octanol or 1-decanol or water) and for ($[BMIM]^+[OcSO_4]^-$ + methanol or 1-butanol or 1-hexanol or 1-octanol or 1-decanol) at T = 298.15 K and atmospheric pressure. The systems exhibit very negative or positive molar excess volumes.

Pereiro and Rodriguez (2007a) determined experimental densities, speed of sound and refractive indices of the binary mixtures of ($[MMIM]^+[MeSO_4]^-$or $[BMIM]^+[MeSO_4]^-$ or $[BMIM]^+[PF_6]^-$ or $[HMIM]^+[PF_6]^-$ or $[MOIM]^+[PF_6]^-$ + ethanol) at T = (293.15 to 303.15) K. The excess molar volume, change in refractive index on mixing and deviation in isentropic compressibility for the above systems were calculated. Pereiro's results showed that the excess molar volumes and deviations in isentropic compressibilities decrease when the temperature in increased for the systems studied. The excess molar volumes are negative.

Bhujrajh and Deenadayalu (2007) reported V_m^E for ($[EMIM]^+[CH_3(OCH_2CH_2)_2OSO_3]^-$ or $[BMIM]^+[CH_3(OCH_2CH_2)_2OSO_3]^-$ or 1- $[MOIM]^+[CH_3(OCH_2CH_2)_2OSO_3]^-$ + methanol) and ($[EMIM]^+[CH_3(OCH_2CH_2)_2OSO_3]^-$ + water) at T = (298.15, 303.15 and 313.15) K. The V_m^E values were found to be negative for all systems.

Zhong and Wang (2007) determined the density of the two binary mixtures formed by ($[BMIM]^+[PF_6]^-$ + aromatic benzyl alcohol or benzaldehyde) over the entire composition and the temperature range (293.15 to 303.15) K and at atmospheric pressure. Zhong's results showed that, V_m^E , decreases slightly when temperature increases. The excess molar volumes are negative.

González *et al.* (2007) measured density and isobaric molar heat capacity for the binary systems containing ionic liquid ($[BPyr]^+[BF_4]^-$ + water or ethanol or nitromethane) at T = (293.15 to 318.15) K and at atmospheric pressure. For the system ($[BPyr]^+[BF_4]^-$ + water),

the excess molar volume is positive, and for the systems ($[BPyr]^+[BF_4]^-$ + ethanol) and ($[BPyr]^+[BF_4]^-$ + nitromethane) are negative.

Golden et al. (2007) studies the density of pure anion $[MMIM]^+[MeSO4]^-$ and its ($[MMIM]^+[MeSO4]^-$ + methanol) at T = (313.15 to 333.15) K and pressure range from (0.1 to 25) MPa using a vibrating tube densimeter. The isothermal compressibilities, isobaric expansivities, and excess volumes were also calculated. The excess molar volumes are negative for all temperature.

Ming-Lan Ge *et al.* (2008) measured densities and viscosities for the binary mixtures of (H_2O + $[BMIM]^+[CF_3SO_3]^-$) were measured over the entire mole fraction range from (303.15 to 343.15) K at atmospheric pressure. The values of excess molar volume were positive for (H_2O + $[BMIM]^+[CF_3SO_3]^-$) mixtures at all temperatures and over the entire range of compositions.

Hofman *et al.* (2008) measured the densities of ($[EMIM]^+[EtSO_4]^-$ + methanol) over the temperature range (283.15 to 333.15) K and pressure range (01-35) MPa. The excess molar volumes were negative at all measured temperatures and pressures over the whole concentration range.

Deenadayalu *et al.* (2009) measured densities for the binary system ($[EMIM]^+[EtSO_4]^-$ + methanol or 1- propanol or 2-propanol) at T = (298.15, 303.15 and 313.15) K. Partial molar volumes were determined from the Redlich-Kister coefficients. The excess molar volumes were negative over the entire composition range for each system at all temperatures. The

excess molar volumes were correlated with the pentic four parameter virial (PFV) equation of state (EoS) model.

Feng *et al.* (2009) evaluated the densities of two binary mixtures formed by ($[BMIM]^+[BF_4]^-$ or $[BMIM]^+[PF_6]^-$ +*N*-methyl-2-pyrrolidinone) have been determined over the full range of composition and range of temperature from T = (298.15 to 313.15) K and at atmospheric pressure. Partial molar volumes, apparent molar volume and partial molar volumes at infinite dilution were calculated from experimental results. Results show that excess molar volume decrease slightly when temperature increases in the system. The results have been used to test the applicability of the Prigogine-Flory-Patterson (PFP) theory.

A literature summary of ternary excess molar volumes is given in Table 2.3.

Table 2.3 V_{123}^{E} from literature for ternary systems for all the same temperature

Author	Systems
Bhujrajh and Deenadayalu 2007	{$[EMIM]^+[CH_3(OCH_2CH_2)_2OSO_3]^-$ (x_1) + methanol (x_2) + water (x_3)}
Bhujrajh and Deenadayalu 2008	{$[EMIM]^+[BETI]^-$ (x_1) + methanol (x_2) + acetone (x_3)}
Gomez *et al.* 2008	{ethanol (x_1) + water (x_2) + $[MMIM]^+[MeSO_4]^-$ (x_3)}
Gonzalez *et al.* 2008 (a)	{ethanol (x_1) + water (x_2) + $[BMIM]^+[MeSO_4]^-$ (x_3)}
Gonzalez *et al.* 2008 (b)	{1-propanol (x_1) + water (x_2) + $[EMIM]^+[EtSO_4]^-$ (x_3)}
Andreatta *et al.* 2009	{methyl acetate (x_1) + methanol (x_2) + $[C_8MIM]^+[Tf_2N]^-$ (x_3)}
Andreatta *et al.* 2010	{ethyl acetate (x_1) + ethanol (x_2) + $[BMIM]^+[Tf_2N]^-$ (x_3)}
Deenadayalu and Bahadur 2010 (a) (this work)	{$[MOA]^+[Tf_2N]^-$ (x_1) + ethanol (x_2) + methyl acetate or ethyl acetate (x_3)}
Deenadayalu and Bahadur 2010 (b) (this work)	{$[MOA]^+[Tf_2N]^-$ (x_1) + methanol (x_2) + methyl acetate or ethyl acetate (x_3)}

Bhujrajh and Deenadayalu (2007) calculated V_m^E from density measurement over the entire composition range for the ternary systems of ($[EMIM]^+[CH_3(OCH_2CH_2)_2OSO_3]^-$ + methanol + water) at T = (298.15 to 313.15) K. The results show the V_m^E values were found to be negative at T = (298.15 and 303.15) K and become positive at T = 313.15 K at higher mole fraction of ionic liquid and at a corresponding decrease in mole fraction of water.

Bhujrajh and Deenadayalu (2008) evaluated the densities of binary and ternary system ($[EMIM]^-$ $[BETI]^-$ + methanol or acetone) and the ternary system($[EMIM]^-$ $[BETI]^-$ + methanol + acetone) respectively at T = (298.15, 303.15 and 313.15) K and the speed of sound data for the binary systems ($[EMIM][CH_3]^+[(OCH_2CH_2)_2OSO_3]^-$ + methanol) at T = 298.15 K. The results show excess molar volumes for the binary system ($[EMIM]^-$ $[BETI]^-$ + methanol) were positive for low mole fraction of methanol, and for the binary system ($[EMIM]^-$ $[BETI]^-$ + acetone) , V_m^E was negative throughout the whole composition range. The ternary excess molar volumes were also negative for all temperatures. The isentropic compressibility for the binary system ($[EMIM][CH_3]^+[(OCH_2CH_2)_2OSO_3]^-$ + methanol) was negative over the entire composition range.

González *et al.* (2008) reported experimental densities, dynamic viscosities, and refractive indices and their derived properties for the ternary system ($[BMIM]^+[MeSO_4]^-$ + ethanol + water) at T = 298.15 K and of its binary systems ($[BMIM]^+[MeSO_4]^-$ ethanol or water) at T = (298.15, 313.15, 328.15) K. These physical properties have been measured over the whole composition range and at 0.1 MPa. The excess molar volume is negative over the entire composition range for both binary and ternary systems. For the ternary systems Cibulka, Singh et al., and Nagata and Sakura equations were used for the correlation.

González *et al.* (2008) determined densities, refractive indices, and dynamic viscosities, of two ternary mixtures, (1-propanol + water + $[EMIM]^+[EtSO_4]^-$) and (2-propanol + water + $[EMIM]^+[EtSO_4]^-$) at 298.15 K over the whole composition range and at atmospheric pressure. Excess molar volumes, refractive index deviations, viscosity deviations, and excess free energies of activation of viscous flow. For the ternary systems Cibulka, Singh et al., and Nagata and Sakura equations were used for the correlation. The excess properties have been used to test several prediction models. The excess molar volumes show negative deviations over the whole range of compositions. The ternary systems, the excess molar volumes are negative for both systems.

Gomez *et al.* (2008) reported experimental densities, dynamic viscosities, and refractive indices of the ternary system (ethanol + water + $[MMIM]^+[MeSO_4]^-$) at $T = 298.15$ K and of its binary systems ($[MMIM]^+[MeSO_4]^-$ + ethanol or water) at several temperatures $T =$ (298.15, 313.15, 328.15) K. Excess molar volumes, viscosity deviations, refractive index deviations and excess free energy of activation for were calculated. Cibulka, Singh et al., and Nagata and Sakura equations were fitted to the ternary data. The ternary excess properties were predicted from binary contributions using geometrical solution models. The excess molar volumes are negative over the entire composition range for both binary and ternary systems.

Andreatta *et al.* (2009) reported experimental densities, dynamic viscosities, and refractive indices of the ternary system (methyl acetate + methanol + $[C_8MIM]^+[Tf_2N]^-$) and its binary mixtures at $T = 298.15$ K. Excess molar volumes as well as molar refraction and viscosity

changes of mixing were calculated. The excess molar volumes were negative over the entire range of composition for both binary and ternary system.

Andreatta *et al.* (2010) reported experimental densities, dynamic viscosities, and refractive indices of the ternary system (ethyl acetate + ethanol + $[BMIM]^+[Tf_2N]^-$) and its binary mixtures at $T = 298.15$ K. Excess molar volumes as well as molar refraction and viscosity changes of mixing were calculated. The excess molar volumes were negative over the entire range of composition for both binary and ternary system.

Deenadayalu and Bahadur (2010) reported experimental densities, and excess molar volume for the ternary systems ($[MOA]^+[Tf_2N]^-$ + methanol + methyl acetate or ethyl acetate) at $T =$ (298.15, 303.15, 313.15) K. The excess molar volume is negative over the entire composition range for both ternary systems. For the ternary system, the Cibulka equation was used for the correlation.

Deenadayalu and Bahadur (2010) reported experimental densities, and excess molar volume for the ternary systems ($[MOA]^+[Tf_2N]^-$ + ethanol + methyl acetate or ethyl acetate) at $T =$ (298.15, 303.15, 313.15) K. The excess molar volume is negative over the entire composition range for both ternary systems. For the ternary system, the Cibulka equation was used for the correlation.

(B) APPARENT MOLAR PROPERTIES

Zafarani- Moatter and Shekaari (2005a) measured the density and sound velocity of the binary mixtures (BMIMBr + water or methanol) at T = (298.15 to 318.15) K and atmospheric pressure. Apparent molar volume and the apparent molar isentropic compressibility values were evaluated from the experimental density and sound velocity data and a Redlich + Mayer type equation was fitted to the data. The apparent molar volume and apparent molar isentropic compressibility at the infinite dilution were also calculated at each temperature. The obtained limiting apparent molar volume values and the limiting slope of the apparent molar volume *versus* molality$^{1/2}$ indicated that (BMIMBr + water) interactions are stronger than the (BMIMBr + methanol) solutions.

Yang *et al.* (2005a) measured the densities of ($[EMIM]^+[EtSO_4]^-$ + water) at T = (278.2 to 338.2) K. Apparent molar volume were treated by Pitzer-Simomson and Clegg-Pitzer theories. The values of Pitzer-Simomson parameters and Cless-Pitzer parameters were obtained by fitting the experimental data.

Zafarani-Moattar and Shekaari (2005b) reported the density, excess molar volume, and speed of sound data for ($[BMIM]^+[PF_6]^-$ + methanol) and ($[BMIM]^+[PF_6]^-$ + acetonitrile) binary mixtures over the entire range of composition for T = (298.15 to 318.15) K. The V_m^E for acetonitrile mixtures are more negative than methanol mixtures. Isentropic compressibility deviation values ($\Delta\kappa_s$) in methanol mixtures are more than acetonitrile mixtures.

Yang *et al.* (2005b) measured the densities of ($[EMIM]^+[EtSO_4]^-$ + water) at T = (278.15 to 333.15) K. The apparent and partial molar volumes and apparent molar expansibilities and the

coefficient of thermal expansibility of the binary solution were calculated. The values of the apparent molar volume, ΦV_B, were fitted by the method of least-squares to a Pitzer's equation to determine the parameters.

Calvar *et al.* (2006) measured densities, refractive indices, speed of sound and isentropic compressibilities of the ternary mixture (ethanol + water + $[BMIM]^+[Cl]^-$), and of the binary subsystems containing the $[BMIM]^+[Cl]^-$ at T = 298.15 K and atmospheric pressure. From the densities the apparent molar volume of the binary systems were calculated.

Zafarani-Moattar and Shekaari (2006) reported density and speed of sound of the systems containing the ionic liquid $[BMIM]^+[PF_6]^-$ and methanol and acetonitrile having a wide range of dielectric constants. For the systems investigated, the apparent molar volumes and apparent molar isentropic compressibilities were determined and fitted to the Redlich–Mayer and the Pitzer equations from which the corresponding limiting values were obtained. Furthermore, using the ionic limiting apparent volume values for $[TBA]^+$ from the literature and limiting apparent molar volume for the ionic liquid and $[TBA][PF_6]$ obtained in the work, the ionic limiting apparent molar volume values for the cation $[BMIM]^+$ in different organic solvents was also estimated. The excess molar volumes are negative.

Gomez *et al.* (2006) measured dynamic viscosities, densities, and refractive indices from T = (298.15 K to 343.15) K for $[C_6MIM]^+[Cl]^-$, and $[C_8MIM]^+[Cl]^-$. Dynamic viscosities and densities have been determined over the whole composition range for (water + $[C_6MIM]^+[Cl]^-$) and (water + $[C_8MIM]^+[Cl]^-$) at T = (298.15, 313.15, 328.15, and 343.15) K and 0.1 MPa of pressure. Densities and viscosities of (water + $[BMIM]^+[Cl]^-$), at T =

(298.15, 313.15, 328.15, and 343.15) K and 0.1 MPa of were measured, and the apparent molar volumes were calculated. The excess molar volumes are both negative and positive for all the systems.

Gomez *et al.* (2006) reported densities, speed of sound and refractive indices from T = (288.15 to 343.15) K (ethanol or water + EMISE). Densities, dynamic viscosities, speed of sound, and isentropic compressibilities were determined over the whole composition range for (ethanol + EMISE) and (water + EMISE) binary systems at T = (298.15, 313.15 and 328.15) K and atmospheric pressure. The excess molar volumes are negative over the whole composition range for the (ethanol + EMISE) system and negative for the binary (water + EMISE) system except for large concentrations of water at T = 298.15 and 313.15 K.

Pereiro and Rodriguez (2007b) measured the experimental densities, speed of sound and refractive indices of binary mixtures ($[MMIM]^+[MeSO_4]^-$, $[BMIM]^+[MeSO_4]^-$, $[HMIM]^+[PF_6]^-$ and $[OMIM]^+[PF_6]^-$ + ethanol) from T = (293.15 to 303.15) K. Excess molar volumes, changes of refractive index on mixing and deviation in isentropic compressibility for the above systems were calculated. The excess molar volumes are negative over the entire composition range for all the binary mixtures except for the system ($[HMIM]^+[PF_6]^-$ + 2-propanol). For the deviations in isentropic compressibility negative values are observed over the entire composition range. In general terms, the excess molar volumes and the deviations properties increase when the temperature is increased.

Widegren and Magee (2007) measured the physical properties of ($[C_6MIM]^+[Tf_2N]^-$ + water). Densities for the temperature range (258.15 to 373.15) K was obtained. Dynamic viscosity for

T = (258.15 to 373.15) K, kinetic viscosity for T = (293.15 to 298.15) K and speed of sound through the mixture for T = (283.15 to 343.15) K.

González *et al*. (2007) measured dynamic viscosities, densities, and speeds of sound of ($[EMIM]^+[EtSO_4]^-$ + methanol, 1-propanol, and 2-propanol) at T = (298.15, 313.15, and 328.15) K and refractive indices at T = 298.15 K and at atmospheric pressure over the whole composition range. Excess molar volumes, excess molar isentropic compressions, and viscosity deviations for the binary systems from T = (298.15 to 328.15) K and refractive deviations at T = 298.15 K was calculated. The excess molar volumes were negative, and decreased as the temperature increased for all binary systems.

Abdulagatov *et al.* (2008) measured densities of ($BMIMBF_4$ + ethanol) binary mixtures. Measurements were performed at T = (298.15 to 398.15) K and at pressures up to 40 MPa. The measured densities were used to study derived volumetric properties such as excess, apparent, and partial molar volumes. It was shown that the values of excess molar volume for ($BMIMBF_4$ + ethanol) mixtures are negative at all measured temperatures and pressures over the whole concentration range. The volumetric (excess, apparent, and partial molar volumes) and structural (direct and total correlation integrals, cluster size) properties of dilute ($BMIMBF_4$ + ethanol) mixtures were studied in terms of the Krichevskii parameter. The Tait-type equation of state were fitted to measured densities.

Singh and Kumar (2008) measured the densities and refractive indices for binary mixtures of ($[MOIM]^+[BF_4]^-$ + ethylene glycol monomethyl ether or diethylene glycol monomethyl ether

or triethylene glycol monomethyl ether). The experimental densities were used to estimate excess molar volumes, apparent molar volumes, partial molar volumes, excess partial molar volumes and their limiting values at infinite dilution. Excess molar volumes are negative over the whole composition range except for the mixtures with a high mole fraction of ionic liquid in ethylene glycol monomethyl ether. The values of excess molar volumes in these mixtures become more negative with the introduction of $–OC_2H_4–$ group in the alkoxyethanol molecule.

Gardas *et al.* (2008) reported density at different temperatures ranging from $T =$ (293.15 to 313.15) K, speed of sound and osmotic coefficients at $T =$ 298.15 K for ($[EMIM]^+[Br]^-$ + water) and osmotic coefficients at $T = 298.15$ K for ($[BMIM]^+[Cl]^-$ + water) in the dilute concentration region. The data were used to obtain compressibilities, expansivity, apparent and limiting molar properties, internal pressure, activity, and activity coefficients for ($[EMIM]^+[Br]^-$ + water).

Wang *et al.* (2009) measured densities for binary mixture ($[C_nMIM]$ Br (n) 8, 10, 12 + ethylene glycol, or *N*, *N*-dimethylformamide, or dimethylsulfoxide) at $T = 298.15$ K. The apparent molar volumes, standard partial molar volumes were derived from the experimental data.

Wu *et al.* (2009) measured densities, for ($[BMIM]^+[BF_4]^-$ + sucrose-water) solutions at $T =$ 298.15 K. The measured densities were used to calculate the apparent molar volumes of

sucrose and $[BMIM]^+[BF_4]^-$ in the studied solutions. Infinite dilution apparent molar volumes have been evaluated.

Sadeghi *et al.* (2009) measured effect of alkyl chain length of ([RMIM][Br], R = propyl (C_3), hexyl (C_6), heptyl (C_7), and octyl (C_8) + water or methanol). The density and speed of sound at different temperatures ranging from T = (288.15 to 308.15) K were obtained. The values of the compressibilities, expansivity and apparent molar properties for ($[C_nMIM][Br]$ + water or methanol) were determined. The Redlich–Mayer and the Pitzer's equations were fitted to the apparent molar volumes and apparent molar isentropic compressibilities from which the corresponding infinite dilution molar properties were obtained.

Haiyan *et al*. (2009) measured the densities of the binary mixtures formed by ($[BMIM][BF_4]$ + benzaldehyde) at the temperature range T = (298.15 to 313.15) K and at atmospheric pressure. Partial molar volumes, apparent molar volumes, and partial molar volumes at infinite dilution were calculated for each binary system. The excess molar volume values are all negative and decreases slightly when temperature increases in the systems studied.

There are no apparent molar volume or apparent molar isentropic compressibility data in the literature for the $[MOA]^+[Tf_2N]^-$ ionic liquid.

CHAPTER 3
IONIC LIQUIDS

3.1 PROPERTIES OF IONIC LIQUIDS

ILs are composed of organic cations and various anions. As numerous combinations of cations and anions are possible, they are considered as "designer solvents" since the IL can be optimized for its physical properties for a specific application (Plechkova and Seddon 2008; Rogers *et al.* 2002; Wu and Marsh 2003; Carmichael and Seddon 2000)**.**

ILs have widely tunable properties with regard to polarity, hydrophobicity and solvent miscibility through the appropriate selection of the anion and cation. They are important because of their unique physical properties, such as low melting point, high thermal stability, non-flammability, no measurable vapour pressure (Welton 1999; Rebelo *et al.* 2005) and good dissolution properties (Baranyai *et al.* 2004) for most organic and inorganic compounds (Welton 1999; Sheldon 2001; Yang *et al.* 2005 b) and a very rich and complex behaviour as solvents which can be modified by changing the nature of the cation or anion (Scurto *at al.* 2004; Gutowki *et al.* 2003; Lachwa *et al.* 2005; Lachwa *et al.* 2006). ILs have high stability to air and moisture, and a wide electrochemical window. The ILs that are moisture and air stable (e.g. with $[Tf_2N]^-$ anion) at room temperature have potential uses for new chemical processes and technologies (Domanska and Pobudkowska 2006; Lozano and De Diego 2004).

Some ILs are highly hydroscopic and small quantities of water or other compounds in the IL causes considerable change in the physical properties (Seddon *et al.* 2000; Calvar *et al.* 2006; González *et al.* 2006).

ILs are different from typical salts such as alkali halides that have very high melting points due to extremely strong Coulombic forces. Their low melting points and unique properties can be tailored to specific processes.

The growing importance of ILs is manifested by the rapidly increasing rate at which papers on the topic are being published. Besides, the fact that many of the initial discoveries have been patented rather than released in the open literature is a measure of their industrial potential. Ionic liquids are salts that are liquid at low temperature - many at room temperature or below - and in a molten form are composed wholly of ions (Davis *et al.* 2003). The adopted upper temperature limit for the classification of IL as room temperature ionic liquid ≤ 100 °C (Visser *et al*. 2002). These low melting points are a result of the chemical composition of RTILs, which contain larger asymmetric organic cations. The asymmetry lowers the lattice energy, and hence the melting point, of the resulting ionic medium. In some cases, even the anions are relatively large and play a role in lowering the melting point (Yang *et al.* 2004). ILs are either organic salts or mixtures consisting of at least one organic component. The term "ionic liquid" includes all classical molten salts, which are composed of more thermally stable ions, such as sodium with chloride or potassium with nitrate; the term dates back as early as 1943 (Barrer, 1943).

3.2 PHYSICAL PROPERTIES OF IONIC LIQUIDS

The physical properties of IL are given below in Figure 3.1

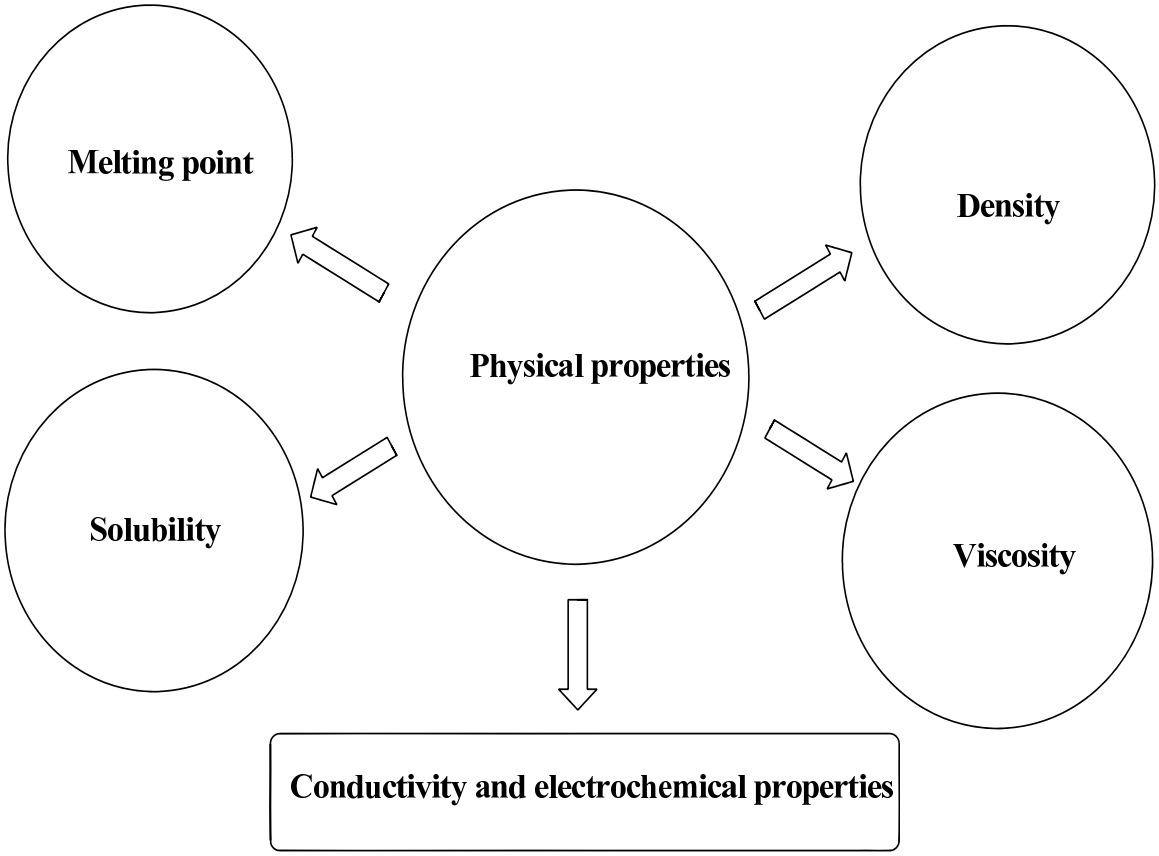

Figure 3.1 Map of physical properties of ionic liquids

3.2.1 Melting point

- The melting point of room temperature ionic liquid is 0-100 ^{o}C.
- The more corban atoms in alkyl side chain, the lower the melting point.
- The greater the anion size, the lower the melting point

3.2.2 Density

- The density of room temperature ionic liquid is generally 1.1 to 1.69 g.cm^{-3}

3.2.3 Viscosity

- The major impact of these compounds' viscosity is attributed for the hydrogen bonds and van der Waals force at room temperature.

3.2.4 Solubility

- The solubility of a phosphonium-based ionic liquid in dense CO_2 is in sharp contrast to the solubility behavior of imidazolium-based ionic liquids. This finding could prove to be quite important for designing a single-phased ionic liquid–CO_2 solvent system (James W. 2005).

The solubility of different species in imidazolium ionic liquids depends mainly on polarity and hydrogen bonding ability. Saturated aliphatic compounds are generally only sparingly soluble in ionic liquids, whereas olefins show somewhat greater solubility, and aldehydes can be completely miscible. This can be exploited in biphasic catalysis, such as hydrogenation and hydrocarbonylation processes, allowing for relatively easy separation of products and/or unreacted substrate(s). Gas solubility follows the same trend, with carbon dioxide gas

showing exceptional solubility in many ionic liquids, carbon monoxide being less soluble in ionic liquids than in many popular organic solvents, and hydrogen being only slightly soluble (similar to the solubility in water) and may vary relatively little between the more commonly used ionic liquids.

RTILs possess a unique array of physico-chemical properties that make them suitable in numerous task-specific applications in which conventional solvents are non-applicable or insufficientlyeffective.

Such properties include:

- high thermal stability,
- high electrical conductivity,
- large electrochemical window,
- low nucleophilicity and capability of providing weekly coordinating or non-coordinating environment,
- very good solvent properties for a wide variety of organic, inorganic and organometallic compounds: in some cases, the solubility of certain solutes in RTILs can be several orders of magnitude higher than that in traditional solvents.

3.2.5 Conductivity and electrochemical properties

- Conductivity and the density of the “IL” are affected by molecular weight; viscosity; the size of the ions.
- Preparation of electrochemical cells and solar panels material from RTIL.

3.2.6 Stability

Several studies have indicated that, certain ionic liquids incorporating 1,3-dialkyl imidazolium cations are generally more resistant than traditional solvents under certain harsh process conditions, such as those occurring in oxidation, photolysis and radiation processes (Yang *et al.* 2004).

3.2.7 Color

High quality ionic liquids incorporating the $[BMIM]^+$ cation and a variety of anions, such as $[PF_6]^-$, $[BF_4]^-$, $[CF_3SO_3]^-$, $[CF_3CO_2]^-$ and $[(CF_3SO_2)_2N]^-$ have been reported to be colorless, even though they are not 100% pure. The color of less pure ionic liquids generally ranges from yellowish to orange (Yang *et al.* 2004).

The formation of the color has been attributed to the use of raw materials with color or excessive heating during the synthesis of the imidazolium salt.

A number of precautions for synthesis of colorless ionic liquids have been described, and a procedure for removal of color from impure ionic liquids using acidic alumina and activated charcoal has also been proposed.

3.2.8 Hygroscopicity

The water content has an influence on the density and viscosity of the ionic liquids. Viscosity measurements indicate that ionic liquids became less viscous with increasing water content. Hydrolysis problems can also occur (Yang *et al.* 2004).

3.2.9 Hydrophopicity

The degree of polarity can be varied by adapting the length of the 1-alkyl chain (in 1,3-

substituted imidazolium cations), and the counterion. Long-chain IL salts have attracted some interest due to their liquid-crystalline (LC) properties (Kolle *et al.* 2004).

The anion chemistry has a large influence on the properties of IL. Though little variation in properties might be expected between same-cation salts of these species, the actual differences can be dramatic: for example, $[BMIM]^+[PF_6]^-$ is immiscible with water, whereas $[BMIM]^+[BF_4]^-$ is water-soluble (Davis *et al.* 2003).

ILs are often moderate to poor conductors of electricity, non-ionising (e.g. non-polar), highly viscous and frequently exhibit a low vapour pressure. The miscibility of ionic liquids with water or organic solvents varies with sidechain length on the cation and anion.

3.3 CHEMICAL PROPERTIES

Despite their extremely low vapor pressures, some ionic liquids can be distilled under vacuum conditions at temperatures near 300 °C (Martyn *et al*. 2006). In the original work by (Martyn *et al.* 2006) the authors wrongly assumed the vapour to be made up of individual, separated ions (Wasserscheid 2006), but it was later proven that the vapours formed consisted of ion-pairs (James *et al.* 2007). Some ionic liquids (such as 1-butyl-3-methylimidazolium nitrate) generate flammable gases on thermal decomposition. Thermal stability and melting point depend on the components of the IL.

3.4 STRUCTURE OF IONIC LIQUIDS

Room temperature ionic liquids consist of bulky and asymmetric organic cations such as 1-alkyl-3-methylimidazolium, 1-alkylpyridinium, N-methyl-N-alkylpyrrolidinium and ammonium ions and is given in Figure 3.2. A wide range of anions are employed, from simple halides, which generally inflect high melting points, to inorganic anions such as

tetrafluoroborate and hexafluorophosphate and to large organic anions like bistriflimide, triflate or tosylate.

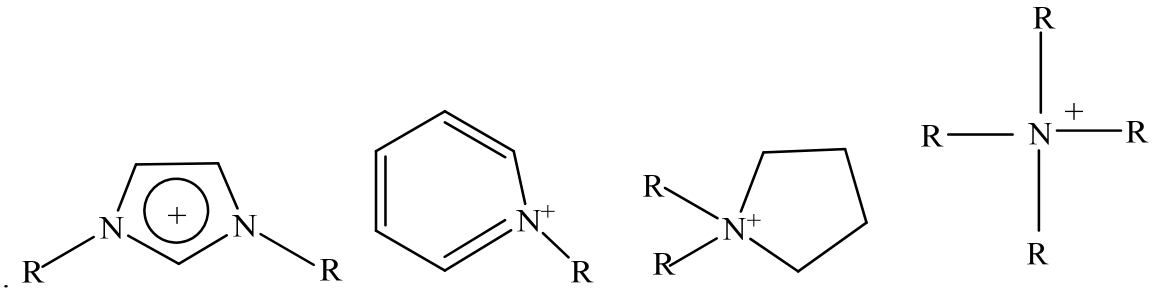

(a) (b) (c) (d)

Figure 3.2 (a) 1-Alkyl-3-methylimidazolium, (b) 1-Alkylpyridinium, (c) N-methyl-N-alkylpyrrolidinium and (d) Ammonium ions

The structures of possible IL cations and anions are presented in Figure 3.3 to 3.16 (Heintz 2005)

Cations **Anions**

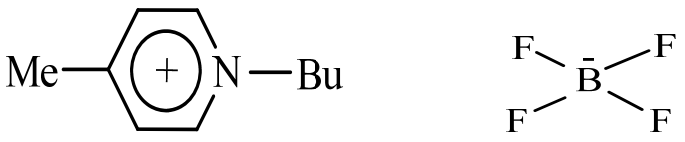

Figure 3.3 4-*n*-Butyl-4-methylpyridinium tetrafluoroborate $[BMDy]^+[BF_4]^-$

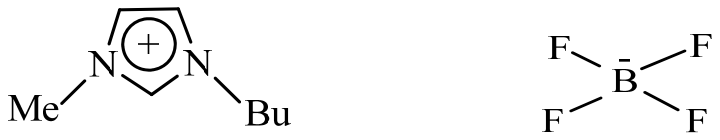

Figure 3.4 1-*n*-Butyl-3-methylimidazolium tetrafluoroborate $[BMIM]^+[BF_4]^-$

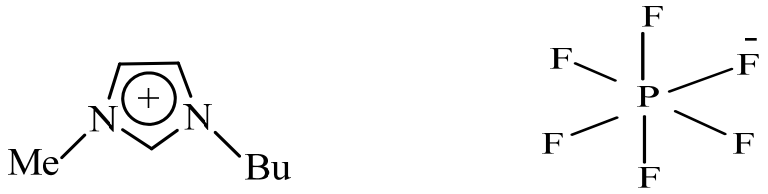

Figure 3.5 1-*n*-Butyl-3-methylimidazolium hexafluorophosphate $[BMIM]^+[PF_6]^-$

Figure 3.6 1-*n*-Butyl-3-methylimidazolium chloride $[BMIM]^+[Cl]^-$

Figure 3.7 1-*n*-Butyl-3-methylimidazolium bromide $[BMIM]^+[Br]^-$

Figure 3.8 1-*n*-Butyl-3-methylimidazolium dicyanamide $[BMIM]^+[DCA]^-$

Figure 3.9 1-*n*-Butyl-3-methylimidazolium trifluoromethanesulfonate $[BMIM]^+[CF_3SO_3]^-$

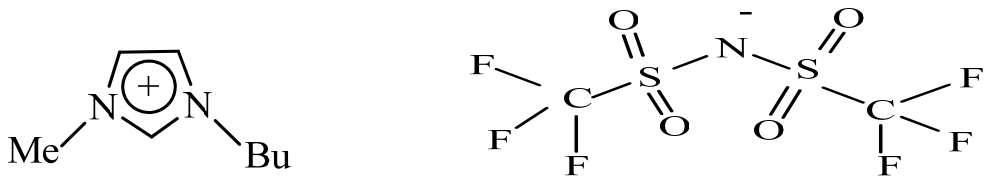

Figure 3.10 1-*n*-Butyl-3-methylimidazolium bis(trifluoromethylsulfonyl)imide $[BMIM]^+[\ Tf_2N]^-$

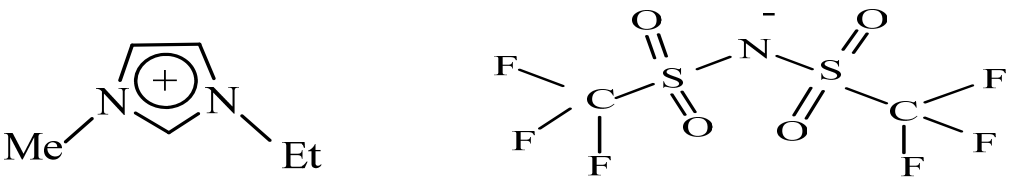

Figure 3.11 1-*n*-Ethyl-3-methylimidazolium bis(trifluoromethylsulfonyl)imide

$[EMIM]^+[\ Tf_2N]^-$

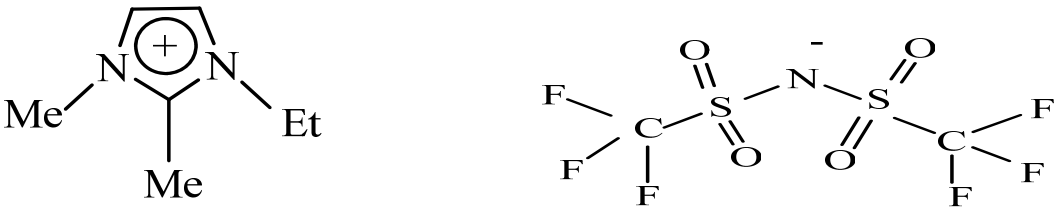

Figure 3.12 1-Ethyl 2, 3-dimethylimidazolium bis(trifluoromethylsulfonyl)imide

$[EMMIM]^+[Tf_2N]^-$

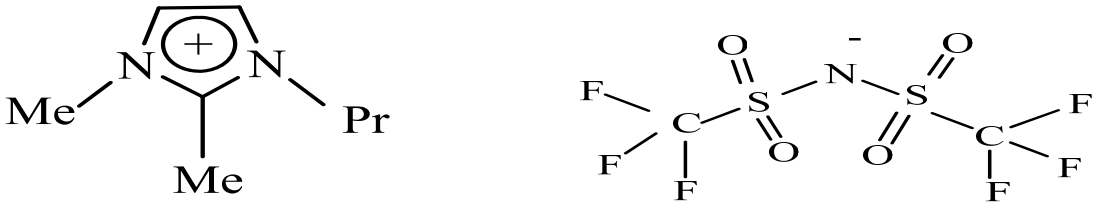

Figure 3.13 2, 3-Dimethyl-1-propylimidazolium bis(trifluoromethylsulfonyl)imide

$[PMMIM]^+[Tf_2N]^-$

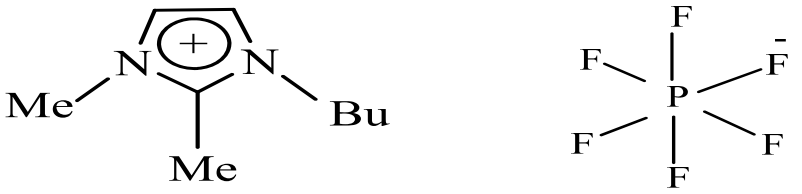

Figure 3.14 1- Butyl-2, 3-dimethyl hexafluorophosphate $[BDMIM]^{+}[PF_6]^{-}$

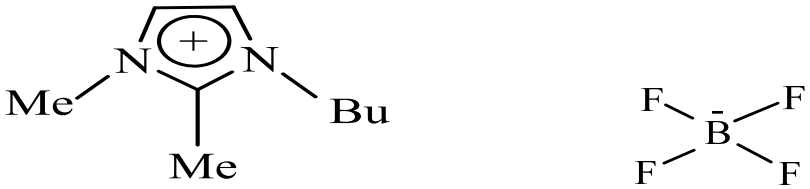

Figure 3.15 1- Butyl-2, 3-dimethyl tetrafluoroborate $[BDMIM]^{+}[BF_4]^{-}$

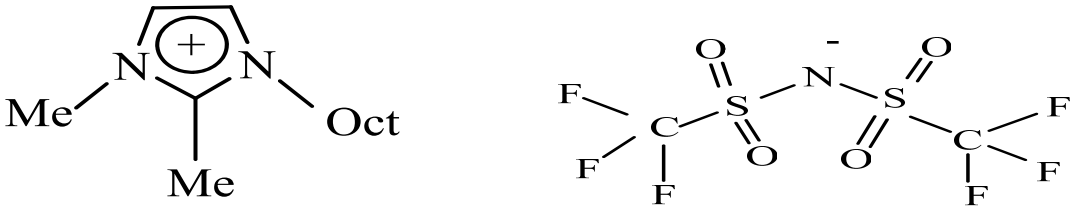

Figure 3.16 1, 2-Dimethyl-3-octylimidazolium bis(trifluoromethylsulfonyl)imide $[MOIM]^{+}[Tf_2N]^{-}$

3.5 ILs AS A REPLACEMENT SOLVENT FOR VOCs

ILs are proving to be increasingly promising as viable media for potential green synthesis and separation processes, as well as, for novel applications, where the unique properties of the IL materials provides new options based upon different chemical and physical properties (Rogers and Seddon 2003).

ILs are being explored as possible environmentally benign solvents (Brennecke and Maginn 2001; Holbrey and Seddon 1999; Seddon *et al.* 2000) because of their negligible vapour pressure (Earle *et al.* 2006; Zaitsau *et al.* 2006; Anthony *et al.* 2001; Dupont *et al.* 2002, Zafarani-Mottar and Shekaari 2006) and as potential replacement solvents for volatile organic compounds (VOCs) (Kaar *et al.* 2003; Poole 2004; Freemantle 1998) currently used in industry (Heintz and Lehman 2003). Implementation of ionic liquids in industry could lead to a reduction in VOC emission and to a more cost-effective use of starting materials because ionic liquids are recyclable (Pereiro and Rodriguez 2006 a; Zafarani-Mottar and Shekaari 2005 a; Domanska and Pobudkowska 2006; Seddon 1997).

VOCs are compounds that impact negatively on the environment. VOCs are released into the environment from indoor activities (example cooking and tobacco smoke) and outdoor activities (example combustion of fuel, emissions from petrochemical and chemical facilities) (Cohen 1996). VOCs are of particular concern since they readily volatilize into the atmosphere and are distributed over large regions leading to a population wide exposure to these chemicals. VOCs are present in liquid and solid processes and waste streams, in consumer products and in fossil fuels. VOCs in the environment present problems that are associated with a) human health problems, b) formation of ozone and c) odor. In most urban regions the concentration of VOCs contributes significantly to the total cancer risk associated with toxic air pollutants. The potential health risk associated with VOCs and their role in the

formation of photochemical smog have led to increasing public concern regarding the presence of VOCs in the environment (Cohen 1996).

One advantage of ILs over VOCs as solvents, for synthetic chemistry, chemical separation and for electrochemistry, is the intrinsic lack of vapour pressure (Rogers and Seddon 2003).

The large liquidus range and favorable solvation behaviour that RTILs possess make them suitable substituents for volatile organic compounds (VOCs). Additionally, they can be used as catalysts (Welton 1999) while combining their power as solvents.

3.6 APPLICATIONS OF IONIC LIQUIDS

ILs have been used in reaction rate enhancement, separations because of higher selectivities, as solvents for higher yields in organic synthesis and in the optimization of compound characteristics through a broad choice of anion and cation combination (Brown *et al.* 1973; Pikkarainen 1982; Chakraborty and Hans-Jörg 2007). ILs can be used as solvents for synthesis, e.g. Diels-Alder cycloaddition reactions (Fischer *et al.* 1999), Friedel-Craft acylation and alkylation, hydrogenation and oxidation reactions and Heck reactions; as biphasic system in combination with an organic solvent or water in extraction and separation technologies; as catalyst immobilizers for the easy recycling of homogeneous catalysts; as electrolytes in electrochemistry (Zhong and Wang 2007).

3.6.1 Energetic application

There are ILs that are able to store large amounts of energy due to the numbers of nitrogen atoms they contain. These nitrogen-rich salts provide several advantages over the current energetic technologies and thus represent potential substitutes. For instance, hydrazine (N_2H_4), the current propellant used in satellite propulsion systems is carcinogenic. One of the advantages of energetic ILs is the high number of nitrogens in cations and anions which

yields high heats of formation and high densities, thereby meeting some of the requirements of good energetic materials. On the other hand, there is low carbon and hydrogen content which is beneficial to oxygen balance. Finally, another feature that makes ILs attractive as potential energetic technologies in industrial and millitary applications is that ILs generates innocuous dinitrogen when they decompose (Singh *et al.* 2006). Examples of energetic ILs are triazolium-, tetrazolium-, urotropinium-, tetrazine- and picrate based salts (Singh *et al.* 2006). RTILs have shown to be ideal propellants for electrospray thrusters because of their high conductivity and immesurable vapor pressure (Chiu *et al.* 2006). NASA has investigated the ionic liquid 1-ethyl-3-methylimidazolium bis(trifluoromethanesulfonyl)imide and approved it through space environmental tests for the NASA's Space Technology 7 - Disturbance Reduction System Mission (ST7-DRS), (Gamero-Castano *et al.* 2003, Ziemer *et al.* 2003).

ILs used in solar cells take the advantage of high ion mobility (Papageorgiou *et al.* 1996).

3.6.2. The Biphasic Acid Scavenging utilising Ionic Liquids (BASIL) process

The first major industrial application of ILs was the BASIL process by BASF, in which

1-methylimidazol was used to scavenge the acid from an existing process. This led to the formation of an IL which was easily removed from the reaction mixture. By the formation of an IL it was possible to increase the space/time yield by a factor of 80,000. (Plechkova and Seddon 2008).

3.6.3 Cellulose Processing

Cellulose is the earth's most widespread natural organic compound and thus highly important as a bio-renewable resource. A more intensive exploitation of cellulose as a bio-renewable feedstock has to date been prevented by the lack of a suitable solvent that can be used in chemical processes (Rogers *et al.* 2003). The addition of ILs to solutions of cellulose can now be produced at technically useful concentrations (Rogers *et al.* 2002). This new technology therefore opens up great potential for cellulose processing.

3.6.4 Dimersol – Difasol

The dimersol process is a traditional way to dimerise short chain alkenes into branched alkenes of higher molecular weight. Nobel laureate Yves Chauvin developed an IL –based process called the Difasol process (Plechkova and Seddon 2008).

3.6.5 Paint additives

ILs can enhance the finish, appearance and drying properties of paints. The company Degussa are marketing ILs under the name of "TEGO Dispers". These products are also added to a pliolite paint range (Plechkova and Seddon 2008).

3.6.6 Air products – ILs as a transport medium for reactive gases

Air products make use of ILs as a medium to transport reactive gases. Reactive gases such as trifluoroborane, phosphine or arsine, are stored in suitable ILs at sub-ambient pressure. This is a significant improvement over pressurized cylinders. The gases are withdrawn from the containers by applying a vacuum (Plechkova and Seddon 2008).

3.6.7 Hydrogen storage

Air Product's Gasguard system relies on the solubility of some gases in ILs. Linde (1996) and his group are exploiting other gases insolubility in ILs. The solubility of hydrogen in ILs is very low. Linde uses the solubility of hydrogen in IL to compress hydrogen in filling stations (Plechkova and Seddon 2008).

3.6.8 Nuclear industry

ILs are extensively explored for various innovative applications in the nuclear industry, including the application of an IL as an extractant/diluent in a solvent extraction system and as an alternative electrolyte media for high temperature pyrochemical processing (Giridhar and Venkatesan 2007).

3.6.9 Separations

ILs have been used for azeotropic (Meindersma *et al.* 2005) and extractive (Jork *et al.* 2005) distillations. Due to having a high thermal stability, ionic liquids could be used as lubricants that are required to work at relatively high temperatures.

ILs are used in various novel micro-extraction techniques (Anderson 2009). In one example, robust absorbent coatings were prepared with polymeric ionic liquids for solid-phase microextraction, e.g. the extraction of esters and fatty acid methyl esters in red and white wines. In another example, hydrophobic ionic liquids were used, via liquid microextraction, to detect organic pollutants (e.g. polyaromatic hydrocarbons) at extremely low (ppb) concentrations in sediment. The partitioning behaviour of various analytes to monocationic and dicationic imidazolium-based micellar aggregates was presented.

Gas separations for CO_2 capture with ILs having amine-functionalised cations or anions was showed that these ionic liquids performed better than traditional aqueous amines

(monoethanolamine, monodiethanolamine, etc.) and that CO_2 solubility in the ionic liquids is higher than that in molecular solvents (Brennecke 2009).

The application map of ILs is given in Figure 3.17

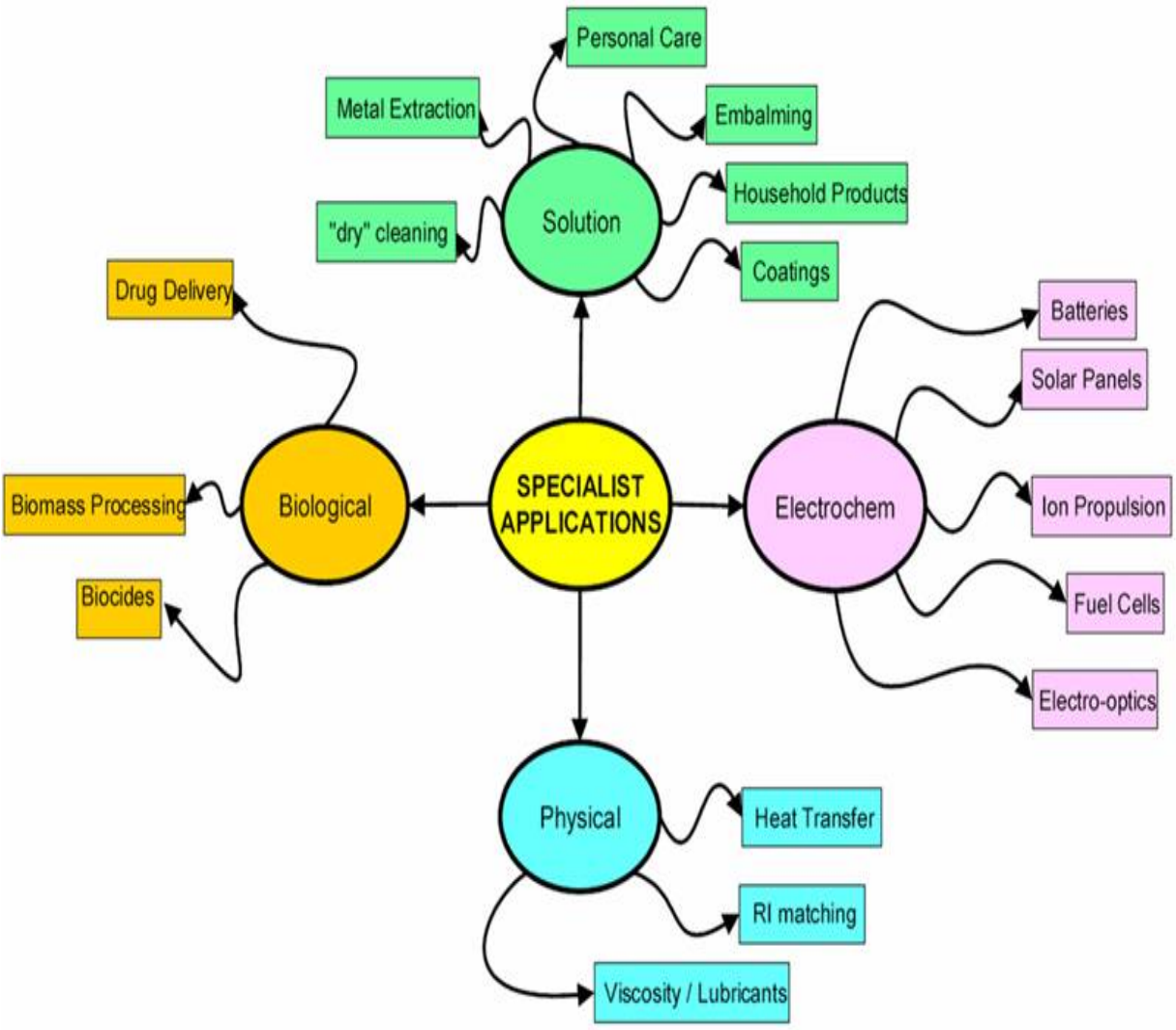

Figure 3.17 Map of the applications of ionic liquids

CHAPTER 4

THEORETICAL FRAMEWORK

(A) TERNARY EXCESS MOLAR VOLUME

Thermophysical and thermodynamic properties of pure liquid and liquid mixtures are of interest to both chemists and chemical engineers. Thermophysical and thermodynamic properties are useful for:

(i) interpretation, correlation and prediction via molecular thermodynamic consideration,

(ii) predicting the properties of mixtures of similar nature,

(iii) the design of industrial equipment with better precision and

(iv) testing current theories of solutions because of their sensitivity to the difference in magnitude of intermolecular forces and geometry of the component molecules.

The excess thermodynamic properties are extensively used to study the deviation of the real liquid mixture from ideality. An ideal solution is defined in terms of two auxiliary functions, the fugacity and the activity. In terms of fugacity, f_{i}, of component *i*, an ideal solution is one in which the fugacity of a component is proportional to its mole fraction over the whole range of composition and a non-zero range of temperature and pressure as expressed by the relation:

$$f_{\mathrm{i}}\,(T, P, x_{\mathrm{i}}) = x_{\mathrm{i}} f_i^0(T, P) \qquad (4.1)$$

where f_i is the fugacity of the component *i* in the solution, f_i^0 is that of the pure component and x_i is the mole fraction.

Alternatively, it is convenient to define an ideal solution in terms of activity of components. Activity, a_i, is equal to its mole fraction over the entire range of composition at all temperatures and pressures.

$$a_i = x_i (0 \leq x_i \leq 1) \tag{4.2}$$

Further, in an ideal solution, chemical potential of the component *i* is given by the relation:

$$\mu_i(T, P, x_i) = \mu_i^0 (T, P) + RT \ln x_i \tag{4.3}$$

where $\mu_i(T, P, x_i)$ denotes the chemical potential of component *i* in solution and $\mu_i^0 (T, P)$ is the chemical potential of pure component *i* at the same temperature and pressure at which the mixture is being studied.

Statistical theory of liquid mixtures gives the following relation for chemical potential

$$\mu_i = RT \ln {Q_i}/{x_i} \tag{4.4}$$

where Q_i denotes the partition function of the component *i*. This relation for chemical potential gives the following expressions for ideal liquid mixtures:

$$G = \sum_{i=1}^{n} n_i \mu_i^0 + RT \sum_{i=1}^{n} n_i \ln x_i \tag{4.5}$$

$$H = \sum_{i=1}^{n} n_i H_i^0 \tag{4.6}$$

$$S = \sum_{i=1}^{n} n_i S_i^0 + R \sum_{i=1}^{n} n_i \ln x_i \tag{4.7}$$

$$V = \sum_{i=1}^{n} n_i V_i^0 \tag{4.8}$$

$$C_p = \sum_{i=1}^{n} n_i (C_p)_i^0 \tag{4.9}$$

where μ_i^0, H_i^0, S_i^0, V_i^0, and $(C_\mathrm{p})_i^0$ are the molar properties of the pure components at the same temperature and pressure as those of the liquid mixture and n_i is the number of moles of the component *i*.

The correction terms which relate the properties of real solutions to those of ideal solutions are called excess functions. An excess thermodynamic fuction (denoted by superscript E) is defined as the difference between the thermodynamic function of mixing of a real mixture and the value corresponding to the ideal solution at the same conditions of temperature, pressure and composition. For an ideal solution all excess functions are zero. The excess volume is given by

$$V^\mathrm{E} = V_\mathrm{real}^\mathrm{M} - V_\mathrm{ideal}^\mathrm{M} \tag{4.10}$$

where V^{E} is excess volume, $V^{\mathrm{M}}_{\mathrm{real}}$ is real volume and $V^{\mathrm{M}}_{\mathrm{ideal}}$ is the ideal volume.

The thermodynamic functions of mixing are useful to understand the behaviour of real solutions. A thermodynamic function of mixing can be given by the expression:

$$Z^{\mathrm{E}} = Z - \sum_{i=1}^{n} x_i Z_i^0 \tag{4.11}$$

where Z^{E} is the thermodynamic function of mixing, Z is the thermodynamic function of the real mixture and Z_i^0 is the value of the property of component *i* in the pure state. Thus the volume of mixing for binary and ternary mixtures are given by,

$$V_{\mathrm{m}}^{\mathrm{E}} = V - (x_1 V_1 + x_2 V_2) \tag{4.12}$$

$$V_{123}^{\mathrm{E}} = V - (x_1 V_1 + x_2 V_2 + x_3 V_3) \tag{4.13}$$

where *V* denotes the molar volume of the mixture, x_1 , x_2, and x_3 are mole fractions of components 1, 2 and 3, respectively. V_1, V_2, and V_3 are molar volumes of the components in the pure state.

Similarly, the free energy of mixing, enthalpy of mixing, and entropy of mixing for ternary mixtures are given by the relations:

$$G^{\mathrm{M}} = RT\ (x_1 \ln x_1 + x_2 \ln x_2 + x_3 \ln x_3) \tag{4.14}$$

$$H^{\mathrm{M}} = H - (x_1 H_1^0 + x_2 H_2^0 + x_3 H_3^0) \tag{4.15}$$

$$S^{\mathrm{M}} = -R\,(x_1 \ln x_1 + x_2 \ln x_2 + x_3 \ln x_3) \tag{4.16}$$

At a given temperature and pressure the partial molar volume and partial molar enthalpy in an ideal solution will be the same as the molar volume and molar enthalpy. Hence, an ideal solution will be formed with no change in volume and no absorption or evolution of heat upon mixing.

The majority of liquid mixtures do not follow the requirement of equation (4.3) and hence they are not ideal in behaviour. The departure of a real mixture from ideality is expressed in terms of activity coefficients in the form:

$$\mu_i\,(T, P, x_i) = \mu_i^0\,(T, P) + RT \ln x_i \gamma_i \tag{4.17}$$

where γ_i is the activity coefficient of component *i*.

Using the general thermodynamic relations the following expressions for G^{E}, S^{E}, H^{E}, V^{E}, U^{E}, and $C_{\mathrm{P}}^{\mathrm{E}}$ can be obtained:

(i) Excess Gibbs free energy

$$G^{\mathrm{E}} = G^{\mathrm{M}}_{\mathrm{real}} - G^{\mathrm{M}}_{\mathrm{ideal}}$$

$$= RT \sum_{\mathrm{i}=1}^{3} x_{\mathrm{i}} \ln \gamma_{\mathrm{i}} \tag{4.18}$$

where

$$G^{\mathrm{E}}_{\mathrm{real}} = RT \sum_{\mathrm{i}=1}^{3} x_{\mathrm{i}} \ \ln \ x_{\mathrm{i}}\gamma_{\mathrm{i}}$$

$$G^{\mathrm{E}}_{\mathrm{ideal}} = RT \sum_{\mathrm{i}=1}^{3} x_{\mathrm{i}} \ \ln \ x_{\mathrm{i}}\gamma_{\mathrm{i}}$$

(ii) Excess entropy

$$S^{\mathrm{E}} = \left[\frac{\delta G^{\mathrm{E}}}{\delta T}\right] P, x$$

$$= -RT \sum_{i=1}^{3} x_i \left(\frac{\delta ln\gamma_i}{\delta T}\right) - R \left(\sum_{i=1}^{3} x_i \ln \gamma_i\right) \qquad (4.19)$$

(iii) Excess enthalpy

$$H^{\mathrm{E}} = -T^2 \left[\frac{\delta (G^{\mathrm{E}}/T)}{\delta T}\right] P, x$$

$$= -RT^2 \sum_{i=0}^{3} x_i \left(\frac{\delta \ln \delta_i}{\delta T}\right) \qquad (4.20)$$

(iv) Excess volume

$$V^E = \left[\frac{\delta \, G^{\mathrm{E}}}{\delta \, P}\right] T, x$$

$$= RT \sum_{i=1}^{3} x_i \frac{\delta \ln \gamma_i}{\delta P} \tag{4.21}$$

(v) Excess energy

$$U^{\mathrm{E}} = H^{\mathrm{E}} - PV^{\mathrm{E}}$$

$$= -RT \left[T \sum_{i=1}^{3} x_i \frac{\delta \ln \gamma_i}{\delta T} + P \sum_{i=1}^{3} x_i \frac{\delta \ln \gamma_i}{\delta P} \right] \tag{4.22}$$

(vi) Excess heat capacity

$$C_{\mathrm{P}}^{\mathrm{E}} = \frac{\delta H^{\mathrm{E}}}{\delta T}$$

$$= -2RT \sum_{i=1}^{3} x_i \frac{\delta \ln \gamma_i}{\delta T} - RT^2 \sum_{i=1}^{3} x_i \frac{\delta^2 \ln \gamma_i}{\delta T^2} \tag{4.23}$$

Excess functions may be positive or negative, their sign and magnitude representing the deviation from ideality. Both, thermodynamic functions of mixing and excess functions become identical in respect of quantities where entropy does not appear. For example, the excess enthalpy H^{E} is identical with the enthalpy of mixing H^{M} and excess volume V^{E} is also identical with volume of mixing V^{M}.

4.1 A BRIEF REVIEW OF THE THEORY OF SOLUTIONS

Theories of solutions were formulated to predict the properties of liquid mixtures. Theories concerning excess volumes of binary liquid mixtures have been reviewed and discussed by (Rowlinson *et al.* 1969; Rowlinson 1970), (Flory 1970), (Scott and Fenby 1969), (Hijmans *et*

al. 1969), (Stokes and Marsh 1972), (Williamson and Scott 1970), (Patterson and Bardin 1970), (Henderson 1974), (Battino 1971), (Sanchez and Lacombe 1976), (Handa and Benson 1979), (Kehiaian 1972) and (Tager and Adamova 1980). Theories concerning multicomponent properties of liquid mixtures have recently been reviewed by (Rastogi 1980), (Rowlinson and Swinton 1982) and (Acree 1984).

In the theories of van der Waals (1890), and van Laar (1906), the properties of liquid mixtures were described in terms of van der Waals equation of state where the characteristic quantities *a* and *b* of the equation of state were treated as composition dependent parameters. The deviation of real solution from ideal behaviour was attributed to the differences in covolume and cohesion which arise due to differences in the interactions of different pair of molecules present in solution. These theories successfully explained certain excess properties in the critical region. (Dolezalek 1908) attempted to account for the non-ideal behaviour of solutions by assuming chemical equlibria, involving either association or solvation or both with all the true molecular species obeying Raoult's law.
Using (Hildebrand 1929) concept of regular solution, (Scatchard 1931; 1932; 1934; 1937) formulated an equation for excess volume

$$V^{\mathrm{E}} = nkU_{\mathrm{V}}^{\mathrm{E}} = nkG^{\mathrm{E}} \tag{4.24}$$

where *n* is the ratio of the internal pressure to the cohesive energy assumed to be the same for the pure and mixed component and *k* is the bulk compressibility which is assumed to be strictly additive in terms of volume fraction. One of the main advantages of the regular solution equation is its simplicity, and the simplicity is retained even when the model is extended to liquid mixtures having more than two components. The derivation for the

multicomponent system is completely analogous to that given for the binary system. However, this theory failed to allow V^{E} and G^{E} to have the oppositive signs in mixtures made up of components which:

(i) follow the same law of corresponding states and

(ii) have the same intrinsic size (i.e. $\sigma_{11} = \sigma_{22}$).

where $\sigma_{11}$and σ_{22} refer to intrinsic size of molecules.

Longuet-Higgins (1951) proposed an equivalent equation using the first order conformal solution theory. The equation takes the form

$$V^{\mathrm{E}} = \frac{\propto TG^{\mathrm{E}}}{\delta^2} \tag{4.25}$$

where $\propto$ is the thermal expansion coefficient. It is assumed to be strictly additive in terms of volume fraction of the components, δ is the solubility parameter of the mixture and is assumed to be simple the average:

$$\delta = \frac{\delta_1 + \delta_2}{2} \tag{4.26}$$

where δ_1 and δ_2 are solubility parameters for component 1 and 2, respectively.

Equations, relating volume change of mixing to energy change of mixing, were deduced by (Wood 1957). These equations could not be used to find any prior reason for V^{E} and U^{E} to

have the same sign. (Mathieson 1958) developed an equation that relates heat of mixing to excess volume and vapour pressure.

$$\left(\frac{\partial \Delta H_{\mathrm{m}}}{\partial x}\right)_{\mathrm{P},\ \mathrm{T}} = \left(\frac{\partial \Delta V_{\mathrm{m}}}{\partial x}\right)_{\mathrm{P},\ \mathrm{T}} \left(\frac{1}{\beta_0 V_0 - \beta_{\mathrm{m}} V_{\mathrm{m}}}\right)_{\mathrm{T},\ \mathrm{x}} \left[\Delta V_{\mathrm{m}} - T\left(\frac{\partial \Delta V_{\mathrm{m}}}{\partial x}\right)_{P,\ x}\right] + \left(\frac{\partial \Delta H_{\mathrm{m}}}{\partial x}\right)_{\Delta \mathrm{V_m},\ \mathrm{T}} \tag{4.27}$$

where β_{m}, and β_0 are respectively the isothermal compressibilities of the mixture and the corresponding additive function for the separate components.

Rowlinson and Mathieson (1959) presented a shorter form of Mathieson's earlier equation, which was similar in form to the one derived by Scatchard (1937).

There are two types of approaches to theories of liquid and liquid mixtures. The first one considers a liquid to be gas-like; a highly non-ideal gas whose properties can be described by some equation of state of which van der Waals is the best known example. The second approach considers a liquid to be solid-like, in a quasicrystalline state, where the molecules vibrate back and forth, about a more or less fixed point in space. X-ray studies, indicated the shorter range order in liquids and supported the solid-like state of liquids. The theory based on this theory of a liquid called lattice theory (Scatchard 1937) was formulated with the aid of statistical mechanics that deals with the evolution of the partition function which is related to thermodynamic functions. Guggenheim (1952) described the crystal lattice model in a comprehensive manner. The lattice model was applied to the liquid state by (Porter 1920), (van Laar and Lorenz 1925), (Heitler 1926), (Guggenheim 1935), (Fowler and Guggenheim 1939), (Hildebrand and Scott 1950). The basic assumptions of this model are:

(i) The factorization of the partition function is valid and the internal partition function remains unchanged in the mixture. The free energy of mixing depends only on the configurational partition function, which is given by

$$Q = Q_{\text{Latt.}}\, Q_{\text{Vibr.}} \tag{4.28}$$

where $Q_{\text{Latt.}}$ is only term that depends on composition and $Q_{\text{Vibr.}}$ is unaffected by mixing.

(ii) The lattice is treated as rigid i.e. $V^{\text{M}} = V^{\text{E}} = 0$ and each site is occupied by a single molecule. The assumption that $V^{\text{E}} = 0$ was not found valid in the case of real solutions. (McGlashan and Morcom 1961) calculated the energies of mixing with zero volume change for pairs of n-alkanes and showed that these agree fairly well with those predicted by this model. However, there is evidence now which show that TS^{E} makes a finite contribution to the free energy, which was not considered while formulating the theory.

Eyring (1936) put forward the first cell-model of the liquid state. This model was used by Lennard-Jones and Devonshire (1937; 1938) and Prigogine and Garikian (1950) to relate the thermodynamic properties of liquid mixtures to intermolecular energy parameters. This model was further developed by Prigogine and Mathhot (1952) to permit G^{E} and V^{E} to have opposite signs (Mathot *et al.* 1953; 1956).

This was later extended by (Prigogine *et al.* 1953; 1957) to the general case where $r_{11}^{*} \neq r_{22}^{*}$. It was assumed that cells of two different sizes exist in the liquid mixtures, cells containing molecules of species 1 and 2. The ratio of the diameters of the cells is then chosen so as to minimize the free energy of mixture. It was shown that a relatively large positive excess volume would result form quite a small difference in molecular size. It follows from this that

negative excess volume which should occur for mixtures of molecules of the same size would only rarely be observed. However, application of cell model theory to binary liquid mixtures showed that experimental excess functions are in poor agreement with those predicted by the model.

Scott (1956) proposed three models for averaging the intermolecular energy parameters of mixtures. These are called 'one fluid', 'two-fluid' and 'three-fluid' models. The first two correspond to Prigogine's crude approximation' and 'refined average potential model, respectively. (Streett and Staveley 1967) analysed the excess functions of simple mixtures, in terms of three models and came to the following conclusions:

(i) All the three models predicted negative values of V^{E} if the molecules of the two components had same size.

(ii) The uncertainties in selecting intermolecular energy parameters would only partly be responsible for the lack of agreement between theory and experiment.

(iii) The 'three- liquid' model predicted a symmetrical dependence of V^{E} on mole fraction while the other two models predicted rather asymmetric V^{E} curves and

(iv) The disagreement between theory and experiment might be due to departure from combination rules in formulating the theory.

Leland *et al.* (1968; 1969) formulated a statistical theory of liquid state. These workers used an approximation for a mixture of the type originally suggested by van der Waals in regard to parameters of the equation of state. Hence the theory was designed as 'one-liquid' van der Waals approximation to a 'two-liquid' model, which took into account the departure from a random distribution induced by differences in intermolecular energy.

Prigogine *et al.* (1953) extended the corresponding states approach, on the basis of the cell model, to chain molecules. The chain molecule was considered as a series of quasi-spherical segments. Balescu (1955) extended Prigogine's average potential model to the solutions which included molecules differing in size and polarity. The equation for an excess peoperty included the two terms (a) contribution of central forces and (b) contribution due to orientataional forces of dipolar origin. This equation failed to predict quantitavely excess volume and excess enthalpy.

The efforts of Kihara (1953), Hamann and Lambert (1954) and Pitzer (1955) to represent intermolecular potential energy between polyatomic molecules led Flory (1965) to believe that the intermolecular energy was effectively determined by the surface interactions of the adjoining molecules. This approximation had the advantage of being adaptable to non-spherical molecules of different size. Flory assumed that the molecule was divided into '*r*' (arbitrary) segments and each segment has intermolecular contact sites. Flory formulated the equation for the intermolecular energy,

$$E_0 = \frac{N\, r\, s\, n}{2v} \tag{4.29}$$

where *N* is the number of molecules, *n* is the constant characterising the energy of interaction for a pair of neighbouring sites and *v* is the volume per segment. Flory deduced the following equation for the partition using Prigogine's treatment of 'rN' chain molecules.

$$Q = Q_{\text{comb.}} [r \left(V^{\frac{1}{3}} - V^{*\frac{1}{3}})^3\right]^{\text{rNC}} \exp\left(\frac{-E_0}{RT}\right) \tag{4.30}$$

Where $Q_{comb.}$ is the combinatorial factor which takes into account the number of ways of interspersing the rN-elements among one another regardless of precise location of each molecules. The above equation can be used to get reduced partition functions and reduced equations of state. The reduced equation of state can then be used to derive an expression for excess volume. The greatest advantage of the Flory theory was its ability to predict all excess thermodynamic quantities with the use of a single interaction parameter, $\theta_{\mathrm{B}}\, X_{\mathrm{AB}}$. (Flory and Abe 1965) applied the theory to binary mixtures and found that the agreement between theoretical and experimental values of excess function was satisfactory.

Eyring and co-workers (1964; 1965; 1965) extended the significant structure theory of pure liquids to binary liquid mixtures based on the assumption that the liquid has three significant structures (i) molecules with solid like freedom (ii) positional degeneracy in the solid like structure and (iii) molecules with gas like freedom. This theory satisfactorily predicted excess Gibbs function for binary liquid mixtures of (carbon tetrachloride + cyclohexane), (carbon tetrachloride + benzene) and (benzene + cyclohexane).

(Flory 1941; 1942) and (Huggins 1941; 1942) independently derived an expression for the entropy of mixing in an athermal solution using the concept of a crystalline lattice model for liquid state. They assumed that polymer molecules in a solution behave like a chain with a large number of equal-sized segments identical in size to the solvent and hence they derived an expression for the excess Gibbs free energy. This expression was further reduced by (Wilson 1964), assuming that the component molecules in the mixture differ not only in their size but also in their intermolecular forces. A study of Wilson's equation by Orye and Prausnitz (1965) showed that excess Gibbs free energies of binary liquid mixtures can be described adequately by Wilson's equation. Wilson's equation has been extended by (Heil and Prausnitz 1966) to the strongly non-ideal polymer solution.

$$\Delta G_{12}^{\text{ex}} = -RT[x_1 \ln(x_1 + x_2 \Lambda_{12}) + x_2 \ln(x_2 + x_1 \Lambda_{21})] \quad (4.31)$$

The new parameters Λ_{12} and Λ_{21} are defined in terms of molar volumes and energies. Using these definitions:

$$\Lambda_{12} = (V_2^0/V_1^0)\, exp[-(g_{12} - g_{11})] \quad (4.32)$$

$$\Lambda_{21} = (V_1^0/V_2^0)\, exp[-(g_{12} - g_{22})] \quad (4.33)$$

Wilson's equation gives not only an expression for the activity coefficient as a function of composition but also an expression for the variation of the acivity coefficient with temperature. This is an important practical advantage in isobaric conditions where temperature varies as the composition changes. An application of Wilson's equation for approximately a hundred miscible binary mixtures of various chemical types showed that the activity coefficient could be satisfactorily described by the Wilson's equation. (Renon and Prausnitz 1968) further developed Wilson's concept of local concentrations with a view to obtain a general equation applicable to miscible and partially miscible liquids. They considered a binary mixture in which each molecule is closely surrounded by other molecules. The immediate vicinity around the any central molecule is referred to as that molecule's cell. In a binary mixture of components 1 and 2, there are two type of cells of which one type contains molecule 1 at its centre and the other contains molecule 2 at its centre. The chemical nature of the molecules surrounding a central molecules depends on the mole fractions, x_1 and x_2.

Prausnitz and co-worker (1975; 1978) proposed the Universal Quasi Chemical (UNIQUAC) model based on a relatively simple two fluid model. Ohta *et al.* (1981) checked the ability of the UNIQUAC model to predict the liquid-vapour pressures of (ethanol + benzene), (ethanol + 2-butanone) and (benzene + 2-butanone) mixtures. However, this model failed to give a satisfactory estimation of vapour-liquid equilibrium data of highly non-ideal mixtures.

The theories of liquid mixtures of more than two components are based on the theories of binary mixtures. (Hildebrand and Scott 1950) and (Scatchard 1931; 1932; 1934; 1937) extended the improved van Laar theory to the liquid solutions containing more than two components with an additional assumption that the excess entropy of mixing is zero at constant temperature and pressure. An expression for the excess Gibbs free energy of ternary systems, proposed by the above workers, takes the form:

$$G^{\mathrm{E}} = (x_1V_1 + x_2V_2 + x_3V_3)\,(\Phi_1\Phi_2A_{12} + \Phi_1\Phi_3A_{13} + \Phi_2\Phi_3A_{23}) \qquad (4.34)$$

where $A_{\mathrm{i\,j}}$ is the binary interaction parameter Φ_1, Φ_2 and Φ_3 are the volume fractions and V_1, V_2 and V_3 are the molar volumes of pure components 1,2 and 3, respectively. The above equation, when modified by suitable mathematical manipulation, will be:

$$G^E = (x_1 + x_2)(\Phi_1 + \Phi_2)G^E + (x_1 + x_3)(\Phi_1 + \Phi_3)G^E + (x_2 + x_3)(\Phi_2 + \Phi_3)G^E \qquad (4.35)$$

This equation is identical to the expression proposed by (Lakhanpal *et al.* 1975; 1976). The above equation can be used to compute excess enthalpy of a ternary mixture. This theory retains its simplicity even when it is extended to multicomponent mixtures.

The significant structure theory of binary liquid mixtures, proposed by (Eyring and co-workers 1964; 1965; 1965) was extended to the liquid mixture of (benzene + cyclohexane +

corban tetrachloride) by (Winhsin and Yapens 1987). It has been observed that the theory gives a satisfactory estimate of excess Gibbs free energy. However, estimation of the thermodynamic properties requires the knowledge of solid state data that are not generally available for liquids.

The Universal Quasi Chemical (UNIQUAC) model, proposed by (Prausntiz and co-workers 1966, 1968) was extended to the mixtures containing three are more components without any additional assumption by the same workers. (Ohta *et al.* 1981) compared the predictions of UNIQUAC model with experimental data for the mixture. (ethanol + benzene + 2-butanone) and concluded that the UNIQUAC model gave a reasonable estimate of multi-component properties. However, the UNIQUAC models fails to gives a satisfactory estimate of vapour-liquid equilibrium data for highly non-ideal systems. In an attempt to improve the predictive ability of UNIQUAC model, (Nagata and Katoh 1980) assumed the energy of mixing U_{12}^{M} for a binary mixture to be of the form:

$$U_{12}^{\mathrm{M}} = x_1\theta_{21}u_{21} + x_2\theta_{12}u_{12} \tag{4.36}$$

where $\theta_{i\,\mathrm{j}}$ is the local area fraction of molecule *i* about a central

$$\theta_{21} = \theta_2 \exp\left(\frac{-u_{21}}{CRT}\right) \Big/ \left[\theta_1 + \theta_2 \exp\left(\frac{-u_{21}}{CRT}\right)\right] \tag{4.37}$$

$$\theta_{12} = \theta_1 \exp\left(\frac{-u_{12}}{CRT}\right) \Big/ \left[\theta_2 + \theta_1 \exp\left(\frac{-u_{12}}{CRT}\right)\right] \tag{4.37a}$$

u_{21} and u_{12} represent the binary interaction parameters and *C* is the proportionality constant. Thus, the excess Gibbs free energy is given by:

$$\frac{G_{12}^{E}}{RT} = x_1 \ln\left(\frac{\Phi_1}{x_1}\right) + x_2 \ln\left(\frac{\Phi_2}{x_2}\right) + \frac{1}{2Z}\left[x_1 q_1 \ln\left(\frac{\theta_1}{\Phi_1}\right) + x_2 q_2 \ln\left(\frac{\theta_2}{\Phi_2}\right)\right] - C x_1 \ln(\theta_1 + \theta_2 \tau'_{21}) - C x_1 \ln(\theta_2 + \theta_1 \tau'_{12}) \quad (4.38)$$

and

$$\tau'_{12} = exp\left(\frac{-u_{12}}{CRT}\right) = exp\left(\frac{-\propto_{12}}{CT}\right) \quad (4.39)$$

This excess Gibbs function equation, called effective UNIQUAC equation was extended to multicomponent mixtures with an additional assumption that the constant *C* is identical in all contributing binary systems. Hence, for a multicomponent mixture, the excess Gibbs free energy equation becomes:

$$\frac{G_{12..n}^{E}}{RT} = \sum_{i=1}^{n} x_i \ln\left(\frac{\Phi_i}{x_i}\right) + \frac{1}{2Z}\sum_{i=1}^{n} x_i q_i \ln\left(\frac{\theta_i}{\Phi_i}\right) - C \sum_{i=1}^{n} x_i \ln\left(\sum_{j} \theta_j \tau'_{j\,i}\right) \quad (4.40)$$

with the activity coefficient γ_i given by

$$\ln \gamma_i = \ln\left(\frac{\Phi_i}{x_i}\right) + 1/2\ zq_i \ln\left(\frac{\theta_i}{\Phi_i}\right) + l_i$$

$$- \frac{\Phi_i}{x_i} \sum_j x_j l_j$$

$$+\ C\left[-\ln\left(\sum_j x_j G_{ji}\right) + 1 - \sum_k \frac{x_k G_{i\,k}}{\sum_j x_j G_{j\,k}} - \ln\left(\frac{\theta_i}{x_i}\right) - 1 + \frac{\theta_i}{x_i}\right] \qquad (4.41)$$

where $G_{j\,i} = \frac{q_j}{q_i}\ \tau'_{j\,i}$

The predictive abilities of UNIQUAC and Effective UNIQUAC models were checked by (Nagata and Katoh 1980) in respect of (acetonitrile + ethanol + cyclohexane) ternary mixture and showed that the latter gives a closed solubility curve. On the other hand, the UNIQUAC equation gives an erroneous prediction of phase separation for (ethanol + cyclohexane) system.

Bronsted and Koefoed (1946) proposed the Principle of Congruence and showed that activity coefficient depends on the average of the carbon atoms per molecule. This principle was applied to a number of binary mixtures by (Desmyter and van der Waals 1958), (Holleman 1963), (Pflug and Benson 1968), (Dantzler and Knobler 1969), (Diaz Pena and Martin 1963), (McGlashan 1961), (Handa *et al.* 1977). (Shana and Canfield 1968) analysed the V^{E} data of the ternary mixture (methane + ethane + propane) at -165 ^{0}C and found that the principle of congruence gives a good estimate of V^E for mixtures which include alkanes beyond n-butane. Vonka and co-workers (1982) predicted excess volumes of multicomponent mixtures using the expression developed for excess free energy as:

$$V_{1\,2\,3}^{\mathrm{E}} = \sum_{i<j} \frac{x_i x_j}{x_i' x_j'} V_{i\,j}^{E} \left(x_i', x_j'\right) \tag{4.42}$$

where $x_i'$and x_j' are defined as $x_i' + x_j' = 1$ and $V_{i\,j}^{E}$ corresponding to binary excess volume at the composition (x_i', x_j') can be obtained by projection of ternary point composition on to the axis of respective binary system in a triangular diagram.

In the normal projection

$$x_i' = \frac{1 + x_i - x_j}{2}, \qquad x_j' = \frac{1 - x_j - x_i}{2}$$

and

$$V_{123}^{\mathrm{E}} = \sum_{i<j} \frac{4\, x_i\, x_j}{1 - (x_i - x_j)^2} V_{i\,j}^{E} \left(x_i',\, x_j'\right) \tag{4.43}$$

This relation is similar to that of (Redlich and Kister 1948) for binary mixtures.

Under direct projection:

$$x_i' = \frac{x_i}{x_i + x_j}, \qquad x_j' = \frac{x_j}{x_i + x_j} \text{ and}$$

$$V_{123}^{\mathrm{E}} = \sum_{i<j} (x_i + x_j)^2\, V_{i\,j}^{E} \left(x_i',\, x_j'\right) \tag{4.44}$$

In parallel projection:

$$V_{123}^{\mathrm{E}} = 1/2 \sum_{i<j} \left[\frac{x_j}{1-x_i} V_{ij}^{E} \left(x_i',\, x_j'\right) + \frac{x_i}{1-x_j} V_{ij}^{E} \left(x_i',\, x_j'\right) \right] \tag{4.45}$$

Garcia and co-workers (1984a; 1984b), computed the ternary excess volumes using the aforesaid projection methods and found that the normal projection method gives the better estimates of ternary data. (Cibulka 1982) also applied these projection methods to a number of ternary mixtures and found that the normal projection method gives a better estimate.

Yet, in another approach efforts were made to develop the predictive expressions on the basis of group contribution methods. The predictive expressions based on this approach, were formulated by (Derr and Deal 1969), (Fredenslund *et al.* 1975; 1977a; 1977b), (Gmehling *et al.* 1978; 1982), (Lai *et al.* 1978), (Ratcliff *et al.* 1971a; 1971b; 1971c; 1971d; 1974; 1969; 1975a; 1975b; 1976) (Siman and Vera 1979) (Skjold-Jorgensen *et al.* 1979) and (Wilson and Deal 1962). Their approach were based on the assumption (i) the physical properties of liquid mixture is a sum of the contributions made by functional groups present in the molecule and (ii) the contribution made by one group in a molecule is independent of that made by another group in the same molecule. The method developed to predict activity coefficients of non-electrolyte mixtures are called Analytical Solution of Groups (ASOG) model (Derr and Deal 1969), and UNIQUAC Functional group activity coefficient (UNIFAC) model.

The ASOG model was suggested by (Derr and Deal 1969) modifying the idea of (Wilson and Deal 1962). In this model, activity coefficient of component *i* in a liquid mixture is divided into two separate contributions. One is the configurational contribution due to differences in molecular size ($\gamma_{\mathrm{i}}^{\mathrm{s}}$) and the other is group interaction contribution due to the differences in intermolecular forces ($\gamma_{\mathrm{i}}^{\mathrm{g}}$).

$$\ln \gamma_i = \ln \gamma_i^s + \ln \gamma_i^g \quad (4.46)$$

The UNIFAC method was developed by (Fredenslund *et al*. 1975) and latter this method was revised and the applicability range was extended by (Fredenslund 1977b) and (Skjold-Jorgensen *et al.* 1979; 1962; 1982) In the UNIFAC method, the molecular activity coefficient is given by the combination of the combinatorial part of UNIQUAC equation and the residual part of the ASOG method.

$$\ln \gamma_i = \ln \gamma_i^c + \ln \gamma_i^r \quad (4.47)$$

The parameters, characterising interaction between the pair of structural groups in a non-electrolyte mixture, can be obtained from experimental values of aforesaid molecular activity coefficients. The parameters are employed to predict activity coefficients for other system which have not been studied experimentally but which cantain the same functional groups. The predicted activity coefficient values are then employed to compute G^E values at different temperatures and are in turn used to compute H^E data. Similarly G^E values, computed as a function of pressure, are used to predict V^E values.

Several empirical equations have been formulated to predict the ternary data from binary results. (Scatchard *et al.* 1952) expressed excess enthalpy and Gibbs free energy for a binary system by the general equation:

$$Z_{i\,j}^E/V = \Phi_i \Phi_j \left[B_{i\,j} + C_{i\,j}\Phi_j + D_{i\,j}\,\Phi_j^2\right] \quad (4.48)$$

and also proposed an expression for excess quantities of ternary mixtures that include symmetrical binaries as:

$$Z^{\mathrm{E}}_{\mathrm{ij}}/V = \sum_{i=1}^{2}\sum_{i>I}^{3} \Phi_i\Phi_j \left[B_{i\,j} + C_{i\,j}\left(1-\Phi_i-\Phi_j\right)/2\right) + D_{i\,j}\left(1-\Phi_i-\Phi_j\right)^2/4\right)\Big] \qquad (4.49)$$

where V is the molar volume of the solution and z is the thermodynamic property referring to either enthalpy or Gibbs free energy. (Wohl 1946 and 1953) developed an expression for excess Gibbs free energy of multicomponent systems in terms of weighted mole fractions called , "q-fractions" and the interaction parameters were determined using contribution from the binary systems. (Redlich and Kister 1948) proposed the equation:

$$Z^{\mathrm{E}}_{123} = x_1x_2\sum_{s=0}^{r} Z^{\mathrm{E}}_{1\,2}(x_1-x_2)^{\mathrm{s}} + x_1x_3\sum_{s=0}^{r} Z^{\mathrm{E}}_{1\,3}(x_1-x_3)^{\mathrm{s}} + x_2x_3\sum_{s=0}^{r} Z^{\mathrm{E}}_{2\,3}(x_2-x_3)^{\mathrm{s}} \quad (4.50)$$

where $Z^{\mathrm{E}}_{\mathrm{ij}}$ is the thermodynamic excess property of binary system. This equation can be used for the computation of excess enthalpy, excess Gibbs free energy and excess volume. Several empirical equations were also proposed by (Tsao and Smith 1953), (Mathieson and Thynne 1956), (Kohler 1960), (Toop 1965), (Colinet 1967), (Lakhanpal *et al.* 1975; 1976), (Jacob and Fitzner 1977), (Rastogi *et al.* 1977a; 1977b) and (Singh *et al.* 1984). However, these empirical expressions served as a point of departure for the mathematical representation of multicomponent excess properties. Differences between predicted values and experimental values are expressed as:

$$Z^{\mathrm{E}}_{123\,(\mathrm{obs})} - Z^{\mathrm{E}}_{123\,(\mathrm{pre})} = x_1x_2x_3Q_{123} \qquad (4.51)$$

with Q functions of varying complexity. However, these predictive relations failed to give good estimate of multicomponent properties.

The theory of solutions described so far attempted to explain the solution non-ideality in terms of physical intermolecular forces. An alternative approach to the study of solution properties, based on a completely different premise, states that molecules in liquid phase interact with each other to form a "new" chemical species and that the observed solution non-ideality is a consequence of the chemical reactions. The hydrogen bond formation between the molecules of a liquid mixture is another common effect that influences the thermodynamic properties of the solution to a greater extent than other specific and physical interaction (Murthy *et al.* 1968 and Arnett *et al.* 1974). The molecules containing hydrogen linked to an electronegative atom exhibit a tendency to associate with each other and to interact with other molecules possessing an accessible electronegative atom. The extent of self-association and intermolecular bonding between unlike molecules vary with composition of the mixtures. For example, the dilution of strong hydrogen bonded liquid by an inert solvent leads to the coverage of hydrogen bond and gradual decrease in contraction of aggregates. This would be attended by the absorption of heat and expansion in volume. The magnitude of volume change will be determined by structure –breaking ability of the inert solvent. If the unlike molecules participate in hydrogen bonding it would result in evolution of heat and contraction in volume. The sign of the excess function will depend on the dominant effect. However, at present, there appears to be no satisfactory theory of solutions which deals with strong orientation effects from which one may reduce excess volume. (Flory 1944) formulated a theory of associated liquid mixtures. This was employed to deduce equations for excess free energy, excess enthalpy and excess entropy. (Nagata 1973 and

1975) proposed an association solution theory to predict excess enthalpy of ternary mixtures, which contains one associated component.

The present study of excess properties of ternary liquid mixtures involving specific and non-specific interactions are utilised for two purposes:

1. To study the non-ideal nature of the liquid mixture and
2. To understand the influence of a third component on pair wise interactions in ternary mixtures.

4.2 EXCESS MOLAR VOLUMES

Excess molar volume of mixing (V^E) is defined as the difference between the volume of mixing of the real mixture and the value corresponding to an ideal mixture at the same conditions of temperature, pressure and composition, which is given by the equation,

$$V^{\mathrm{E}} = V^{\mathrm{M}}_{\mathrm{real}} - V^{\mathrm{M}}_{\mathrm{ideal}} \qquad (4.52)$$

Volume changes occur because of the combination of the following factors:

(i) Difference in size and shape of the components,

(ii) Difference in the intermolecular interaction energy between like and unlike molecules,

(iii) Formation of new chemical species,

(iv) Hydrogen bonding and

(v) Structural changes such as in the correlation of molecular orientations

Excess molar volume data of liquid mixtures are utilised to understand, the departure of the real system from ideality, the nature of the specific interactions between the molecules of the components. Excess volumes are also useful in conversion of excess thermodynamics functions determined at constant pressure to the condition of mixing at constant volume, in determining composition from density measurement of mixtures, in obtaining the second virial cross coefficient

The excess molar volume $V_{\mathrm{m}}^{\mathrm{E}}$ is defined as (McGlashan 1979; Walas 1985; Letcher 1975):

$$V_{\mathrm{m}}^{\mathrm{E}} = V_{\mathrm{mix}} - \sum_{i=1}^{\mathrm{N}} x_{\mathrm{i}} V_{\mathrm{i}}^{0} \tag{4.53}$$

where x_{i} is the mole fraction of component *i,* $V_{\mathrm{mix}} = V_{\mathrm{real}}$ and V_{i}^{0} are the molar volumes of the mixture and pure component *i*, respectively. For a binary mixture:

$$V_{\mathrm{m}}^{\mathrm{E}} = V_{\mathrm{mix}} - (x_1 V_1^0 + x_2 V_2^0) \tag{4.54}$$

The change in volume on mixing two liquids, 1 and 2 can be attributed to a number of processes (Letcher 1975):

(a) The breakdown of 1-1 and 2-2 intermolecular interaction which have a positive effect on the volume,

(b) The formation of 1-2 intermolecular interaction which results in a decrease of the volume of the mixture,

(c) Packing effect caused by the difference in the size and shape of the component species and which may have positive or negative effect on the particular species involved and

(d) Formation of new chemical species (Redhi 2003).

There is no volume change upon mixing two liquids to form a thermodynamically ideal solution at constant temperature and pressure, but a volume change may occur when two real liquids are mixed (Battino 1971).

Volume change on mixing of binary liquid mixtures, $V_{\mathrm{m}}^{\mathrm{E}}$, at constant pressure and temperature is of interest to chemists and chemical engineers, and is an indicator of the non-idealities present in real mixtures. It is also important to thermochemists because it serves as a sensitive indicator for the applicability of liquid theories to liquid mixtures [Redhi 2003].

In reality it is impossible to apportion with any strong conviction the contributing effects of the intermolecular interactions of the dissimilar molecules, because of the packing effect (Deenadayalu 2000).

The volume, (V), of a mixture is a function of temperature, (T), pressure, (P), and number of moles, (n), etc:

$$V = V(T, P, n_1, n_2, n_3 \ldots\ldots n_{\mathrm{f}}) \tag{4.55}$$

At constant temperature and pressure this is:

$$V = V(n_1, n_2, n_3 \ldots\ldots n_{\mathrm{f}}) \tag{4.56}$$

The volume of the unmixed liquid components V_{unmix} at the constant temperature and pressure may be written as:

$$V_{\mathrm{m,unmix}} = \sum_{i=1}^{\mathrm{N}} x_i V_{\mathrm{m,i}}^0 = V_{\mathrm{m,ideal}} \tag{4.57}$$

where $V_{\mathrm{m,i}}^0$ is the molar volume of the pure species *i*.

Once the liquids have been mixed together the volume of the mixture $V_{\mathrm{m,mix}}$ is not normally the sum of the volumes of the pure liquids but is given by:

$$V_{\mathrm{m,mix}} = \left(V_{\mathrm{m,real}}\right) \neq x_1 V_{\mathrm{m},1} + x_2 V_{\mathrm{m},2} \ldots\ldots x_{\mathrm{i}} V_{\mathrm{m,i}} = \sum_{\mathrm{i}=1}^{\mathrm{N}} x_{\mathrm{i}} V_{\mathrm{m,i}} \tag{4.58}$$

The excess molar volume of binary, $V_{\mathrm{m}}^{\mathrm{E}}$, and ternary, $V_{\mathrm{m}}^{\mathrm{E}}$, mixing is given by:

$$V_{\mathrm{m}}^{\mathrm{E}} = V_{\mathrm{m,mix}} - V_{\mathrm{m,unmix}} = V_{\mathrm{m,real}} - V_{\mathrm{m,ideal}} = \sum_{\mathrm{i}=1}^{\mathrm{N}} x_{\mathrm{i}} (V_{\mathrm{m,i}} - V_{\mathrm{m,i}}^0) \tag{4.59}$$

where $V_{\mathrm{m}}^{\mathrm{E}}$ is the excess molar volume of the binary and ternary system at constant temperature and pressure (Smith and Pagni 1998).

4.3 CORRELATION AND PREDICTION THEORIES FOR V_{123}^{E}

Ternary excess molar volumes can be calculated using the predictive expressions proposed by (Redlich-Kister 1948), (Kohler 1960), (Tsao-Smith 1953), (Jacob-Fitzner 1977) and (Cibulka 1982).

(i) Redlich-Kister equation

$$V_{123}^{\mathrm{E}} = \sum_{\mathrm{j}>i} V_{\mathrm{m,ij}}^{\mathrm{E}} \left(x_{\mathrm{i}}, x_{\mathrm{j}}\right), \tag{4.60}$$

where

$$V_{\mathrm{ij}}^{\mathrm{E}} = x_{\mathrm{i}} x_{\mathrm{j}} \sum_{\mathrm{s}=0}^{\mathrm{n}} (A_{\mathrm{s}})_{\mathrm{i\,j}} \left(x_{\mathrm{i}} - x_{\mathrm{j}}\right)^{\mathrm{s}}$$

x_{i} and x_{j} are the mole fractions of the component in ternary mixture and *s* is the number of parameters.

(ii) Kohler's equation

$$V_{123}^{\mathrm{E}} = (x_1 + x_2)^2 \, V_{12}^{\mathrm{E}} + (x_1 + x_3)^2 \, V_{13}^{\mathrm{E}} + (x_2 + x_3)^2 \, V_{23}^{\mathrm{E}} \tag{4.61}$$

where

$$V_{ij}^{E} = x_i' x_j' \sum_{s=0}^{n} (A_s)_{i\,j} \left(x_i' - x_j'\right)^s$$

at composition (x_i', x_j'), such that

$$x_i' = 1 - x_j' = {}^{x_i}/_{(x_i + x_j)}$$

where x_i and x_j are the ternary mole fractions.

(iii) Tsao-Smith equation

$$V_{123}^{E} = x_2(1 - x_1)^{-1}\, V_{12}^{E} + x_3(1 - x_1)^{-1}\, V_{13}^{E} + (1 - x_1) \tag{4.62}$$

Where V_{12}^{E}, V_{13}^{E} and V_{23}^{E} are the binary excess molar volumes at composition (x_i', x_j'), such that $x_i' = x_1$ for 1,2 and 1,3 binary systems and $x_2' = {}^{x_2}/_{(x_2 + x_3)}$ for 2, 3 binary system.

(iv) Jacob-Fitzner equation

$$V_{123}^{E} = \frac{x_1 x_2 V_{12}^{E}}{\left(x_1 + {}^{x_3}/_{2}\right)\left(x_2 + {}^{x_3}/_{2}\right)} + \frac{x_1 x_3 V_{13}^{E}}{\left(x_1 + {}^{x_2}/_{2}\right)\left(x_3 + {}^{x_2}/_{2}\right)} + \frac{x_2 x_3 V_{23}^{E}}{\left(x_2 + {}^{x_1}/_{2}\right)\left(x_3 + {}^{x_1}/_{2}\right)} \tag{4.63}$$

Where V_{12}^{E}, V_{13}^{E} and V_{23}^{E} are the binary excess molar volumes at composition $(x_{\mathrm{i}}^{'}, x_{\mathrm{j}}^{'})$, such that $x_{\mathrm{i}} - x_{\mathrm{j}} = x_{\mathrm{i}}^{'} - x_{\mathrm{j}}^{'}$

However, simple mathematical manipulations show that the Redlich- Kister equation yields results similar to those of Jacob-Fitzner.

(v) Cibulka's equation

$$V_{123}^{\mathrm{E}} = \sum \frac{x_{\mathrm{i}} x_{\mathrm{j}}}{x_{\mathrm{i}}^{'} x_{\mathrm{j}}^{'}} V_{\mathrm{i\,j}}^{\mathrm{E}} \left(x_{\mathrm{i}}^{'}, x_{\mathrm{j}}^{'}\right) \tag{4.64}$$

Where $V_{\mathrm{i\,j}}^{\mathrm{E}}$ is the binary excess molar volume at $(x_{\mathrm{i}}^{'}, x_{\mathrm{j}}^{'})$ composition such that $x_{\mathrm{i}}^{'} + x_{\mathrm{j}}^{'} = 1$. $x_{\mathrm{i}}^{'}$ and $x_{\mathrm{j}}^{'}$ can be obtained as projections in the triangle diagram as normal, direct and parallel projections.

(a) For normal projection

$$x_{\mathrm{i}}^{'} = \frac{\left(1 + x_{\mathrm{i}} - x_{\mathrm{j}}\right)}{2}, \quad x_{\mathrm{j}}^{'} = \frac{\left(1 + x_{\mathrm{j}} - x_{\mathrm{i}}\right)}{2},$$

and $$V_{123}^{E} = \sum_{\mathrm{i<j}} \frac{4 x_{\mathrm{i}} x_{\mathrm{j}}}{1 - (x_{\mathrm{i}} - x_{\mathrm{j}})^2} V_{\mathrm{ij}}^{\mathrm{E}} \left(x_{\mathrm{i}}^{'}, x_{\mathrm{j}}^{'}\right) \tag{4.65}$$

This relation is similar to Redlich- Kister expression.

(b) For direct projection

$$x_{\mathrm{i}}' = \frac{x_{\mathrm{i}}}{x_{\mathrm{i}} + x_{\mathrm{j}}}, \quad x_{\mathrm{j}}' = \frac{x_{\mathrm{j}}}{x_{\mathrm{i}} + x_{\mathrm{j}}}$$

$$\text{and} \quad V_{123}^{E} = \sum_{\mathrm{i<j}} (x_{\mathrm{i}} - x_{\mathrm{j}})^2 \, V_{ij}^{\mathrm{E}}\left(x_{\mathrm{i}}', x_{\mathrm{j}}'\right) \tag{4.66}$$

This is similar to Kohler's expression.

(c) For parallel projection

The binary contributions can be written as the arithmetic mean contribution of the points of ternary compositions.

$x_{\mathrm{i}}'(1) = x_{\mathrm{i}}, x_{\mathrm{j}}'(1) = 1 - x_{\mathrm{i}}$ and

$x_i'(2) = 1 - x_j, \qquad x_j'(2) = x_j$

This yields the relation

$$V_{123}^{\mathrm{E}} = \frac{1}{2} \sum_{\mathrm{i<}j} \frac{x_{\mathrm{j}}}{1 - x_{\mathrm{i}}} \, V_{\mathrm{ij}}^{\mathrm{E}}\left(x_{\mathrm{i}}, 1 - x_{\mathrm{j}}\right) + \frac{x_{\mathrm{i}}}{1 - x_{\mathrm{j}}} \, V_{\mathrm{ij}}^{\mathrm{E}}\left(1 - x_{\mathrm{j}}, \, x_{\mathrm{i}}\right) \tag{4.67}$$

In this work the Cibulka equation was used to correlate the ternary excess molar volumes using the binary excess molar volume parameters.

(B) APPARENT MOLAR PROPERTIES

4.4 APPARENT MOLAR VOLUME AND DERIVED PROPERTIES

A solution of volume V, is prepared using n_1 moles of solvent (e.g. water) and n_j moles of solute, Thus:

$$V = n_1 V_{1(aq)} + n_j V_{j(aq)} \quad (4.68)$$

where $V_{1(aq)}$ is the partial molar volume of the solvent (i) and $V_{j(aq)}$ is the partial molar volume of the solute (j) Equation (4.68) can be rewritten in terms of the molar volume of the solvent, V_m which is calculated from the density of the pure solvent and its molar mass. At a given T and P, density is given by

$\rho_1 = M_1/V_1$.

$V_{j(aq)}$ is replaced in equation (4.68) by the apparent molar volume, (V_ϕ), equation (4.69).

$$V = n_1 V_1 + n_j V_\phi \quad (4.69)$$

There is only one unknown variable. The apparent molar volume (V_ϕ), depends on the composition of the solution, the solute, T and P.

The apparent molar volumes, V_ϕ , was calculated from the experimental density values using equation (4.70):

$$V_\phi = \frac{M}{d} - \frac{(d - d_0)}{mdd_0} \tag{4.70}$$

where m is molality of the solute and d and d_0 are the densities of the solution and pure solvent, respectively; M is molar mass of solute.

A Redlich-Mayer type equation was fitted to the apparent molar volume data using the following Redlich-Mayer equation (4.71):

$$V_\phi = V_\phi^0 + S_\mathrm{v} m^{\frac{1}{2}} + B_\mathrm{v} m \tag{4.71}$$

where V_ϕ^0 is the apparent molal volume at infinite dilution, which is also known as the partial molar volume of the solute. S_v and B_v are empirical parameters.

The temperature dependence of V_ϕ^0 can be expressed as:

$$V_\phi^0 = A + BT + CT^2 \tag{4.72}$$

where *A*, *B*, and *C* are empirical parameters and *T* is the temperature. The limiting apparent molar expansibility E_ϕ^0 can be obtained by differentiating equation (4.72) with respect to temperature to obtained equation (4.73):

$$E_\phi^0 = \left(\partial V_\phi^0 / \partial T\right)_p = B + 2CT \qquad (4.73)$$

4.5 SOUND VELOCITY

Sound velocity data gives direct and precise information about the adiabatic properties of the liquids. The measurement of sound velocity in liquids provides a means for obtaining some equilibrium thermodynamic data which are not readily obtained by other experimental methods. The ultrasonic sound velocity in a liquid or a liquid mixture is mainly determined by its intermolecular properties. Langeman and Correy (1942) discussed sound velocity in liquids as the sum of 'bond velocities'. Rendall (1942) has shown a close agreement between the experimental and theoretical values calculated from the adiabatic compressibility measurements. Sound velocity is closely related to the derivatives of equations of state. Auslander *et al.* (1971), Samal *et al.* (1972), Aziz *et al.* (1972), Pool *et al.* (1972) and Younglove (1965), showed that there is a close relation between sound velocity and thermodynamic properties.

According to Eyring *et al.* (1937), Hirschfeldera *et al.* (1937) and Kincaid *et al.* (1937) molecules in the liquid state are loosely packed so as to leave some free space in between them. A sound wave is pictured as travelling with infinite velocity within a molecule and the gas kinetic velocities through space between the molecules of the liquid. The space is termed

as the available volume, V_a. The molecules thus short circuit all but a fraction of the path and the sound velocity is given by:

$$u_{\text{lib}} = \left(\frac{V}{V_a}\right)^{1/3} u_{\text{gas}} = \left(\frac{V}{V_a}\right)^{1/3} \left(\frac{\gamma RT}{M}\right)^{1/2} \tag{4.74}$$

were V is the free volume, V_a is the available volume, u_{gas} is sound velocities in the gas, T is the temperature and R is the gas constant. Sound velocity in liquid u_{liq} can be calculated from the free volume V. Depending upon the model of liquid assumed, the calculation of V gives different values. Kittel (1946) derived a simpler relation for u_{liq} using Tonk's equation (1936) as,

$$u_{\text{lib}} = \left(\frac{V}{V_a}\right)\left(\frac{3\gamma_{\text{lib}}}{\gamma_{\text{gas}}}\right)^{1/2} u_{\text{gas}} \tag{4.75}$$

V_a has been back calculated using experimental sound velocity data of liquids with the application of equation (4.76) and compared with those obtained from thermal expansion data. The relation gives a satisfactory estimate of sound velocity in some liquids.

4.5.1 THEORIES OF SOUND

4.5.1.1 Free length theory (FLT)

The concept of intermolecular free length i.e the distance between surfaces of two molecules, used to explain the sound velocity in pure liquids and liquid mixtures was introduced by (Jacobson 1951; 1952a; 1952b). According to Jacobson:

$$u_{\text{lib}} = \frac{K}{L_{\text{f}}\,\rho^{1/2}} \tag{4.76}$$

where *K* is a temperature dependent constant, ρ is the density and L_f is the free length in the liquid. Free length theory (FLT) of Jacobson was used by different investigators (Rai *et al.* 1989), (Kaulgud *et al.* 1963; 1960; 1962; 1971), (Seshadri *et al.* 1973; 1974), and (Prakash *et al.* 1975) to evaluate the sound velocities in the liquid mixtures. In a mixture:

$$u_{\text{mix}}\,L_{\text{mix}}\,\rho_{\text{mix}}^{1/2} = K \tag{4.77}$$

where u_{mix} and ρ_{mix} are sound velocity and density, respectively. L_{mix} is the free length in the mixture. Free length (L_{f}) of pure liquids is calculated using the relation:

$$L_{\text{f}} = \frac{K}{u_{\text{exp}}\,\rho_{\text{exp}}^{1/2}} \tag{4.78}$$

where u_{exp} and ρ_{exp} are experimentally determined sound velocity and density, respectively.

The surface area *Y*, per mole for the pure component is calculated using the following expression:

$$Y = \frac{2V_{\mathrm{a}}}{L_{\mathrm{f}}} \tag{4.79}$$

and $V_{\mathrm{a}} = V_{\mathrm{T}} - V_0$, where V_{a} is the available volume per mole, and V_0 and V_{T} are the molar volumes at absolute zero and at absolute temperature *T*, respectively. The values of V_0 were obtained using critical temperature as shown below:

$$V_0 = V_{\mathrm{T}} \left(1 - \frac{T}{T_{\mathrm{C}}}\right)^{0.3} \tag{4.80}$$

L_{mix} is calculated employing the expression:

$$L_{\mathrm{mix}} = \frac{2\left[V - \sum_{i=1}^{3} x_{\mathrm{i}} V_0^{\mathrm{i}}\right]}{\sum_{\mathrm{i}=1}^{3} x_{\mathrm{i}} y_{\mathrm{i}}} \tag{4.81}$$

where x_{i} and V_0^{i} represents mole fraction and molar volume at absolute zero of component *i*, respectively *V* represents molar volume of mixture.

4.5.1.2 Collision Factor Theory (CFT)

Schaaffs (1940; 1963; 1974) developed the following formula for sound velocity in pure liquids on the basis of collision factor theory (CFT):

$$u = u_\infty S r_f = u_\infty S \frac{B}{V} \quad (4.82)$$

where u_∞ = 1600 m.s^{-1}, S is the collision factor, $r_f = B/V$ is the space filling factor, B is the actual volume of the molecules per mole of liquid. Nutsch-Kuhnkies (1965) extended this concept to the binary liquid mixtures and showed that:

$$u_{mix} = u_\infty S_{mix} r_{f\,mix} \quad (4.83)$$

This may be written as:

$$u_{mix} = u_\infty [x_1 S_1 + x_2 S_2] \frac{[x_1 B_1 + x_2 B_2]}{V} \quad (4.84)$$

Rai *et al.* (1989) extended such studies to the ternary liquid mixtures to show that:

$$u_{mix} = u_\infty [x_1 S_1 + x_2 S_2 + x_3 S_3] \frac{[x_1 B_1 + x_2 B_2 + x_3 B_3]}{V} \quad (4.85)$$

The suffixes 1, 2 and 3 denote the components 1, 2 and 3, respectively. The actual volume of the molecule per mole for the pure components, *B* and is calculated using the following equation

$$B = \frac{4\pi}{3} r_{\mathrm{m}}^{3} N \tag{4.86}$$

where r_{m} is the molecular radius and *N* is the Avagadro number. The value of r_{m} has been obtained from Schaaff `s semi-empirical formula (4.87) and expression (4.88) suggested by Rao and Venkataseshaiah (1969).

$$\mathrm{r_m} = \sqrt[3]{a\left[1 - b\left(\sqrt{1 + 1/3b - 1}\right)\right]} \tag{4.87}$$

$$\mathrm{r_m} = \sqrt[3]{a\left[1 - b\left(\sqrt{1 + 1/b - 1}\right)\right]} \tag{4.88}$$

a and *b* of the above equations are given by

$$a = \frac{3V}{16\pi N} \;\; and \;\; b = \frac{\gamma RT}{MU^2} \tag{4.89}$$

where γ and M are specific heat ratio and molecular weight, respectively and other symbols have their usual meanings. The molecular diameter d, ($d = 2r_{\mathrm{m}}$) of pure liquids can also be computed from the data of surface tension (σ) and critical temperature (T_{c}) of pure liquids using the equation (Chaturvedi *et al.* 1979).

$$d^{5/2} = \frac{1}{7.21 \times 10^{19}} \cdot \frac{V\sigma^{1/4}}{T_{\mathrm{C}}^{1/4}} \tag{4.90}$$

4.5.1.3 Nomoto relation

Nomoto (1956; 1958) developed the following relation for sound velocity in binary liquid mixtures:

$$u = \left[\frac{x_1R_1 + x_2R_2}{x_1V_1 + x_2V_2}\right]^3 \tag{4.91}$$

Rai *et al.* (1989) extended the above equation for sound velocity to ternary liquid mixtures:

$$u = \left[\frac{x_1R_1 + x_2R_2 + x_3R_3}{x_1V_1 + x_2V_2 + x_3V_3}\right]^3 \tag{4.92}$$

where x and V are the mole fraction and molar volume respectively, R is molecular sound velocity and is related to molecular weight (M_i) sound velocity (u) and density (ρ_i) of the component i, as follows:

$$R_i = \frac{M_i}{\rho_i} u_i^{1/3} \tag{4.93}$$

4.6 ISENTROPIC COMPRESSIBILITY

Another thermodynamic property which influences the interactions between the molecules in the liquid mixture is called the isentropic compressibility, κ_S. This can be defined as

$$\kappa_S = \frac{-1}{V}\left(\frac{\partial V}{\partial P}\right) \tag{4.94}$$

κ_S can be determined both by direct and indirect methods. In the indirect method it is computed from ultrasonic sound velocity (u) and density (ρ) using the equation:

$$\kappa_S = u^{-2}\,\rho^{-1} \tag{4.95}$$

The above equation was used in this work for the calculation of the isentropic compressibility for the binary mixtures. For an ideal mixture isentropic compressibility is considered to be

additive in terms of volume fraction. The difference between the compressibility of a real solution and that of an ideal solution is called excess isentropic compressibility. Unlike excess volume and excess enthalpy, excess compressibility is a complicated fuction expressed by:

$$\kappa^{\mathrm{E}} = -\frac{1}{V}\left(\frac{\partial \mathrm{V}}{\partial \mathrm{P}}\right)_{\mathrm{T}} + \left[\frac{1}{x_1V_1 + x_2V_2 + x_3V_3}\right]\left[\frac{\partial\,(x_1V_1 + x_2V_2 + x_3V_3)}{\partial\, P}\right]_{\mathrm{T}} \tag{4.96}$$

where V_1, V_2 and V_3 are molar volumes of pure components 1, 2 and 3, respectively at constant pressure and temperature. By introducing excess volume of the solution equation (4.96) can be converted into the form:

$$\kappa^{\mathrm{E}} = -\frac{1}{V}\left(\frac{\partial \mathrm{V}}{\partial \mathrm{P}}\right)_{\mathrm{T}} + \left[\frac{V^{\mathrm{E}}}{x_1V_1 + x_2V_2 + x_3V_3}\right]\left[\frac{(\kappa_1x_1V_1 + \kappa_2x_2V_2 + \kappa_3x_3V_3)}{(x_1V_1 + x_2V_2 + x_3V_3)}\right] \tag{4.97}$$

where κ^{E} is made up of two terms: one is proportional to V^{E} and other to $\left(\frac{\partial \mathrm{V}}{\partial \mathrm{P}}\right)$. An attempt to formulate a theoretical expression for compressibility was made after the publication of average potential model (Prigogine *et al.* 1950; 1952). Compressibility data relating to many liquid mixtures were used to test this theory. The agreement between theoretical and experimental values was found to be good (Jeener 1956; Sackmann *et al.* 1961; Reddy *et al.* 1964; Holder *et al.* 1962).

Flory and Abe (1965) defined excess compressibility as:

$$\kappa^{\mathrm{E}} = -\frac{1}{V}\left(\frac{\partial \mathrm{V}^{\mathrm{E}}}{\partial \mathrm{P}}\right)_T = -\frac{1}{V}\left(\frac{\partial \bar{V}^{\mathrm{E}}}{\partial \mathrm{P}}\right)_T \tag{4.98}$$

where

$$\bar{V} - \bar{V}^{0} = \bar{V}^{\mathrm{E}} = \frac{V^{\mathrm{E}}}{x_1 V_1^* + x_2 V_2^*}$$

And $\bar{V}^{0} = \Phi_1 \bar{V}_1 + \Phi_2 \bar{V}_2$

Φ_1 and Φ_1 are segment fractions, V_1^* and V_2^* are characteristic volumes.

The equation (4.98) can be expressed as:

$$\kappa^{\mathrm{E}} = \kappa - \left(\Phi_1 \bar{V}_1 \kappa_1 + \Phi_2 \bar{V}_2 \kappa_2\right) \bar{V}^{-1} \tag{4.99}$$

The compressibility, κ, is evaluated from an equation of state. The equation for excess compressibility setting $P = 0$ may be written in the form:

$$\kappa^{\mathrm{E}} = \frac{3\bar{V}^{2}}{P^{*}}\left[\left(\bar{V}^{\frac{1}{3}} - 1\right)^{-1} - 3\right]^{-1} - \left[\Phi_1 \bar{V}_1 \kappa_1 + \Phi_2 \bar{V}_2 \kappa_2\right]\bar{V}^{-1} \qquad (4.100)$$

The excess compressibilities predicted by the above equation were compared with experimental results for a number of binary liquid mixtures by Flory and Abe (1965). The agreement between the theoretical and experimental data was found to be satisfactory.

Ewing and Marsh (1974) defined κ by the equation:

$$\kappa = -\frac{1}{V}\left(\frac{\partial \mathrm{V}^{\mathrm{E}}}{\partial \mathrm{P}}\right)_T \qquad (4.101)$$

where V denotes molar volume of one mole of mixture and $\left(\frac{\partial \mathrm{V}^{\mathrm{E}}}{\partial \mathrm{P}}\right)_T$ is the pressure coefficient of excess molar volumes at constant temperature. Rao and Naidu (1974) defined a quantity $\Delta\kappa_{\mathrm{s}}$ as:

$$\Delta\kappa_{\mathrm{s}} = \kappa_s - \kappa_s^{id} \qquad (4.102)$$

where $\Delta\kappa_s$ is the deviation in isentropic compressibilities, κ_s and κ_s^{id} are the isentropic compressibilities of the real and ideal mixtures, respectively. The ideal isentropic compressibility is calculated using the relation:

$$\kappa_s^{id} = \sum_{i=1}^{n} \Phi_i \kappa_{si} \tag{4.103}$$

where Φ_i and κ_{si} are volume fraction and isentropic compressibility of pure component *i*, respectively However, deviation in isentropic compressibilities ($\Delta\kappa_s$) are used to study the departure of a real mixtures from ideality and to understand the nature and strength of interactions between molecules in a liquid mixture.

4.7 APPARENT MOLAR ISENTROPIC COMPRESSIBILITY AND DERIVED PROPERTIES

The apparent molar isentropic compressibility, κ_ϕ , is computed from equation. (4.104):

$$\kappa_\phi = \frac{(\kappa_s d_0 - \kappa_{s0} d)}{m d d_0} + \frac{\kappa_s M}{d} \tag{4.104}$$

where *m* is molality of the solute, *d* and d_0 are the densities of the solution and pure solvent, respectively; *M* is molar mass of solute. κ_{s0} and κ_s are the isentropic compressibility of pure solvent and mixture, respectively.

A Redlich-Mayer type equation was fitted to the apparent molar isentropic compressibility data using the following Redlich-Mayer equation (4.105):

$$\kappa_{\phi} = \kappa_{\phi}^{0} + S_{\mathrm{k}} m^{1/2} + B_{\mathrm{k}} m \qquad (4.105)$$

where κ_{ϕ}^{0} is the apparent molal volume at infinite dilution, which is also known as the partial molar volume of the solute. S_{k} and B_{k} are empirical parameters.

CHAPTER 5

EXPERIMENTAL

(A) EXCESS MOLAR VOLUMES AND APPARENT MOLAR VOLUMES

5.1 EXPERIMENTAL METHODS FOR MEASUREMENT OF EXCESS MOLAR VOLUMES

The binary excess molar volume, $V_{\mathrm{m}}^{\mathrm{E}}$, at a constant concentration of x_1 of component 1 and x_2 of component 2 are defined as

$$V_{\mathrm{m}}^{\mathrm{E}} = V_{\text{mixture}} - \left[x_1 V_1^0 + x_2 V_2^0\right] \tag{5.1}$$

where $V_{\mathrm{i}}^{\mathrm{o}}$ is molar volume of the mixture pure components. The excess molar volume, $V_{\mathrm{m}}^{\mathrm{E}}$, upon mixing two liquids may be measured either directly or indirectly. The direct measurements involve mixing the liquids and determining the volume change (dilatometric method) and the indirect measurements involve measuring the density of the pure liquid and the density of the mixture by (pycnometer or densitometer) and calculating, $V_{\mathrm{m}}^{\mathrm{E}}$, or V_{123}^{E} using equations (5.2 and 5.3) (Battino 1971; Letcher 1975; Handa and Benson 1979; Beath *et al.* 1969; Pflug and Benson 1968; Stokes and Marsh 1972; Marsh 1980, 1984; Kumaran and McGlashan 1977; Govender 1996; Nevines 1997; Redhi 2003). The latter method was used in this work. A summary of the various techniques (direct and indirect methods) are given here.

5.1.1 Direct method

The direct method measures the volume change that occurs when the liquids are mixed. Direct methods of measurement of, V_m^E, include batch dilatometer and continuous dilution dilatometer.

Batch dilatometer is characterized by the determination of a single data point per loading of the apparatus and continuous dilatometer is characterized by the determination of many data points per loading of the apparatus [Handa and Benson 1979; Nevines 1997; Redhi 2003).

5.1.1.1 Batch dilatometer

An example of a batch dilatometer is shown in Figure 5.1.

The dilatometer is filled with known masses of pure liquids, which are separated by mercury. The height of mercury in the calibrated graduated column is noted. The liquids are mixed by rotating the dilatometer and the volume change on mixing is indicated by the change in the height of the mercury in the calibrated capillary. The, V_m^E, is determined from the volume change and the masses of the components. It was reported that a precision of $\pm$ 0.003 $cm^3 \cdot mol^{-1}$ in the, V_m^E, could be achieved over the temperature range of (280 to 350) K using this technique. A disadvantage of this apparatus is that it is difficult to fill the dilatometer and this is usually accomplished using a syringe. A major source of error in this method is the determination of the composition as is it necessary to weigh the dilatometer as it contains mercury. This results in large errors in the measured mass. The error associated with taking a difference in large masses is usually quiet significant (Keyes and Hildebrand 1917; Nevines 1997; Redhi 2003).

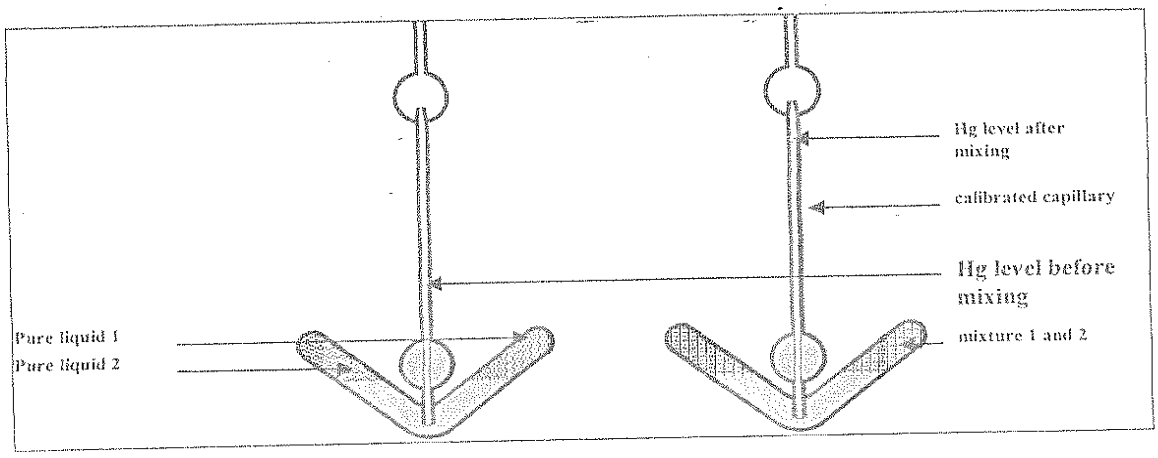

Figure 5.1 A typical batch dilatometer

5.1.1.2 Continuous dilatometer

This technique has become more popular than the batch technique because it is less time consuming and more data is generated per loading. The mode of operation involves the successive addition of one liquid into the reservoir, which contains the other liquid and detecting the volume change that accompanies the addition.

The dilatometer of Kumaran and McGlashan (1977) which is based on the design of Bottomly and Scott (1974) is presented in Figure 5.2. Both are considered superior to other continuous dilatometer because mercury and the liquids do not pass through the greased gas. The instrument of Kumaran and McGlashan (1977) is considered an improvement on the one

developed by Bottomly and Scott (1974) because it is easier to load. Kumaran and McGlashan (1977) reported a precision of $0.0003\ \mathrm{cm^3 \cdot mol^{-1}}$ in V_m^E for their apparatus.

A measurement is made by filling the burette (e) with one of the pure liquids and the bulb (d) with the other pure liquid. As the dilatometer is tilted some of the mercury is displaced into the burette through a capillary (c) and collects at the bottom of the burette. This displaced mercury forces some of the pure liquid from the burette into the bulb through the higher capillary (b). After mixing the change in volume is registered as a change in the level of the mercury in the calibrated capillary (a). The amount of pure liquid that is displaced is determined from the height of the mercury in the burette. Because mercury is used, a capillary pressure effect is possible and the compressibility of mercury has to be considered when determining the excess molar volume.

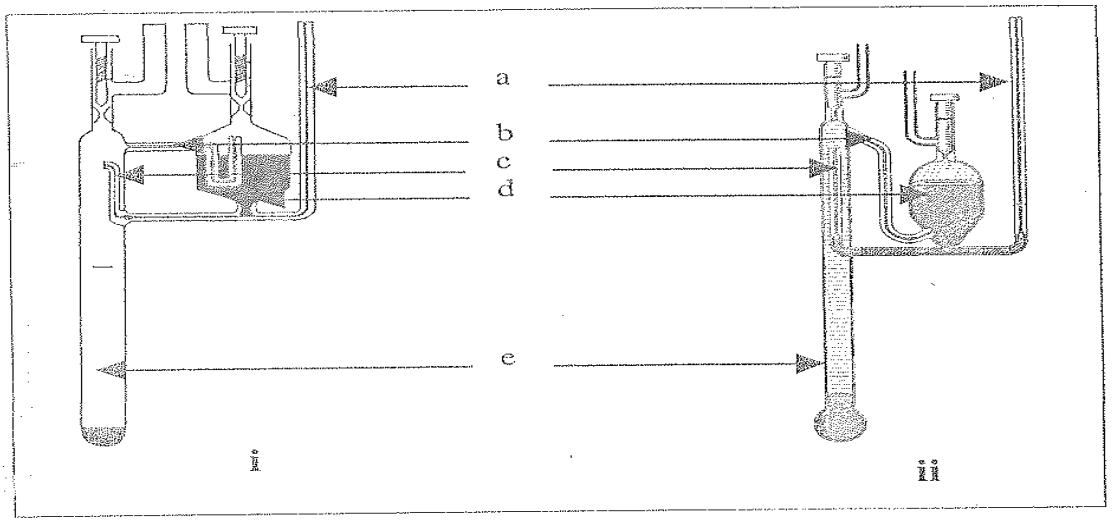

Figure 5.2 Continuous dilatometer (i) design of Bottomly and Scott, (ii) design of Kumaran and McGlashan. a; calibrated capillary from which the volume change is determined, b; liquid capillary, c; mercury capillary, d; bulb that contains mercury, e; burette liquid 2

5.1.2 Indirect determination

As the development of the dilatometer was accompanied by a greater accuracy than was possible from density measurement techniques, the latter method became less popular for determination of V_m^E. However the development of highly accurate vibrating tube densitometers has made it possible to determine, V_m^E , with acceptable accuracy from density measurements. This method is also very simple.

The excess molar volume for a binary V_m^E and ternary V_{123}^E mixtures are determined from density measurements using the following equations, respectively:

$$V_m^E = \frac{x_1 M_1 + x_2 M_2}{\rho} - \frac{x_1 M_1}{\rho_1} - \frac{x_2 M_2}{\rho_2} \quad (5.2)$$

$$V_{123}^E = \frac{x_1 M_1 + x_2 M_2 + x_3 M_3}{\rho} - \frac{x_1 M_1}{\rho_1} - \frac{x_2 M_2}{\rho_2} - \frac{x_3 M_3}{\rho_3} \quad (5.3)$$

where x_1 , x_2 and x_3 are the mole fractions, M_1 , M_2 and M_3 are molar masses, ρ_1, ρ_2 , ρ_3 and ρ are the densities where 1, 2 and 3 refers to the component 1, 2 and 3, respectively and ρ is the density of the mixture (Govender 1996; Nevines 1997; Redhi 2003).

5.1.2.1 Pycnometry

Pycnometry involves the determination of the mass for a fixed volume. A vessel with a known volume is filled with a liquid mixture of known composition. It is then weighed and

this mass, together with the composition and volume of the vessel is used to determine V_m^E. A pycnometer capable of a precision of 5×10^{-6} g·cm^{-3} for density measurement translates into a precision of 0.001 cm^3· mol^{-1} for V_m^E has been reported by (Wood and Bruisie 1943). The pycnometer based on the design of (Wood and Bruisie 1943) is shown in Figure 5.3.

5.1.2.2 Magnetic float densimeter

The mode of operation of a magnetic float densimeter is based on the determination of the height of a magnetic float in a liquid mixture. The height of this magnetic float in the presence of a known magnetic field is a function of the buoyancy of the liquid. The buoyancy of the liquid is related to the density of the liquid. An instrument with a precision 3×10^{-6} g·cm^{-3} has been reported and this translates to a precision of 0.0008 cm^3·mol^{-1} (Franks and Smith 1967). The magnetic float densitometer based on the design of (Franks and Smith 1967) is shown in Figure 5.4.

5.1.2.3 Mechanical oscillating densitometer

Mechanical oscillating (vibrating tube) densimeters coupled to digital output displays are widely used in the chemical industry, and in research laboratories to measure densities of pure liquids and liquid mixtures. The frequency of the vibrating tube containing a liquid that is subjected to a constant electric stimulation is related to the density of the liquid. According to Handa and Benson (1979), the frequency of a vibration of an undamped oscillator (e.g. tube containing a liquid) connected by a spring with a constant elasticity, *c*, is related to the mass of the oscillator, *M*, by using the following equation:

$$2\pi\nu = \left(\frac{c}{M}\right)^{\frac{1}{2}} \tag{5.4}$$

Since the oscillator is a hollow tube, M is the sum of the contents in the tube and the true mass M_0. If a liquid with a density, ρ, fills the hollow which has a volume V, then:

$$M = M_0 + \rho V \tag{5.5}$$

This mass, together with the composition and volume of the vessel is used to determine V_m^E.

The pycnometer based on the design of (Wood and Bruisie 1943) is shown in Figure 5.3.

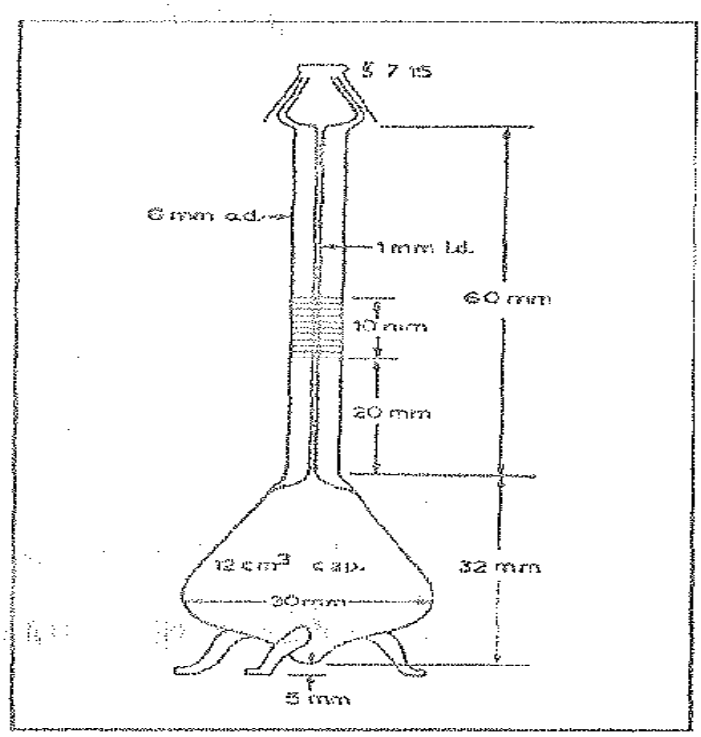

Figure 5.3 The pycnometer based on the design of Wood and Bruisie

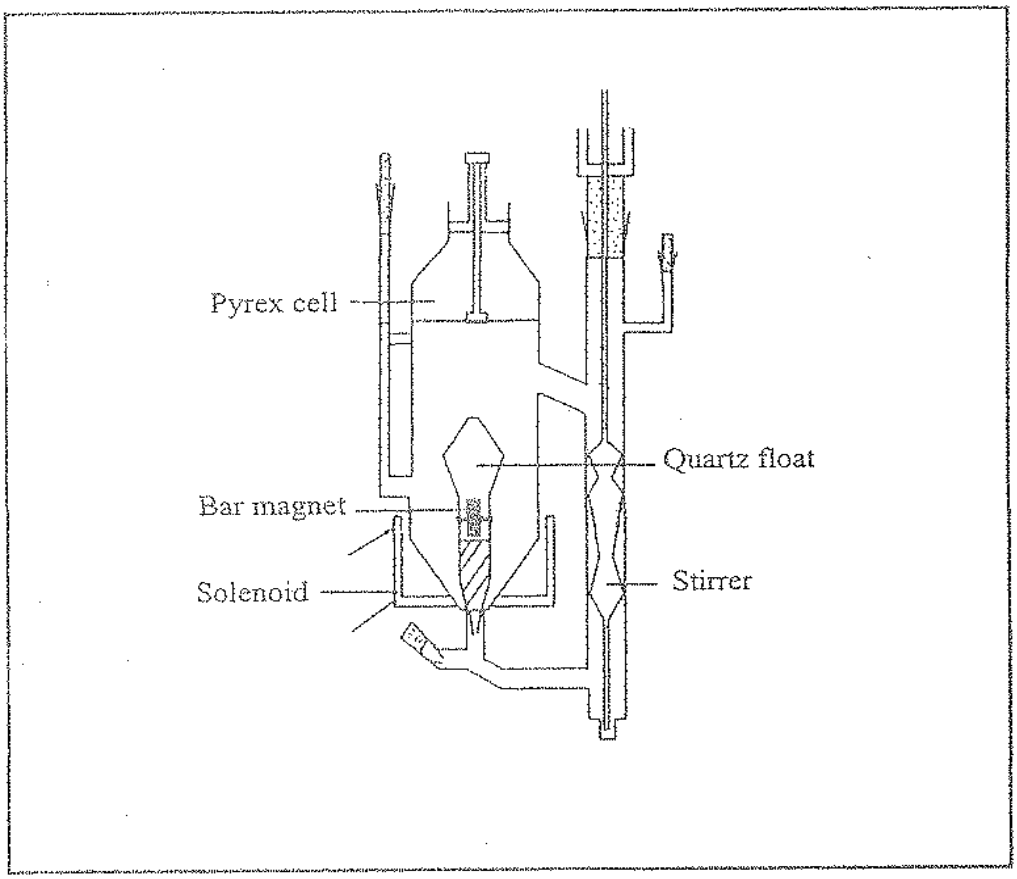

Figure 5.4 Magnetic float densitometer

Substitution of equation (5.5) into equation (5.4) and solving for ρ:

$$\rho = -\frac{M_0}{V} + \left(\frac{c}{4\pi^2}\right)\left(\frac{1}{V^2}\right) \tag{5.6}$$

where $\frac{-M_0}{V}$ and $\frac{c}{4\pi^2 V}$ are constants. Therefore the following equation is valid:

$$\rho = A + B\left(\frac{1}{\nu}\right)^2 \tag{5.7}$$

where $\frac{-M_0}{V}$ and $\frac{c}{4\pi V^2}$

The constants A and B are characteristics of the oscillator. τ is termed the period and density is given the symbol, ρ, hence:

$$\rho = A + B\tau^2 \tag{5.8}$$

where A and B are determined by calibration. This involves determining the period for two substances of known density.

Since densities are measured relative to a reference material:

$$\rho - \rho_o = B\left(\tau^2 - \tau_o^2\right) \tag{5.9}$$

Commercially available vibrating tube densimeters with a precision of 0.001 % are available. This implies a precision of 0.003 $cm^3 \cdot mol^{-1}$ in the measurement of V_m^E (Nevines 1997).

In this work the Anton Paar DMA 38 vibrating tube densitometer was used to measure the densities of the binary and ternary mixtures and is described below.

5.2 EXPERIMENTAL APPARATUS AND METHOD USED IN THIS WORK

5.2.1 Vibrating tube densitomer (Anton Paar DMA 38)

The density measured is based on the oscillation of a vibrating U-shaped sample tube. This tube is filled with the liquid sample mixture and the relationship between the period τ and the density ρ of the mixture is given by:

$$\rho = A + B\tau^2 \qquad (5.10)$$

The constants A and B are instrument constants for each individual oscillator and can be determined by two calibration measurements with samples of known density, e.g. dry air and de-ionised water.

A diagram of the Anton Paar DMA 38 apparatus used in this work is shown in Figure 5.5.

5.2.2 Mode of operation

The density measurements are based on the electromagnetically induced oscillation of the glass U-tube. One complete back and forth movement of a vibration is a period its duration is the period of oscillation τ. The number of periods per second is the frequency ν.

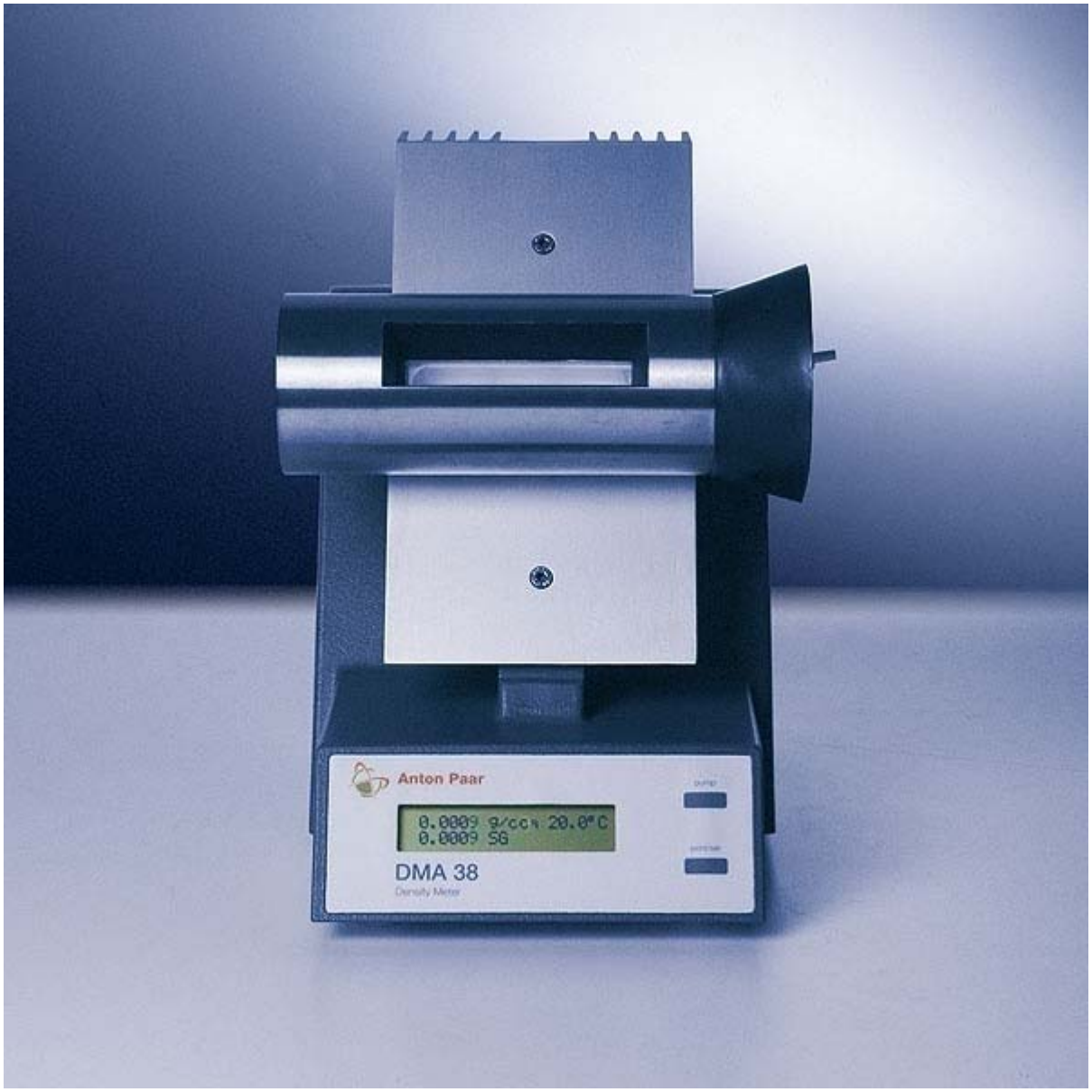

Figure 5.5 DMA 38 Densitometer

Each glass tube vibrates at a characteristic or natural frequency. This changes when the tube is filled with a liquid mixture.

As the frequency is a function of mass. When the mass increases, the frequency decreases in other words the period of oscillation τ increases:

$$\nu = \frac{1}{\tau} \tag{5.11}$$

A magnet is fixed to the measurement tube which is made to oscillate by a transmitter. A sensor measures the period of oscillation τ.

The period of oscillation is obtained from the equation:

$$\tau = 2\pi\sqrt{\frac{\left(\rho V_c + m_c\right)}{K}} \tag{5.12}$$

where ρ is the density of the sample in measurement, V_c is the volume of sample (capacity of tube), m_c is the mass of the measured tube, K is the measurement tube constant.

It follows that

$$\rho = \frac{K\tau^2}{4\pi^2 V_c} - \frac{m_c}{V_c} \tag{5.13}$$

The density and the period oscillation τ are related as follows:

$$\rho = A\tau^2 + B \tag{5.14}$$

$$\rho = \frac{K\tau^2}{4\pi^2 V_c} \quad \text{and} \quad B = -\frac{m_c}{V_c}$$

A and *B* are constants which are determined by the elasticity, structure and mass of the measurement tube. In this work the density was given as the output from the DMA 38 densitometer.

5.2.3 Materials

The water content in all chemicals was determined by a Karl Fischer Coulometer [Metrohm 831]. Mass percent water content was found to be in 0.0400 % in $[MOA]^+[Tf_2N]^-$, 0.0400 % in $[BMIM]^+[MeSO_4]^-$, 0.0400 % in 0.0040 % in methanol, 0.0040 % in ethanol, 0.0040 % in 1-propanol, 0.006 % in methyl acetate, 0.006 % in ethyl acetate and 0.006 % in nitromethane.

Methanol was first dried with potassium carbonate and then distilled before being used. Ethanol was first dried with magnesium turnings and then distilled before being used (Riddick and Bunger 1986). The ionic liquids, methyl acetate, ethyl acetate and nitromethane were used without any further purification.

A summary of the pure chemicals their suppliers and purities used in this work is given in Table 5.1. The experimental and literature values of densities and speed of sound of the pure compound is given in Tables 5.2 and 5.3.

Three density values for $[MOA]^{+}[Tf_2N]^{-}$ were obtained 1.1093, 1.1069 and 1.1070 because different bottles of the same chemical were used.

Table 5.1 Chemicals, their suppliers and mass % purity

Chemicals	Supplier	Mass % Purity
Methanol	Fulka	99.8
Ethanol	Fulka	99.8
Methyl acetate	Sigma-Aldrich	99.0
Ethyl acetate	Sigma-Aldrich	99.7
Nitromethane	Sigma-Aldrich	99.0
$[MOA]^+[Tf_2N]^-$	Fulka	98.0
$[BMIM]^+[MeSO_4]^-$	Sigma-Aldrich	97.0

Table 5.2 Densities, ρ, of pure chemicals at T = (298.15, 303.15, and 313.15) K

Chemicals	ρ / g·cm^{-3}			
	Literature	Experimental		
	T/K 298.15	T/K 298.15	T/K 303.15	T/K 313.15
Methanol	0.7869[a]	0.7866	0.7818	0.7728
Ethanol	0.7852[a]	0.7864	0.7818	0.7734
1-Propanol	0.7994[a]	0.7996	0.7818	0.7734
Methyl acetate	0.9270[b]	0.9271	0.9205	0.9079
Ethyl acetate	0.8944[b]	0.8947	0.8885	0.8751
Nitromethane	1.13117[c]	1.1309	1.1244	1.1115
$[MOA]^+ Tf_2N]^-$	1.1093[a]	1.1069	1.1032	1.0957
$[BMIM]^+ [MeSO_4]^-$	1.20775[c]	1.2080	1.2048	1.1988

[a] (Sibiya and Deenadayalu 2008)

[b] (Gonzalez *et al.* 2007)

[c] (Iglesias-Otero *et al.* 2008)

Table 5.3 Speed of sound, u, of pure chemicals at T = (298.15, 303.15, 308.15 and 313.15) K

Chemicals	u / m·s^{-1}				
	Literature	Experimental			
	T/K 298.15	T/K 298.15	T/K 303.15	T/K 308.15	T/K 313.15
Methanol	1108[a]	1102	1086	1074	1052
Ethanol	1152[a]	1149	1128	1098	1086
Methyl acetate	1155[b]	1146	1128	1110	1092
Ethyl acetate	1141[b]	1141	1118	1096	1073
$[MOA]^+ Tf_2N]^-$		1260	1242	1230	1212

[a](Aminabhavi and Banerjee 1998)

[b](Oswal *et al.* 2004)

5.2.4 Preparation of mixtures

(a) V_{123}^{E}

Ternary mixtures with composition spanning the entire mole fraction range were prepared. This was verified by plotting the composition on a ternary plot as given in Figure 5.6. Ternary mixture were prepared for z values covering the entire composition range where $z = x_3/x_1$, x_1 is the mole fraction of the ILs and x_3 is the mole fraction of methyl acetate or ethyl acetate or nitromethane. For each z value the density of the binary mixture of (IL + an alkyl acetate or nitromethane) was determined at each temperature. The density was used to calculate the V_m^E values and plotted with the literature binary data to ensure that it fitted with the literature data. Each ternary mixture was prepared by transferring via syringe, the pure liquids into stoppered bottles to prevent evaporation. The IL was first filled into an air–tight stoppered 5 cm^3 glass vial and weighed. An OHAUS mass balance was used to determine the mass of each component of the mixture. The mixture was shaken in order to homogenize the solution since the ionic liquid is slightly viscous. The injection of the solution into the densimeter was done slowly to avoid formation of bubbles inside the vibrating tube of the densimeter. The mass balance has a precision of 0.0001 g.

(b) V_ϕ

Binary mixtures with composition spanning the lower concentration range of the ionic liquid were prepared. Each binary mixture was prepared by transferring via syringe, the pure liquids into stoppered bottles to prevent evaporation. The IL was first filled into an air–tight stoppered 5 cm^3 glass vial and weighed. An OHAUS mass balance was used to determine the mass of each component of the mixture. The mixture was shaken in order to homogenize the solution since the ionic liquid is slightly viscous. The injection of the solution into the densimeter was done as for the ternary mixtures.

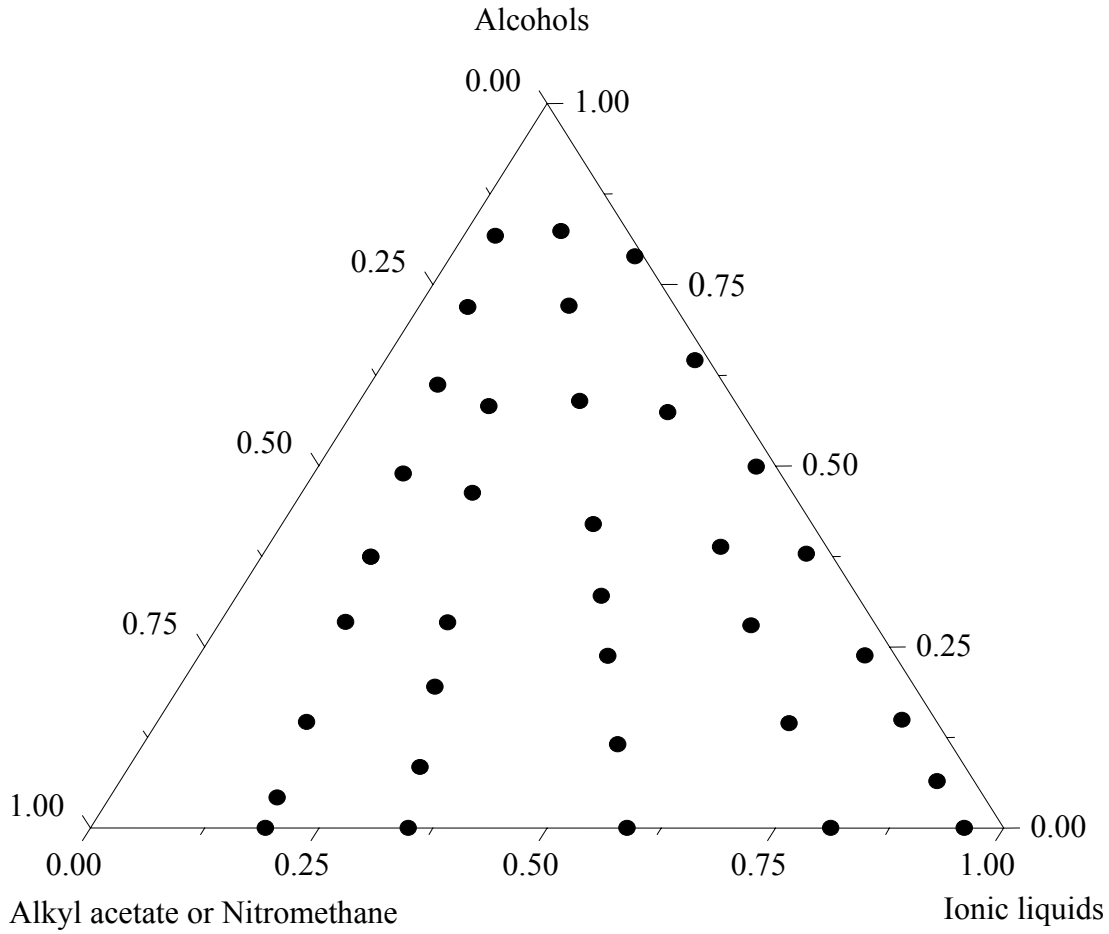

Figure 5.6 Typical plot showing *z* values covering the entire composition range.

5.2.5 Experimental procedure for instrument

The densities were measured using an Anton Paar DMA 38 vibrating U-tube densimeter. The densimeter consists of a built-in thermostat controller capable of maintaining temperature precisely to ± 0.01 K and measuring density to ± 0.0001 g·cm^{-3}.

Prior to each experimental run, the cell was first flushed with ethanol. After flushing compressed dry air was blown through the cell. Ultra pure water supplied by SH Calibration Service GmbH Graz (used as the calibration standard) was then introduced into the cell by means of a glass syringe. The injection process was carried out slowly, enabling the liquid to properly wet the walls of the cell, and also to alleviate the risk of trapping air bubbles in the U-tube. The sample was always filled past its nodal points and the syringe was left in place at the nodal point during each measurement. The density of air and water was set for the calibration. The solution mixtures were introduced into the sample cell in exactly the same manner as for the ultra pure water. Density values of water, pure solvents and air were determined after a series of density measurements to permit a continuous check on accuracy of the density determinations.

This was further verified by repeated measurements of the same solution at different times. Using the density and the composition of the mixtures, the ternary excess molar volume,V_{123}^{E}, were calculated from experimental density using the equation (5.15) as given below:

$$V_{123}^{\mathrm{E}} = \frac{x_1M_1 + x_2M_2 + x_3M_3}{\rho} - \frac{x_1M_1}{\rho_1} - \frac{x_2M_2}{\rho_2} - \frac{x_3M_3}{\rho_3} \qquad (5.15)$$

where x_1 , x_2 and x_3 are mole fractions, M_1 , M_2 and M_3 are molecular masses, ρ_1, ρ_2 and ρ_3 are densities of the pure components, where "1" , "2" and "3" refer to the IL , alcohol and alkyl acetate or nitromethane, respectively, and ρ is the density of the mixture.

The apparent molar volume, V_ϕ , of the binary system was calculated from the experimental density using equation (5.16) below:

$$V_\phi = \frac{M}{d} - \frac{(d - d_0)}{mdd_0} \tag{5.16}$$

where m is molality of the solute ($[MOA]^+ [Tf_2N]^-$ or methanol or ethanol) (mol·kg^{-1}) and d and d_0 are the densities (kg·m^{-3}) of the solution and pure solvent, respectively; M is molar mass of $[MOA]^+ [Tf_2N]^-$ or methanol or ethanol (kg·mol^{-1}).

5.2.6 Specifications of the Anton Paar DMA 38 instrument

Accuracy : 1×10^{-3} g·cm^{-3}

Min. Sample Volume : I cm^3

Measuring Range : 0 -3 g·cm^{-3}

Temperature Range : 15 – 40 ^{o}C

Pressure Range : 10 bar (145 psi)

5.2.7 Validation of experimental technique

The experimental technique was assessed by the determination of the excess molar volumes for the test system {octane (x_1) + toluene (x_2)} at T = 298.15 K and comparing it with the literature values (Moravkova and Linek 2008). The difference between experimental and literature $V^{\mathrm{E}}_{\mathrm{m}}$ were within the experimental error. The maximum uncertainty in binary $V^{\mathrm{E}}_{\mathrm{m}}$ is ± 0.007 cm^3· mol^{-1}.

The comparison of the calculated and literature binary V_m^E data is plotted in Figure 5.7

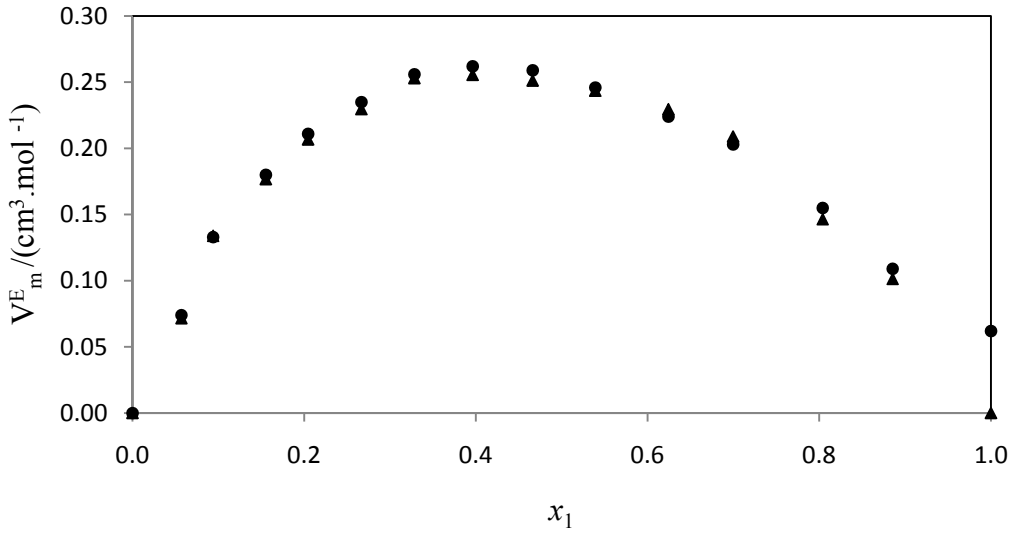

Figure 5.7 Comparison of the binary V_m^E from this work with the literature results for the mixture {$C_6H_5CH_3$(x_1) + C_6H_{14}(x_2)} at T = 298.15 K, ●, literature results; ▲, this work

5.2.8 Systems studied in this work

In this work the V_{123}^E of mixing were determined at T = (298.15, 303.15 and 313.15) K for ([MOA]$^+$[Tf_2N]$^-$ + alcohol + alkyl acetate) and T = 298.15 K for ([BMIM]$^+$[$MeSO_4$]$^-$ + alcohol + nitromethane). Binary V_m^E data for each ternary system was taken from the literature (Sibiya and Deenadayalu 2008, 2009; Iglesias-Otero *et al*. 2008; Nakanishi *et al.* 1970; Cerdeirina *et al.* 1999; González *et al.* 2007). For the ([BMIM]$^+$[$MeSO_4$]$^-$ + alcohol + nitromethane) ternary system V_{123}^E was only done at T = 298.15 K because no binary data was available at T = (303.15 and 313.15) K.

The V_ϕ of the binary mixtures were determined at T = (298.15, 303.15, 308.15 and 313.15) K for the IL [MOA]$^+$[Tf_2N]$^-$.

The follow (IL + alcohol + alkyl acetate or nitromethane) ternary, V_{123}^{E} systems and binary V_{ϕ}, and κ_{ϕ} systems (IL + alcohol or alkyl acetate) and (alcohol + alkyl acetate) were studied:

Ternary V_{123}^{E} systems (IL + alcohol + alkyl acetate or nitromethane)

1. {methyltrioctylammonium bis(trifluoromethylsulfonyl)imide + methanol + methyl acetate} at T = (298.15, 303.15 and 313.15) K.

2. {methyltrioctylammonium bis(trifluoromethylsulfonyl)imide + methanol + ethyl acetate} at T = (298.15, 303.15 and 313.15) K

3. {methyltrioctylammonium bis(trifluoromethylsulfonyl)imide + ethanol + methyl acetate} at T = (298.15, 303.15 and 313.15) K

4. {methyltrioctylammonium bis(trifluoromethylsulfonyl)imide + ethanol + ethyl acetate} at T = (298.15, 303.15 and 313.15) K

5. (1-butyl-3-methylimidazolium methyl sulphate + methanol + nitromethane) at T = 298.15 K

6. (1-butyl-3-methylimidazolium methyl sulphate + ethanol + nitromethane) at T = 298.15 K

7. (1-butyl-3-methylimidazolium methyl sulphate + 1-propanol + nitromethane) at T = 298.15 K

Binary V_{ϕ} systems ($[MOA]^{+}[Tf_2N]^{-}$ + alcohol or alkyl acetate) and (alcohol + alkyl acetate)

1. {methyltrioctylammonium bis(trifluoromethylsulfonyl)imide + methanol} at T = (298.15, 303.15, 308.15 and 313.15) K

2. {methyltrioctylammonium bis(trifluoromethylsulfonyl)imide + methyl acetate} at T = (298.15, 303.15, 308.15 and 313.15) K

3. {methyltrioctylammonium bis(trifluoromethylsulfonyl)imide + ethanol} at T = (298.15, 303.15, 308.15 and 313.15) K

4. {methyltrioctylammonium bis(trifluoromethylsulfonyl)imide + ethyl acetate} at T = (298.15, 303.15, 308.15 and 313.15) K

5. (methanol + methyl acetate) at T = (298.15, 303.15, 308.15 and 313.15) K

6. (methanol + ethyl acetate) at T = (298.15, 303.15, 308.15 and 313.15) K

7. (ethanol + methyl acetate) at T = (298.15, 303.15, 308.15 and 313.15) K

8. (ethanol + ethyl acetate) at T = (298.15, 303.15, 308.15 and 313.15) K

(B) ISENTROPIC COMPRESSIBILITY AND APPARENT MOLAR ISENTROPIC COMPRESSIBILITY

5.3 Introduction

Measurement of the speed of sound, u, in liquids is a powerful source of information (e.g. to detect small changes in gas composition or the effects of small concentrations changes) about the thermophysical properties of chemical substances and their mixtures (Azevedo and Szydlowski 2004).

Speed of sound and density, are used to calculate isentropic compressibility by means of the Newton-Laplace equation.

$$k_s = \frac{1}{\rho u^2} \quad . \tag{5.17}$$

Density and isentropic compressibility are used to calculate the apparent molar isentropic compressibility by using the equation below:

$$\kappa_\phi = \frac{(\kappa_s d_0 - \kappa_{s0} d)}{m d d_0} + \frac{\kappa_s M}{d} \tag{5.18}$$

where m is molality of the solute ($[MOA]^+[Tf_2N]^-$ or methanol or ethanol) (mol·kg^{-1}) and d and d_0 are the densities (kg·m^{-3}) of the solution and pure solvent, respectively; M is molar mass of $[MOA]^+[Tf_2N]^-$ or methanol or ethanol (kg·mol^{-1}) and κ_{s0} and κ_s are the isentropic compressibility of pure solvent and mixture, respectively.

5.3.1 Ultrasonic interferometer

The instrument used in this work is a Mittal multifrequency ultrasonic interferometer M-81G. It is a simple and direct device to determine the ultrasonic velocity in liquids with a high degree of accuracy.

It consists of a:

i) high frequency generator, which is designed to excite the quartz plate fixed at the bottom of the measuring cell at its resonance frequency to generate ultrasonic waves in the experimental liquid in the measuring cell. A macro-ammeter senses the changes in the current

and two controls for the purpose of sensitivity regulation and initial adjustments of the micro-ammeter are provided on the high frequency generator.

ii) measuring cell, which is a specially designed double walled cell for maintaining the temperature of the liquid constant during the experiment. A fine micrometer screw is provided at the top, which can lower or raise the reflector plate in the cell through a known distance. It has a quartz plate fixed at the bottom.

A diagram showing the Ultrasonic Interferometer M-81G and interferometer is shown in Figures 5.8 and 5.9.

Figure 5.8 Ultrasonic interferometer M-81G

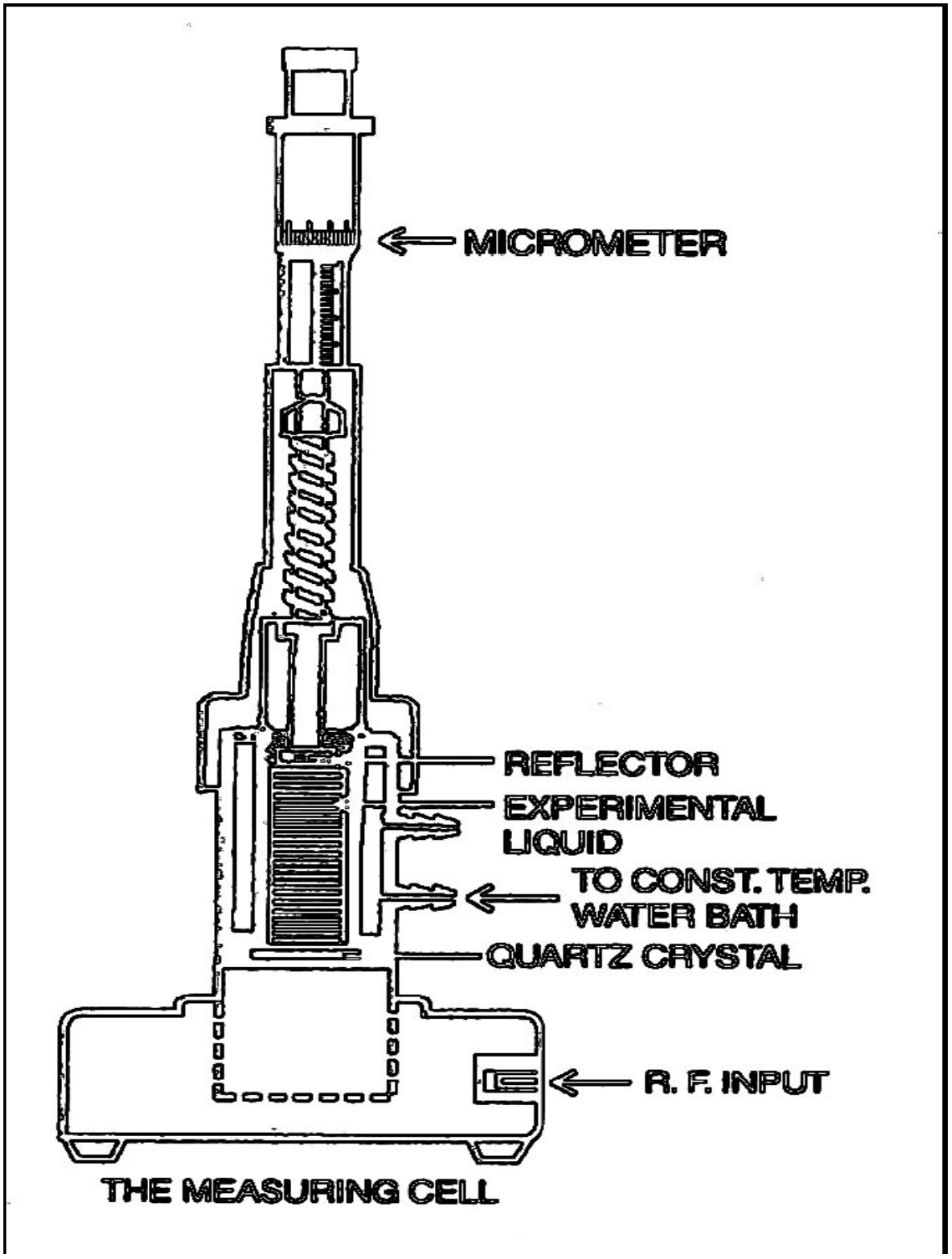

Figure 5.9 Diagram of interferometer

5.3.2 Working principle

The principle used in the measurement of velocity, V, is based on the accurate determination of the wavelength, λ, in the medium. Ultrasonic waves of known frequency ν are produced by a quartz plate cell. A movable plate kept parallel to the quartz plate reflects the waves. If the separation between these plates is exactly a whole multiple of the sound wavelength, standing waves are formed in the medium. The acoustic resonance gives rise to an electrical reaction on the generator driving the quartz plate and the anode current of the generator becomes maximum.

If the distance between the reflector and crystal is increased or decreased and the variation is exactly one half wavelength, (λ/2) or multiple of it, anode current again becomes maximum. From the knowledge of wavelength, (λ), the velocity, (V), can be obtained by the relation:

Velocity =Wavelength × frequency

$$V = \lambda \times \nu \tag{5.19}$$

5.3.3 Systems studied in this work

In this work the speed of sound was measured over the entire composition range at T = (298.15, 303.15, 308.15 and 313.15) K for the systems ($[MOA]^+[Tf_2N]^-$ + alcohol or alkyl acetates) and (alcohol + alkyl acetates) using a multifrequency ultrasonic interferometer M-81G at 3 MHz. The isentropic compressibility and the apparent molar isentropic compressibility were then calculated from the speed of sound values.

The systems studied in this work is given below:

1. {methyltrioctylammonium bis(trifluoromethylsulfonyl)imide + methanol}
2. {methyltrioctylammonium bis(trifluoromethylsulfonyl)imide + methyl acetate}
3. {methyltrioctylammonium bis(trifluoromethylsulfonyl)imide + ethanol}
4. {methyltrioctylammonium bis(trifluoromethylsulfonyl)imide + ethyl acetate}
5. (methanol + methyl acetate)
6. (methanol + ethyl acetate)
7. (ethanol + methyl acetate)
8. (ethanol + ethyl acetate)

CHAPTER 6

RESULTS

(A) TERNARY EXCESS MOLAR VOLUME

6.1 V_{123}^{E}

The ternary excess molar volumes for the systems ($[MOA]^+[Tf_2N]^-$ + methanol or ethanol + methyl acetate or ethyl acetate) and ($[BMIM]^+[MeSO_4]^-$ + methanol or ethanol or 1-propanol + nitromethane) were calculated from the experimental density values using equation (6.1)

$$V_{123}^{E} = \frac{x_1M_1 + x_2M_2 + x_3M_3}{\rho} - \frac{x_1M_1}{\rho_1} - \frac{x_2M_2}{\rho_2} - \frac{x_3M_3}{\rho_3} \qquad (6.1)$$

where x_1 , x_2 and x_3 are mole fractions, M_1 , M_2 and M_3 are molecular masses, ρ_1 , ρ_2 and ρ_3 are densities of the pure components, where "1" , "2" and "3" refer to the IL, an alcohol and alkyl acetate or nitromethane respectively, and ρ is the density of the mixture.

The density and V_{123}^{E} data are given in Tables 6.1-6.7 for the systems ($[MOA]^+[Tf_2N]^-$ + methanol or ethanol + methyl acetate or ethyl acetate) at T = (298.15, 303.15 and 313.15) K and ($[BMIM]^+[MeSO_4]^-$ + methanol or ethanol or 1-propanol + nitromethane) at T = 298.15 K. The graphs of V_{123}^{E} at constant z values ($z = x_3/x_1$) were plotted in Figures 6.1-6.15 for the systems {$[MOA]^+[Tf_2N]^-$ + methanol or ethanol + methyl acetate or ethyl acetate} at T = (298.15, 303.15 and 313.15) K and{ $[BMIM]^+[MeSO_4]^-$ + methanol or ethanol or 1-propanol + nitromethane} at T = 298.15 K.

The Cibulka equation was used to correlate the ternary data using the binary parameters obtained from the Redlich-Kister equation. The binary Redlich-Kister parameters used for the Cibulka equation correlation is given in Appendix 1. The Cibulka equation is given below:

$$V_{123}^{\mathrm{E}} = \sum_{i,j=1,2;1,3;2,3} V_{\mathrm{ij}}^{\mathrm{E}}\left(x_i, x_j\right) \quad + \quad x_1 x_2 x_3 (b_0 + b_1 x_1 + b_2 x_2) \tag{6.2}$$

where x_1, x_2 and x_3 are the mole fractions of IL, alcohols and methyl acetate, or ethyl acetate or nitromethane, respectively. It contains three parameters (b_0, b_1, b_2) included in the last term of equation (6.2) which is a correction over the binary contributions. The correlation coefficients and the standard deviation, σ_{s}, (rmsd) values are given in the Table 6.8-6.9 for all the ternary systems. The graphs obtained from using the Cibulka parameters are given in Figures 6.16-6.30.

The standard deviations (σ_{s}) is defined as:

$$\sigma_{\mathrm{s}} = [(V_{123\,\mathrm{exp}}^{\mathrm{E}} - V_{123\,\mathrm{cal}}^{\mathrm{E}})^2/n - k]^{1/2} \tag{6.3}$$

where n is the number of experimental points and k is the number of coefficients used in the Cibulka correlation equation.

6.1.1 $[MOA]^+[Tf_2N]^-$

The ternary excess molar volumes were calculated using equation (6.1) from the experimental density, ρ, values for each temperature. For each temperature , ρ, values were obtained for a fixed z value where ($z = x_3/x_1$) z = 0.30, 0.50, 1.00, 1.50, 4.00, 9.00 for the ($[MOA]^+[Tf_2N]^-$ + methanol + methyl acetate), z = 7.50, 3.36, 1.80, 1.00, 0.43, 0.10 for the ($[MOA]^+[Tf_2N]^-$ + methanol + ethyl acetate), z = 0.10, 0.20, 0.50, 1.00, 1.50, 4.00, 9.00 for the ($[MOA]^+[Tf_2N]^-$ + ethanol + methyl acetate) and z = 0.08, 0.25, 0.40, 0.80,1.30, 4.00 9.00 for the ($[MOA]^+[Tf_2N]^-$ + ethanol + ethyl acetate) systems.

The z values were kept constant with only a change in x_2. This was to ensure that the entire composition range was covered.

The excess molar volumes for the ternary systems ($[MOA]^+[Tf_2N]^-$ + methanol or ethanol + methyl acetate or ethyl acetate) were obtained at three temperatures namely T = (298.15, 303.15 and 313.15) K.

6.1.2 $[BMIM]^+[MeSO_4]^-$

The ternary excess molar volumes were calculated using equation (6.1) from the experimental density, ρ, values for each temperature. For each temperature, ρ, values were obtained for a fixed z value where ($z = x_3/x_1$) for z = 4.21, 1.87, 0.70, 0.23 and 0.04.

The z values were kept constant with only a change in x_2. This was to ensure that the entire composition range was covered.

The excess molar volumes for the ternary systems {$[BMIM]^+[MeSO_4]^-$ + methanol or ethanol or 1-propanol + nitromethane} were obtained at temperatures T = 298.15 K.

Table 6.1 Density, ρ, and ternary excess molar volume, V^{E}_{123}, for ([MOA]$^{+}$[Tf$_2$N]$^{-}$ + methanol + methyl acetate) at T = (298.15, 303.15, and 313.15) K

x_1	x_2	ρ / g·cm^{-3}	V^{E}_{123} / cm^3· mol^{-1}
{[MOA]$^{+}$[Tf$_2$N]$^{-}$ (x_1) + methanol (x_2) + methyl acetate (x_3)}			
T = 298.15 K			
0.0596	0.7022	0.9620	-0.67
0.1006	0.4969	1.0045	-0.88
0.1434	0.2835	1.0298	-1.02
0.1637	0.1812	1.0380	-1.03
0.1999	0.0000	1.0485	-0.89
0.1564	0.6090	1.0295	-0.85
0.2382	0.4046	1.0566	-1.08
0.2791	0.3018	1.0650	-1.13
0.3329	0.1681	1.0735	-1.21
0.3995	0.0000	1.0814	-1.33
0.2615	0.6078	1.0605	-1.02
0.3983	0.4026	1.0812	-1.20
0.5309	0.2037	1.0921	-1.32
0.5997	0.1004	1.0960	-1.36
0.6659	0.0000	1.0989	-1.34
0.1867	0.7573	1.0385	-0.78
0.3606	0.5313	1.0768	-1.14
0.5182	0.3263	1.0914	-1.28
0.6259	0.1863	1.0975	-1.35
0.7709	0.0000	1.1029	-1.28
0.0397	0.6030	0.9401	-0.30
0.0696	0.3023	0.9866	-0.57
0.0899	0.1012	1.0042	-0.49
0.1000	0.0000	1.0106	-0.37
0.0641	0.8718	0.9545	-0.42

0.1195	0.7608	1.0070	-0.62
0.2418	0.5164	1.0565	-1.00
0.3478	0.3045	1.0754	-1.21
0.4567	0.0867	1.0865	-1.31
0.5000	0.0000	1.0898	-1.38
	T = 303.15 K		
0.0596	0.7022	0.9610	-0.93
0.1006	0.4969	1.0040	-1.32
0.1434	0.2835	1.0280	-1.41
0.1637	0.1812	1.0363	-1.49
0.1999	0.0000	1.0460	-1.30
0.1564	0.6090	1.0285	-1.24
0.2382	0.4046	1.0556	-1.63
0.2791	0.3018	1.0635	-1.66
0.3329	0.1681	1.0720	-1.83
0.3995	0.0000	1.0792	-1.88
0.2615	0.6078	1.0590	-1.43
0.3983	0.4026	1.0797	-1.79
0.5309	0.2037	1.0902	-1.95
0.5997	0.1004	1.0938	-1.96
0.6659	0.0000	1.0965	-1.92
0.1867	0.7573	1.0370	-1.07
0.3606	0.5313	1.0752	-1.63
0.5182	0.3263	1.0898	-1.95
0.6259	0.1863	1.0955	-2.00
0.7709	0.0000	1.1002	-1.78
0.0397	0.6030	0.9374	-0.44
0.0696	0.3023	0.9855	-0.98
0.0899	0.1012	1.0016	-0.81
0.1000	0.0000	1.0069	-0.59
0.0641	0.8718	0.9530	-0.58

0.1195	0.7608	1.0065	-0.97
0.2418	0.5164	1.0560	-1.60
0.3478	0.3045	1.0740	-1.81
0.4567	0.0867	1.0845	-1.91
0.5000	0.0000	1.0875	-1.93
	T = 313.15 K		
0.0596	0.7022	0.9526	-1.15
0.1006	0.4969	0.9960	-1.60
0.1434	0.2835	1.0206	-1.80
0.1637	0.1812	1.0278	-1.71
0.1999	0.0000	1.0370	-1.43
0.1564	0.6090	1.0210	-1.54
0.2382	0.4046	1.0485	-2.01
0.2791	0.3018	1.0570	-2.17
0.3329	0.1681	1.0652	-2.30
0.3995	0.0000	1.0720	-2.27
0.2615	0.6078	1.0520	-1.78
0.3983	0.4026	1.0730	-2.22
0.5309	0.2037	1.0840	-2.57
0.5997	0.1004	1.0876	-2.61
0.6659	0.0000	1.0905	-2.69
0.1867	0.7573	1.0295	-1.33
0.3606	0.5313	1.0686	-2.07
0.5182	0.3263	1.0834	-2.48
0.6259	0.1863	1.0891	-2.57
0.7709	0.0000	1.0932	-2.12
0.0397	0.6030	0.9267	-0.49
0.0696	0.3023	0.9750	-1.05
0.0899	0.1012	0.9916	-0.92
0.1000	0.0000	0.9983	-0.87
0.0641	0.8718	0.9433	-0.65

0.1195	0.7608	0.9970	-1.02
0.2418	0.5164	1.0485	-1.88
0.3478	0.3045	1.0672	-2.25
0.4567	0.0867	1.0778	-2.41
0.5000	0.0000	1.0805	-2.35

Table 6.2 Density, ρ, and ternary excess molar volume, V^{E}_{123}, for ([MOA]$^{+}$[Tf$_2$N]$^{-}$ + methanol + ethyl acetate) at T = (298.15, 303.15, and 313.15) K

x_1	x_2	ρ /g·cm^{-3}	V^{E}_{123} / cm^3· mol^{-1}
{[MOA]$^{+}$[Tf$_2$N]$^{-}$ (x_1) + methanol (x_2) + ethyl acetate (x_3)}			
	T = 298.15 K		
0.9077	0.0000	1.1045	-0.57
0.7075	0.2218	1.0986	-0.72
0.6265	0.3103	1.0955	-0.87
0.5123	0.4369	1.0895	-1.03
0.4200	0.5381	1.0823	-1.09
0.3364	0.6294	1.0727	-1.09
0.2604	0.7133	1.0585	-0.86
0.1850	0.7964	1.0371	-0.76
0.0890	0.9021	0.9762	-0.19
0.6987	0.0000	1.0965	-1.58
0.6273	0.1024	1.0938	-1.61
0.5613	0.1987	1.0908	-1.64
0.4837	0.3085	1.0857	-1.51
0.4165	0.4048	1.0808	-1.61
0.3460	0.5047	1.0734	-1.59
0.2786	0.6019	1.0623	-1.34
0.1999	0.7139	1.0429	-1.14
0.1330	0.8099	1.0135	-0.83
0.0864	0.8764	0.9764	-0.45
0.5009	0.0000	1.0815	-1.59
0.4467	0.1065	1.0779	-1.60
0.3995	0.2022	1.0742	-1.62
0.3453	0.3073	1.0689	-1.67
0.2937	0.4119	1.0621	-1.64
0.2509	0.5004	1.0547	-1.60

0.1982	0.6035	1.0410	-1.38
0.1465	0.7071	1.0212	-1.17
0.0484	0.9033	0.9315	-0.54
0.1053	0.5406	1.0018	-1.96
0.1292	0.4363	1.0145	-2.13
0.1534	0.3307	1.0232	-2.13
0.1771	0.2272	1.0293	-2.02
0.2028	0.1153	1.0339	-1.77
0.0421	0.6392	0.9450	-1.78
0.0775	0.3360	0.9840	-2.30
0.1032	0.1156	0.9950	-1.93
0.0852	0.7613	0.9825	-1.18
0.1371	0.6161	1.0185	-1.67
0.1918	0.4630	1.0391	-1.96
0.2564	0.2820	1.0528	-2.00
0.3312	0.0727	1.0613	-1.64
0.3571	0.0000	1.0627	-1.30
	$T = 303.15$ K		
0.9077	0.0000	1.1006	-0.50
0.7075	0.2218	1.0943	-0.52
0.6265	0.3103	1.0915	-0.81
0.5123	0.4369	1.0859	-1.11
0.4200	0.5381	1.0781	-1.02
0.3364	0.6294	1.0679	-0.92
0.2604	0.7133	1.0535	-0.69
0.1850	0.7964	1.0291	-0.23
0.0890	0.9021	0.9724	-0.25
0.6987	0.0000	1.0921	-1.40
0.6273	0.1024	1.0895	-1.49
0.5613	0.1987	1.0865	-1.54
0.4837	0.3085	1.0819	-1.58

0.4165	0.4048	1.0765	-1.55
0.3460	0.5047	1.0691	-1.55
0.2786	0.6019	1.0580	-1.32
0.1999	0.7139	1.0388	-1.16
0.1330	0.8099	1.0095	-0.87
0.0864	0.8764	0.9731	-0.56
0.5009	0.0000	1.0769	-1.46
0.4467	0.1065	1.0734	-1.52
0.3995	0.2022	1.0698	-1.58
0.3453	0.3073	1.0644	-1.62
0.2937	0.4119	1.0576	-1.61
0.2509	0.5004	1.0498	-1.50
0.1982	0.6035	1.0366	-1.38
0.1465	0.7071	1.0169	-1.20
0.0484	0.9033	0.9269	-0.55
0.1053	0.5406	0.9978	-2.08
0.1292	0.4363	1.0115	-2.39
0.1534	0.3307	1.0198	-2.36
0.1771	0.2272	1.0255	-2.20
0.2028	0.1153	1.0304	-2.02
0.0421	0.6392	0.9420	-1.99
0.0775	0.3360	0.9820	-2.71
0.1032	0.1156	0.9915	-2.21
0.0852	0.7613	0.9799	-1.39
0.1371	0.6161	1.0144	-1.75
0.1918	0.4630	1.0354	-2.10
0.2564	0.2820	1.0492	-2.18
0.3312	0.0727	1.0575	-1.80
0.3571	0.0000	1.0582	-1.29
	T = 313.15 K		
0.9077	0.0000	1.0933	-0.67

0.7075	0.2218	1.0865	-0.49
0.6265	0.3103	1.0830	-0.55
0.5123	0.4369	1.0762	-0.55
0.4200	0.5381	1.0683	-0.54
0.3364	0.6294	1.0579	-0.49
0.2604	0.7133	1.0438	-0.41
0.1850	0.7964	1.0213	-0.30
0.0890	0.9021	0.9631	-0.19
0.6987	0.0000	1.0848	-1.71
0.6273	0.1024	1.0815	-1.53
0.5613	0.1987	1.0778	-1.35
0.4837	0.3085	1.0723	-1.16
0.4165	0.4048	1.0665	-1.09
0.3460	0.5047	1.0580	-0.92
0.2786	0.6019	1.0472	-0.86
0.1999	0.7139	1.0272	-0.70
0.1330	0.8099	0.9977	-0.52
0.0864	0.8764	0.9620	-0.35
0.5009	0.0000	1.0693	-1.80
0.4467	0.1065	1.0650	-1.60
0.3995	0.2022	1.0606	-1.45
0.3453	0.3073	1.0543	-1.31
0.2937	0.4119	1.0470	-1.24
0.2509	0.5004	1.0386	-1.07
0.1982	0.6035	1.0249	-0.95
0.1465	0.7071	1.0046	-0.78
0.0484	0.9033	0.9181	-0.59
0.1053	0.5406	0.9904	-2.43
0.1292	0.4363	1.0026	-2.59
0.1534	0.3307	1.0109	-2.58
0.1771	0.2272	1.0172	-2.54

0.2028	0.1153	1.0215	-2.28
0.0421	0.6392	0.9330	-2.18
0.0775	0.3360	0.9730	-3.01
0.1032	0.1156	0.9820	-2.51
0.0852	0.7613	0.9710	-1.47
0.1371	0.6161	1.0055	-1.83
0.1918	0.4630	1.0271	-2.30
0.2564	0.2820	1.0410	-2.43
0.3312	0.0727	1.0490	-2.01
0.3571	0.0000	1.0504	-1.68

Table 6.3 Density, ρ, and ternary excess molar volume, V_{123}^{E}, for ([MOA]$^{+}$[Tf$_2$N]$^{-}$ + ethanol + methyl acetate) at T = (298.15, 303.15, and 313.15) K

x_1	x_2	ρ/g·cm^{-3}	V_{123}^{E} / cm^3· mol^{-1}
{[MOA]$^{+}$[Tf$_2$N]$^{-}$ (x_1) + ethanol (x_2) + methyl acetate (x_3)}			
T = 298.15 K			
0.0749	0.6258	0.9632	-1.12
0.1169	0.4168	1.0045	-1.34
0.1364	0.3192	1.0182	-1.39
0.1538	0.2310	1.0278	-1.31
0.1698	0.1531	1.0348	-1.15
0.1853	0.0738	1.0410	-1.01
0.2000	0.0000	1.0459	-0.81
0.1027	0.7434	0.9780	-1.27
0.1503	0.6244	1.0121	-1.50
0.1925	0.5203	1.0325	-1.60
0.2331	0.4192	1.0465	-1.56
0.2715	0.3211	1.0575	-1.62
0.3078	0.2305	1.0655	-1.57
0.3488	0.1269	1.0728	-1.48
0.4001	0.0000	1.0800	-1.31
0.3199	0.5191	1.0630	-1.90
0.3879	0.4186	1.0745	-1.95
0.4542	0.3194	1.0825	-1.85
0.5085	0.2373	1.0878	-1.78
0.5645	0.1554	1.0920	-1.59
0.6150	0.0747	1.0955	-1.50
0.6651	0.0000	1.0984	-1.38
0.7456	0.1825	1.1013	-1.79
0.8255	0.0955	1.1046	-1.67

0.6689	0.2667	1.0975	-1.91
0.5834	0.3603	1.0921	-1.99
0.3778	0.5858	1.0704	-1.96
0.4298	0.4420	1.0789	-2.00
0.5290	0.3133	1.0888	-1.91
0.5744	0.2537	1.0922	-1.82
0.6623	0.1403	1.0978	-1.70
0.7436	0.0352	1.1018	-1.53
0.0133	0.8671	0.8448	-0.11
0.0266	0.7352	0.8873	-0.14
0.0486	0.5134	0.9393	-0.29
0.0590	0.4113	0.9590	-0.49
0.0681	0.3176	0.9730	-0.51
0.0765	0.2306	0.9845	-0.55
0.0924	0.0761	1.0020	-0.52
0.1013	0.0000	1.0082	-0.27
0.0874	0.8256	0.9601	-1.17
0.1555	0.6893	1.0118	-1.52
0.2868	0.4268	1.0589	-1.81
0.3826	0.2354	1.0760	-1.72
0.4678	0.0663	1.0857	-1.45
0.5003	0.0000	1.0888	-1.37
	T = 303.15 K		
0.0749	0.6258	0.9584	-1.14
0.1169	0.4168	0.9985	-1.21
0.1364	0.3192	1.0118	-1.19
0.1538	0.2310	1.0218	-1.16
0.1698	0.1531	1.0298	-1.15
0.1853	0.0738	1.0368	-1.14
0.2000	0.0000	1.0428	-1.14
0.1027	0.7434	0.9755	-1.53

0.1503	0.6244	1.0100	-1.85
0.1925	0.5203	1.0300	-1.93
0.2331	0.4192	1.0440	-1.92
0.2715	0.3211	1.0551	-2.03
0.3078	0.2305	1.0632	-2.04
0.3488	0.1269	1.0706	-2.00
0.4001	0.0000	1.0780	-1.93
0.3199	0.5191	1.0603	-2.22
0.3879	0.4186	1.0715	-2.23
0.4542	0.3194	1.0798	-2.24
0.5085	0.2373	1.0850	-2.16
0.5645	0.1554	1.0895	-2.09
0.6150	0.0747	1.0932	-2.10
0.6651	0.0000	1.0962	-2.05
0.7456	0.1825	1.0985	-2.21
0.8255	0.0955	1.1020	-2.16
0.6689	0.2667	1.0946	-2.27
0.5834	0.3603	1.0892	-2.32
0.3778	0.5858	1.0675	-2.23
0.4298	0.4420	1.0758	-2.25
0.5290	0.3133	1.0857	-2.19
0.5744	0.2537	1.0895	-2.23
0.6623	0.1403	1.0950	-2.12
0.7436	0.0352	1.0992	-2.06
0.0133	0.8671	0.8403	-0.14
0.0266	0.7352	0.8824	-0.16
0.0486	0.5134	0.9339	-0.28
0.0590	0.4113	0.9540	-0.53
0.0681	0.3176	0.9690	-0.67
0.0765	0.2306	0.9807	-0.75
0.0924	0.0761	0.9980	-0.72

0.1013	0.0000	1.0045	-0.52
0.0874	0.8256	0.9562	-1.25
0.1555	0.6893	1.0097	-1.86
0.2868	0.4268	1.0560	-2.11
0.3826	0.2354	1.0735	-2.16
0.4678	0.0663	1.0835	-2.03
0.5003	0.0000	1.0866	-1.98
0.0397	0.6030	0.9374	-0.44
0.0696	0.3023	0.9855	-0.98
0.0899	0.1012	1.0016	-0.81
0.1000	0.0000	1.0069	-0.59
0.0641	0.8718	0.9530	-0.58
0.1195	0.7608	1.0065	-0.97
0.2418	0.5164	1.0560	-1.59
0.3478	0.3045	1.0740	-1.81
0.4567	0.0867	1.0845	-1.91
0.5000	0.0000	1.0875	-1.93
0.0749	0.6258	0.9584	-1.14
0.1169	0.4168	0.9985	-1.21
0.1364	0.3192	1.0118	-1.19
0.1538	0.2310	1.0218	-1.16
0.1698	0.1531	1.0298	-1.15
0.1853	0.0738	1.0368	-1.14
0.2000	0.0000	1.0428	-1.14
0.1027	0.7434	0.9755	-1.53
0.1503	0.6244	1.0100	-1.85
0.1925	0.5203	1.0300	-1.93
0.2331	0.4192	1.0440	-1.92
0.2715	0.3211	1.0551	-2.03
0.3078	0.2305	1.0632	-2.04
0.3488	0.1269	1.0706	-2.00

0.4001	0.0000	1.0780	-1.93
0.3199	0.5191	1.0603	-2.22
0.3879	0.4186	1.0715	-2.23
0.4542	0.3194	1.0798	-2.24
0.5085	0.2373	1.0850	-2.16
0.5645	0.1554	1.0895	-2.09
0.6150	0.0747	1.0932	-2.10
0.6651	0.0000	1.0962	-2.05
0.7456	0.1825	1.0985	-2.21
0.8255	0.0955	1.1020	-2.16
0.6689	0.2667	1.0946	-2.27
0.5834	0.3603	1.0892	-2.32
0.3778	0.5858	1.0675	-2.23
0.4298	0.4420	1.0758	-2.25
0.5290	0.3133	1.0857	-2.19
0.5744	0.2537	1.0895	-2.23
0.6623	0.1403	1.0950	-2.12
0.7436	0.0352	1.0992	-2.06
0.0133	0.8671	0.8403	-0.14
0.0266	0.7352	0.8824	-0.16
0.0486	0.5134	0.9339	-0.28
0.0590	0.4113	0.9540	-0.53
0.0681	0.3176	0.9690	-0.67
0.0765	0.2306	0.9807	-0.75
0.0924	0.0761	0.9980	-0.72
0.1013	0.0000	1.0045	-0.52
0.0874	0.8256	0.9562	-1.25
0.1555	0.6893	1.0097	-1.86
0.2868	0.4268	1.0560	-2.11
0.3826	0.2354	1.0735	-2.16
0.4678	0.0663	1.0835	-2.03

0.5003	0.0000	1.0866	-1.98
	T = 313.15 K		
0.0749	0.6258	0.9490	-1.15
0.1169	0.4168	0.9920	-1.63
0.1364	0.3192	1.0055	-1.68
0.1538	0.2310	1.0159	-1.75
0.1698	0.1531	1.0235	-1.71
0.1853	0.0738	1.0290	-1.48
0.2000	0.0000	1.0335	-1.23
0.1027	0.7434	0.9655	-1.40
0.1503	0.6244	1.0002	-1.73
0.1925	0.5203	1.0199	-1.76
0.2331	0.4192	1.0360	-2.08
0.2715	0.3211	1.0475	-2.28
0.3078	0.2305	1.0560	-2.40
0.3488	0.1269	1.0635	-2.33
0.4001	0.0000	1.0705	-2.26
0.3199	0.5191	1.0545	-2.73
0.3879	0.4186	1.0662	-2.85
0.4542	0.3194	1.0740	-2.91
0.5085	0.2373	1.0792	-2.86
0.5645	0.1554	1.0838	-2.85
0.6150	0.0747	1.0870	-2.69
0.6651	0.0000	1.0895	-2.56
0.7456	0.1825	1.0925	-2.93
0.8255	0.0955	1.0958	-2.84
0.6689	0.2667	1.0888	-3.01
0.5834	0.3603	1.0834	-3.00
0.3778	0.5858	1.0612	-2.64
0.4298	0.4420	1.0698	-2.80
0.5290	0.3133	1.0800	-2.90

0.5744	0.2537	1.0835	-2.88
0.6623	0.1403	1.0890	-2.82
0.7436	0.0352	1.0930	-2.75
0.0133	0.8671	0.8312	-0.13
0.0266	0.7352	0.8727	-0.14
0.0486	0.5134	0.9238	-0.27
0.0590	0.4113	0.9445	-0.61
0.0681	0.3176	0.9610	-0.96
0.0765	0.2306	0.9725	-1.03
0.0924	0.0761	0.9895	-1.01
0.1013	0.0000	0.9955	-0.76
0.0874	0.8256	0.9472	-1.22
0.1555	0.6893	1.0045	-2.37
0.2868	0.4268	1.0500	-2.64
0.3826	0.2354	1.0672	-2.71
0.4678	0.0663	1.0770	-2.59
0.5003	0.0000	1.0795	-2.38

Table 6.4 Density, ρ, and ternary excess molar volume, V_{123}^{E}, for ([MOA]$^{+}$[Tf$_2$N]$^{-}$ + ethanol + ethyl acetate) at T = (298.15, 303.15, and 313.15) K

x_1	x_2	ρ/g·cm^{-3}	V_{123}^{E} / cm^3· mol^{-1}
{[MOA]$^{+}$[Tf$_2$N]$^{-}$ (x_1) + ethanol (x_2) + ethyl acetate (x_3)}			
		T = 298.15 K	
0.0786	0.6570	0.9640	-2.13
0.1260	0.4501	1.0005	-2.20
0.1490	0.3499	1.0129	-2.24
0.1706	0.2558	1.0220	-2.18
0.1903	0.1698	1.0288	-2.09
0.2102	0.0831	1.0343	-1.91
0.1558	0.6476	1.0090	-1.70
0.2011	0.5454	1.0290	-1.87
0.2465	0.4425	1.0426	-1.81
0.2901	0.3430	1.0529	-1.79
0.3320	0.2492	1.0605	-1.71
0.3827	0.1344	1.0679	-1.59
0.4423	0.0000	1.0749	-1.49
0.3292	0.5326	1.0598	-1.59
0.4037	0.4268	1.0712	-1.51
0.4702	0.3320	1.0788	-1.42
0.5302	0.2472	1.0843	-1.33
0.5935	0.1556	1.0888	-1.15
0.6508	0.0754	1.0928	-1.20
0.7044	0.0000	1.0965	-1.44
0.7542	0.1847	1.0985	-0.81
0.8378	0.0943	1.1021	-0.70
0.6755	0.2697	1.0943	-0.87
0.5880	0.3644	1.0885	-0.93
0.3800	0.5892	1.0645	-0.63
0.9251	0.0000	1.1051	-0.52

0.2454	0.6932	1.0380	-1.13
0.3145	0.6067	1.0555	-1.27
0.4388	0.4513	1.0750	-1.28
0.5427	0.3214	1.0855	-1.27
0.5911	0.2609	1.0890	-1.15
0.6845	0.1441	1.0947	-0.99
0.7707	0.0363	1.0995	-1.11
0.7998	0.0000	1.1012	-1.27
0.0275	0.7642	0.8975	-1.84
0.0523	0.5520	0.9475	-2.52
0.0642	0.4497	0.9631	-2.61
0.0863	0.2603	0.9836	-2.53
0.1069	0.0833	0.9960	-2.16
0.0885	0.8373	0.9575	-1.15
0.1595	0.7066	1.0085	-1.48
0.3006	0.4468	1.0545	-1.67
0.4074	0.2497	1.0710	-1.44
0.5054	0.0693	1.0815	-1.38
0.5436	0.0000	1.0853	-1.55
	T = 303.15 K		
0.0786	0.6570	0.9600	-2.24
0.1260	0.4501	0.9976	-2.49
0.1490	0.3499	1.0105	-2.63
0.1706	0.2558	1.0195	-2.59
0.1903	0.1698	1.0260	-2.46
0.2102	0.0831	1.0310	-2.21
0.1558	0.6476	1.0068	-2.04
0.2011	0.5454	1.0260	-2.11
0.2465	0.4425	1.0393	-2.02
0.2901	0.3430	1.0493	-1.95
0.3320	0.2492	1.0567	-1.84

0.3827	0.1344	1.0639	-1.68
0.4423	0.0000	1.0706	-1.49
0.3292	0.5326	1.0563	-1.74
0.4037	0.4268	1.0675	-1.61
0.4702	0.3320	1.0747	-1.38
0.5302	0.2472	1.0800	-1.24
0.5935	0.1556	1.0847	-1.13
0.6508	0.0754	1.0888	-1.19
0.7044	0.0000	1.0923	-1.34
0.7542	0.1847	1.0944	-0.68
0.8378	0.0943	1.0980	-0.55
0.6755	0.2697	1.0904	-0.84
0.5880	0.3644	1.0846	-0.92
0.3800	0.5892	1.0612	-0.80
0.9251	0.0000	1.1012	-0.45
0.2454	0.6932	1.0350	-1.35
0.3145	0.6067	1.0525	-1.50
0.4388	0.4513	1.0710	-1.28
0.5427	0.3214	1.0810	-1.09
0.5911	0.2609	1.0848	-1.05
0.6845	0.1441	1.0905	-0.86
0.7707	0.0363	1.0952	-0.91
0.7998	0.0000	1.0970	-1.12
0.0275	0.7642	0.8940	-1.99
0.0523	0.5520	0.9445	-2.76
0.0642	0.4497	0.9610	-2.99
0.0863	0.2603	0.9815	-2.97
0.1069	0.0833	0.9930	-2.51
0.0885	0.8373	0.9535	-1.21
0.1595	0.7066	1.0060	-1.77
0.3006	0.4468	1.0506	-1.75

0.4074	0.2497	1.0670	-1.47
0.5054	0.0693	1.0772	-1.33
0.5436	0.0000	1.0810	-1.49
	T = 313.15 K		
0.0786	0.6570	0.9525	-2.52
0.1260	0.4501	0.9905	-2.92
0.1490	0.3499	1.0022	-2.92
0.1706	0.2558	1.0106	-2.81
0.1903	0.1698	1.0170	-2.69
0.2102	0.0831	1.0220	-2.46
0.1558	0.6476	0.9992	-2.26
0.2011	0.5454	1.0183	-2.35
0.2465	0.4425	1.0314	-2.24
0.2901	0.3430	1.0414	-2.19
0.3320	0.2492	1.0487	-2.06
0.3827	0.1344	1.0557	-1.87
0.4423	0.0000	1.0625	-1.72
0.3292	0.5326	1.0480	-1.74
0.4037	0.4268	1.0590	-1.54
0.4702	0.3320	1.0666	-1.40
0.5302	0.2472	1.0720	-1.28
0.5935	0.1556	1.0765	-1.09
0.6508	0.0754	1.0810	-1.29
0.7044	0.0000	1.0848	-1.56
0.7542	0.1847	1.0865	-0.59
0.8378	0.0943	1.0902	-0.48
0.6755	0.2697	1.0825	-0.77
0.5880	0.3644	1.0765	-0.80
0.3800	0.5892	1.0528	-0.67
0.9251	0.0000	1.0934	-0.35
0.2454	0.6932	1.0268	-1.35

0.3145	0.6067	1.0446	-1.56
0.4388	0.4513	1.0630	-1.29
0.5427	0.3214	1.0730	-1.07
0.5911	0.2609	1.0768	-1.03
0.6845	0.1441	1.0825	-0.82
0.7707	0.0363	1.0876	-1.03
0.7998	0.0000	1.0898	-1.41
0.0275	0.7642	0.8858	-2.17
0.0523	0.5520	0.9368	-3.11
0.0642	0.4497	0.9535	-3.41
0.0863	0.2603	0.9736	-3.43
0.1069	0.0833	0.9837	-2.85
0.0885	0.8373	0.9452	-1.28
0.1595	0.7066	0.9978	-1.86
0.3006	0.4468	1.0425	-1.87
0.4074	0.2497	1.0590	-1.62
0.5054	0.0693	1.0695	-1.60
0.5436	0.0000	1.0734	-1.80

Table 6.5 Density, ρ, and ternary excess molar volume, V_{123}^{E} , for ([BMIM]$^{+}$[MeSO$_4$]$^{-}$ + methanol + nitromethane) at T = 298.15 K

x_1	x_2	ρ/g·cm^{-3}	V_{123}^{E} /cm^3·mol^{-1}
{[BMIM]$^{+}$[MeSO$_4$]$^{-}$ (x_1) + methanol (x_2) + nitromethane (x_3)}			
	T = 298.15 K		
0.0485	0.7471	0.9590	-0.90
0.0903	0.5290	1.0484	-0.92
0.1099	0.4269	1.0808	-0.90
0.1452	0.2429	1.1325	-1.07
0.1771	0.0765	1.1642	-0.78
0.1332	0.6173	1.0583	-1.64
0.1998	0.4256	1.1148	-1.36
0.2390	0.3114	1.1383	-1.05
0.2971	0.1467	1.1678	-0.78
0.0603	0.8974	0.9177	-0.75
0.1591	0.7290	1.0420	-1.52
0.2494	0.5752	1.1014	-1.45
0.3119	0.4692	1.1292	-1.28
0.3705	0.3690	1.1494	-1.06
0.4720	0.1965	1.1752	-0.59
0.5271	0.1026	1.1866	-0.38
0.3706	0.5428	1.1285	-1.29
0.4692	0.4211	1.1541	-1.05
0.5494	0.3222	1.1700	-0.84
0.6151	0.2409	1.1798	-0.55
0.7242	0.1053	1.1943	-0.23
0.8468	0.1150	1.1971	-0.12
0.7200	0.2475	1.1835	-0.37

Table 6.6 Density, ρ, and ternary excess molar volume, V_{123}^{E} , for ([BMIM]$^{+}$[MeSO$_4$]$^{-}$ + ethanol + nitromethane) at T = 298.15 K

x_1	x_2	ρ/g·cm^{-3}	V_{123}^{E} /cm^3·mol^{-1}
{[BMIM]$^{+}$[MeSO$_4$]$^{-}$ (x_1) + ethanol (x_2) + nitromethane (x_3)}			
	T = 298.15 K		
0.0628	0.6726	0.9542	-0.82
0.1076	0.4385	1.0460	-0.93
0.1263	0.3412	1.0798	-0.96
0.1568	0.1824	1.1278	-0.83
0.1813	0.0545	1.1620	-0.65
0.1640	0.5288	1.0495	-1.35
0.2297	0.3403	1.1088	-1.08
0.2898	0.1676	1.1530	-0.82
0.3109	0.1070	1.1660	-0.67
0.0829	0.8588	0.9140	-0.75
0.2045	0.6517	1.0345	-1.33
0.3024	0.4850	1.0961	-1.27
0.3638	0.3807	1.1250	-1.08
0.4175	0.2891	1.1465	-0.90
0.5020	0.1454	1.1751	-0.62
0.2942	0.6370	1.0644	-1.29
0.4439	0.4523	1.1250	-1.16
0.5383	0.3359	1.1513	-0.86
0.6637	0.1808	1.1783	-0.39
0.7482	0.0757	1.1937	-0.16
0.8775	0.0829	1.1970	-0.11
0.7787	0.1862	1.1823	-0.23
0.6796	0.2898	1.1659	-0.49

Table 6.7 Density, ρ, and ternary excess molar volume, V_{123}^{E} , for ([BMIM]$^{+}$[MeSO$_4$]$^{-}$ + 1-propanol + nitromethane) at T = 298.15 K

x_1	x_2	ρ / g·cm^{-3}	V_{123}^{E} /cm^3·mol^{-1}
{[BMIM]$^{+}$[MeSO$_4$]$^{-}$ (x_1) + 1-propanol (x_2) + nitromethane (x_3)}			
	T = 298.15 K		
0.0979	0.4893	1.0039	-0.54
0.1372	0.2842	1.0785	-0.59
0.1637	0.1460	1.1255	-0.51
0.1836	0.0423	1.1604	-0.49
0.0745	0.6116	0.9571	-0.44
0.1199	0.3745	1.0463	-0.59
0.0539	0.7187	0.9152	-0.36
0.0350	0.8172	0.8747	-0.17
0.1871	0.4625	1.0490	-0.91
0.2495	0.2834	1.1083	-0.77
0.2803	0.1947	1.1339	-0.59
0.3188	0.0841	1.1655	-0.53
0.1454	0.5823	1.0045	-0.97
0.1639	0.7208	0.9770	-0.83
0.1037	0.8234	0.9210	-0.56
0.2412	0.5892	1.0355	-0.92
0.3410	0.4193	1.0954	-0.83
0.3993	0.3203	1.1244	-0.71
0.4477	0.2377	1.1457	-0.57
0.5197	0.1153	1.1745	-0.43
0.3456	0.5736	1.0644	-0.79
0.4964	0.3876	1.1240	-0.68
0.5841	0.2794	1.1512	-0.57
0.6930	0.1447	1.1792	-0.35
0.8948	0.0648	1.1969	-0.02

0.8141	0.1492	1.1825	-0.08
0.7289	0.2382	1.1665	-0.31

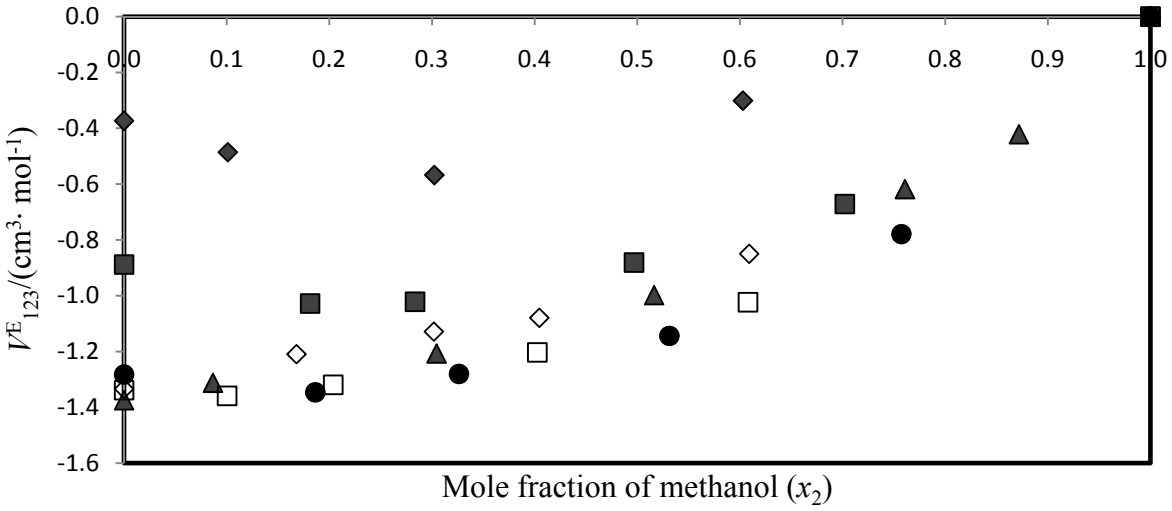

FIGURE 6.1 Graph of ternary excess molar volumes, V^E_{123} , for {[MOA]$^+$[Tf$_2$N]$^-$ (x_1) + methanol (x_2) + methyl acetate (x_3)} against mole fraction of methanol at T = 298.15 K. The symbols represent experimental data at constant $z = x_3/x_1$: ●, z = 0.30; □, z = 0.50; ▲, z = 1.00; ◊, z = 1.50; ■, z = 4.00; ♦, z = 9.00.

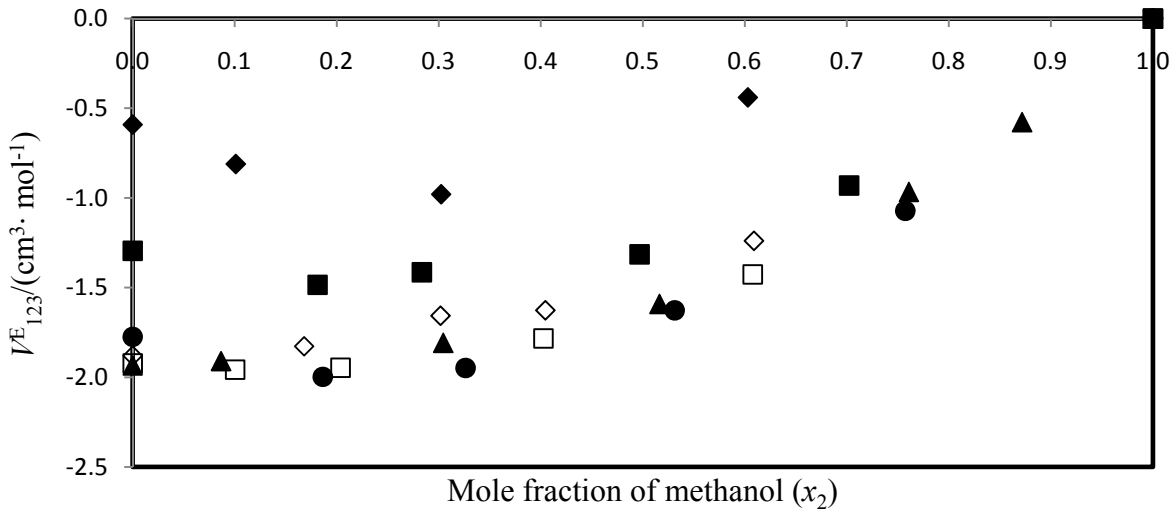

FIGURE 6.2 Graph of ternary excess molar volumes, V^{E}_{123} , for {[MOA]$^+$[Tf$_2$N]$^-$ (x_1) + methanol (x_2) + methyl acetate (x_3)} against mole fraction of methanol at T = 303.15 K. The symbols represent experimental data at constant $z = x_3/x_1$: ●, z = 0.30; □, z = 0.50; ▲, z = 1.00; ◊, z = 1.50; ■, z = 4.00; ♦, z = 9.00.

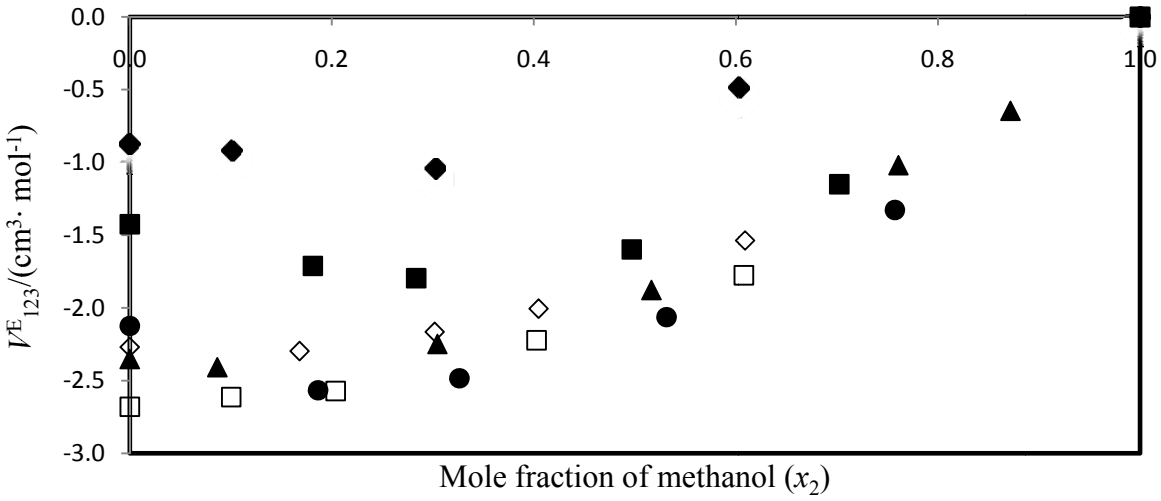

FIGURE 6.3 Graph of ternary excess molar volumes, V^E_{123} , for {[MOA]$^+$[Tf$_2$N]$^-$ (x_1) + methanol (x_2) + methyl acetate (x_3)} against mole fraction of methanol at T = 313.15 K . The symbols represent experimental data at constant $z = x_3/x_1$: ●, z = 0.30; □, z = 0.50; ▲, z = 1.00; ◊, z = 1.50; ■, z = 4.00; ♦, z = 9.00.

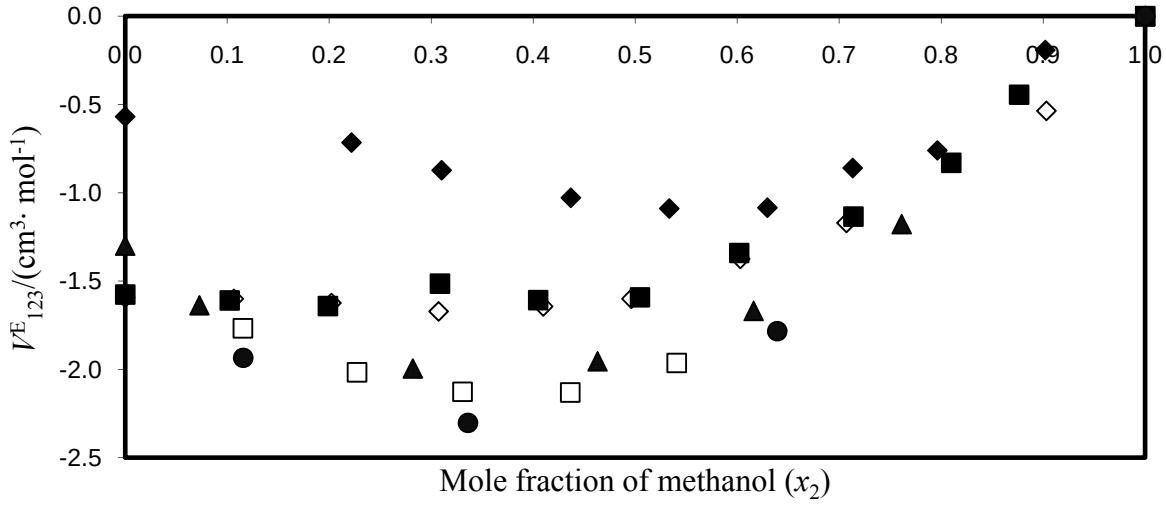

FIGURE 6.4 Graph of ternary excess molar volumes, V^E_{123} , for {[MOA]$^+$[Tf$_2$N]$^-$ (x_1) + methanol (x_2) + ethyl acetate (x_3)} against mole fraction of methanol at T = 298.15 K. The symbols represent experimental data at constant $z = x_3/x_1$: ●, z = 7.50; □, z = 3.36; ▲, z = 1.80; ◊, z = 1.00; ■, z = 0.43; ♦, z = 0.10.

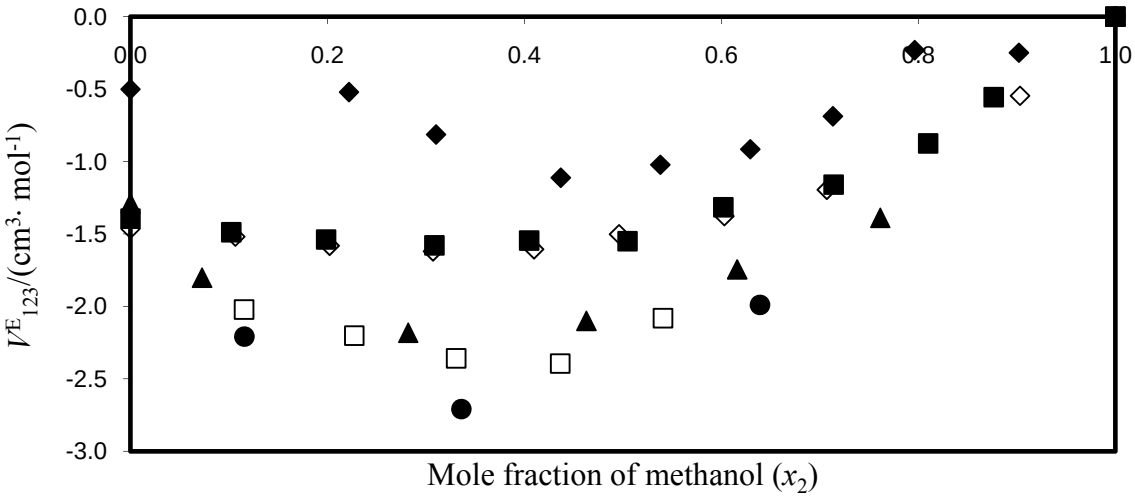

FIGURE 6.5 Graph of ternary excess molar volumes, V^E_{123} , for {[MOA]$^+$[Tf$_2$N]$^-$ (x_1) + methanol (x_2) + ethyl acetate (x_3)} against mole fraction of methanol at T = 303.15 K. The symbols represent experimental data: at constant $z = x_3/x_1$ ●, z = 7.50; □, z = 3.36; ▲, z = 1.80; ◊, z = 1.00; ■, z = 0.43; ♦, z = 0.10.

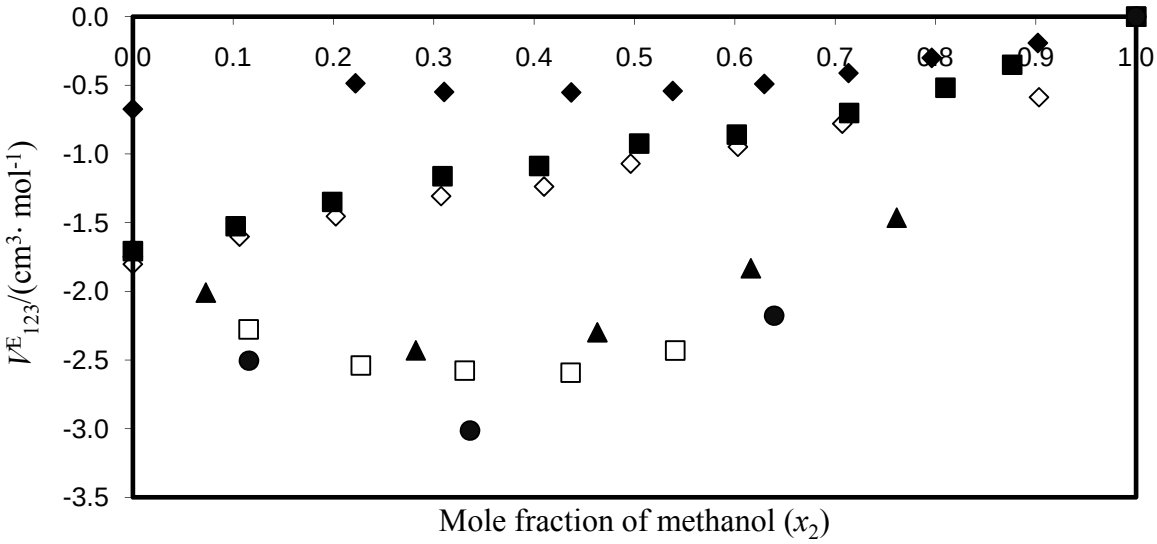

FIGURE 6.6 Graph of ternary excess molar volumes, V^{E}_{123} , for {[MOA]$^+$[Tf$_2$N]$^-$ (x_1) + methanol (x_2) + ethyl acetate (x_3)} against mole fraction of methanol at T = 313.15 K. The symbols represent experimental data at constant $z = x_3/x_1$: ●, z = 7.50; □, z = 3.36; ▲, z = 1.80; ◊, z = 1.00; ■, z = 0.43; ♦, z = 0.10.

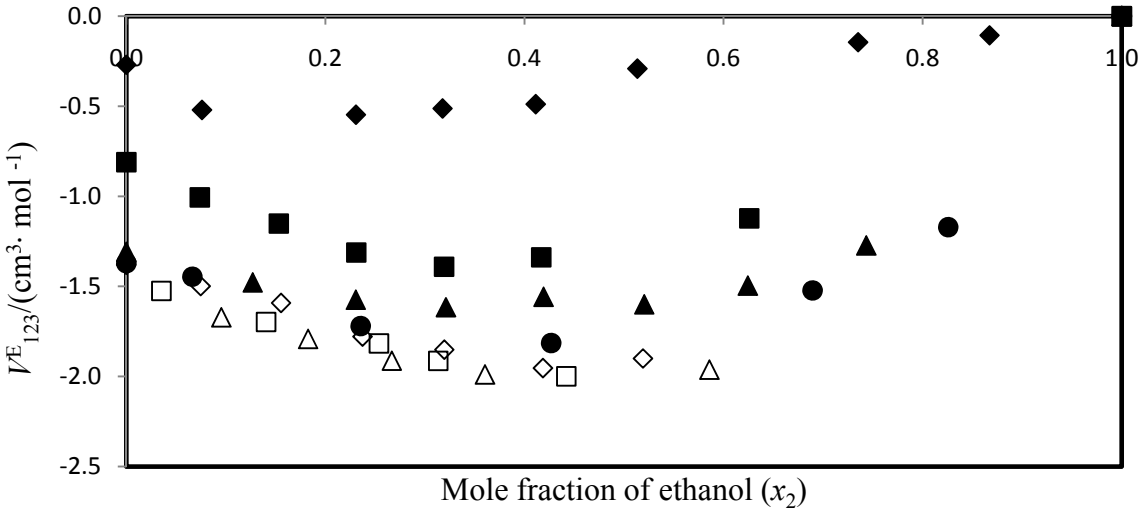

FIGURE 6.7 Graph of ternary excess molar volumes, V^{E}_{123} , for {[MOA]$^+$[Tf$_2$N]$^-$ (x_1) + ethanol (x_2) + methyl acetate (x_3)} against mole fraction of ethanol at T = 298.15 K. The symbols represent experimental data at constant $z = x_3/x_1$: Δ, z = 0.10 □, z = 0.20; ◊, z = 0.50; ●, z = 1.00; ▲, z = 1.50; ■, z = 4.00; ♦, z = 9.00.

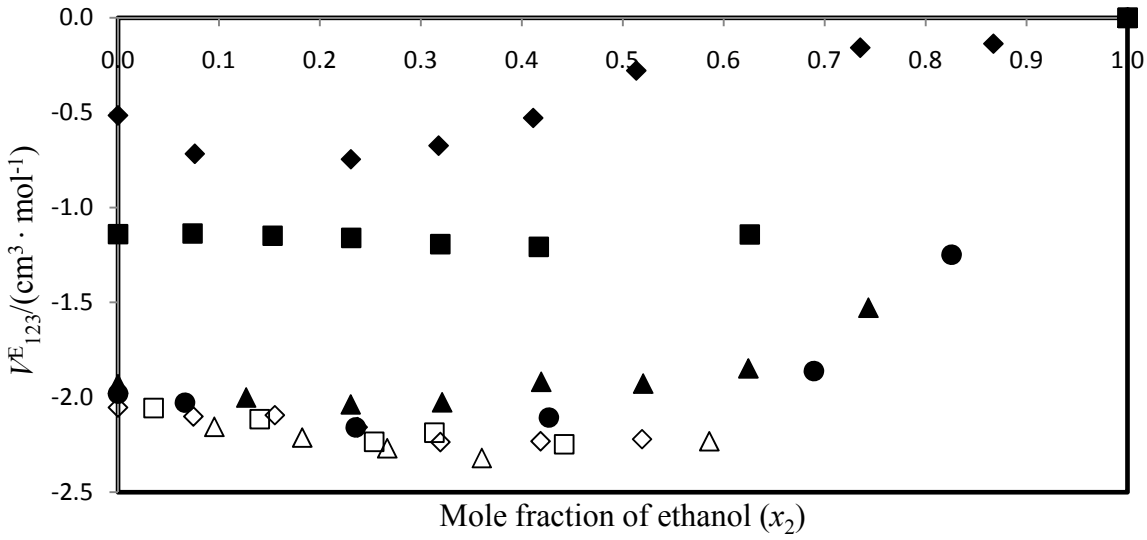

FIGURE 6.8 Graph of ternary excess molar volumes, V^E_{123} , for {$[MOA]^+[Tf_2N]^-$ (x_1) + ethanol (x_2) + methyl acetate (x_3)} against mole fraction of ethanol at T = 303.15 K. The symbols represent experimental data at constant $z = x_3/x_1$: Δ, z = 0.10 □, z = 0.20; ◊, z = .50; ●, z = 1.00; ▲, z = 1.50; ■, z = 4.00; ♦, z = 9.00.

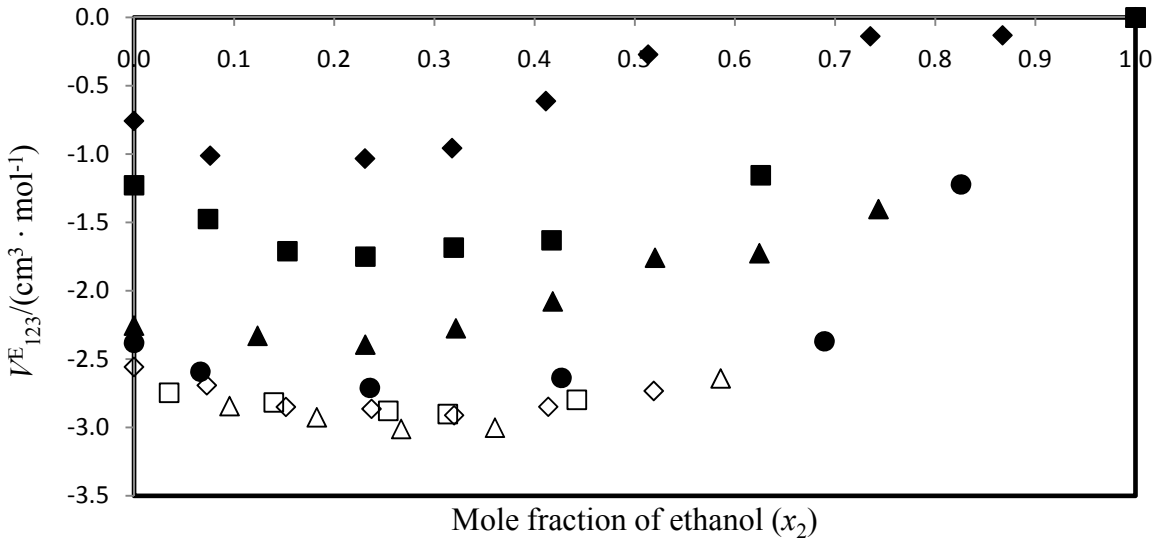

FIGURE 6.9 Graph of ternary excess molar volumes, V^{E}_{123} , for {$[MOA]^+[Tf_2N]^-$ (x_1) + ethanol (x_2) + methyl acetate (x_3)} against mole fraction of ethanol at T = 313.15 K. The symbols represent experimental data at constant $z = x_3/x_1$: Δ, z = 0.10 □, z = 0.20; ◊, z = .50; ●, z = 1.00; ▲, z = 1.50; ■, z = 4.00; ♦, z = 9.00.

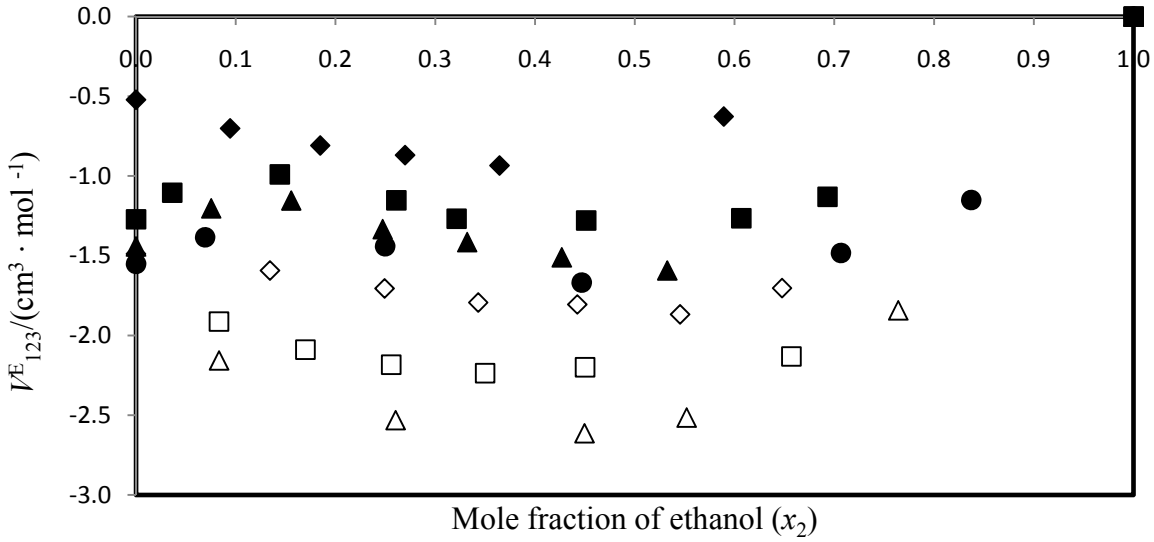

FIGURE 6.10 Graph of ternary excess molar volumes, V^E_{123} , for {[MOA]$^+$[Tf$_2$N]$^-$ (x_1) + ethanol (x_2) + ethyl acetate (x_3)} against mole fraction of ethanol at T = 298.15 K. The symbols represent experimental data at constant $z = x_3/x_1$: ♦, z = 0.08; ■, z = 0.25; ▲, z = 0.40; ●, z = 0.80; ◊, z = 1.30; □, z = 4.00; Δ, z = 9.00.

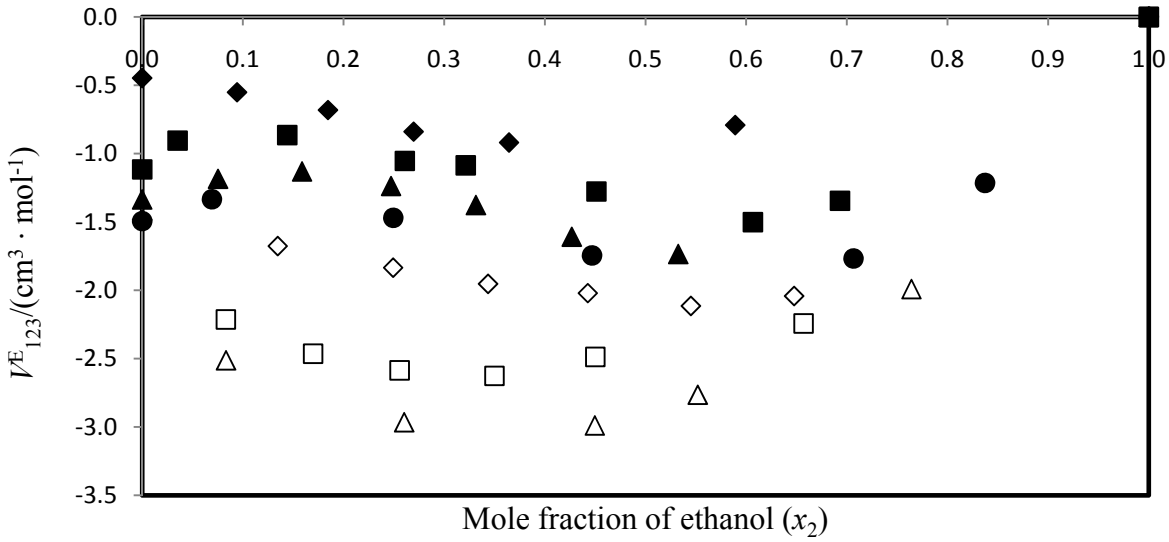

FIGURE 6.11 Graph of ternary excess molar volumes, V^E_{123} , for {$[MOA]^+[Tf_2N]^-$ (x_1) + ethanol (x_2) + ethyl acetate (x_3)} against mole fraction of ethanol at T = 303.15 K. The symbols represent experimental data at constant $z = x_3/x_1$: ♦, z = 0.08; ■, z = 0.25; ▲, z = 0.40; ●, z = 0.80; ◊, z = 1.30; □, z = 4.00; Δ, z = 9.00.

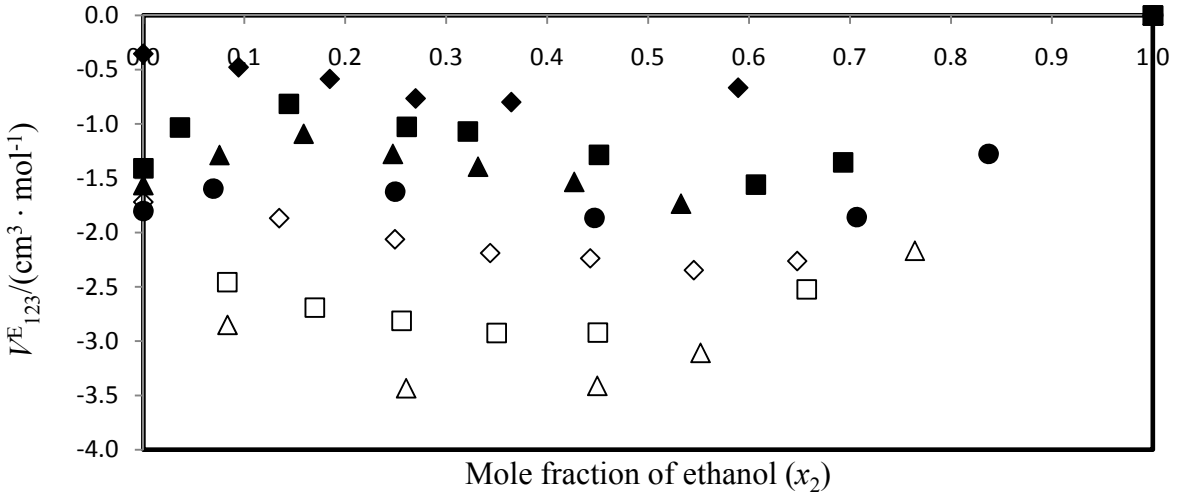

FIGURE 6.12 Graph of ternary excess molar volumes, V^{E}_{123} , for {$[MOA]^+[Tf_2N]^-$ (x_1) + ethanol (x_2) + ethyl acetate (x_3)} against mole fraction of ethanol at T = 313.15 K. The symbols represent experimental data at constant $z = x_3/x_1$: ♦, z = 0.08; ■, z = 0.25; ▲, z = 0.40; ●, z = 0.80; ◊, z = 1.30; □, z = 4.00; Δ, z = 9.00.

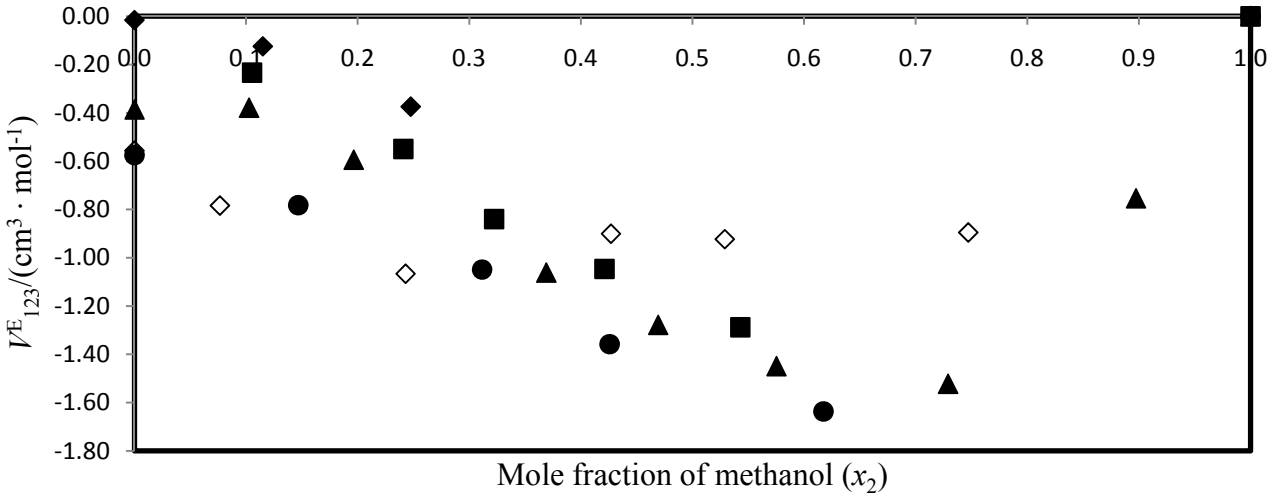

FIGURE 6.13 Graph of ternary excess molar volumes, V^E_{123} , for {[BMIM]$^+$[MeSO$_4$]$^-$ (x_1) + methanol (x_2) + nitromethane (x_3)} against mole fraction of methanol at T = 298.15 K. The symbols represent experimental data at constant $z = x_3/x_1$: ♦, z = 0.04; ■, z = 0.23; ▲, z = 0.72; ●, z = 1.80; ◊, z = 4.21.

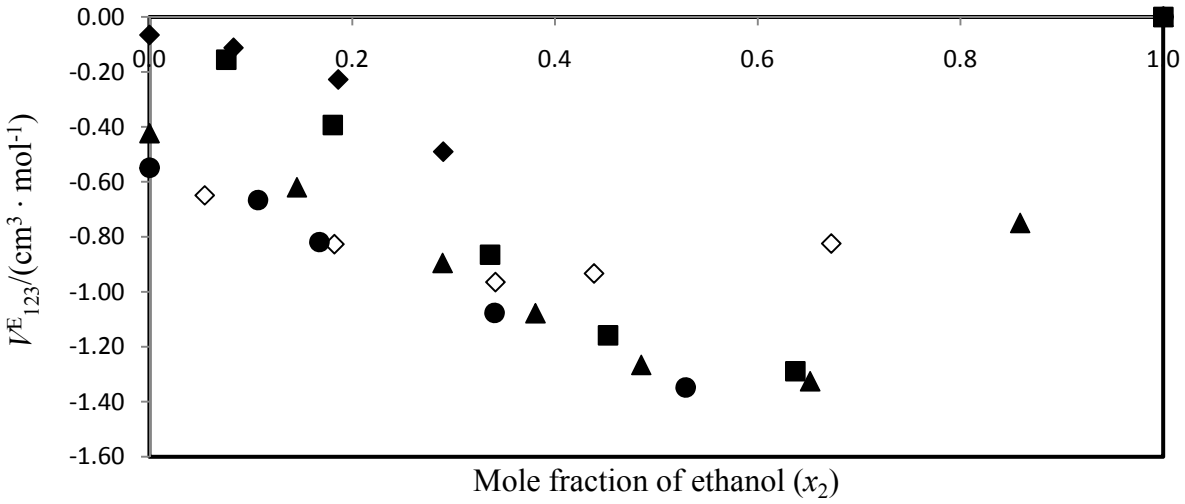

FIGURE 6.14 Graph of ternary excess molar volumes, V^E_{123} , for {$[BMIM]^+[MeSO_4]^-$ (x_1) + ethanol (x_2) + nitromethane (x_3)} against mole fraction of ethanol at T = 298.15 K. The symbols represent experimental data at constant $z = x_3/x_1$: ♦, z = 0.04; ■, z = 0.23; ▲, z = 0.72; ●, z = 1.80; ◊, z = 4.21.

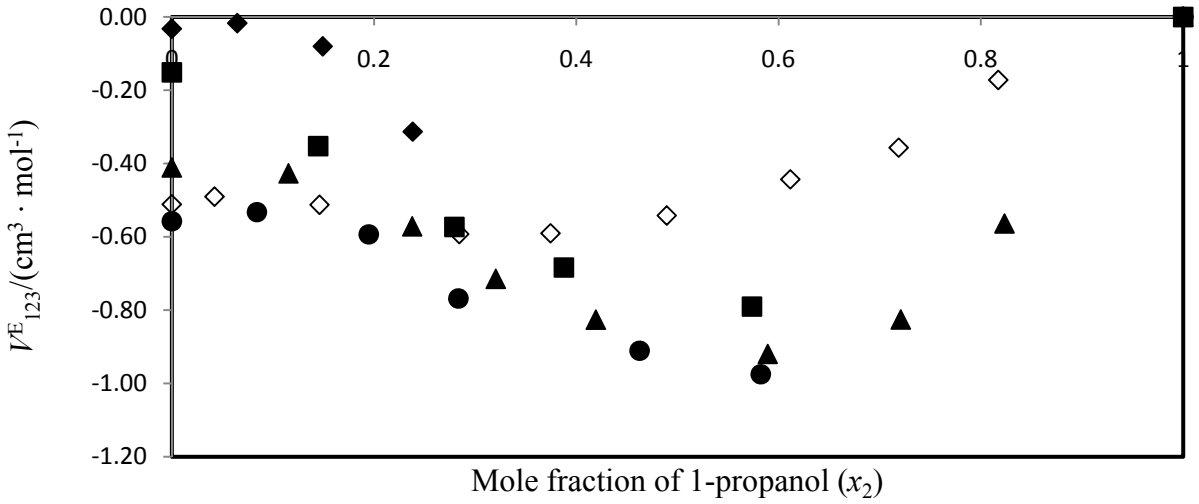

FIGURE 6.15 Graph of ternary excess molar volumes, V^E_{123} , for {[BMIM]$^+$[MeSO$_4$]$^-$ (x_1) + 1-propanol (x_2) + nitromethane (x_3)} against mole fraction of 1-propanol at T = 298.15 K. The symbols represent experimental data at constant $z = x_3/x_1$: ♦, z = 0.04; ■, z = 0.23; ▲, z = 0.72; ●, z = 1.80; ◊, z = 4.21.

Table 6.8 Smoothing Coefficients b_n, and Standard Deviation σ_S , for the Cibulka Equation at T = (298.15, 303.15 and 313.15) K

T/K	b_0	b_1	b_2	σ_S
{$[MOA]^+[Tf_2N]^-$ (x_1) + methanol (x_2) + methyl acetate (x_3)}				
298.15	17.48	-34.92	-110.91	0.22
303.15	15.59	- 43.06	-144.46	0.28
313.15	18.49	- 44.98	-172.17	0.37
{$[MOA]^+[Tf_2N]^-$ (x_1) + methanol (x_2) + ethyl acetate (x_3)}				
298.15	-32.53	57.30	-111.75	0.45
303.15	- 48.60	86.45	-113.99	0.50
313.15	- 62.20	122.03	- 88.56	0.63
{$[MOA]^+[Tf_2N]^-$ (x_1) + ethanol (x_2) + methyl acetate (x_3)}				
298.15	4.61	- 53.26	-103.39	0.26
303.15	25.78	-137.97	-129.45	0.31
313.15	10.57	- 86.23	-123.08	0.36
{$[MOA]^+[Tf_2N]^-$ (x_1) + ethanol (x_2) + ethyl acetate (x_3)}				
298.15	- 46.38	59.78	- 67.80	0.44
303.15	-53.66	27.80	- 80.78	0.54
313.15	-78.56	119.70	- 62.88	0.50

Table 6.9 Smoothing Coefficients b_n, and Standard Deviation σ_S, for the Cibulka Equation at $T = 298.15$ K

T/K	b_0	b_1	b_2	σ_S
{[BMIM]$^+$[MeSO$_4$]$^-$ (x_1) + methanol (x_2) + nitromethane (x_3)}				
298.15	35.60	-52.47	- 185.50	0.74
{[BMIM]$^+$[MeSO$_4$]$^-$ (x_1) + ethanol (x_2) + nitromethane (x_3)}				
298.15	14.68	-29.73	- 133.66	0.74
{[BMIM]$^+$[MeSO$_4$]$^-$ (x_1) + 1-propanol (x_2) + nitromethane (x_3)}				
298.15	5.86	-9.83	- 86.03	0.31

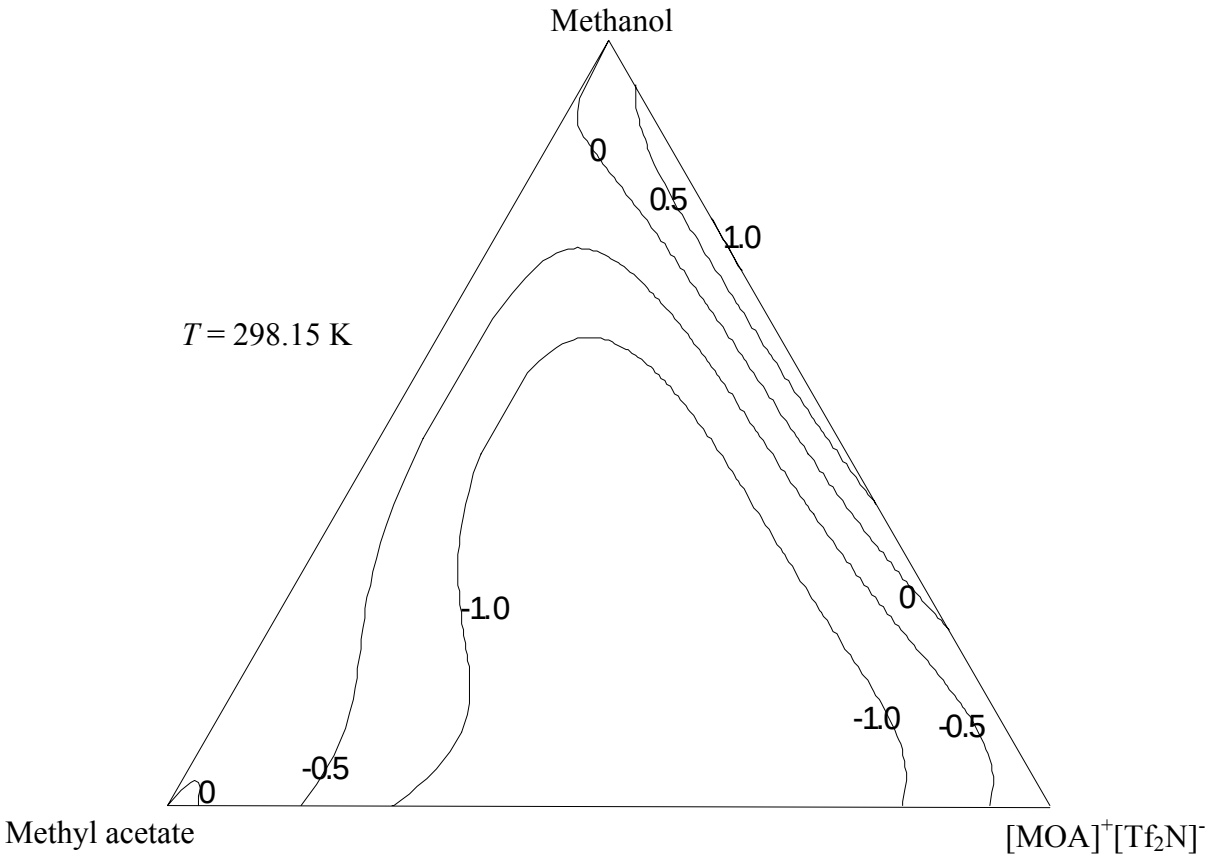

FIGURE 6.16 Graph obtained from the Cibulka equation for the ternary system {[MOA] $^{+}$[Tf_2N] $^{-}$ (x_1) + methanol (x_2) + methyl acetate (x_3)} at T = 298.15 K.

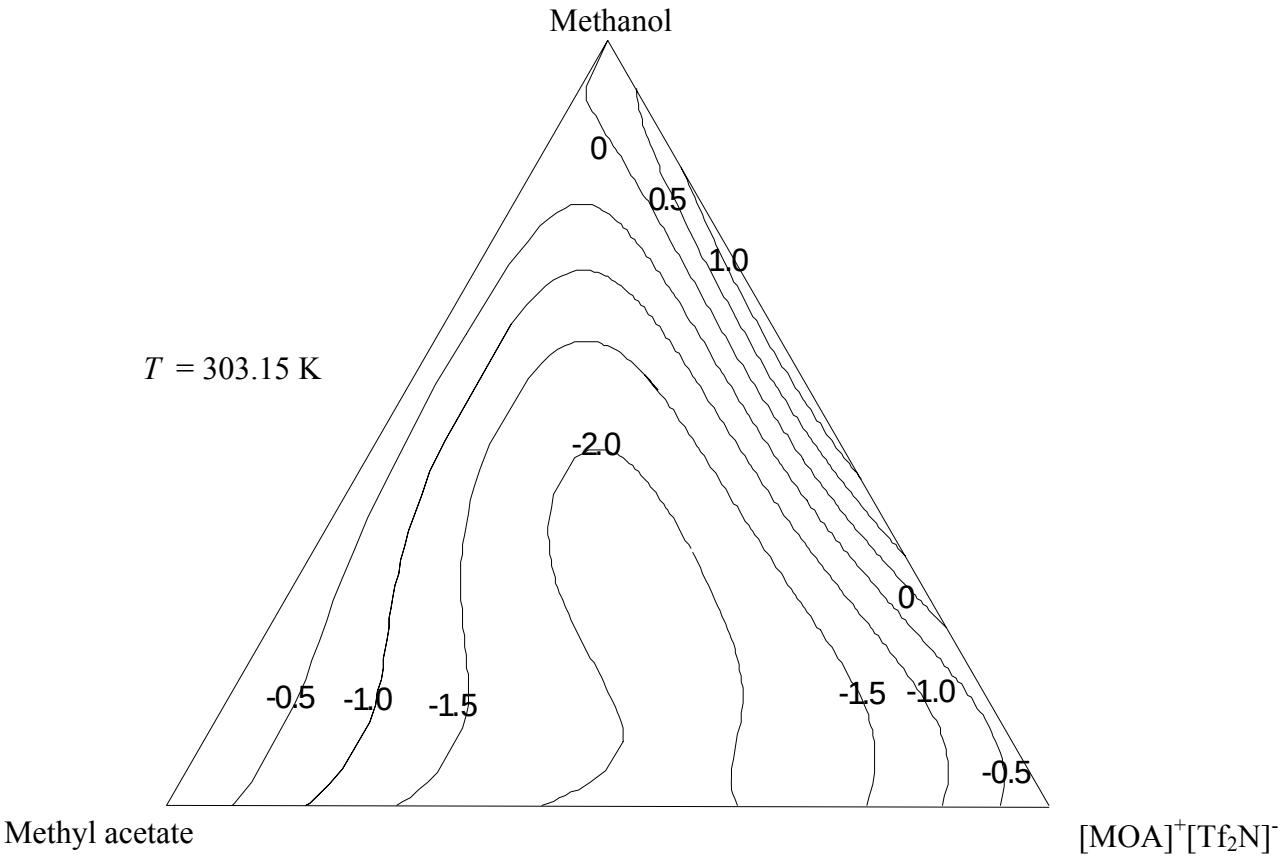

FIGURE 6.17 Graph obtained from the Cibulka equation for the ternary system {[MOA]$^+$[Tf$_2$N]$^-$ (x_1) + methanol (x_2) + methyl acetate (x_3)} at T = 303.15 K.

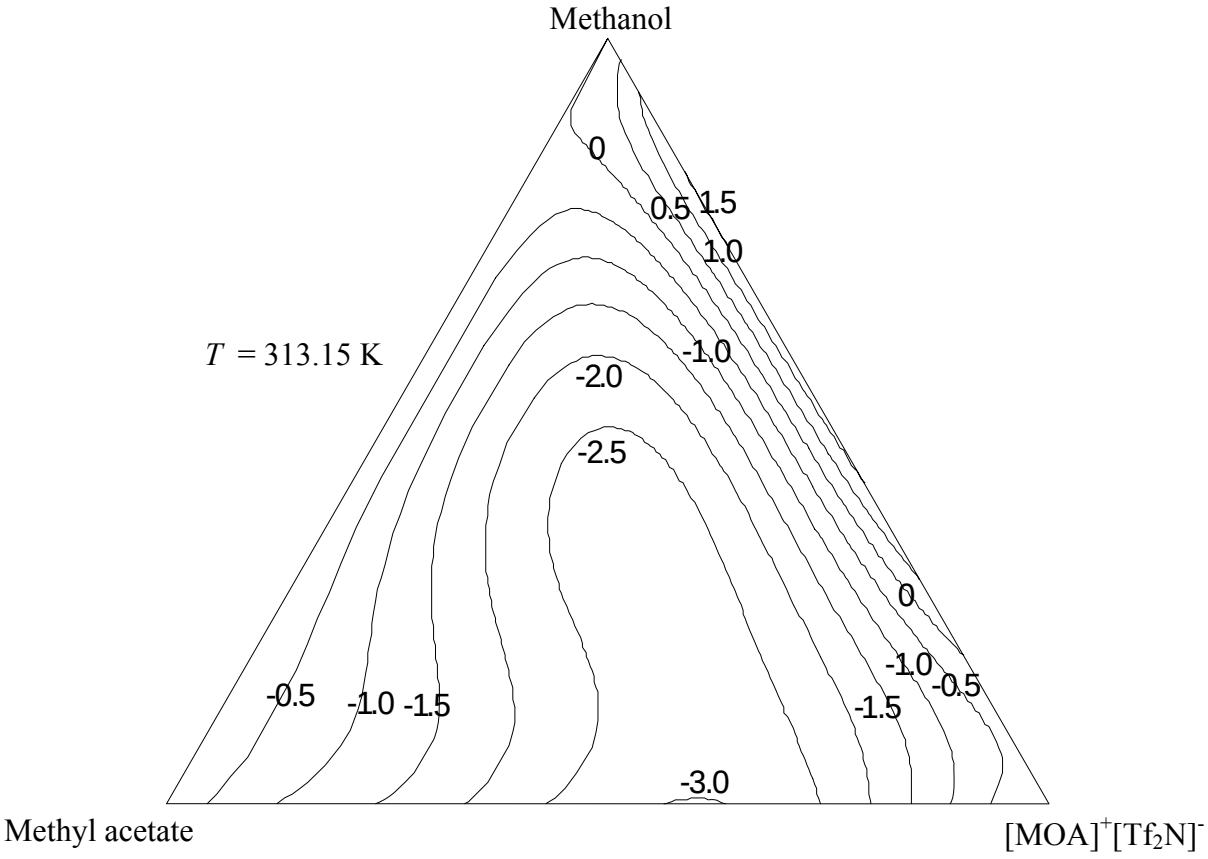

FIGURE 6.18 Graph obtained from the Cibulka equation for the ternary system {[MOA] $^{+}$[Tf_2N] $^{-}$ (x_1) + methanol (x_2) + methyl acetate (x_3)} at T = 313.15 K.

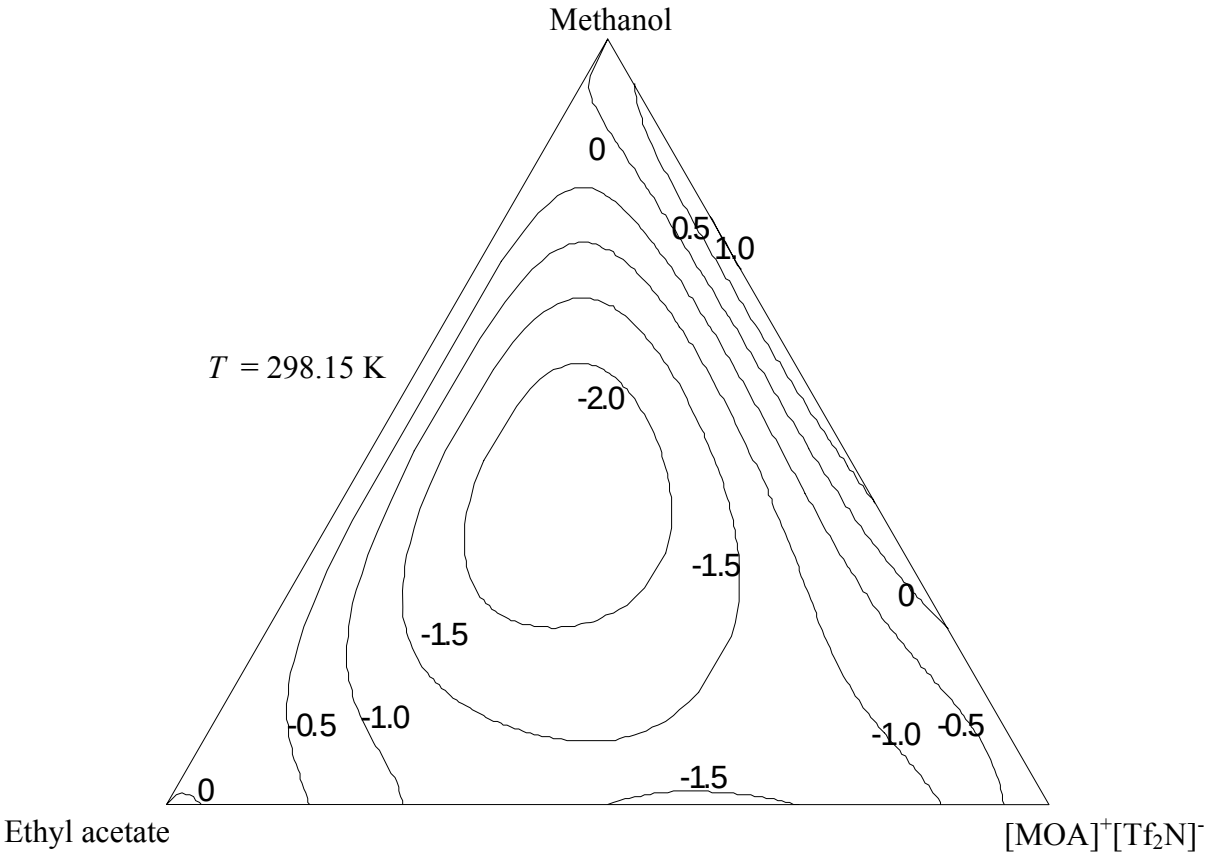

FIGURE 6.19 Graph obtained from the Cibulka equation for the ternary system {[MOA] $^{+}$[Tf_2N] $^{-}$ (x_1) + methanol (x_2) + ethyl acetate (x_3)} at T = 298.15 K.

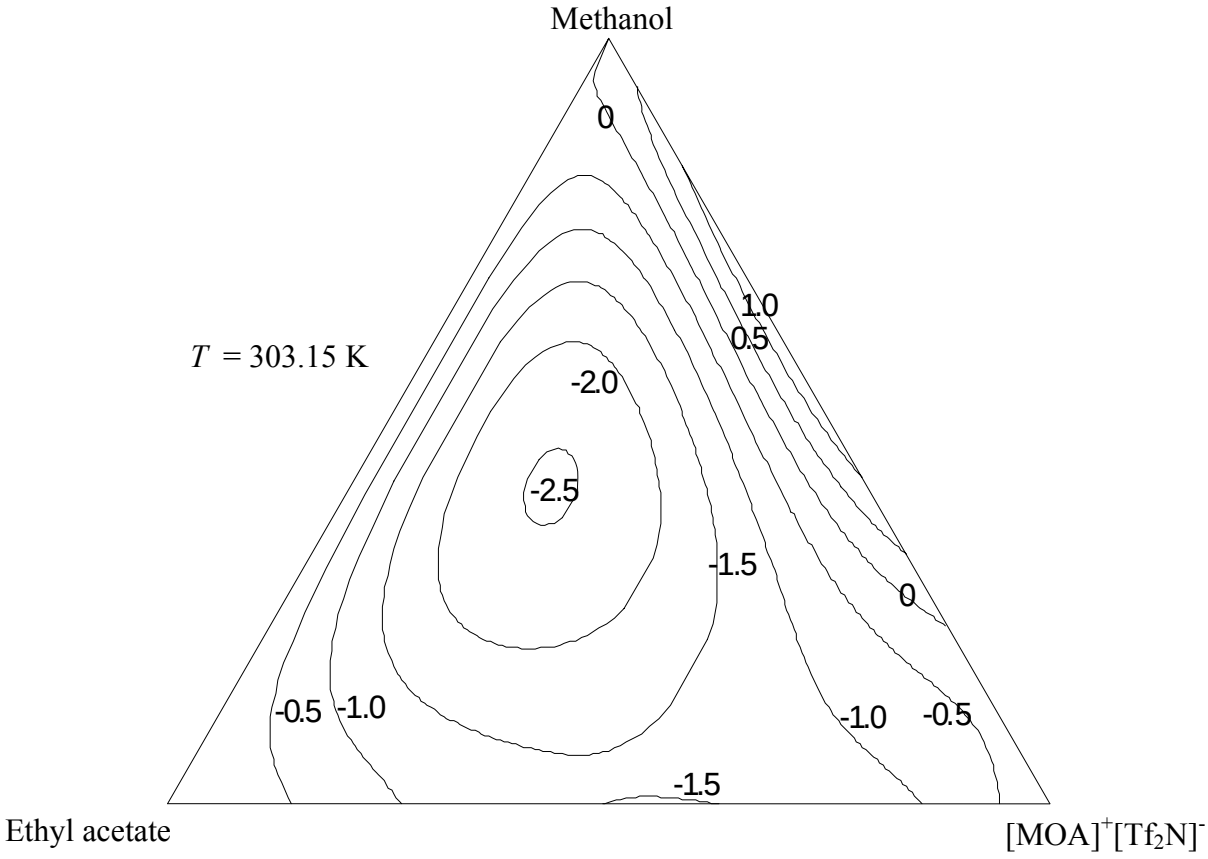

FIGURE 6.20 Graph obtained from the Cibulka equation for the ternary system {[MOA] $^{+}$[Tf_2N] $^{-}$ (x_1) + methanol (x_2) + ethyl acetate (x_3)} at T = 303.15 K.

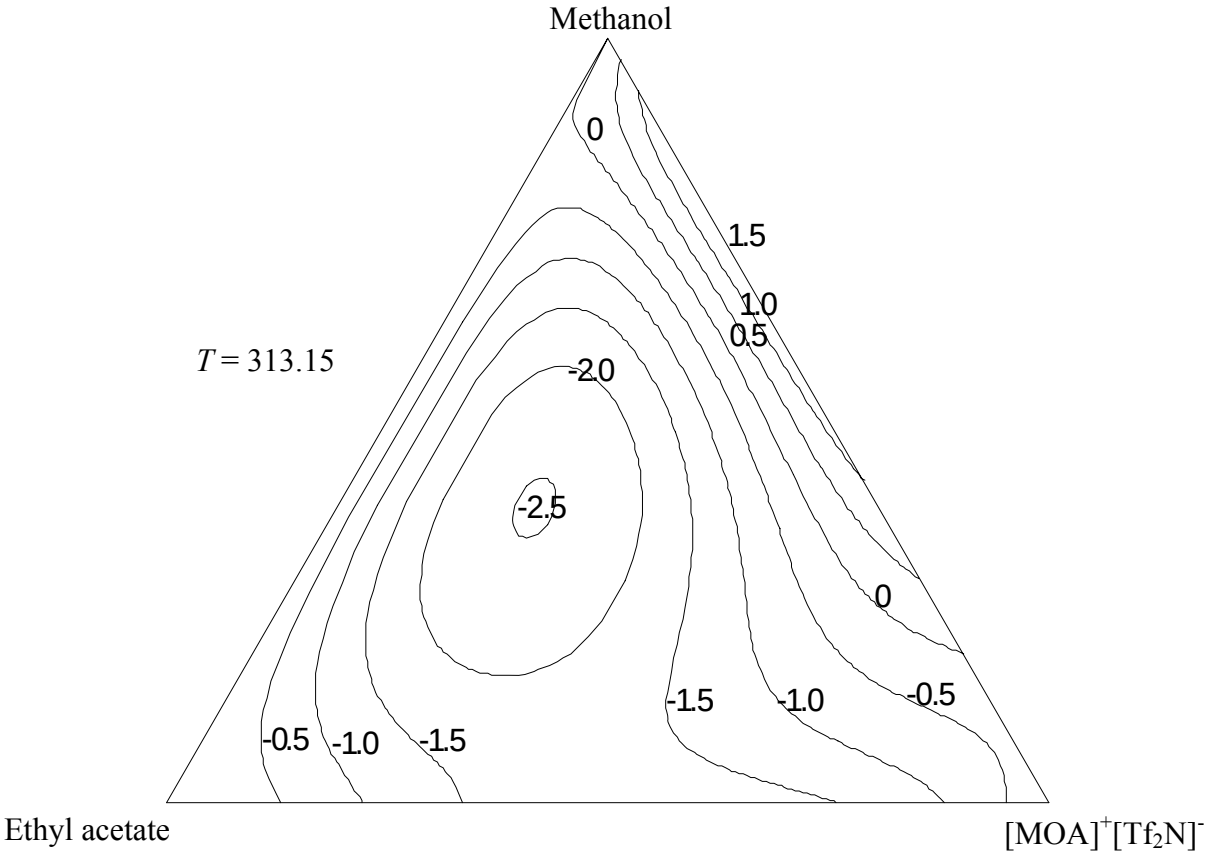

FIGURE 6.21 Graph obtained from the Cibulka equation for the ternary system {[MOA] $^{+}$[Tf_2N] $^{-}$ (x_1) + methanol (x_2) + ethyl acetate (x_3)} at T = 313.15 K.

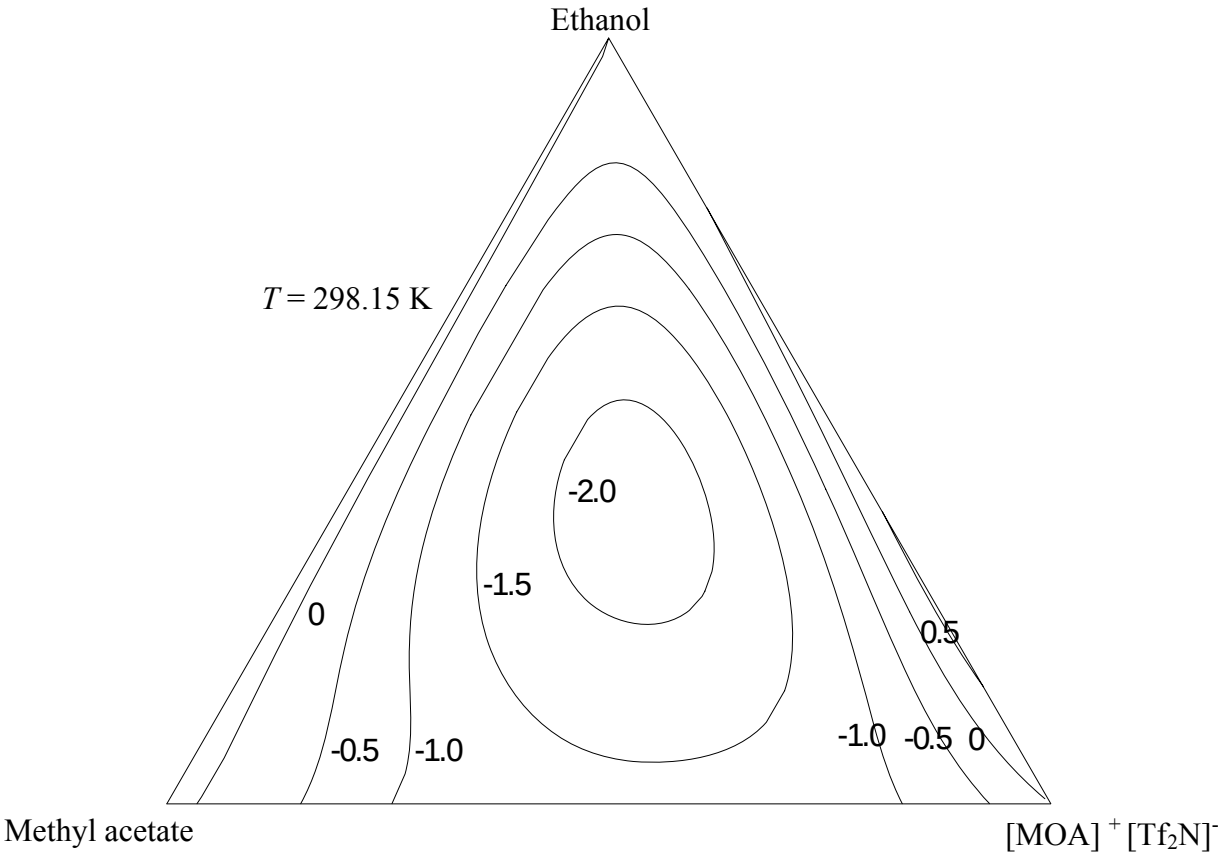

FIGURE 6.22 Graph obtained from the Cibulka equation for the ternary system {[MOA]$^+$[Tf$_2$N]$^-$ (x_1) + ethanol (x_2) + methyl acetate (x_3)} at T = 298.15 K.

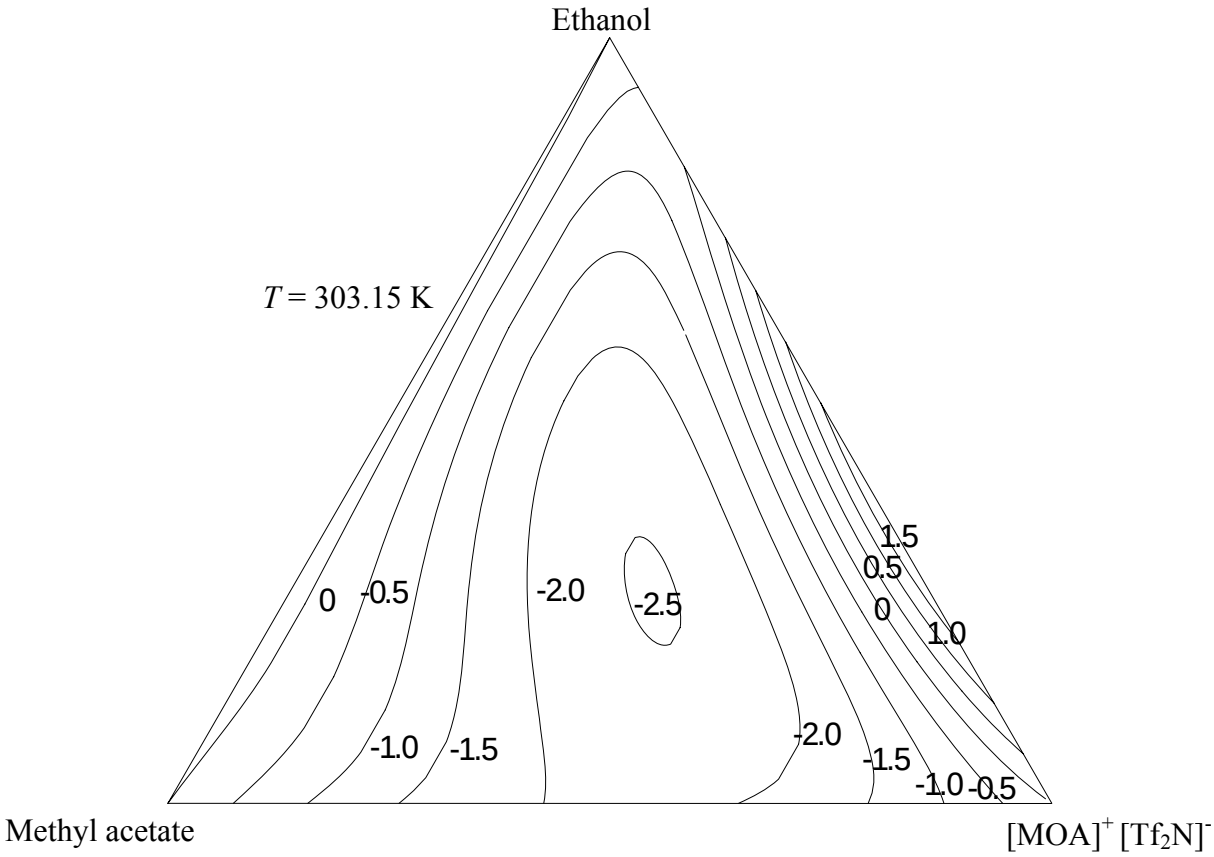

FIGURE 6.23 Graph obtained from the Cibulka equation for the ternary system {[MOA]$^+$[Tf_2N]$^-$ (x_1) + ethanol (x_2) + methyl acetate (x_3)} at T = 303.15 K.

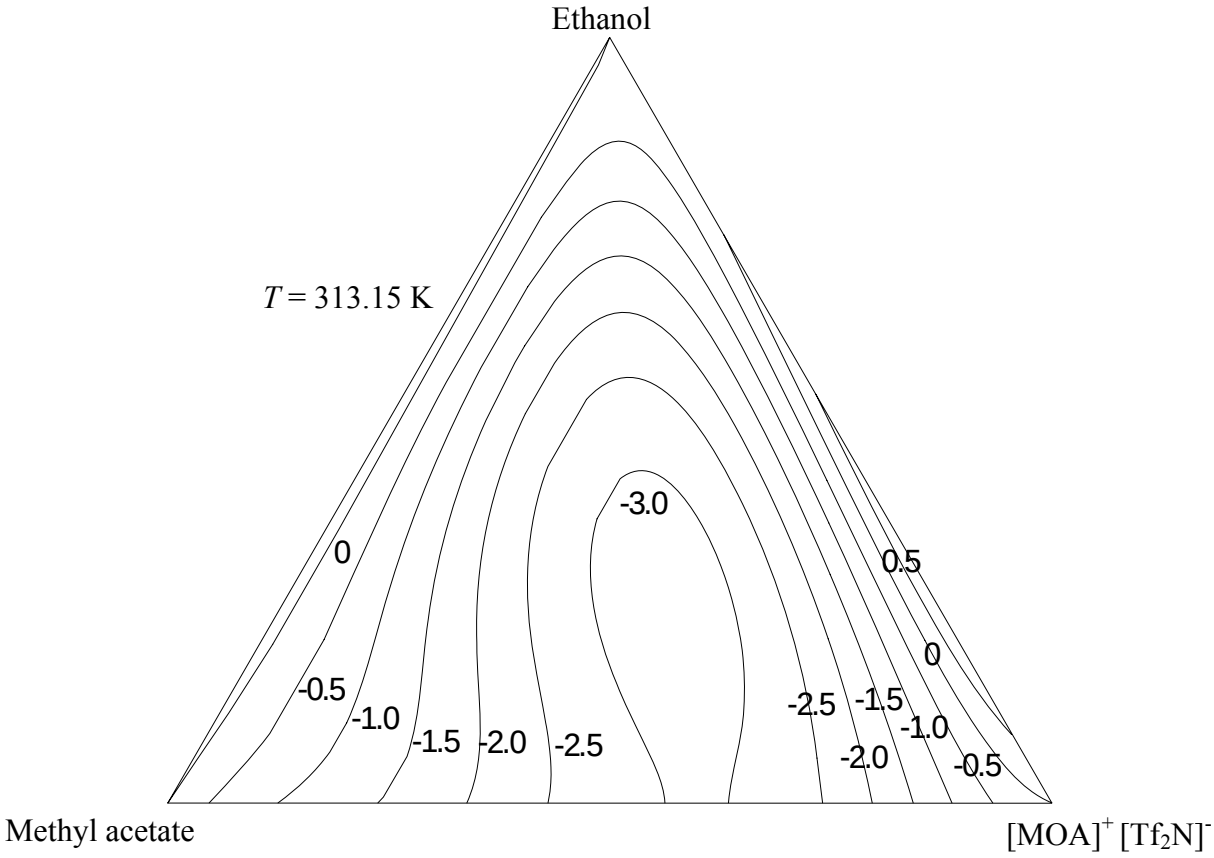

FIGURE 6.24 Graph obtained from the Cibulka equation for the ternary system {[MOA] $^{+}$[Tf_2N] $^{-}$ (x_1) + ethanol (x_2) + methyl acetate (x_3)} at T = 313.15 K.

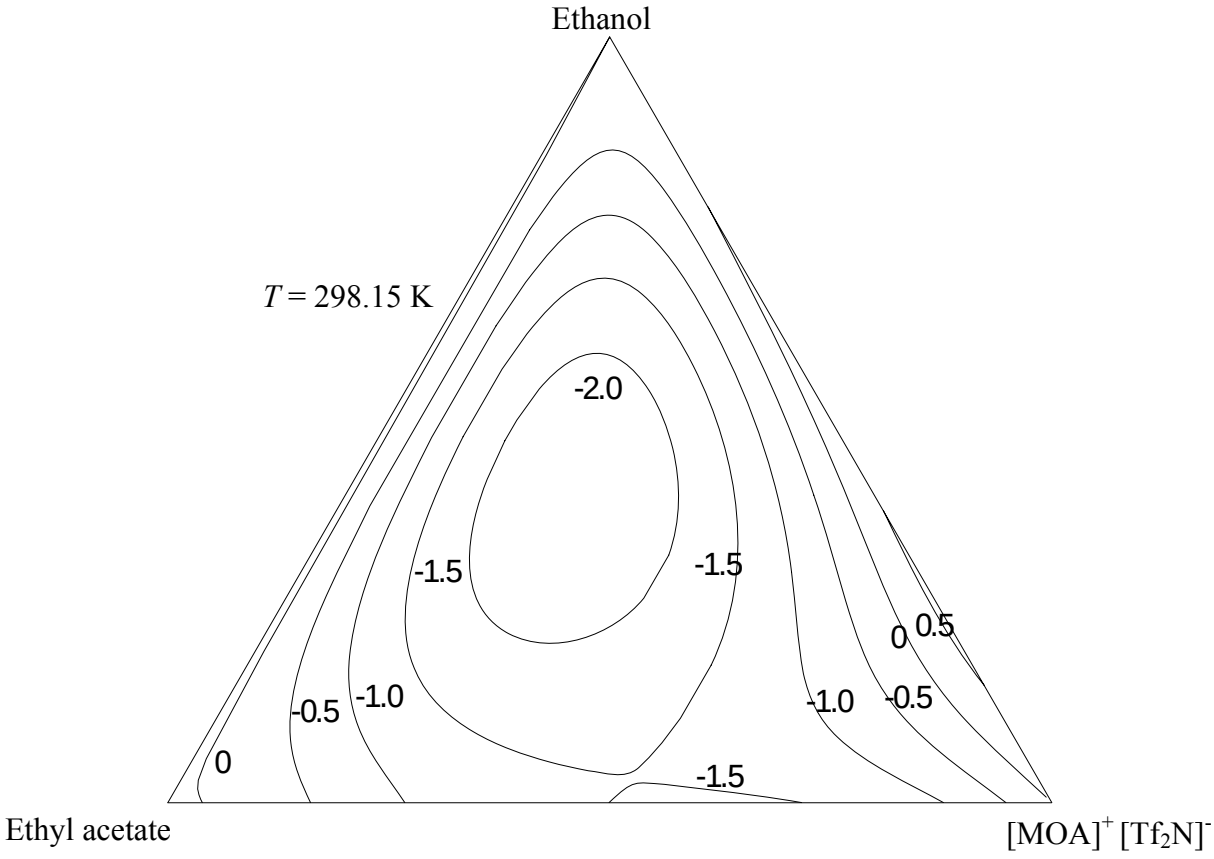

FIGURE 6.25 Graph obtained from the Cibulka equation for the ternary system {[MOA] $^{+}$[Tf_2N] $^{-}$ (x_1) + ethanol (x_2) + ethyl acetate (x_3)} at T = 298.15 K.

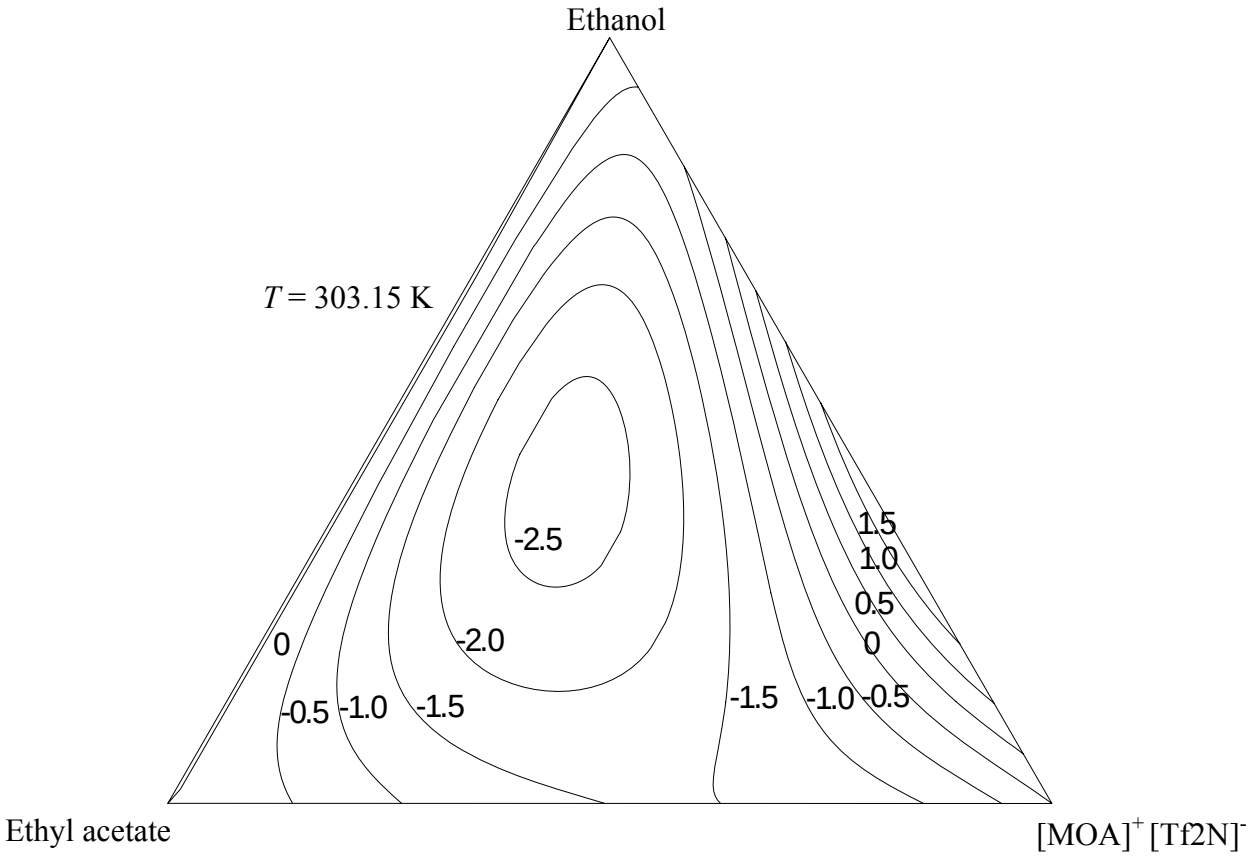

FIGURE 6.26 Graph obtained from the Cibulka equation for the ternary system {[MOA] $^{+}$[Tf_2N] $^{-}$ (x_1) + ethanol (x_2) + ethyl acetate (x_3)} at T = 303.15 K.

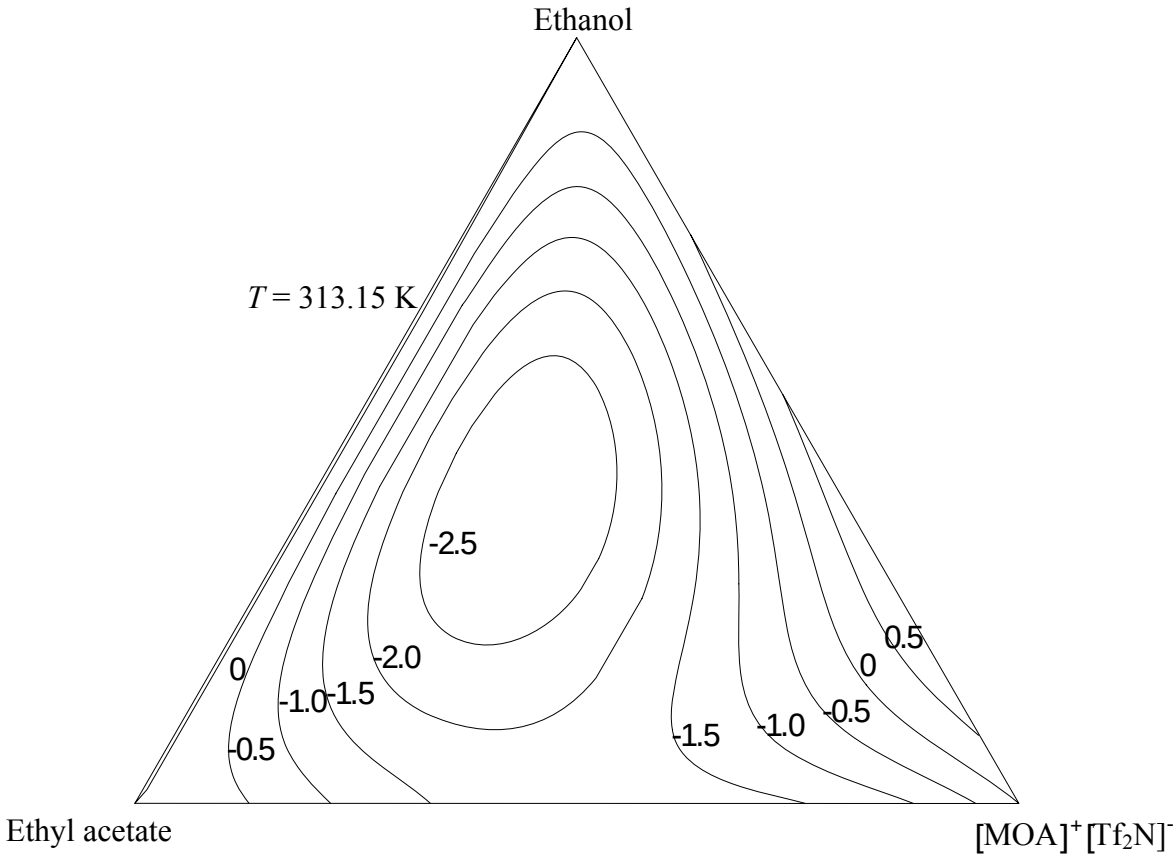

FIGURE 6.27 Graph obtained from the Cibulka equation for the ternary system {[MOA]$^+$[Tf$_2$N]$^-$ (x_1) + ethanol (x_2) + ethyl acetate (x_3)} at T = 313.15 K.

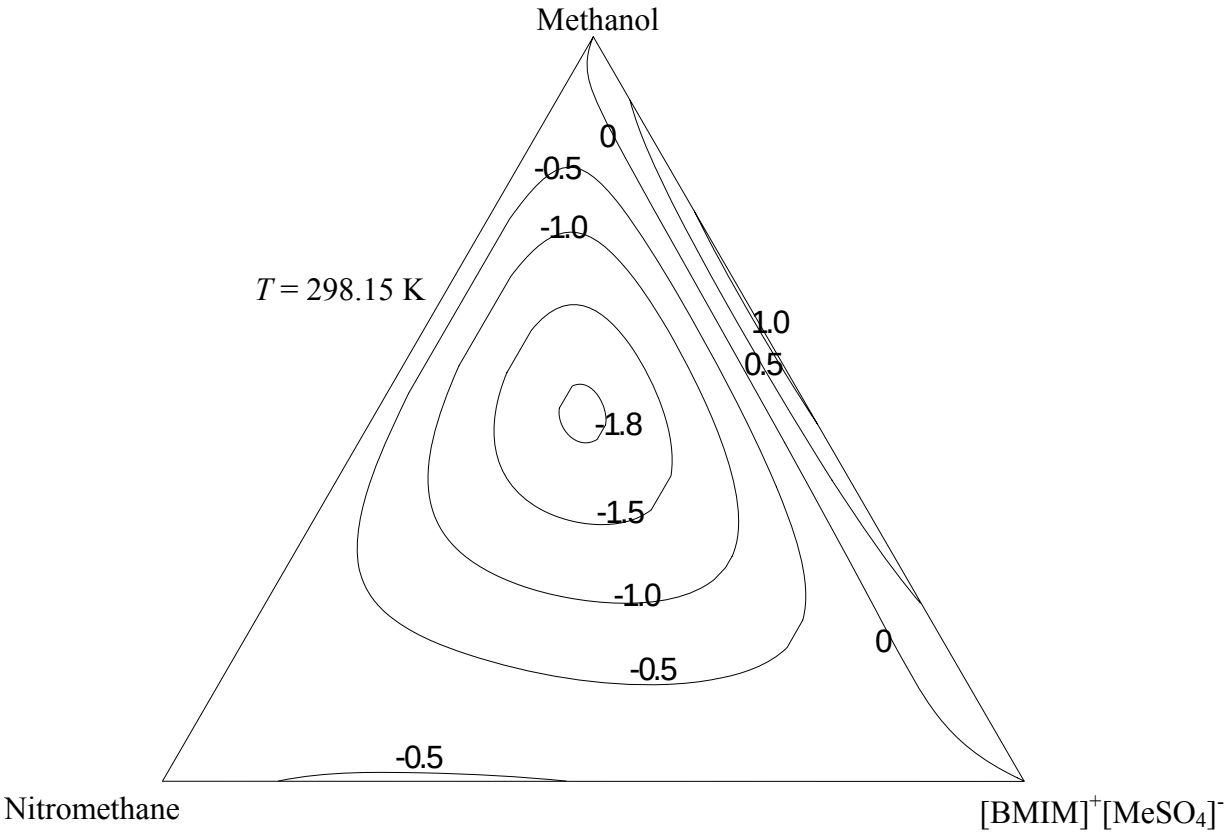

FIGURE 6.28 Graph obtained from the Cibulka equation for the ternary system {$[BMIM]^+[MeSO_4]^-$ (x_1) + methanol (x_2) + nitromethane (x_3)} at T = 298.15 K.

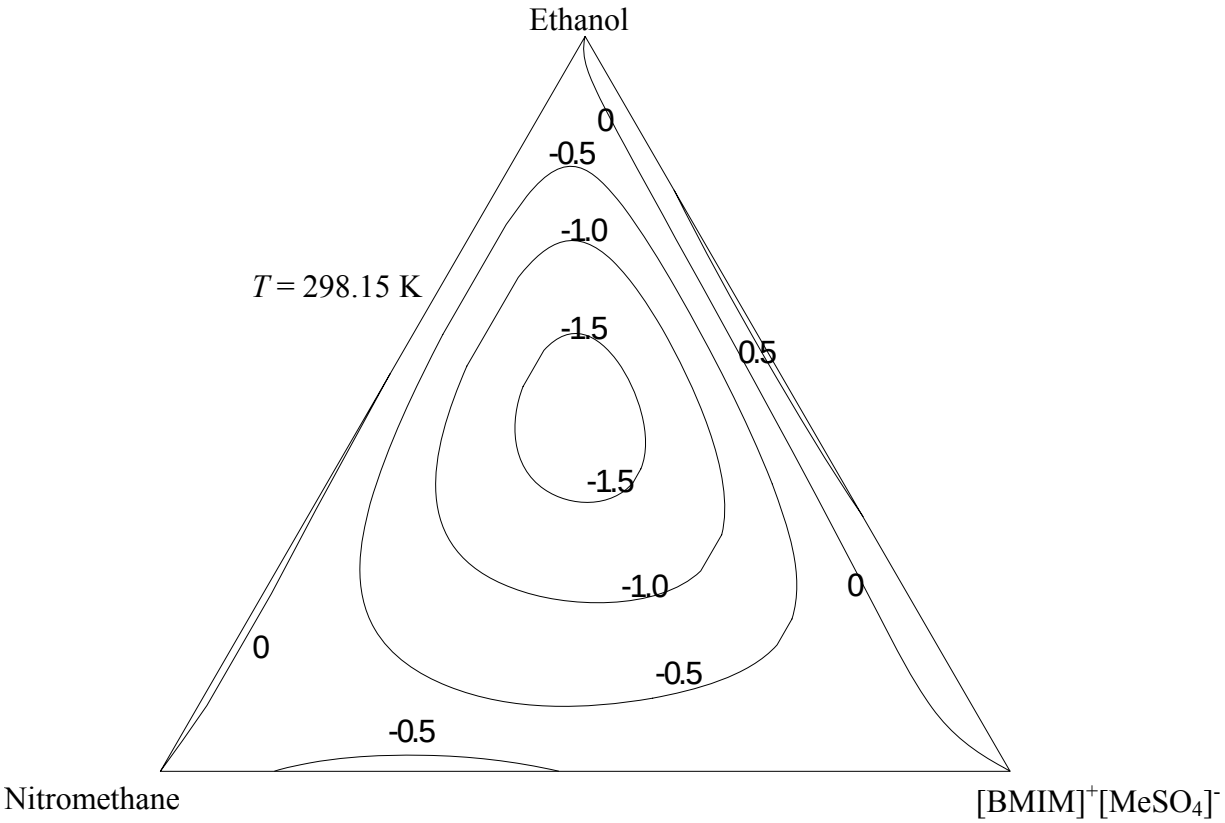

FIGURE 6.29 Graph obtained from the Cibulka equation for the ternary system {$[BMIM]^+[MeSO_4]^-$ (x_1) + ethanol (x_2) + nitromethane (x_3)} at $T = 298.15$ K.

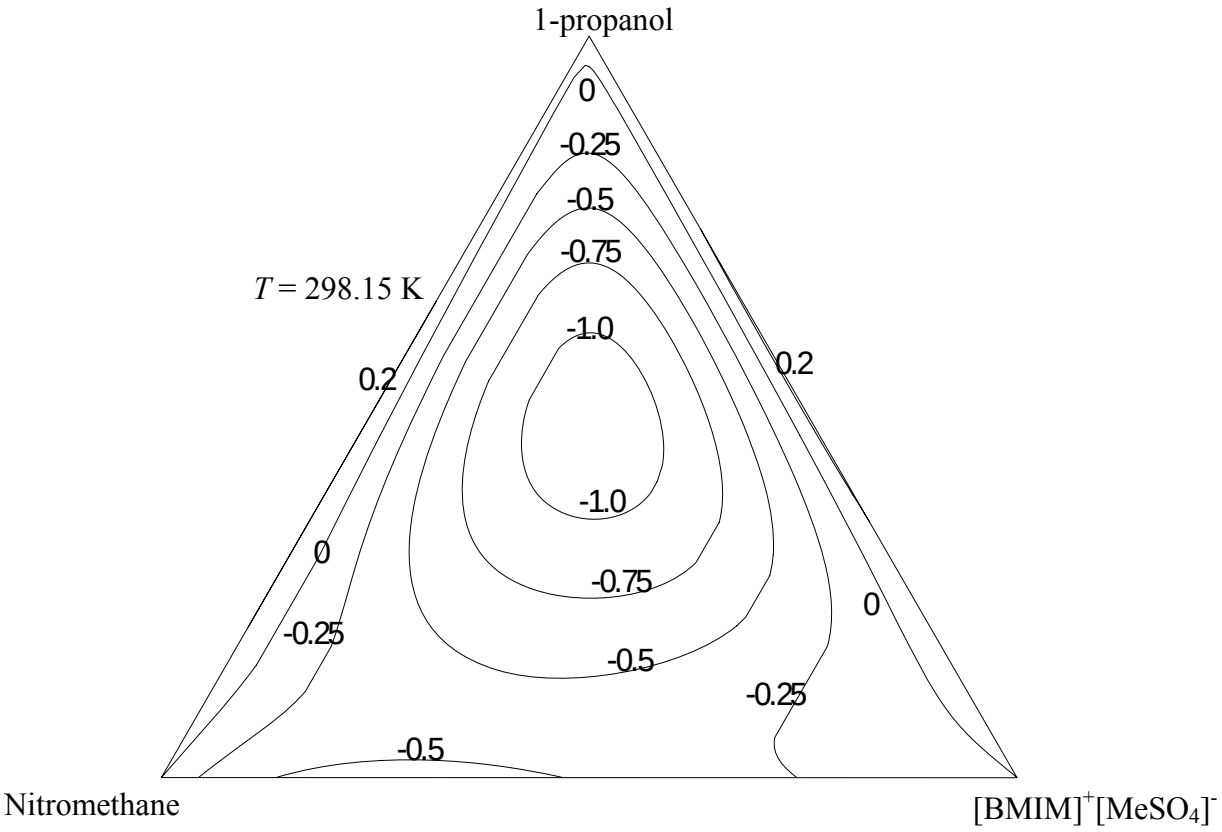

FIGURE 6.30 Graph obtained from the Cibulka equation for the ternary system {[BMIM]$^+$[MeSO$_4$]$^-$ (x_1) + 1-propanol (x_2) + nitromethane (x_3)} at T = 298.15 K.

(B) APPARENT MOLAR PROPERTIES

The apparent molar volumes of the studied systems {$[MOA]^+[Tf_2N]^-$ + methanol or ethanol or methyl acetate or ethyl acetate}, (methanol + methyl acetate or ethyl acetate) , (ethanol + methyl acetate or ethyl acetate) were calculated from the experimental density values, using equation (6.4):

$$V_\phi = \frac{M}{d} - \frac{(d - d_0)}{mdd_0} \tag{6.4}$$

where m is molality of the solute ($[MOA]^+ [Tf_2N]^-$ or methanol or ethanol) (mol·kg^{-1}) and d and d_0 are the densities (kg·m^{-3}) of the solution and pure solvent, respectively, M is molar mass of $[MOA]^+ [Tf_2N]^-$ or methanol or ethanol (kg·mol^{-1}).

A Redlich-Mayer type equation was fitted to the apparent molar volume data using the following equation (6.5):

$$V_\phi = V_\phi^0 + S_v m^{\frac{1}{2}} + B_v m \tag{6.5}$$

where V_ϕ^0 is the apparent molar volume at infinite dilution, which is also known as the partial molar volume at infinite dilution of the solute, S_v and B_v are empirical parameters related to intermolecular interactions.

The temperature dependence of V_ϕ^0 can be expressed as:

$$V_\phi^0 = A + BT + CT^2 \quad (6.6)$$

where A, B, and C are empirical parameters and T is the temperature. The limiting apparent molar expansibility E_ϕ^0 can be obtained by differentiating equation (6.6) with respect to temperature to obtained equation (6.7):

$$E_\phi^0 = \left(\partial V_\phi^0 / \partial T\right)_p = B + 2CT \quad (6.7)$$

The speed of sound of the studied systems {$[MOA]^+[Tf_2N]^-$ + methanol or ethanol or methyl acetate or ethyl acetate}, (methanol + methyl acetate or ethyl acetate) and (ethanol + methyl acetate or ethyl acetate) were measured at T = (298.15, 303.15, 308.15 and 313.15) K and at 3 MHz. The isentropic compressibility, κ_s, was calculated from the Newton-Laplace equation:

$$\kappa_s = \frac{1}{du^2} \quad (6.8)$$

The apparent molar isentropic compressibility, κ_ϕ, of the studied systems {$[MOA]^+[Tf_2N]^-$ + methanol or ethanol or methyl acetate or ethyl acetate}, (methanol + methyl acetate or ethyl

acetate) and (ethanol + methyl acetate or ethyl acetate) were calculated at T = (298.15, 303.15, 308.15 and 313.15) K from the experimental density values, using equation (6.9)

$$\kappa_\phi = \frac{(\kappa_s d_0 - \kappa_{s0} d)}{m d d_0} + \frac{\kappa_s M}{d} \tag{6.9}$$

where κ_{s0} and κ_s are the isentropic compressibility of pure solvent and mixture, respectively.

A Redlich-Mayer type equation was used for correlating the experimental apparent molar isentropic compressibility data using the following Redlich-Mayer equation (6.10):

$$\kappa_\phi = \kappa_\phi^0 + S_k m^{1/2} + B_k m\,, \tag{6.10}$$

where k_ϕ^0 is the limiting apparent molar isentropic compressibility, S_k and B_k are empirical parameters relating to intermolecular interaction.

6.2 APPARENT MOLAR VOLUME AND DERIVED PROPERTIES

6.2.1 Apparent molar volume

The apparent molar volumes were calculated from equation (6.4). The apparent molar volumes for the binary systems {methyltrioctylammonium bis (trifluoromethylsulfonyl) imide $[MOA]^+[Tf_2N]^-$ + methanol or ethanol or methyl acetate or ethyl acetate}, (methanol + methyl acetate or ethyl acetate) and (ethanol + methyl acetate or ethyl acetate) were obtained at four temperatures namely (298.15, 303.15, 308.15 and 313.15) K.

The results for density, ρ, and apparent molar volumes V_ϕ for {$[MOA]^+[Tf_2N]^-$ + methanol or ethanol or methyl acetate or ethyl acetate}, (methanol + methyl acetate or ethyl acetate) and (ethanol + methyl acetate or ethyl acetate) are given in Tables 6.10 – 6.17 and V_ϕ versus molality $m^{1/2}$ are plotted in Figures 6.31 – 6.38.

Table 6.10 Molality, m, densities, ρ, apparent molar volumes, V_ϕ, for ($[MOA]^+$ $[Tf_2N]^-$ + methyl acetate) at T = (298.15, 303.15, 308.15 and 313.15) K

Molality, m	ρ / kg· m^{-3}	$10^6 \cdot V_\phi$ / m^3· mol^{-1}
	($[MOA]^+$ $[Tf_2N]^-$ + methyl acetate)	
	T = 298.15 K	
0.0271	930.8	531
0.0587	934.2	551
0.0847	936.5	562
0.1257	940.4	567
0.1587	943.4	569
0.2262	949.5	570
0.3162	956.9	571
	T = 303.15 K	
0.0271	923.9	546
0.0587	927.3	560
0.0847	929.8	567
0.1257	933.8	570
0.1587	937.0	571
0.2262	943.2	571
0.3162	949.8	576
	T = 308.15 K	
0.0271	917.3	562
0.0587	920.7	569
0.0847	923.0	577
0.1257	927.0	578
0.1587	930.1	578
0.2262	936.1	579
0.3162	943.5	580
	T = 313.15 K	
0.0271	911.1	574
0.0587	914.4	578
0.0847	917.0	580
0.1257	921.0	581
0.1587	924.1	581
0.2262	930.1	582
0.3162	936.9	585

Table 6.11 Molality, m, densities, ρ, apparent molar volumes, V_ϕ , for ($[MOA]^+ [Tf_2N]^-$ + ethyl acetate) at T = (298.15, 303.15, 308.15 and 313.15) K

Molality, m	ρ / kg·m^{-3}	$10^6 \cdot V_\phi$ / m^3·mol^{-1}
	($[MOA]^+ [Tf_2N]^-$ + ethyl acetate)	
	T = 298.15 K	
0.0692	903.0	564.7
0.1377	910.7	567.2
0.2691	923.8	570.1
0.4006	935.1	572.4
0.6119	950.4	575.0
0.8299	963.4	577.0
1.0059	972.5	577.9
1.2799	984.5	579.1
2.1321	1011.1	581.2
2.9994	1029.3	581.5
	T = 303.15 K	
0.0692	897.1	567.4
0.1377	904.8	569.9
0.2691	918.0	572.4
0.4006	929.4	574.5
0.6119	944.9	576.9
0.8299	958.3	578.3
1.0059	967.5	579.3
1.2799	979.7	580.4
2.1321	1006.9	582.3
2.9994	1025.5	582.6
	T = 308.15 K	
0.0692	891.3	570.0
0.1377	899.1	571.6
0.2691	912.4	574.1
0.4006	924.0	575.8
0.6119	939.7	578.2
0.8299	953.3	579.5
1.0059	962.6	580.6
1.2799	974.8	582.0
2.1321	1001.9	584.4
2.9994	1019.5	585.8
	T = 313.15 K	
0.0692	885.0	571.0
0.1377	892.9	572.7
0.2691	906.5	574.5
0.4006	918.3	576.3
0.6119	934.5	578.2
0.8299	948.4	579.6
1.0059	957.9	580.7
1.2799	970.2	582.5
2.1321	997.0	586.0
2.9994	1013.8	588.4

Table 6.12 Molality, m, densities, ρ, apparent molar volumes, V_ϕ , for ($[MOA]^+ [Tf_2N]^-$ + methanol) at T = (298.15, 303.15, 308.15) and 313.15 K

Molality, m	ρ / kg· m^{-3}	$10^6 \cdot V_\phi$ / m^3· mol^{-1}
	($[MOA]^+[Tf_2N]^-$ + methanol)	
	T = 298.15K	
0.0692	800.0	503
0.1378	810.3	531
0.2690	828.4	545
0.6119	867.3	555
1.2787	919.4	562
2.1304	960.4	568
3.1162	993.5	568
5.1733	1024.6	576
7.7906	1049.0	578
	T = 303.15 K	
0.0692	795.2	507
0.1378	805.5	534
0.2690	823.5	548
0.6119	862.5	557
1.2787	914.6	564
2.1304	953.3	573
3.1162	986.1	573
5.1733	1014.7	583
7.7906	1038.7	584
	T = 308.15 K	
0.0692	789.8	525
0.1378	800.8	535
0.2690	818.1	554
0.6119	858.3	557
1.2787	909.9	566
2.1304	941.1	584
3.1162	970.8	586
5.1733	1008.8	586
7.7906	1034.4	586
	T = 313.15	
0.0692	785.0	529
0.1378	796.1	537
0.2690	813.5	555
0.6119	854.0	558
1.2787	903.4	572
2.1304	937.0	586
3.1162	964.2	590
5.1733	995.8	595
7.7906	1020.0	596

Table 6.13 Molality, m, densities, ρ, apparent molar volumes, V_ϕ , for ([MOA]$^+$ [Tf_2N]$^-$ + ethanol) at T = (298.15, 303.15, 308.15 and 313.15) K

Molality, m	ρ / kg·m^{-3}	$10^6 \cdot V_\phi$ / m^3·mol^{-1}
	([MOA]$^+$[Tf_2N]$^-$ + ethanol)	
	T = 298.15K	
0.0692	793.5	565.3
0.1378	806.2	557.9
0.2691	824.1	552.2
0.4006	844.7	546.2
0.6112	868.3	549.2
0.8299	883.8	563.9
1.0077	892.6	575.7
1.2800	910.2	576.9
2.1306	954.4	574.3
3.0002	984.0	573.9
	T = 303.15 K	
0.0692	789.3	569.2
0.1378	802.0	561.7
0.2691	819.9	556.8
0.4006	840.6	549.4
0.6112	864.6	550.6
0.8299	879.9	566.0
1.0077	888.9	577.3
1.2800	906.5	578.6
2.1306	951.0	575.6
3.0002	981.2	574.7
	T = 308.15 K	
0.0692	785.2	575.7
0.1378	797.9	564.6
0.2691	815.8	557.2
0.4006	836.4	550.5
0.6112	860.4	551.9
0.8299	875.8	567.3
1.0077	884.8	578.9
1.2800	902.4	580.2
2.1306	946.9	577.4
3.0002	977.7	576.0
	T = 313.15	
0.0692	781.2	579.9
0.1378	793.7	567.5
0.2691	811.7	560.0
0.4006	832.3	552.0
0.6112	856.3	553.5
0.8299	866.2	569.5
1.0077	880.7	580.7
1.2800	898.3	582.1
2.1306	942.5	579.7
3.0002	973.7	577.8

Table 6.14 Molality, m, densities, ρ, apparent molar volumes, V_ϕ , for (methanol + methyl acetate) at T = (298.15, 303.15, 308.15 and 313.15) K

Molality, m	ρ / kg·m^{-3}	$10^6 \cdot V_\phi$ / m^3·mol^{-1}
	(methanol + methyl acetate)	
	T = 298.15 K	
0.0497	927.6	18.2
0.0811	927.4	27.4
0.1474	927.2	32.2
0.2862	926.6	35.8
0.3555	925.8	38.2
0.4917	925.3	38.4
0.7286	924.4	38.7
0.9736	923.3	39.0
1.4044	921.7	39.1
2.4424	916.9	39.8
3.8983	911.4	39.9
	T = 303.15 K	
0.0497	920.8	22.9
0.0811	920.6	30.4
0.1474	920.4	34.0
0.2862	919.9	36.5
0.3555	919.2	38.5
0.4917	918.4	39.5
0.7286	917.4	39.6
0.9736	916.4	39.7
1.4044	914.6	39.9
2.4424	910.3	40.1
3.8983	905.0	40.1
	T = 308.15 K	
0.0497	914.1	32.6
0.0811	913.9	36.5
0.1474	913.4	40.0
0.2862	912.8	40.1
0.3555	912.4	40.5
0.4917	911.7	40.8
0.7286	910.5	41.0
0.9736	909.3	41.0
1.4044	907.2	41.2
2.4424	902.5	41.2
3.8983	896.4	41.3
	T = 313.15 K	
0.0497	907.9	37.7
0.0811	907.6	41.3
0.1474	907.1	42.7
0.2862	906.2	43.0
0.3555	905.7	43.2
0.4917	904.6	43.8
0.7286	903.0	43.9
0.9736	901.3	44.0
1.4044	898.4	44.0
2.4424	891.7	44.2
3.8983	883.0	44.3

Table 6.15 Molality, m, densities, ρ, apparent molar volumes, V_ϕ , for (methanol + ethyl acetate) at T = (298.15, 303.15, 308.15 and 313.15) K

Molality, m	ρ / kg·m^{-3}	$10^6 \cdot V_\phi$ / m^3·mol^{-1}
	(methanol + ethyl acetate)	
	T = 298.15 K	
0.0495	894.8	25.7
0.1474	894.9	31.6
0.2878	894.7	34.5
0.3556	894.4	35.8
0.4905	893.6	37.9
0.7268	892.2	39.7
0.9740	890.5	41.0
1.4085	888.2	41.6
2.4454	886.1	40.4
3.0005	886.0	39.7
	T = 303.15 K	
0.0495	888.7	30.9
0.1474	888.6	35.2
0.2878	888.5	36.1
0.3556	888.3	36.8
0.4905	887.7	38.2
0.7268	886.4	39.8
0.9740	884.9	40.9
1.4085	882.6	41.6
2.4454	879.8	41.0
3.0005	879.1	40.5
	T = 308.15 K	
0.0495	882.8	33.7
0.1474	882.7	36.3
0.2878	882.4	37.6
0.3556	882.1	38.5
0.4905	881.6	39.2
0.7268	880.6	40.1
0.9740	879.1	41.2
1.4085	877.0	41.8
2.4454	873.8	41.4
3.0005	873.1	40.8
	T = 313.15 K	
0.0495	876.9	36.5
0.1474	876.8	37.4
0.2878	876.4	38.8
0.3556	876.2	39.1
0.4905	875.8	39.5
0.7268	874.8	40.4
0.9740	873.8	40.8
1.4085	871.6	41.7
2.4454	868.4	41.5
3.0005	867.9	40.9

Table 6.16 Molality, m, densities, ρ, apparent molar volumes, V_ϕ , for (ethanol + methyl acetate) at T = (298.15, 303.15, 308.15 and 313.15) K

Molality, m	ρ / kg·m^{-3}	$10^6 \cdot V_\phi$ / m^3·mol^{-1}
	(ethanol + methyl acetate)	
	T = 298.15 K	
0.0357	926.8	56.2
0.1020	926.3	57.7
0.2098	925.5	58.1
0.3417	924.5	58.4
0.5068	923.1	58.9
0.6769	921.8	59.0
0.9775	919.5	59.1
1.7016	914.4	59.1
2.7125	907.8	59.2
3.0001	905.8	59.3
	T = 303.15 K	
0.0357	920.3	56.7
0.1020	919.8	58.2
0.2098	919.0	58.6
0.3417	918.0	58.8
0.5068	916.7	59.1
0.6769	915.4	59.3
0.9775	913.1	59.5
1.7016	908.0	59.5
2.7125	901.5	59.5
3.0001	899.7	59.6
	T = 308.15 K	
0.0357	914.0	57.1
0.1020	913.5	58.6
0.2098	912.7	59.0
0.3417	911.7	59.3
0.5068	910.4	59.6
0.6769	909.1	59.7
0.9775	906.9	59.8
1.7016	901.9	59.8
2.7125	895.4	59.9
3.0001	893.5	60.0
	T = 313.15 K	
0.0357	907.8	57.6
0.1020	907.3	59.1
0.2098	906.5	59.5
0.3417	905.5	59.8
0.5068	904.1	60.3
0.6769	902.8	60.4
0.9775	900.6	60.4
1.7016	895.5	60.5
2.7125	889.0	60.5
3.0001	887.1	60.6

Table 6.17 Molality, m, densities, ρ, apparent molar volumes, V_ϕ , for (ethanol + ethyl acetate) at T = (298.15, 303.15, 308.15 and 313.15) K

Molality, m	ρ / kg·m^{-3}	$10^6 \cdot V_\phi$ / m^3·mol^{-1}
	(ethanol + ethyl acetate)	
	T = 298.15 K	
0.0357	894.7	62.0
0.1025	894.2	61.3
0.2087	893.5	60.5
0.3504	892.6	60.2
0.5065	891.7	59.8
0.6771	890.7	59.7
0.9772	889.1	59.4
1.7008	885.5	59.1
2.7122	880.6	59.1
3.0012	879.4	59.0
	T = 303.15 K	
0.0357	888.2	62.5
0.1025	887.7	61.8
0.2087	887.0	61.1
0.3504	886.1	60.7
0.5065	885.3	60.1
0.6771	884.4	59.8
0.9772	883.0	59.3
1.7008	879.4	59.2
2.7122	874.7	59.2
3.0012	873.5	59.2
	T = 308.15 K	
0.0357	882.7	63.0
0.1025	882.2	62.2
0.2087	881.5	61.5
0.3504	880.6	61.1
0.5065	879.8	60.5
0.6771	878.9	60.2
0.9772	877.4	59.9
1.7008	874.0	59.6
2.7122	869.3	59.6
3.0012	868.1	59.5
	T = 313.15 K	
0.0357	877.0	63.5
0.1025	876.5	62.7
0.2087	875.8	62.0
0.3504	874.9	61.6
0.5065	874.0	61.2
0.6771	873.2	60.7
0.9772	871.8	60.2
1.7008	868.3	60.0
2.7122	863.7	60.0
3.0012	862.5	59.9

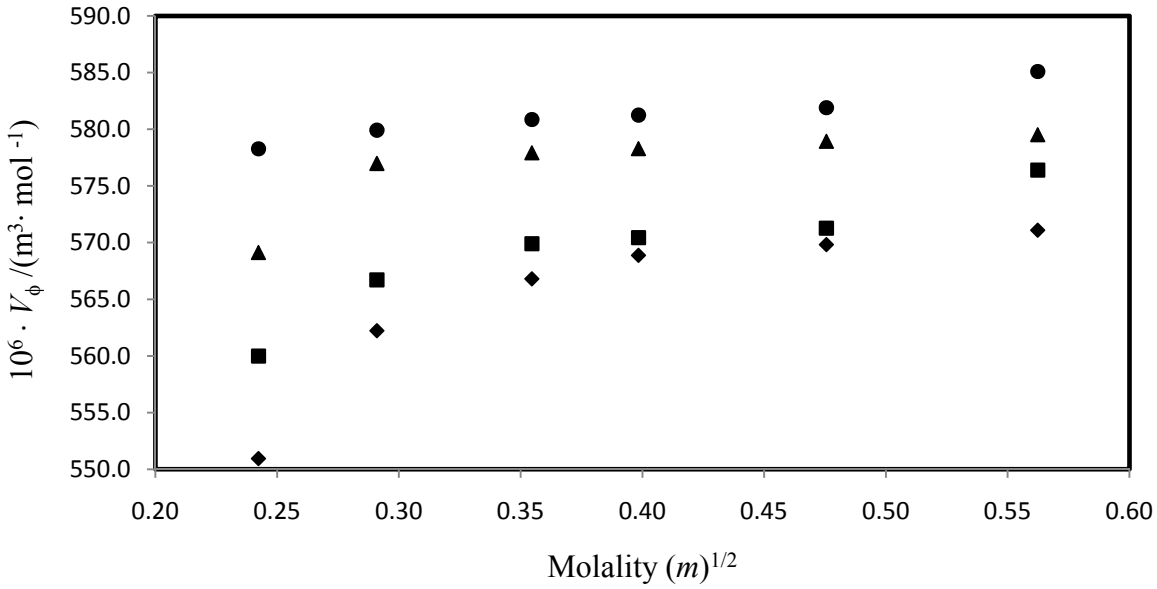

FIGURE 6.31 Apparent molar volume (V_ϕ) versus molality $(m)^{1/2}$ of binary mixture of ([MOA]$^+$[Tf$_2$N]$^-$ + methyl acetate) at T = 298.15 K (♦), 303.15 K (■), 308.15 K (▲) and 313.15 K (•).

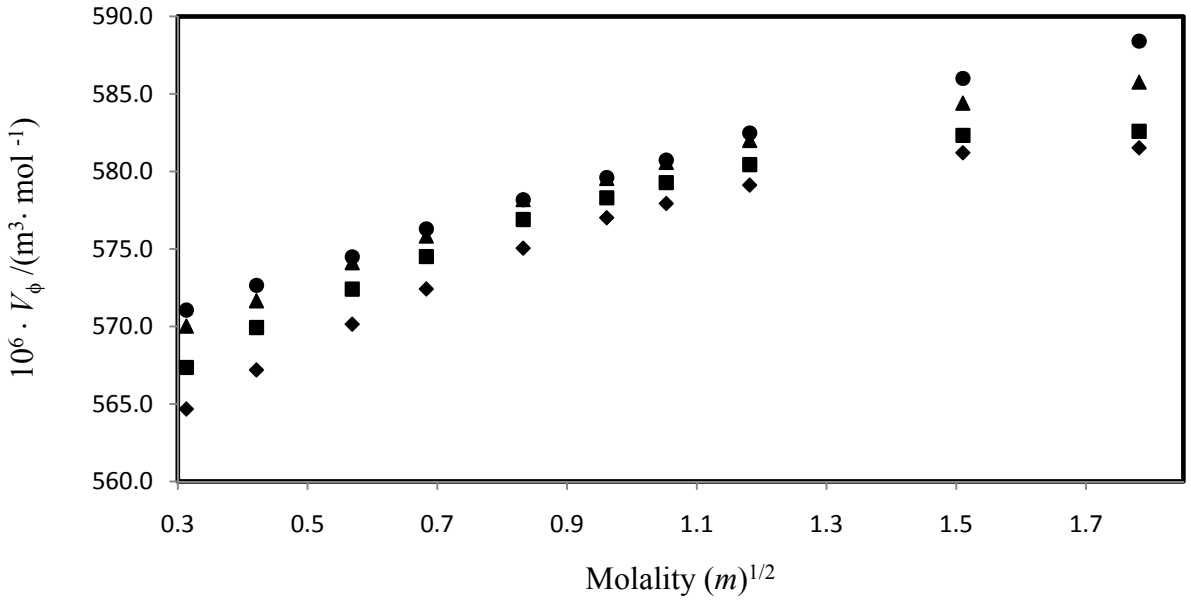

FIGURE 6.32 Apparent molar volume (V_ϕ) versus molality $(m)^{1/2}$ of binary mixture of ([MOA]$^+$[Tf$_2$N]$^-$ + ethyl acetate) at T = 298.15 K (♦), 303.15 K (■), 308.15 K (▲) and 313.15 K (•).

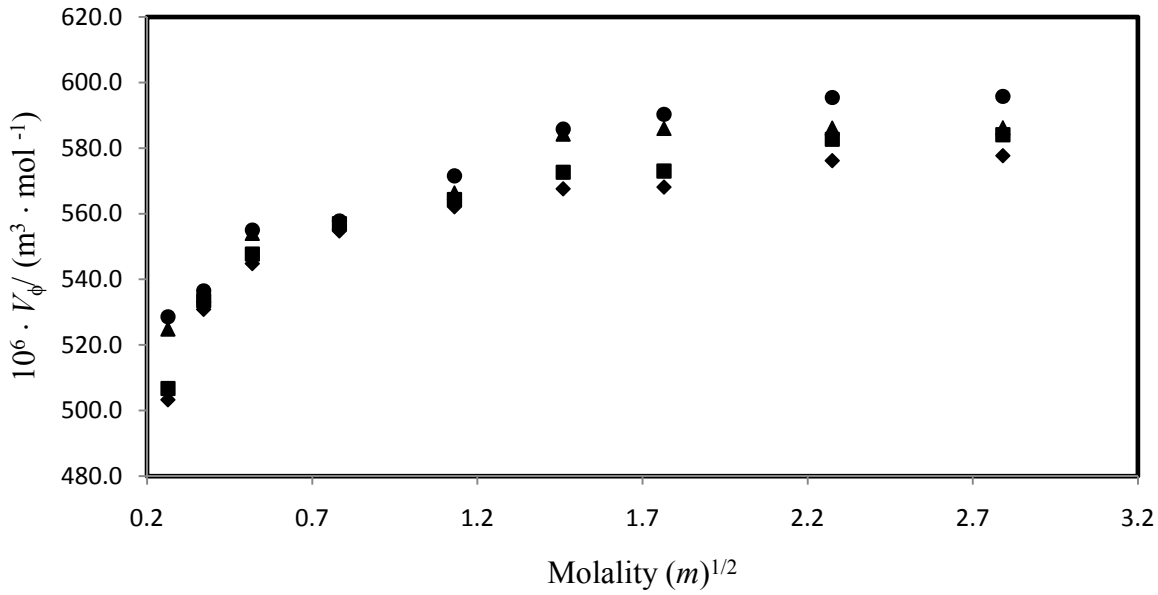

FIGURE 6.33 Apparent molar volume (V_ϕ) versus molality $(m)^{1/2}$ of binary mixture of ([MOA]$^+$[Tf$_2$N]$^-$ + methanol) at T = 298.15 K (♦), 303.15 K (■), 308.15 K (▲) and 313.15 K (•).

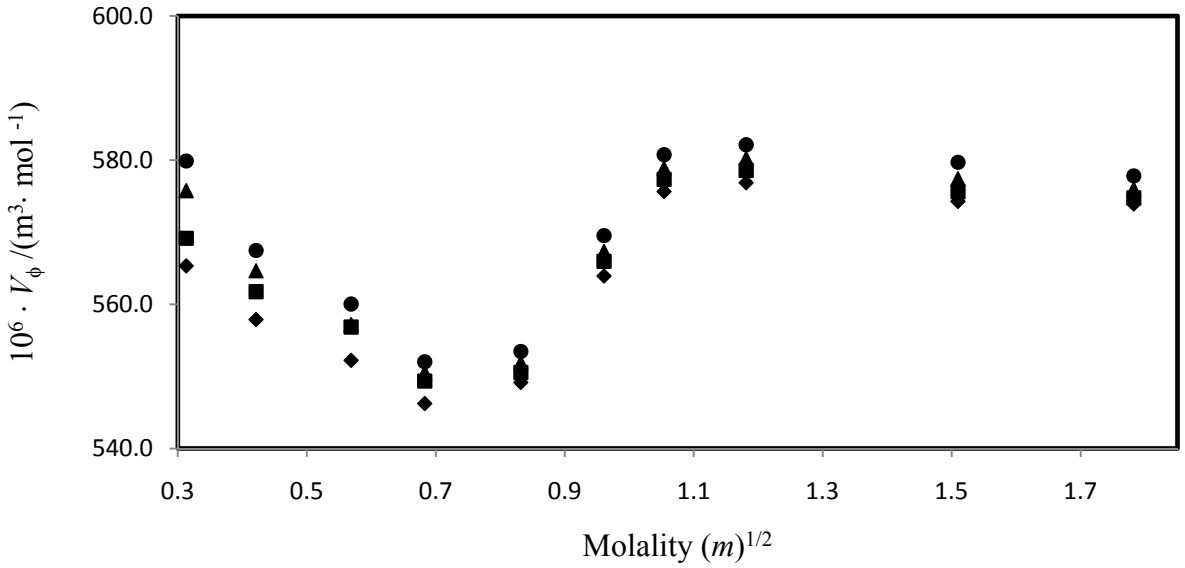

FIGURE 6.34 Apparent molar volume (V_ϕ) versus molality $(m)^{1/2}$ of binary mixture of ([MOA]$^+$[Tf$_2$N]$^-$ + ethanol) at T = 298.15 K (♦), 303.15 K (■), 308.15 K (▲) and 313.15 K (•).

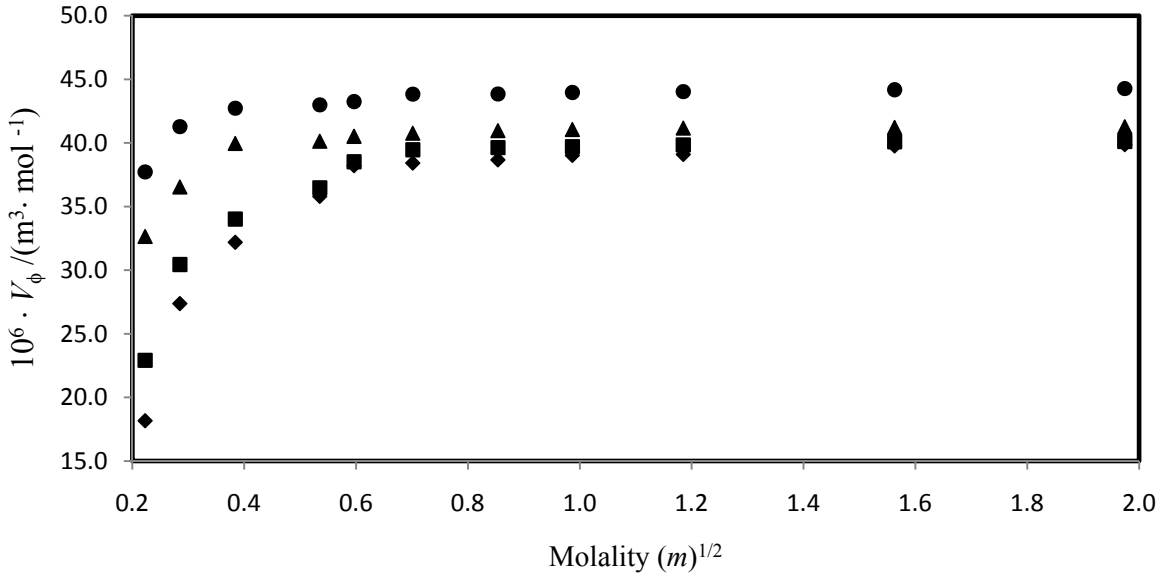

FIGURE 6.35 Apparent molar volume (V_ϕ) versus molality $(m)^{1/2}$ of binary mixture of (methanol + methyl acetate) at T = 298.15 K (♦), 303.15 K (■), 308.15 K (▲) and 313.15 K (•).

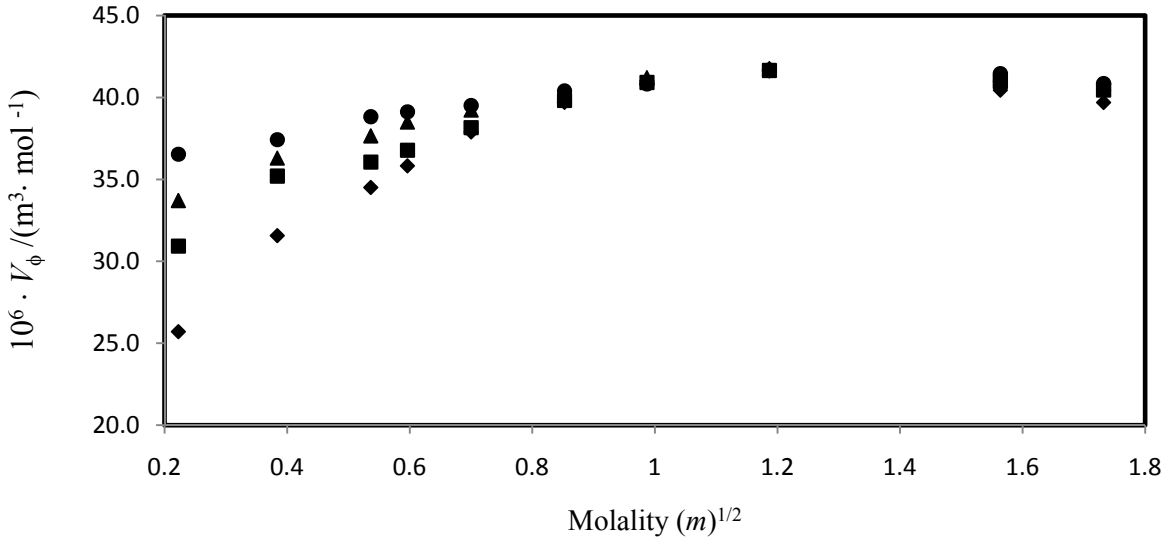

FIGURE 6.36 Apparent molar volume (V_ϕ) versus molality $(m)^{1/2}$ of binary mixture of (methanol + ethyl acetate) at T = 298.15 K (♦), 303.15 K (■), 308.15 K (▲) and 313.15 K (•).

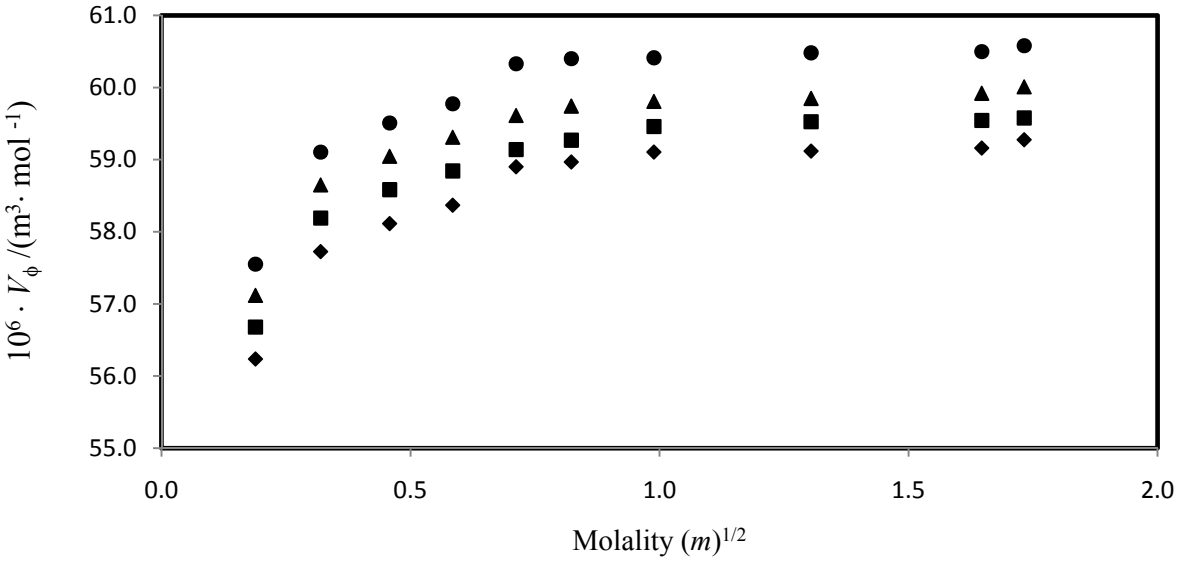

FIGURE 6.37 Apparent molar volume (V_ϕ) versus molality $(m)^{1/2}$ of binary mixture of (ethanol + methyl acetate) at T = 298.15 K (♦), 303.15 K (■), 308.15 K (▲) and 313.15 K (•).

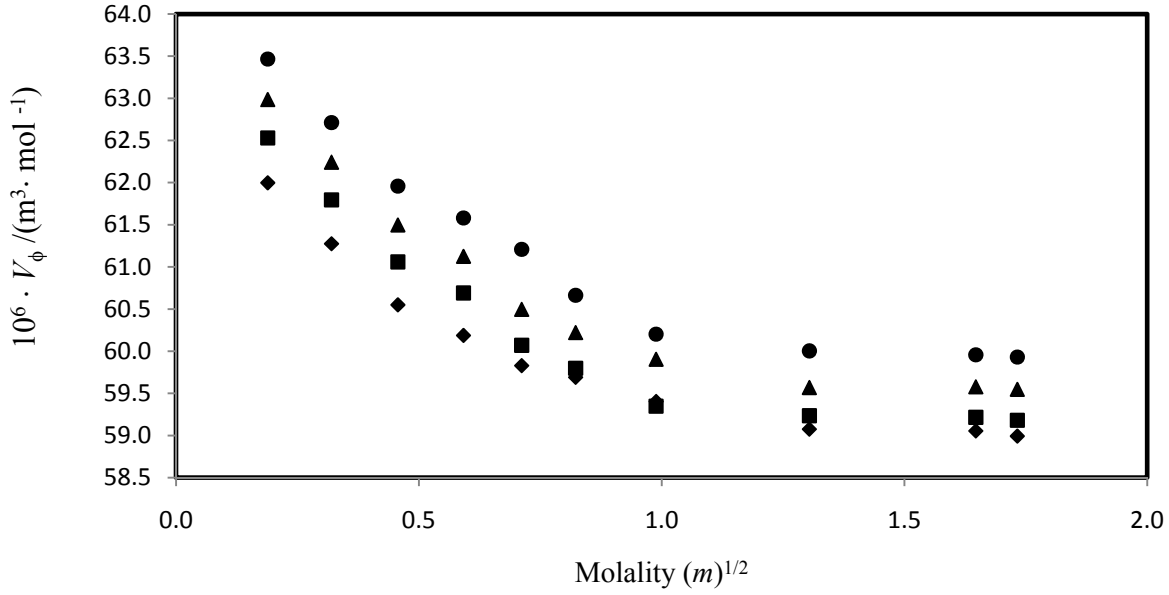

FIGURE 6.38 Apparent molar volume (V_ϕ) versus molality $(m)^{1/2}$ of binary mixture of (ethanol + ethyl acetate) at T = 298.15 K (♦), 303.15 K (■), 308.15 K (▲) and 313.15 K (•).

6.2.2 Partial molar volumes at infinite dilution

For the systems {$[MOA]^+[Tf_2N]^-$ + methanol or ethanol or methyl acetate or ethyl acetate}, (methanol + methyl acetate or ethyl acetate) and (ethanol + methyl acetate or ethyl acetate) the partial molar volume at infinite dilution, V_ϕ^0 , and empirical parameters S_v and B_v were obtained from the Redlich-Mayer equation coefficients using equation (6.5) and partial molar volumes at infinite dilution, V_ϕ^0 , the coefficients S_v , B_v and standard deviations, σ_v , obtained for all the systems studied are given in Table 6.18.

6.2.3 Limiting apparent molar expansibility

The limiting apparent molar expansibility E_ϕ^0 values calculated using equation (6.7) are given in Table 6.19 for the systems {$[MOA]^+[Tf_2N]^-$ + methanol or ethanol or methyl acetate or ethyl acetate}, (methanol + methyl acetate or ethyl acetate) and (ethanol + methyl acetate or ethyl acetate).

Table 6.18 The values of V_ϕ^0, S_v, B_v, and standard deviation, σ_v, obtained for each binary system at the experimental temperatures

T/ *K*	$10^6 \cdot V_\phi^0$ / $m^3 \cdot mol^{-1}$	$10^6 \cdot S_v$ / $m^3 \cdot mol^{-3/2} \cdot kg^{1/2}$	$10^6 \cdot B_v$ / $m^3 \cdot mol^{-2} \cdot kg$	$10^6 \cdot \sigma_v$
		([MOA]$^+$[Tf$_2$N]$^-$ + methyl acetate)		
298.15	477.2	405.2	-429.8	2.8
303.15	516.9	225.9	-220.2	2.7
308.15	538.6	176.7	-187.7	1.8
313.15	567.8	48.4	-34.0	1.0
		([MOA]$^+$[Tf$_2$N]$^-$ + ethyl acetate)		
298.15	557.5	29.3	-8.9	0.12
303.15	561.2	26.1	-7.9	0.13
308.15	564.7	21.0	-5.1	0.13
313.15	567.0	15.7	-1.9	0.13
		([MOA]$^+$[Tf$_2$N]$^-$ + methanol)		
298.15	502.8	68.5	-15.5	9.6
303.15	505.4	68.9	-15.0	9.1
308.15	512.8	69.2	-15.6	5.3
313.15	515.3	70.1	-14.0	4.1
		([MOA]$^+$[Tf$_2$N]$^-$ + ethanol)		
298.15	553.9	4.5	5.8	10.0
303.15	559.6	-0.7	7.2	10.0
308.15	566.3	-10.9	11.5	11.0
313.15	571.1	-16.0	13.7	11.3
		(methanol + methyl acetate)		
298.15	17.2	37.1	-13.5	3.5
303.15	21.8	30.3	-11.1	2.7
308.15	32.9	14.1	-5.2	1.7
313.15	38.1	9.9	-3.6	1.1
		(methanol + ethyl acetate)		
298.15	19.0	36.5	-14.4	0.52
303.15	26.8	22.5	-8.4	0.49
308.15	30.3	17.3	-6.5	0.18
313.15	34.1	10.7	-3.9	0.20
		(ethanol + methyl acetate)		
298.15	55.7	5.6	-2.2	0.31
303.15	56.3	5.5	-2.1	0.30
308.15	56.8	5.3	-2.0	0.34
313.15	57.1	5.9	-2.3	0.34
		(ethanol + ethyl acetate)		
298.15	62.8	-5.3	1.9	0.12
303.15	63.6	-6.6	2.3	0.11
308.15	64.1	-6.5	2.3	0.09
313.15	64.6	-6.5	2.2	0.11

Table 6.19 The infinite dilution apparent molar expansibility, E_{ϕ}^{0}, values for each binarysystem at T = (298.15, 303.15, 308.15 and 313.15) K

Solute	Solvent	E_{ϕ}^{0} / $cm^3 \cdot mol^{-1} \cdot K^{-1}$			
		T = 298.15 K	T = 303.15 K	T = 308.15 K	T = 313.15 K
$[MOA]^+[Tf_2N]^-$	Methyl acetate	7.44	6.39	5.34	4.29
$[MOA]^+[Tf_2N]^-$	Ethyl acetate	0.85	0.71	0.57	0.43
$[MOA]^+[Tf_2N]^-$	Methanol	0.91	0.90	0.89	0.88
$[MOA]^+[Tf_2N]^-$	Ethanol	1.29	1.21	1.12	1.05
Methanol	Methyl acetate	1.39	1.45	1.51	1.57
Methanol	Ethyl acetate	1.58	1.18	0.78	0.38
Ethanol	Methyl acetate	0.14	0.11	0.08	0.05
Ethanol	Ethyl acetate	0.16	0.13	0.10	0.07

6.3 Isentropic compressibility

The isentropic compressibilities, κ_S, were calculated from the Newton-Laplace equation (6.8) for the binary system {$[MOA]^+[Tf_2N]^-$ + methanol or ethanol or methyl acetate or ethyl acetate}, (methanol + methyl acetate or ethyl acetate) , (ethanol + methyl acetate or ethyl acetate) and {$[BMIM]^+[MeSO_4]^-$ + } at T = (298.15, 303.15, 308.15 and 313.15) K are presented in Tables 6.20 - 6.27 and κ_S, versus molality m are plotted in Figures 6.39 – 6.46.

6.3.1 Apparent molar isentropic compressibility

The apparent molar isentropic compressibility were calculated from equation (6.9).

The results for speed of sound, u, apparent molar isentropic compressibility κ_ϕ, for the binary system {$[MOA]^+[Tf_2N]^-$ + methanol or ethanol or methyl acetate or ethyl acetate}, (methanol + methyl acetate or ethyl acetate) , (ethanol + methyl acetate or ethyl acetate) and {$[BMIM]^+[MeSO_4]^-$ + } at T = (298.15, 303.15, 308.15 and 313.15) K are presented in Tables 6.20 - 6.27 and κ_ϕ, versus molality $m^{1/2}$ are plotted in Figures 6.47 – 6.54.

Table 6.20 Molality, m, densities, ρ, speed of sound, u, isentropic compressibilities, κ_s, and apparent molar isentropic compressibilities, κ_ϕ, for $([MOA]^+ [Tf_2N]^-$ + methyl acetate) at T = (298.15, 303.15, 308.15 and 313.15) K

Molality, m	ρ/ kg·m^{-3}	u / m·s^{-1}	$10^{12}\cdot \kappa_s$ / Pa^{-1}	$10^{15}\cdot \kappa_\phi$ / m^3·mol^{-1}·Pa^{-1}
		$([MOA]^+ [Tf_2N]^-$ + methyl acetate)		
		T = 298.15 K		
0.0271	930.8	1146	818.0	297.3
0.0587	934.2	1140	823.7	493.9
0.0847	936.5	1134	830.4	580.0
0.1257	940.4	1128	835.7	596.0
0.1587	943.4	1122	842.0	618.6
0.2262	949.5	1110	854.8	646.0
0.3162	956.9	1092	876.4	687.8
		T = 303.15 K		
0.0271	923.9	1140	832.8	-391.2
0.0587	927.3	1134	838.6	184.7
0.0847	929.8	1128	845.3	367.0
0.1257	933.8	1122	850.7	456.1
0.1587	937.0	1116	856.9	508.8
0.2262	943.2	1104	869.9	573.3
0.3162	949.8	1086	892.7	647.6
		T = 308.15 K		
0.0271	917.3	1134	847.7	-1145.3
0.0587	920.7	1128	853.6	-154.7
0.0847	923.0	1122	860.6	142.9
0.1257	927.0	1116	866.1	310.5
0.1587	930.1	1110	872.6	398.7
0.2262	936.1	1098	886.1	503.8
0.3162	943.5	1080	908.7	598.2
		T = 313.15 K		
0.0271	911.1	1 128	862.6	-1977.5
0.0587	914.4	1 122	868.7	-526.6
0.0847	917.0	1 116	875.6	-116.2
0.1257	921.0	1 110	881.2	141.1
0.1587	924.1	1 104	887.9	268.2
0.2262	930.1	1 092	901.6	417.8
0.3162	936.9	1 074	925.3	547.6

Table 6.21 Molality, m, densities, ρ, speed of sound, u, isentropic compressibilities, κ_s , and apparent molar isentropic compressibilities, κ_ϕ , for $([MOA]^+ [Tf_2N]^-$ + ethyl acetate) at T = (298.15, 303.15, 308.15 and 313.15) K

Molality, m	ρ/ kg·m^{-3}	u / m·s^{-1}	$10^{12}\cdot \kappa_s$ /Pa^{-1}	$10^{15}\cdot \kappa_\phi$ / m^3·mol^{-1}·Pa^{-1}
		($[MOA]^+ [Tf_2N]^-$ + ethyl acetate)		
		T = 298.15 K		
0.0692	903.0	1140	852.1	14249.1
0.1377	910.7	1149	831.7	7222.8
0.2691	923.8	1152	815.7	3854.1
0.4006	935.1	1155	801.6	2696.0
0.6119	950.4	1161	780.6	1875.2
0.8299	963.4	1164	766.1	1474.1
1.0059	972.5	1170	751.2	1269.0
1.2799	984.5	1179	730.7	1061.5
2.1321	1011.1	1200	686.8	759.3
2.9994	1029.3	1206	668.0	637.4
		T = 303.15 K		
0.0692	897.1	1122	885.5	14904.1
0.1377	904.8	1125	873.3	7632.8
0.2691	918.0	1128	856.1	4070.8
0.4006	929.4	1131	841.1	2846.2
0.6119	944.9	1140	814.3	1967.7
0.8299	958.3	1146	794.6	1537.0
1.0059	967.5	1158	770.8	1308.9
1.2799	979.7	1161	757.3	1105.4
2.1321	1006.9	1170	725.5	805.5
2.9994	1025.5	1182	698.0	668.5
		T = 308.15 K		
0.0692	891.3	1104	920.5	15595.0
0.1377	899.1	1107	907.6	7983.3
0.2691	912.4	1110	889.5	4255.6
0.4006	924.0	1113	873.7	2973.5
0.6119	939.7	1116	854.4	2076.0
0.8299	953.3	1122	833.3	1620.4
1.0059	962.6	1128	816.5	1393.5
1.2799	974.8	1137	793.5	1164.2
2.1321	1001.9	1152	752.1	839.1
2.9994	1019.5	1161	727.7	701.1
		T = 313.15 K		
0.0692	885.0	1077	974.1	16620.9
0.1377	892.9	1080	960.2	8504.3
0.2691	906.5	1083	940.5	4528.8
0.4006	918.3	1086	923.3	3162.1
0.6119	934.5	1092	897.4	2192.4
0.8299	948.4	1098	874.6	1709.5
1.0059	957.9	1107	851.9	1461.1
1.2799	970.2	1113	832.0	1226.5
2.1321	997.0	1131	784.1	879.2
2.9994	1013.8	1140	759.0	735.4

Table 6.22 Molality, m, densities, ρ, speed of sound, u, isentropic compressibilities, κ_s , and apparent molar isentropic compressibilities, κ_ϕ , for ([MOA]$^+$ [Tf_2N]$^-$ + methanol) at T = (298.15, 303.15, 308.15 and 313.15) K

Molality, m	ρ/ kg·m^{-3}	u / m·s^{-1}	$10^{12}\cdot \kappa_s$ / Pa^{-1}	$10^{15}\cdot \kappa_\phi$ / m^3·mol^{-1}·Pa^{-1}
([MOA]$^+$ [Tf_2N]$^-$ + methanol)				
		T = 298.15K		
0.0692	800.0	1116	1003.6	-288.7
0.1378	810.3	1122	980.3	-93.4
0.2690	828.4	1128	948.7	53.2
0.6119	867.3	1140	887.2	160.5
1.2787	919.4	1164	802.8	208.6
2.1304	960.4	1176	752.9	251.9
3.1162	993.5	1188	715.3	271.2
5.1733	1024.6	1212	664.4	288.9
7.7906	1049.0	1224	636.3	300.6
		T = 303.15 K		
0.0692	795.2	1110	1020.7	-661.2
0.1378	805.5	1116	996.8	-281.3
0.2690	823.5	1122	964.6	-41.1
0.6119	862.5	1134	901.6	120.1
1.2787	914.6	1158	815.4	191.0
2.1304	953.3	1170	766.3	247.9
3.1162	986.1	1182	725.8	268.8
5.1733	1014.7	1206	677.6	294.3
7.7906	1038.7	1218	649.0	307.6
		T = 308.15 K		
0.0692	789.8	1104	1038.8	-880.1
0.1378	800.8	1110	1013.5	-409.8
0.2690	818.1	1116	981.4	-97.3
0.6119	858.3	1128	915.7	90.1
1.2787	909.9	1152	828.1	179.9
2.1304	941.1	1164	784.3	258.2
3.1162	970.8	1176	744.8	283.5
5.1733	1008.8	1200	688.4	297.2
7.7906	1034.4	1212	658.1	310.3
		T = 313.15		
0.0692	785.0	1098	1056.6	-1556.7
0.1378	796.1	1104	1030.6	-753.7
0.2690	813.5	1110	997.7	-273.8
0.6119	854.0	1122	930.2	12.1
1.2787	903.4	1146	842.9	150.8
2.1304	937.0	1158	795.9	239.1
3.1162	964.2	1170	757.6	276.1
5.1733	995.8	1194	704.4	303.0
7.7906	1020.0	1206	674.1	319.3

Table 6.23 Molality, m, densities, ρ, speed of sound, u, isentropic compressibilities, κ_s , and apparent molar isentropic compressibilities, κ_ϕ , for ([MOA]$^+$ [Tf_2N]$^-$ + ethanol) at T = (298.15, 303.15, 308.15 and 313.15) K

Molality, m	ρ / kg·m^{-3}	u / m·s^{-1}	$10^{12}\cdot \kappa_s$ / Pa^{-1}	$10^{15}\cdot \kappa_\phi$ / m^3·mol^{-1}·Pa^{-1}
		([MOA]$^+$[Tf_2N]$^-$ + ethanol)		
		T = 298.15K		
0.0692	793.5	1149	954.6	18091.2
0.1378	806.2	1152	934.7	9151.5
0.2691	824.1	1158	904.9	4779.3
0.4006	844.7	1170	864.8	3219.9
0.6112	868.3	1176	832.8	2191.5
0.8299	883.8	1179	814.0	1707.4
1.0077	892.6	1182	801.9	1474.4
1.2800	910.2	1188	778.4	1223.1
2.1306	954.4	1200	727.6	852.5
3.0002	984.0	1218	685.0	683.8
		T = 303.15 K		
0.0692	789.3	1128	995.7	18961.4
0.1378	802.0	1134	969.6	9539.9
0.2691	819.9	1140	938.5	4982.0
0.4006	840.6	1149	901.1	3371.3
0.6112	864.6	1158	862.5	2279.6
0.8299	879.9	1161	843.1	1776.4
1.0077	888.9	1164	830.3	1533.0
1.2800	906.5	1170	805.9	1271.3
2.1306	951.0	1182	752.6	885.0
3.0002	981.2	1200	707.8	708.4
		T = 308.15 K		
0.0692	785.2	1107	1039.3	19903.4
0.1378	797.9	1116	1006.3	9955.3
0.2691	815.8	1122	973.7	5194.9
0.4006	836.4	1134	929.7	3495.9
0.6112	860.4	1140	894.3	2375.1
0.8299	875.8	1146	869.4	1840.3
1.0077	884.8	1149	856.1	1587.9
1.2800	902.4	1158	826.4	1309.6
2.1306	946.9	1170	771.5	911.0
3.0002	977.7	1179	735.8	739.2
		T = 313.15		
0.0692	781.2	1086	1085.4	20897.9
0.1378	793.7	1104	1033.7	10280.8
0.2691	811.7	1110	999.9	5362.9
0.4006	832.3	1116	964.7	3645.3
0.6112	856.3	1125	922.7	2462.3
0.8299	866.2	1131	902.5	1919.8
1.0077	880.7	1134	883.0	1645.4
1.2800	898.3	1146	847.6	1349.4
2.1306	942.5	1155	795.3	943.6
3.0002	973.7	1158	765.9	772.5

Table 6.24 Molality, m, densities, ρ, speed of sound, u, isentropic compressibilities, κ_s , and apparent molar isentropic compressibilities, κ_ϕ , for (methanol + methyl acetate) at T = (298.15, 303.15, 308.15 and 313.15) K

Molality, m	ρ / kg·m^{-3}	u / m·s^{-1}	$10^{12}\cdot \kappa_s$ / Pa^{-1}	$10^{15}\cdot \kappa_\phi$ / m^3·mol^{-1}·Pa^{-1}
		(methanol + methyl acetate)		
		T = 298.15 K		
0.0497	927.6	1164	795.7	-545.7
0.0811	927.4	1158	804.1	-209.1
0.1474	927.2	1155	808.5	-69.3
0.2862	926.6	1152	813.2	-2.1
0.3555	925.8	1146	822.5	34.4
0.4917	925.3	1143	827.2	44.4
0.7286	924.4	1134	841.2	61.8
0.9736	923.3	1131	846.7	61.0
1.4044	921.7	1128	852.7	57.3
2.4424	916.9	1125	861.7	52.0
3.8983	911.4	1122	871.6	48.6
		T = 303.15 K		
0.0497	920.8	1158	809.9	-945.7
0.0811	920.6	1152	818.5	-450.4
0.1474	920.4	1149	823.0	-200.7
0.2862	919.9	1146	827.7	-69.5
0.3555	919.2	1140	837.1	-19.4
0.4917	918.4	1137	842.3	7.3
0.7286	917.4	1128	856.7	38.0
0.9736	916.4	1125	862.2	43.4
1.4044	914.6	1122	868.5	45.9
2.4424	910.3	1119	877.3	45.5
3.8983	905.0	1116	887.2	44.8
		T = 308.15 K		
0.0497	914.1	1152	824.3	-1374.2
0.0811	913.9	1146	833.2	-709.1
0.1474	913.4	1140	842.4	-304.7
0.2862	912.8	1137	847.4	-121.0
0.3555	912.4	1134	852.3	-75.3
0.4917	911.7	1131	857.5	-32.9
0.7286	910.5	1122	872.4	12.4
0.9736	909.3	1119	878.3	25.1
1.4044	907.2	1116	885.1	34.1
2.4424	902.5	1113	894.5	39.8
3.8983	896.4	1110	905.4	42.2
		T = 313.15 K		
0.0497	907.9	1146	838.7	-1849.2
0.0811	907.6	1140	847.8	-993.8
0.1474	907.1	1137	852.8	-492.8
0.2862	906.2	1134	858.1	-214.9
0.3555	905.7	1128	867.8	-135.4
0.4917	904.6	1122	878.1	-63.3
0.7286	903.0	1116	889.2	-13.0
0.9736	901.3	1110	900.5	13.5
1.4044	898.4	1107	908.3	28.0
2.4424	891.7	1104	920.1	39.1
3.8983	883.0	1098	939.4	46.1

Table 6.25 Molality, m, densities, ρ, speed of sound, u, isentropic compressibilities, κ_s , and apparent molar isentropic compressibilities, κ_ϕ , for (methanol + ethyl acetate) at T = (298.15, 303.15, 308.15 and 313.15) K

Molality, m	ρ / kg·m^{-3}	u / m·s^{-1}	$10^{12}\cdot \kappa_s$ / Pa^{-1}	$10^{15}\cdot \kappa_\phi$ / m^3·mol^{-1}·Pa^{-1}
		(methanol + ethyl acetate)		
		T = 298.15 K		
0.0495	894.8	1116	897.3	20294.4
0.1474	894.9	1119	892.4	6799.2
0.2878	894.7	1122	887.8	3479.7
0.3556	894.4	1125	883.4	2809.4
0.4905	893.6	1128	879.5	2038.3
0.7268	892.2	1125	885.6	1397.6
0.9740	890.5	1134	873.3	1038.2
1.4085	888.2	1137	870.9	727.6
2.4454	886.1	1140	868.4	432.2
3.0005	886.0	1143	863.9	356.2
		T = 303.15 K		
0.0495	888.7	1092	943.6	21488.2
0.1474	888.6	1095	938.6	7201.5
0.2878	888.5	1098	933.6	3684.4
0.3556	888.3	1101	928.7	2973.6
0.4905	887.7	1104	924.3	2156.2
0.7268	886.4	1107	920.6	1462.3
0.9740	884.9	1110	917.2	1097.4
1.4085	882.6	1113	914.6	768.9
2.4454	879.8	1116	912.6	457.4
3.0005	879.1	1122	903.6	375.5
		T = 308.15 K		
0.0495	882.8	1065	998.7	22894.5
0.1474	882.7	1068	993.2	7671.8
0.2878	882.4	1071	988.0	3926.2
0.3556	882.1	1074	982.8	3169.1
0.4905	881.6	1077	977.9	2297.2
0.7268	880.6	1080	973.6	1556.7
0.9740	879.1	1089	959.2	1155.2
1.4085	877.0	1092	956.2	809.0
2.4454	873.8	1095	954.5	481.7
3.0005	873.1	1098	950.0	397.5
		T = 313.15 K		
0.0495	876.9	1044	1046.3	23322.0
0.1474	876.8	1047	1040.4	7815.9
0.2878	876.4	1050	1034.9	4000.8
0.3556	876.2	1053	1029.3	3230.0
0.4905	875.8	1056	1023.9	2341.0
0.7268	874.8	1059	1019.3	1585.5
0.9740	873.8	1062	1014.7	1188.5
1.4085	871.6	1065	1011.5	831.2
2.4454	868.4	1068	1009.6	493.9
3.0005	867.9	1071	1004.5	409.0

Table 6.26 Molality, m, densities, ρ, speed of sound, u, isentropic compressibilities, κ_s , and apparent molar isentropic compressibilities, κ_ϕ , for (ethanol + methyl acetate) at T = (298.15, 303.15, 308.15 and 313.15) K

Molality(m)	ρ / kg·m^{-3}	u / m·s^{-1}	$10^{12}\cdot \kappa_s$ / Pa^{-1}	$10^{15}\cdot \kappa_\phi$ / m^3·mol^{-1}·Pa^{-1}
		(ethanol + methyl acetate)		
		T = 298.15 K		
0.0357	926.8	1152	813.0	24640.8
0.1020	926.3	1149	817.7	8693.9
0.2098	925.5	1146	822.7	4278.6
0.3417	924.5	1143	827.9	2662.0
0.5068	923.1	1140	833.6	1823.3
0.6769	921.8	1137	839.2	1386.8
0.9775	919.5	1134	845.7	983.2
1.7016	914.4	1131	854.9	592.5
2.7125	907.8	1128	865.7	395.5
3.0001	905.8	1122	877.0	367.3
		T = 303.15 K		
0.0357	920.3	1131	849.5	25926.7
0.1020	919.8	1128	854.5	9148.5
0.2098	919.0	1125	859.8	4502.9
0.3417	918.0	1122	865.3	2801.9
0.5068	916.7	1119	871.2	1918.8
0.6769	915.4	1116	877.1	1459.7
0.9775	913.1	1113	884.1	1035.1
1.7016	908.0	1110	893.9	623.9
2.7125	901.5	1107	905.2	416.4
3.0001	899.7	1104	911.9	384.6
		T = 308.15 K		
0.0357	914.0	1110	888.0	27289.3
0.1020	913.5	1107	893.3	9630.4
0.2098	912.7	1104	898.9	4740.6
0.3417	911.7	1101	904.8	2950.1
0.5068	910.4	1098	911.1	2020.6
0.6769	909.1	1095	917.4	1537.3
0.9775	906.9	1092	924.7	1090.0
1.7016	901.9	1089	934.9	657.0
2.7125	895.4	1086	946.9	438.6
3.0001	893.5	1080	959.5	407.4
		T = 313.15 K		
0.0357	907.8	1086	934.0	28899.6
0.1020	907.3	1083	939.7	10199.9
0.2098	906.5	1080	945.8	5021.6
0.3417	905.5	1077	952.1	3125.4
0.5068	904.1	1074	958.9	2141.5
0.6769	902.8	1071	965.7	1629.4
0.9775	900.6	1068	973.5	1155.5
1.7016	895.5	1065	984.5	696.8
2.7125	889.0	1062	997.4	465.3
3.0001	887.1	1056	1010.9	432.3

Table 6.27 Molality, m, densities, ρ, speed of sound, u, isentropic compressibilities, κ_s , and apparent molar isentropic compressibilities, κ_ϕ , for (ethanol + ethyl acetate) at T = (298.15, 303.15, 308.15 and 313.15) K

Molality(m)	ρ / kg·m^{-3}	u / m·s^{-1}	$10^{12}\cdot \kappa_s$ / Pa^{-1}	$10^{15}\cdot \kappa_\phi$ / m^3·mol^{-1}·Pa^{-1}
		(ethanol + ethyl acetate)		
		T = 298.15 K		
0.0357	894.7	1150.8	844.0	26495.8
0.1025	894.2	1149.0	847.1	9287.1
0.2087	893.5	1147.2	850.4	4604.6
0.3504	892.6	1143.0	857.5	2786.0
0.5065	891.7	1140.0	862.9	1955.1
0.6771	890.7	1138.8	865.7	1480.3
0.9772	889.1	1136.4	870.9	1047.5
1.7008	885.5	1131.0	882.8	632.1
2.7122	880.6	1128.0	892.5	420.4
3.0012	879.4	1122.0	903.3	389.6
		T = 303.15 K		
0.0357	888.2	1134.0	875.5	27687.5
0.1025	887.7	1130.4	881.6	9736.3
0.2087	887.0	1128.0	886.0	4832.7
0.3504	886.1	1123.2	894.5	2927.6
0.5065	885.3	1119.0	902.1	2058.6
0.6771	884.4	1116.0	907.9	1563.4
0.9772	883.0	1113.0	914.2	1107.2
1.7008	879.4	1110.0	922.9	665.4
2.7122	874.7	1107.0	932.9	442.4
3.0012	873.5	1101.0	944.4	410.1
		T = 308.15 K		
0.0357	882.7	1114.8	911.6	29007.6
0.1025	882.2	1110.0	920.0	10223.8
0.2087	881.5	1098.0	941.0	5164.3
0.3504	880.6	1092.0	952.3	3136.1
0.5065	879.8	1090.8	955.3	2193.6
0.6771	878.9	1086.0	964.7	1671.7
0.9772	877.4	1083.0	971.7	1184.3
1.7008	874.0	1080.0	980.9	711.6
2.7122	869.3	1074.0	997.3	475.8
3.0012	868.1	1068.0	1009.9	441.2
		T = 313.15 K		
0.0357	877.0	1092.0	956.2	30625.8
0.1025	876.5	1089.0	962.0	10760.5
0.2087	875.8	1077.0	984.4	5437.7
0.3504	874.9	1069.2	999.8	3314.0
0.5065	874.0	1066.8	1005.4	2323.9
0.6771	873.2	1062.0	1015.4	1771.0
0.9772	871.8	1059.0	1022.8	1254.6
1.7008	868.3	1056.0	1032.8	754.1
2.7122	863.7	1053.0	1044.2	501.5
3.0012	862.5	1044.0	1063.8	467.8

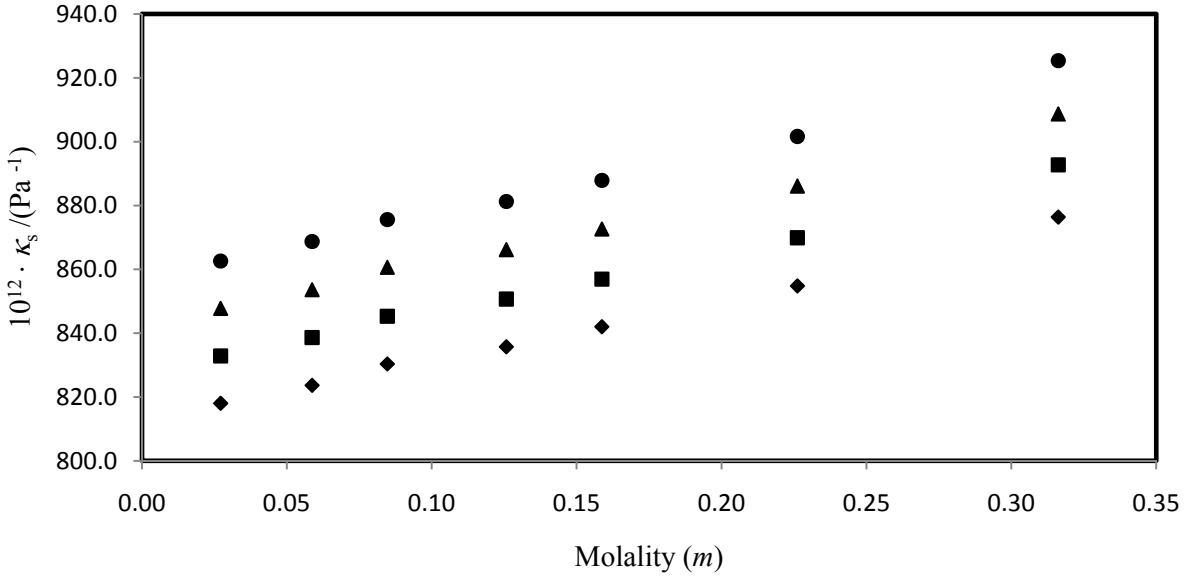

FIGURE 6.39 Isentropic compressibility (κ_s) versus molality (m) of binary mixture of ([MOA]$^+$[Tf$_2$N]$^-$ + methyl acetate) at T = 298.15 K (♦), 303.15 K (■), 308.15 K (▲) and 313.15 K (•).

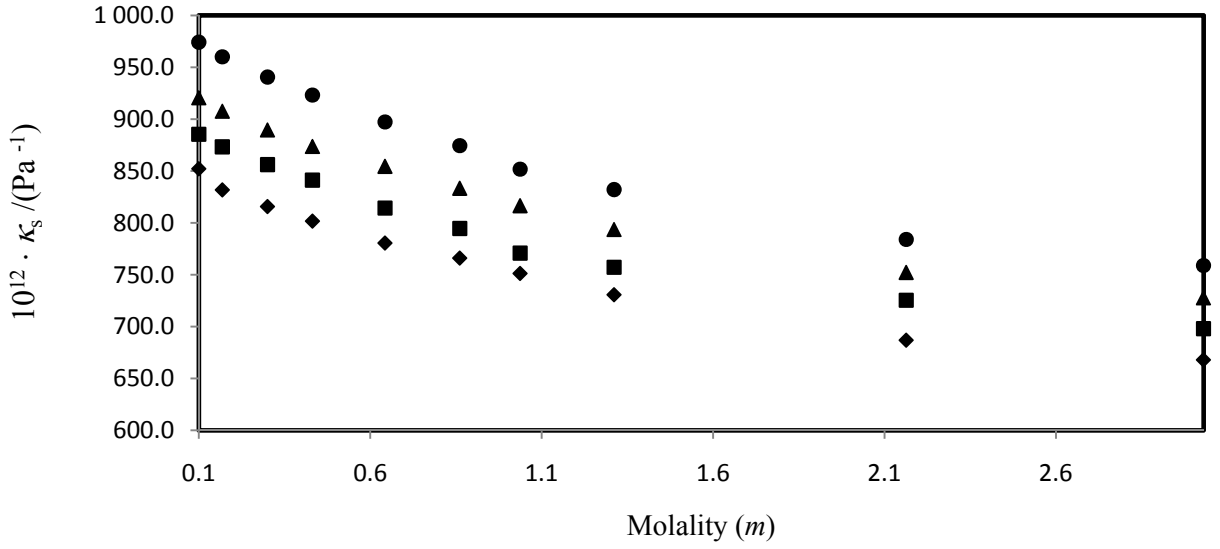

FIGURE 6.40 Isentropic compressibility (κ_s) versus molality (m) of binary mixture of ([MOA]$^+$[Tf$_2$N]$^-$ + ethyl acetate) at T = 298.15 K (♦), 303.15 K (■), 308.15 K (▲) and 313.15 K (•).

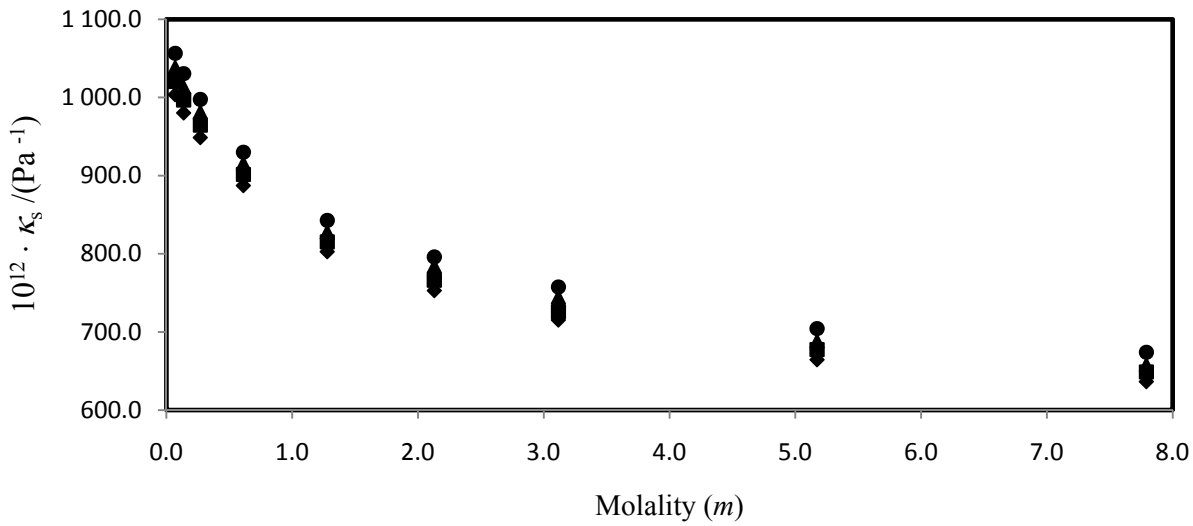

FIGURE 6.41 Isentropic compressibility (κ_s) versus molality (m) of binary mixture of ([MOA]$^+$[Tf$_2$N]$^-$ + methanol) at T = 298.15 K (♦), 303.15 K (■), 308.15 K (▲) and 313.15 K (•).

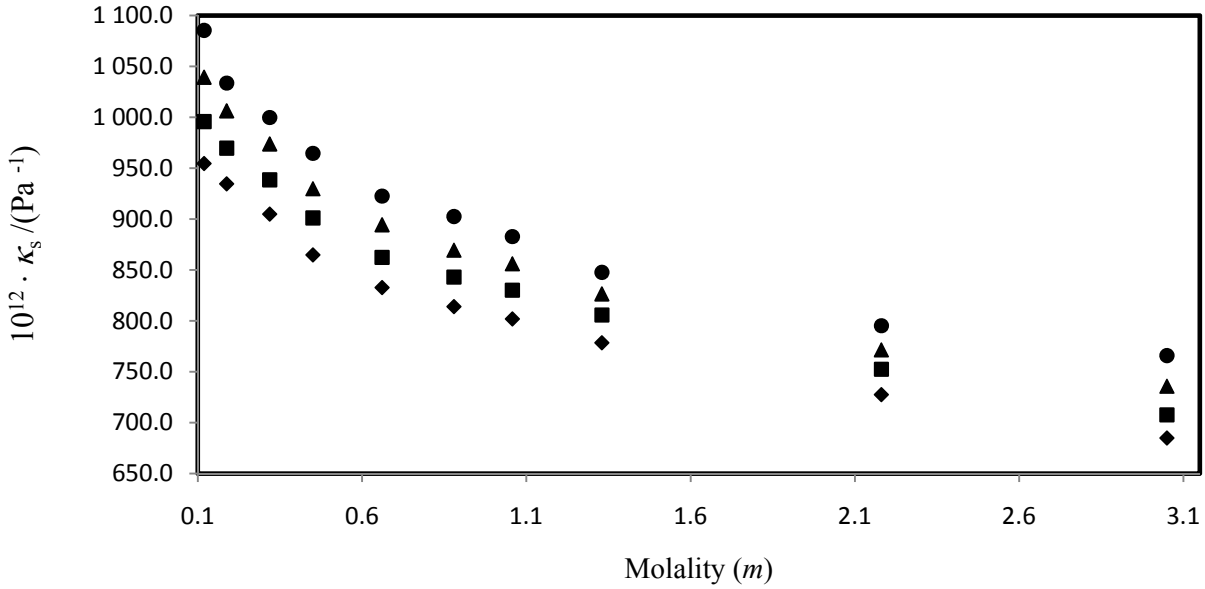

FIGURE 6.42 Isentropic compressibility (κ_s) versus molality (m) of binary mixture of ([MOA]$^+$[Tf$_2$N]$^-$ + ethanol) at T = 298.15 K (♦), 303.15 K (■), 308.15 K (▲) and 313.15 K (•).

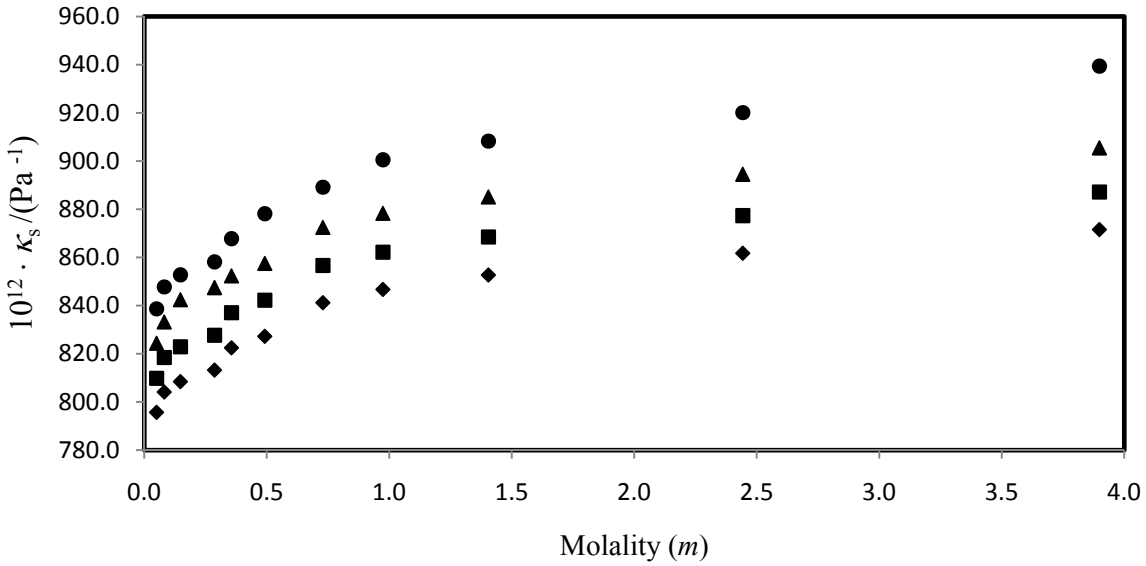

FIGURE 6.43 Isentropic compressibilitiy (κ_s) versus molality (m) of binary mixture of (methanol + methyl acetate) at T = 298.15 K (♦), 303.15 K (■), 308.15 K (▲) and 313.15 K (•).

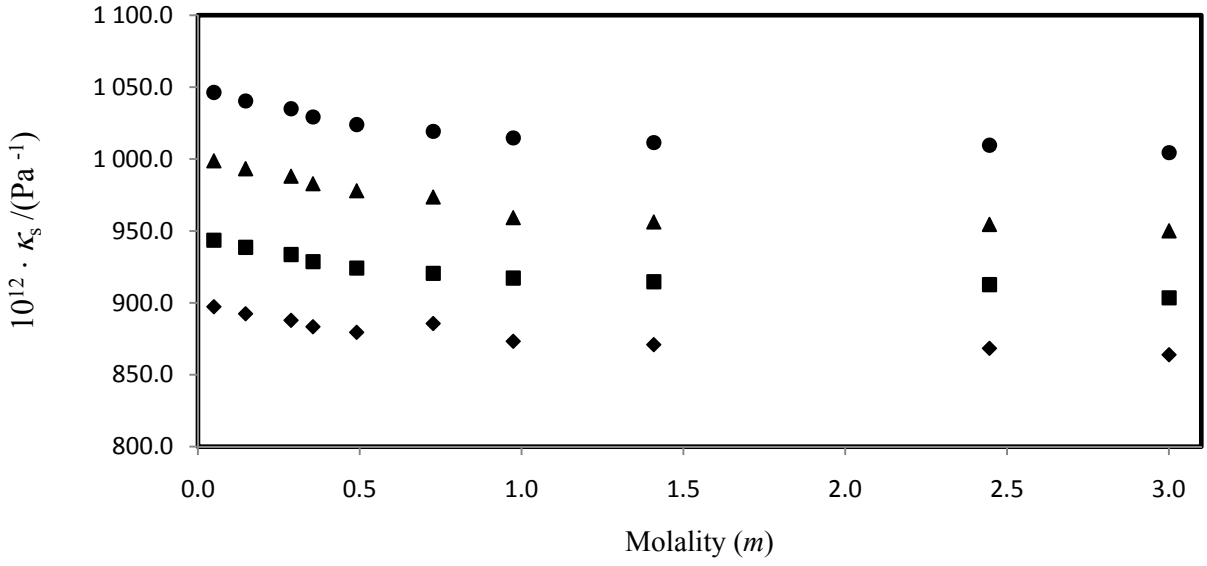

FIGURE 6.44 Isentropic compressibilitiy (κ_s) versus molality (m) of binary mixture of (methanol + ethyl acetate) at T = 298.15 K (♦), 303.15 K (■), 308.15 K (▲) and 313.15 K (•).

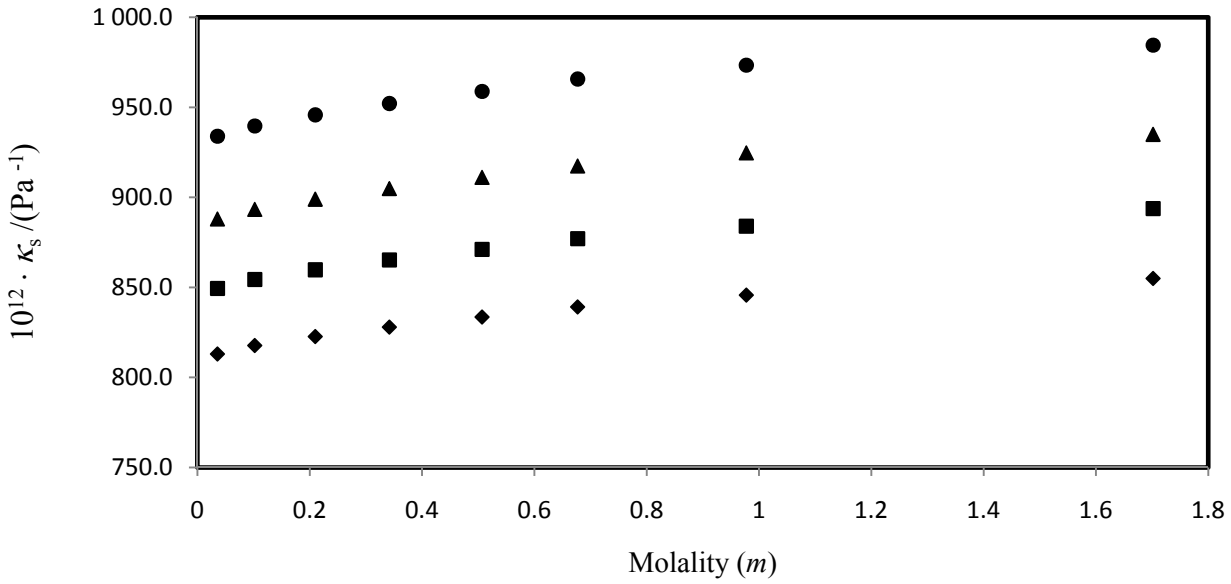

FIGURE 6.45 Isentropic compressibilitiy (κ_s) versus molality (m) of binary mixture of (ethanol + methyl acetate) at T = 298.15 K (♦), 303.15 K (■), 308.15 K (▲) and 313.15 K (•).

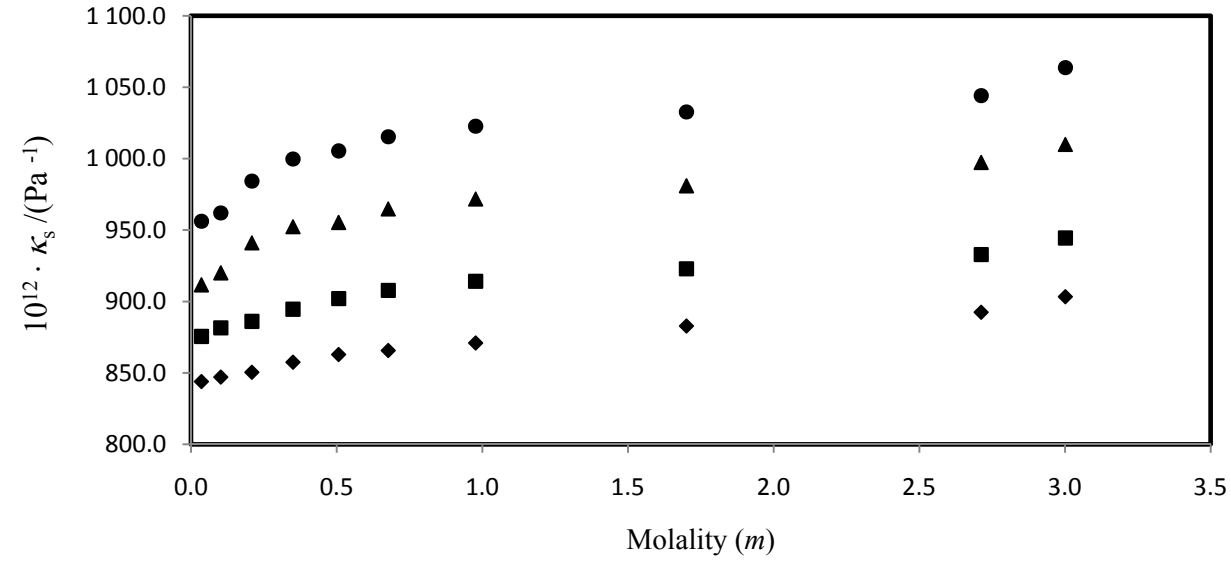

FIGURE 6.46 Isentropic compressibilitiy (κ_s) versus molality (m) of binary mixture of (ethanol + ethyl acetate) at T = 298.15 K (♦), 303.15 K (■), 308.15 K (▲) and 313.15 K (•).

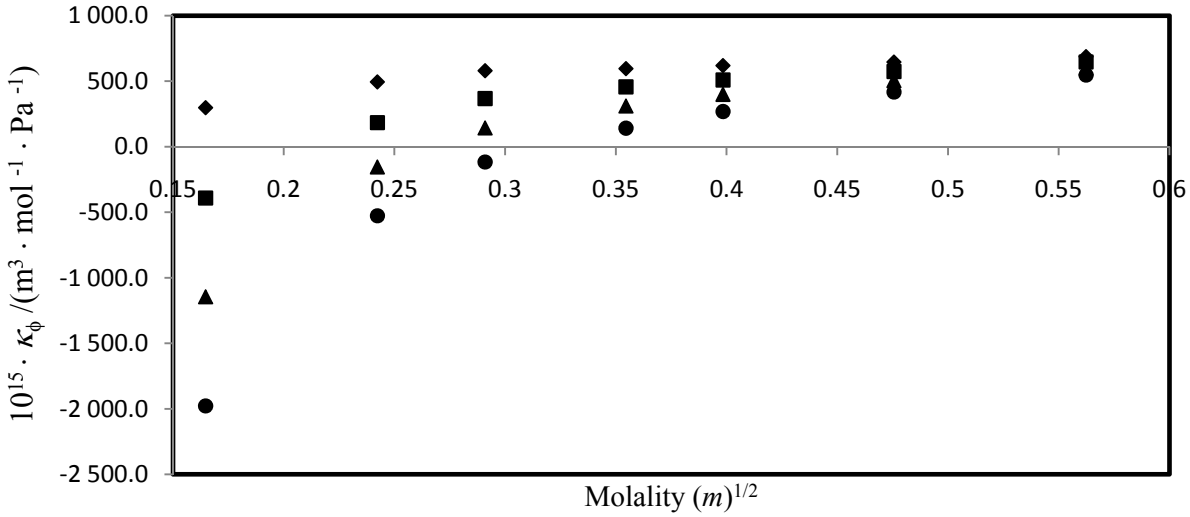

FIGURE 6.47 Apparent molar isentropic compressibility (κ_ϕ) versus molality $(m)^{1/2}$ of binary mixture of ($[MOA]^+[Tf_2N]^-$ + methyl acetate) at T = 298.15 K (♦), 303.15 K (■), 308.15 K (▲) and 313.15 K (•).

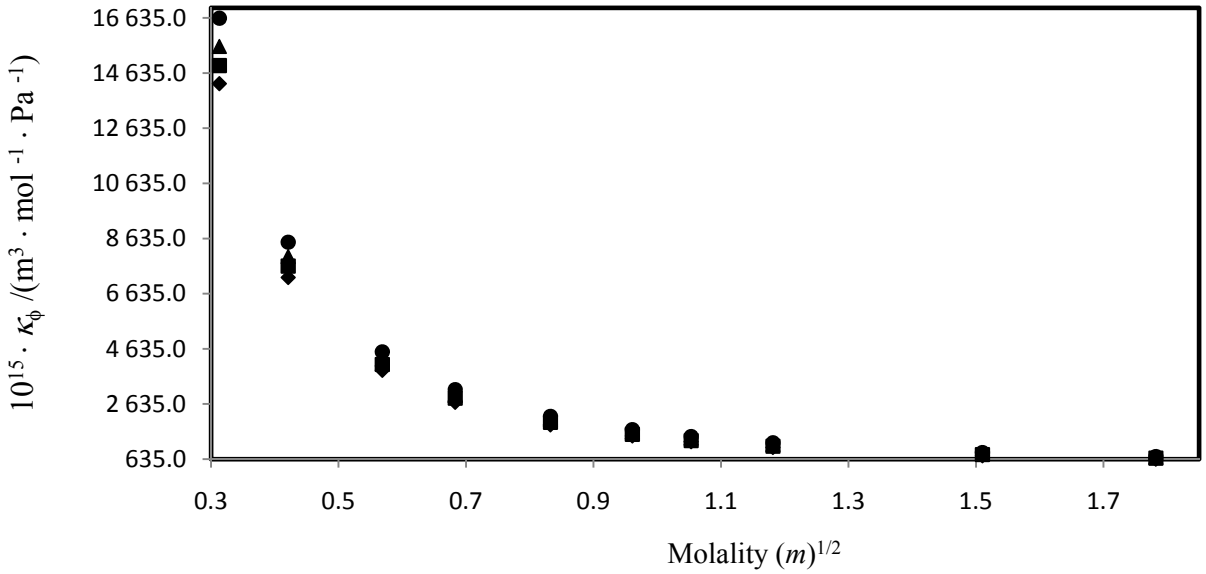

FIGURE 6.48 Apparent molar isentropic compressibility (κ_ϕ) versus molality $(m)^{1/2}$ of binary mixture of ($[MOA]^+[Tf_2N]^-$ + ethyl acetate) at T = 298.15 K (♦), 303.15 K (■), 308.15 K (▲) and 313.15 K (•).

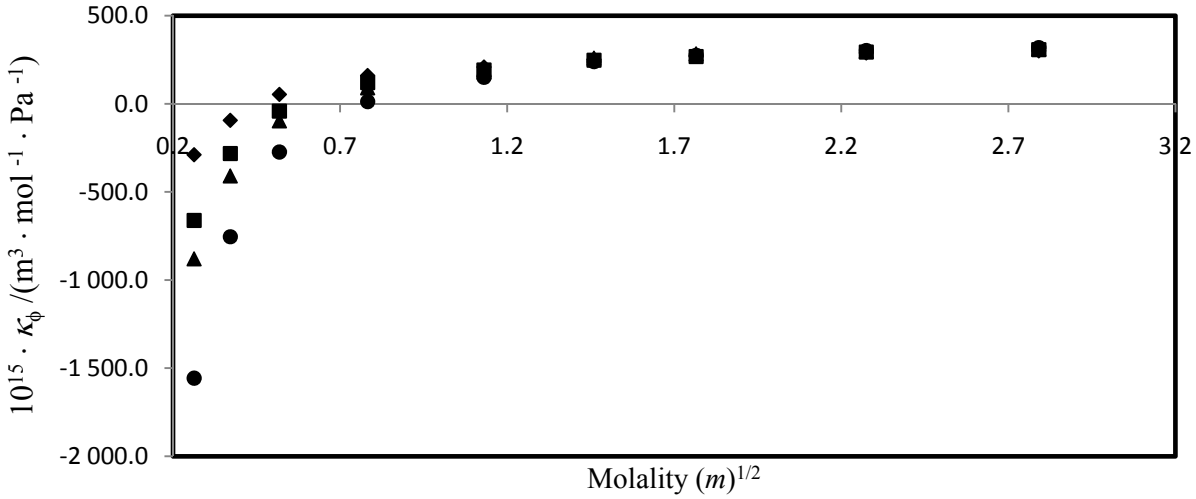

FIGURE 6.49 Apparent molar isentropic compressibility (κ_ϕ) versus molality $(m)^{1/2}$ of binary mixture of ($[MOA]^+[Tf_2N]^-$ + methanol) at T = 298.15 K (♦), 303.15 K (■), 308.15 K (▲) and 313.15 K (•).

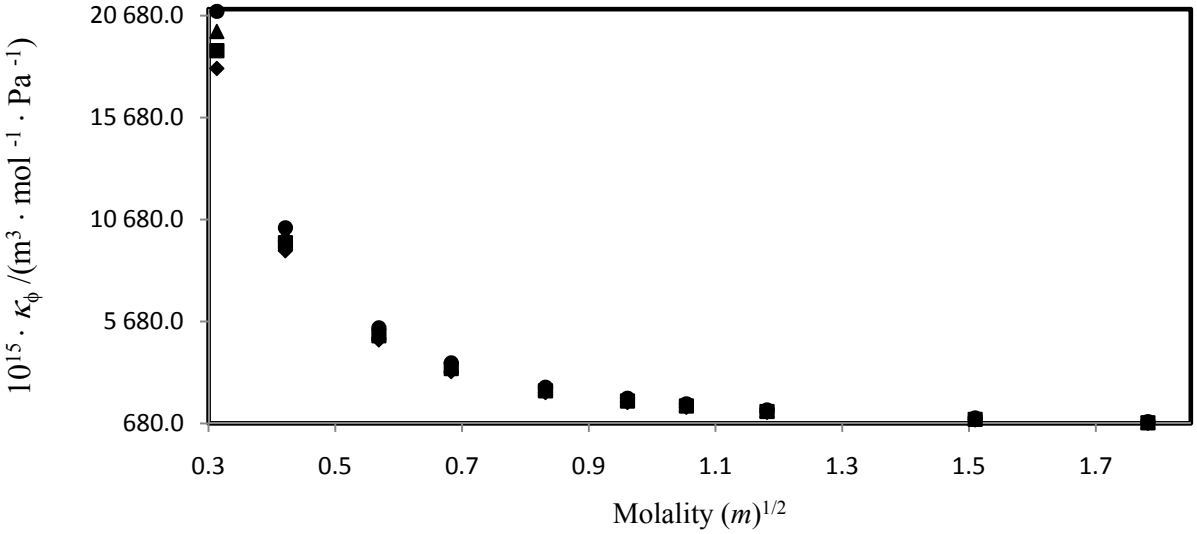

FIGURE 6.50 Apparent molar isentropic compressibility (κ_ϕ) versus molality $(m)^{1/2}$ of binary mixture of ($[MOA]^+[Tf_2N]^-$ + ethanol) at T = 298.15 K (♦), 303.15 K (■), 308.15 K (▲) and 313.15 K (•).

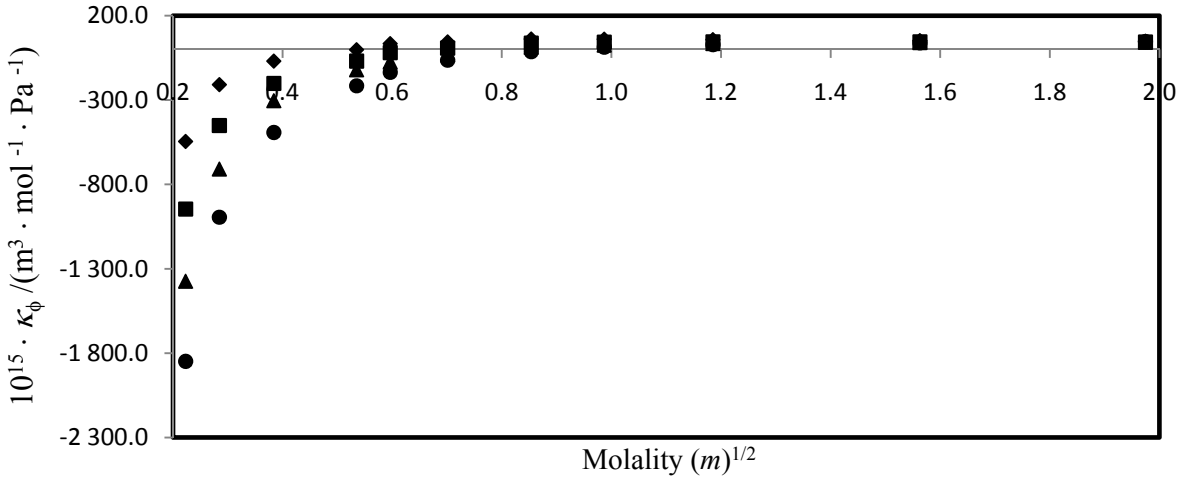

FIGURE 6.51 Apparent molar isentropic compressibility (κ_ϕ) versus molality $(m)^{1/2}$ of binary mixture of (methanol + methyl acetate) at T = 298.15 K (♦), 303.15 K (■), 308.15 K (▲) and 313.15 K (•).

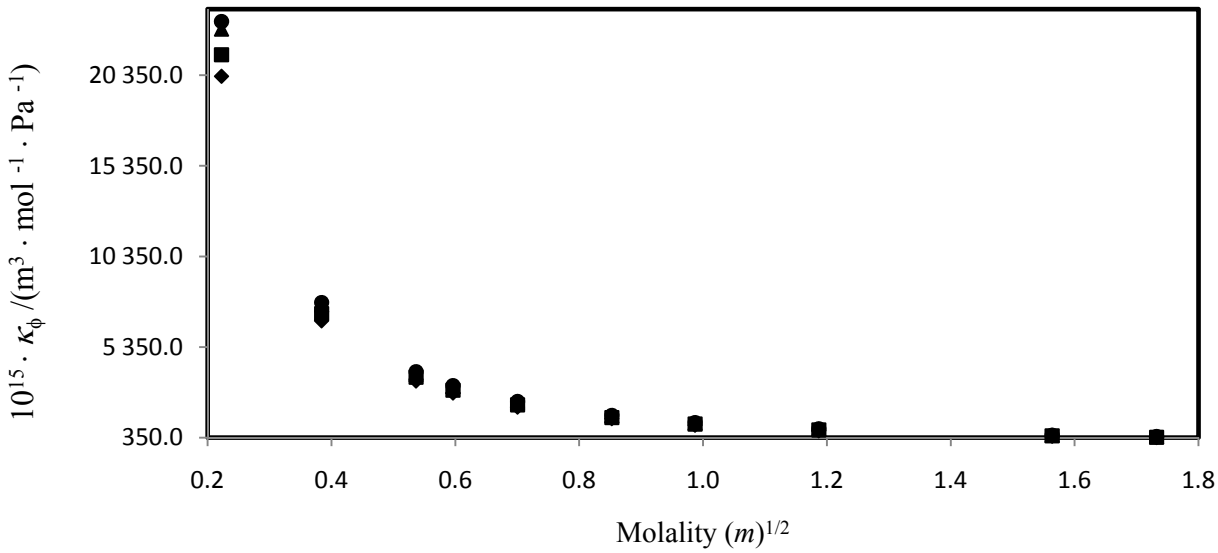

FIGURE 6.52 Apparent molar isentropic compressibility (κ_ϕ) versus molality $(m)^{1/2}$ of binary mixture of (methanol + ethyl acetate) at T = 298.15 K (♦), 303.15 K (■), 308.15 K (▲) and 313.15 K (•).

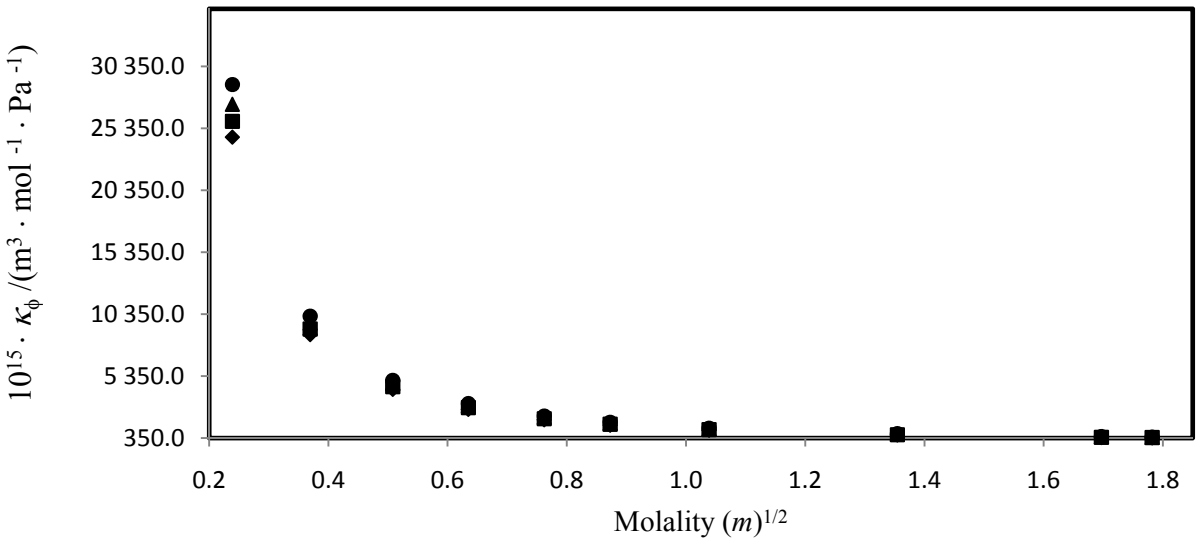

FIGURE 6.53 Apparent molar isentropic compressibility (κ_ϕ) versus molality $(m)^{1/2}$ of binary mixture of (ethanol + methyl acetate) at T = 298.15 K (♦), 303.15 K (■), 308.15 K (▲) and 313.15 K (•).

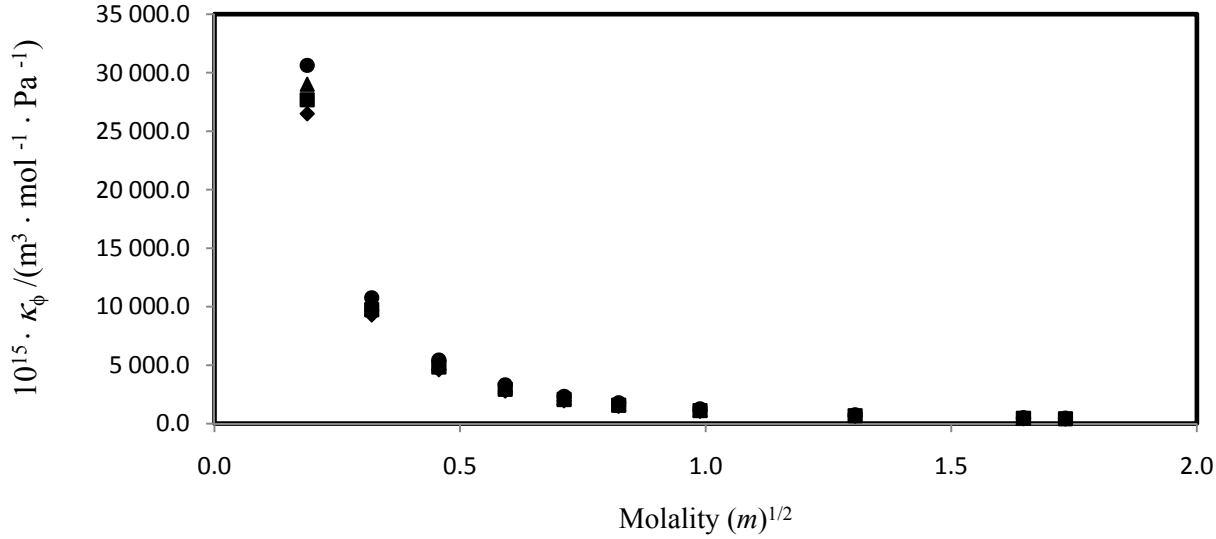

FIGURE 6.54 Apparent molar isentropic compressibility (κ_ϕ) versus molality $(m)^{1/2}$ of binary mixture of (ethanol + ethyl acetate) at T = 298.15 K (♦), 303.15 K (■), 308.15 K (▲) and 313.15 K (•).

6.3.2 The limiting apparent molar isentropic compressibility

The limiting apparent molar isentropic compressibility, k_{ϕ}^{0}, and empirical parameters S_{k} and B_{k} obtained from the Redlich-Mayer coefficients, using equations 6.10 for the binary systems {$[MOA]^{+}[Tf_2N]^{-}$ + methanol or ethanol or methyl acetate or ethyl acetate}, (methanol + methyl acetate or ethyl acetate) and (ethanol + methyl acetate or ethyl acetate) at T = (298.15, 303.15, 308.15 and 313.15) K are given together with the standard deviations, σ_{k} in Tables 6.28.

Table 6.28 The values of κ_ϕ^0, S_k, B_k, and standard deviation, σ_k, from obtained for each binary systems at the experimental temperatures

T/K	$10^{15}\cdot \kappa_\phi^0$ / $m^3\cdot mol^{-1}\cdot Pa^{-1}$	$10^{15}\cdot S_k$ / $m^3\cdot mol^{-3/2}\cdot kg^{1/2}\cdot Pa^{-1}$	$10^{15}\cdot B_k$ / $m^3\cdot mol^{-2}\cdot kg\cdot Pa^{-1}$	$10^{15}\cdot \sigma_k$
		([MOA]$^+$[Tf$_2$N]$^-$ + methyl acetate)		
298.15	-97.4	3068.5	-3044.3	36.1
303.15	-1535.5	8927.4	-9148.7	91.1
308.15	-3143.2	15574.2	-16149.4	149.4
313.15	- 4885.4	22683.6	-23568.0	216.5
		([MOA]$^+$[Tf$_2$N]$^-$ + ethyl acetate)		
298.15	17842.4	-28645.3	11186.5	1859.1
303.15	18731.7	-30069.7	11741.0	1924.5
308.15	19580.3	-31404.8	12257.1	2017.1
313.15	20882.8	-33528.1	13088.1	2149.1
		([MOA]$^+$[Tf$_2$N]$^-$ + methanol)		
298.15	-320.3	629.3	-151.2	77.6
303.15	-674.5	1034.6	-254.3	146.3
308.15	-900.1	1302.2	-323.5	182.4
313.15	-1543.7	2033.4	-509.4	306.8
		([MOA]$^+$[Tf$_2$N]$^-$ + ethanol)		
298.15	22736.8	-36824.7	14407.7	2387.8
303.15	23803.0	-38578.5	15097.5	2511.7
308.15	24963.8	-40523.2	15869.8	2648.9
313.15	26102.3	-42439.8	16635.9	2815.2
		(methanol + methyl acetate)		
298.15	-515.6	1008.3	-383.0	115.3
303.15	-935.6	1689.0	-631.2	177.8
308.15	-1369.9	2400.3	-891.9	252.1
313.15	-1885.4	3240.9	-1196.6	321.0
		(methanol + ethyl acetate)		
298.15	23724.9	-41535.2	16795.8	3045.2
303.15	25127.4	-44001.5	17794.8	3223.2
308.15	26780.0	-46905.3	18969.1	3431.6
313.15	27275.3	-47764.9	19316.9	3496.9
		(ethanol + methyl acetate)		
298.15	25970.9	-46858.2	19141.9	3979.0
303.15	27326.2	-49301.1	20139.1	4186.5
308.15	28763.2	-51892.9	21198.1	4406.1
313.15	30460.5	-54952.0	22447.5	4665.7
		(ethanol + ethyl acetate)		
298.15	27932.6	-50385.9	20576.5	4278.0
303.15	29201.1	-52636.7	21489.1	4462.8
308.15	30612.3	-55076.8	22467.8	4654.2
313.15	32294.1	-58097.0	23699.5	4921.7

CHAPTER 7

DISCUSSION

7.1 TERNARY EXCESS MOLAR VOLUMES

The results obtained in this work for the ternary excess molar volume systems ($[MOA]^+[Tf_2N]^-$ + methanol or ethanol + methyl acetate or ethyl acetate) at T = (298.15, 303.15 and 313.15) K and ($[BMIM]^+[MeSO_4]^-$ + methanol or ethanol or 1-propanol + nitromethane) at T = 298.15 K over the entire composition range are discussed in terms of intermolecular interactions. V_{123}^{E} systems available in the literature are compared with our results to relate the structure of ILs to volume changes.

The values of V_{123}^{E} represents the difference between the molar volume of a real solution and the molar volume of an ideal solution. The magnitude and the sign of V_{123}^{E} are the result of different effects taking place in the mixture. These effects relate to: (1) the breakdown of self-associated molecules or the breaking of intermolecular bonds (a positive volume), (2) the negative contribution of volume due to the packing effect and/ or (ion-dipole) strong intermolecular interactions between the different molecules (Deenadayalu *et al.* 2008). For each ternary system the corresponding binary systems were obtained from the literature. The binary data was used for obtaining the Redlich-Kister parameters. The V_{123}^{E} data was correlated by the Cibulka equation (6.2).

7.1.1 ([MOA]$^+$[Tf$_2$N]$^-$ + methanol + methyl acetate)

For the system ([MOA]$^+$[Tf$_2$N]$^-$ + methanol + methyl acetate) the three binary systems are ([MOA]$^+$[Tf$_2$N]$^-$ + methanol) (Deenadayalu *et al*. 2008), ([MOA]$^+$[Tf$_2$N]$^-$ + methyl acetate) (Deenadayalu *et al*. 2010), and (methanol + methyl acetate) (González *et al.* 2007). For the binary system ([MOA]$^+$[Tf$_2$N]$^-$ + methanol) at all temperatures and at high mole fractions of methanol V_m^E is positive and becomes negative for mole fractions of IL greater than 0.85 due to the packing of small methanol molecules into the IL matrices. At the higher mole fractions of methanol the positive V_m^E is due to the breakdown of the hydrogen bonding in the methanol molecules (Deenadayalu *et al*. 2008). Table 7.1 is a summary of V_{min}^E values for the binary systems related to [MOA]$^+$[Tf$_2$N]$^-$ ternary systems. From Table 7.1, it can be seen that the system ([MOA]$^+$[Tf$_2$N]$^-$ + methanol) V_{min}^E decrease with an increase in the temperature (Deenadayalu *et al*. 2008).

The V_m^E data of ([MOA]$^+$[Tf$_2$N]$^-$ + methyl acetate) at all temperature and at all mole fractions of IL is negative due to the packing of small methyl acetate molecules into the IL matrices (Deenadayalu *et al.* 2010). From Table 7.1, it can be seen that the system ([MOA]$^+$[Tf$_2$N]$^-$ + methyl acetate) V_{min}^E decrease with an increase in the temperature (Deenadayalu *et al.* 2010).

The V_m^E data of (methanol + methyl acetate) at T = (298.15, and 303.15) K is negative due to the strong interactions between unlike molecules through hydrogen bonding (Gómez *et al.* 2007). The experimental data are not available in the literature at T = 313.15 K. From Table 7.1, it can be seen that the system (methanol + methyl acetate) V_{min}^E increase with an increase in the temperature at fixed composition of methanol (Gómez *et al.* 2007).

Table 7.2, lists $V_{123\,min}^E$ for all ternary systems for the [MOA]$^+$[Tf$_2$N]$^-$.

From Table 7.2, it can be seen that the system ([MOA]$^+$[Tf$_2$N]$^-$ + methanol

+ methyl acetate) the minimum ternary excess molar volumes, $V^{E}_{123\,min}$, decrease with a decrease in z values (increase in mole fraction of IL except at z = 0.30 at T = (298.15, and 313.15) K. The $V^{E}_{123\,min}$ also decrease with an increase in the temperature. This trend was also observed for the ternary system ($[EMIM]^{+}[BETI]^{-}$ + methanol + acetone) (Deenadayalu *et al.* 2008).

Table 7.1 The $V_{\min}^{E}$ for the five binary systems at T = (298.15, 303.15, and 313.15) K from literature for the ([MOA]$^{+}$[Tf$_2$N]$^{-}$ + methanol + methyl acetate or ethyl acetate) ternary systems

T/K	x_1	x_2	$V_{\min}^{E}$/cm^3·mol^{-1}
	[MOA]$^{+}$[Tf$_2$N]$^{-}$ + methanol		
298.15	0.8522	0.1478	-0.234[a]
303.15	0.8522	0.1478	-0.292[a]
313.15	0.9345	0.0655	-0.344[a]
	[MOA]$^{+}$[Tf$_2$N]$^{-}$ + methyl acetate		
298.15	0.5029	0.4971	-1.397[b]
303.15	0.6106	0.3894	-2.223[b]
313.15	0.6106	0.3894	-3.333[b]
	[MOA]$^{+}$[Tf$_2$N]$^{-}$ + ethyl acetate		
298.15	0.5450	0.4550	-1.579[b]
303.15	0.5450	0.4550	-1.551[b]
313.15	0.5450	0.4550	-1.834[b]
	Methanol + methyl acetate		
298.15	0.5006	0.4994	-0.072[c]
303.15	0.5006	0.4994	-0.065[c]
	Methanol + ethyl acetate		
298.15	0.5963	0.4037	-0.077[c]
303.15	0.5963	0.4037	-0.071[c]

[a] (Deenadayalu *et al.* 2008).

[b] (Deenadayalu *et al.* 2010).

[c] (González *et al.* 2007).

Table 7.2 The minimum excess molar volume, $V^{E}_{123\,min}$ for each ternary systems ([MOA]$^{+}$[Tf$_2$N]$^{-}$ + methanol + methyl acetate or ethyl acetate) at constant z values and at each temperature

x_1	x_2	x_3	z	$V^{E}_{123\,min}$/cm^3·mol^{-1}
		([MOA]$^{+}$[Tf$_2$N]$^{-}$ + methanol + methyl acetate)		
		T = 298.15 K		
0.0696	0.3023	0.6280	9.00	-0.57
0.1637	0.1812	0.6551	4.00	-1.03
0.3329	0.1681	0.4990	1.50	-1.21
0.4567	0.0867	0.4567	1.00	-1.31
0.5997	0.1004	0.2998	0.50	-1.36
0.6259	0.1863	0.1878	0.30	-1.35
		T = 303.15 K		
0.0696	0.3023	0.6280	9.00	-0.98
0.1637	0.1812	0.6551	4.00	-1.49
0.3329	0.1681	0.4990	1.50	-1.83
0.4567	0.0867	0.4567	1.00	-1.91
0.5997	0.1004	0.2998	0.50	-1.96
0.6259	0.1863	0.1878	0.30	-2.00
		T = 313.15 K		
0.0696	0.3023	0.6280	9.00	-1.05
0.1434	0.2835	0.5732	4.00	-1.80
0.3329	0.1681	0.4990	1.50	-2.30
0.4567	0.0867	0.4567	1.00	-2.41
0.5997	0.1004	0.2998	0.50	-2.61
0.6259	0.1863	0.1878	0.30	-2.57
		([MOA]$^{+}$[Tf$_2$N]$^{-}$ + methanol + ethyl acetate)		
		T = 298.15 K		
0.0775	0.3360	0.5865	7.50	-2.30
0.1292	0.4363	0.4345	3.36	-2.13
0.2564	0.2820	0.4616	1.80	-2.00
0.3453	0.3073	0.3473	1.00	-1.67
0.5613	0.1987	0.2400	0.43	-1.64
0.4200	0.5381	0.0420	0.10	-1.09
		T = 303.15 K		
0.0775	0.3360	0.5865	7.50	-2.71
0.1292	0.4363	0.4345	3.36	-2.39
0.2564	0.2820	0.4616	1.80	-2.18
0.3453	0.3073	0.3473	1.00	-1.62
0.4837	0.3085	0.2078	0.43	-1.58
0.5312	0.4369	0.0507	0.10	-1.11
		T = 313.15 K		
0.0775	0.3360	0.5865	7.50	-3.01
0.1292	0.4363	0.4345	3.36	-2.59
0.2564	0.2820	0.4616	1.80	-2.43
0.4467	0.1065	0.4468	1.00	-1.60
0.6273	0.1024	0.2703	0.43	-1.53
0.5312	0.4369	0.0507	0.10	-0.55

The values of $V^{E}_{123\,min}$ -1.36, -2.00, and -2.61 $cm^3 \cdot mol^{-1}$ for each temperature is greater than that for the ($[MOA]^+[Tf_2N]^-$ + methyl acetate) binary system (Deenadayalu *et al.* 2010). From Figures 6.1 to 6.3, the values of excess molar volumes, V^{E}_{123} , decrease with an increase the moles fraction of ionic liquid at fixed mole fraction of methanol at each temperature and is negative for all ternary composition curves. The negative values of V^{E}_{123} for IL, methanol and methyl acetate show that the effect due to the (ion- dipole) interactions between methanol methyl acetate and the IL and or packing effect are dominating over the dipolar orders in methanol and methyl acetate (Deenadayalu *et al.* 2008).

The interactions between IL ions with methanol and methyl acetate can occur through the cation of the IL and lone pair of electrons on the methanol and methyl acetate as well as accommodation of smaller methanol molecules into the interstices of the IL (Deenadayalu *et al.* 2008). Figure 6.16 to 6.18, is the ternary excess molar volume graphs obtained from using the Cibulka equation parameters for the system ($[MOA]^+[Tf_2N]^-$ + methanol + methyl acetate) at the three temperatures. At high mole fraction of methanol the V^{E}_{123} values are positive corresponding to the binary ($[MOA]^+[Tf_2N]^-$ + methanol) system (Sibiya and Deenadayalu 2008).

The binary ($[MOA]^+[Tf_2N]^-$ + methyl acetate) and (methanol + methyl acetate) V^{E}_{m} are negative at all compositions and temperatures. From Figure 6.16 to 6.18, it can be seen that for the ternary system the negative V^{E}_{123} extends over most of the three component V^{E}_{123} region i.e. the region of high mole fraction of methanol and V^{E}_{123} decrease with an increase in the temperatures.

7.1. 2 ([MOA]$^+$[Tf$_2$N]$^-$ + methanol + ethyl acetate)

For the ternary system ([MOA]$^+$[Tf$_2$N]$^-$ + methanol + ethyl acetate), the three binary systems are: ([MOA]$^+$[Tf$_2$N]$^-$ + methanol), ([MOA]$^+$[Tf$_2$N]$^-$ + ethyl acetate), and (methanol + ethyl acetate). The binary data of ([MOA]$^+$[Tf$_2$N]$^-$ + ethyl acetate) at all temperatures, (Deenadayalu *et al.* 2010) and at all mole fractions of IL V_m^E is negative due to the packing of small ethyl acetate molecules into the IL matrices. In general the V_m^E values decrease with an increase in temperature (Deenadayalu *et al.* 2010). From Table 7.1, for the system ([MOA]$^+$[Tf$_2$N]$^-$ + ethyl acetate) V_{min}^E decrease with an increase in the temperature except T = 303.15 K at fixed composition of IL (Deenadayalu *et al*. 2010).

The binary data of (methanol + ethyl acetate) (Gómez *et al.* 2007) at T = (298.15, and 303.15) K, at all mole fraction of methanol the V_m^E is small negative due to the weak interactions between unlike molecules through hydrogen bonding. The experimental data are not available in the literature at T = 313.15 K. The V_m^E increase slightly with an increase in the temperature of the system (Gómez *et al.* 2007). From the Table 7.1, for the system {methanol + ethyl acetate} V_{min}^E also increase with an increase in the temperature at fixed composition of methanol (Gómez *et al.* 2007).

From Table 7.2, it can be seen that for the ternary system ([MOA]$^+$[Tf$_2$N]$^-$ + methanol + ethyl acetate) V_{123min}^E increase with a decrease in z values at each temperature. $V_{123\,min}^E$ decrease with an increase in the temperature in the range of the z values from 7.50 to 1.80, and increases with temperature from the range of the z values from 1.00 to 0.10 except at T = 303.15 K and z = 0.10 where it decreases. This trend was also observed for the ternary system ([EMIM]$^+$[BETI]$^-$ + methanol + acetone) with temperature (Deenadayalu *et al.* 2008). The values of $V_{123\,min}^E$ -2.30, -2.71, and -3.01 cm^3· mol^{-1} at each temperature is less than the ([MOA]$^+$[Tf$_2$N]$^-$ + ethyl acetate) binary system (Deenadayalu *et al.* 2010). From Figure 6.4 to

6.6, the values of ternary excess molar volumes, V_{123}^{E} , decreases with a decrease in the moles fraction of ionic liquid at fixed mole fraction of methanol at each temperature and is negative for all ternary composition curves. The negative values of V_{123}^{E} for IL, methanol and ethyl acetate show that the effect due to the (ion- dipole) interactions between methanol, as well as, ethyl acetate and the IL and packing effect are dominating over the dipolar orders in methanol and ethyl acetate (Deenadayalu *et al.* 2008). The (ion- dipole) interactions between IL ions with methanol and ethyl acetate can occur through the cation of the IL and lone pair of electrons on the methanol and ethyl acetate, as well as accommodation of smaller methanol molecules into the interstices of the IL (Deenadayalu *et al.* 2008).

Figure 6.19 to 6.21, is the ternary excess molar volume graphs obtained from using the Cibulka equation parameters for the system ($[MOA]^{+}[Tf_2N]^{-}$ + methanol + ethyl acetate) at the three temperatures. The V_{123}^{E} values is more negative for ($[MOA]^{+}[Tf_2N]^{-}$ + methanol + ethyl acetate) system than for ($[MOA]^{+}[Tf_2N]^{-}$ + methanol + methyl acetate) system at all temperatures and also decrease with an increase in the temperature. The binary ($[MOA]^{+}[Tf_2N]^{-}$ + ethyl acetate) and (methanol + ethyl acetate) is greater than ($[MOA]^{+}[Tf_2N]^{-}$ + methanol) this indicates there is a complex intermolecular interactions between these molecules. The Cibulka equation was used to correlate the ternary data and indicated that the ternary contribution (three –body effect) is dominant.

7.1.3. ([MOA]$^+$[Tf$_2$N]$^-$ + ethanol + methyl acetate) ternary system

For the ternary system ([MOA]$^+$[Tf$_2$N]$^-$ + ethanol + methyl acetate) the three binary systems are: ([MOA]$^+$[Tf$_2$N]$^-$ + ethanol) (Deenadayalu *et al.* 2008), ([MOA]$^+$[Tf$_2$N]$^-$ + methyl acetate) (Deenadayalu *et al.* 2010), and (ethanol + methyl acetate) (González *et al.* 2007). The binary V_m^E data for ([MOA]$^+$[Tf$_2$N]$^-$ + ethanol) at all temperatures and at high mole fractions of ethanol are negative and becomes positive for mole fraction of IL greater than 0.17 (Deenadayalu *et al.* 2008). V_m^E is negative due to the packing of small ethanol molecules into the IL matrices (Deenadayalu *et al.* 2008). For low mole fractions of ethanol V_m^E is positive due to a break down of the hydrogen bonding in the ethanol molecules (Deenadayalu *et al.* 2008). The trend for ([MOA]$^+$[Tf$_2$N]$^-$ + ethanol) is the opposite of that for the ([MOA]$^+$[Tf$_2$N]$^-$ + methanol) binary system due to the alkanol having an addition CH_2 group that changes the intermolecular interaction (Deenadayalu *et al.* 2008). Table 7.3 is a summary of V_{min}^E values for the binary systems related to [MOA]$^+$[Tf$_2$N]$^-$ ternary systems. From Table 7.3 for the system ([MOA]$^+$[Tf$_2$N]$^-$ + ethanol) V_{min}^E decrease with an increase in the temperature except at T = 313.15 K. For the binary V_m^E data of

([MOA]$^+$[Tf$_2$N]$^-$ + methyl acetate) at all temperatures, at all mole fractions of methyl acetate the V_m^E is negative due to the packing of small methyl acetate molecules into the IL matrices (Deenadayalu *et al.* 2008). From Table 7.3, for the system ([MOA]$^+$[Tf$_2$N]$^-$ + methyl acetate) V_{min}^E decrease with an increase in the temperature at T = (298.15, 303.15 and 313.15) K. The binary V_m^E data of (ethanol + methyl acetate) at T = (298.15 and 303.15) K, at all mole fractions of ethyl acetate V_m^E is positive, and opposite in sign to (methanol + methyl acetate) and (methanol + ethyl acetate) due to the decrease in the ester chain length (González *et al.* 2007). The experimental data are not available in the

literature at T = 313.15 K. From Table 7.3, V^{E}_{min} for the system (ethanol + methyl acetate) increase with an increase in the temperature (González *et al.* 2007).

From Table 7.4, for the ternary system ($[MOA]^{+}[Tf_2N]^{-}$ + ethanol + methyl acetate) V^{E}_{123min}, decrease with a decrease in z values except at z = 0.10 at T = 298.15 K and z = 0.20 at T = 313.15 K. The $V^{E}_{123\,min}$ decreases with an increase in the temperature except at z = 4.00 at temperature T = 303.15 K. The values of $V^{E}_{123\,min}$ -2.00, -2.32, and -3.01 $cm^3 \cdot mol^{-1}$ at each temperature is less than the ($[MOA]^{+}[Tf_2N]^{-}$ + methyl acetate) binary system except at T = 313.15 K (Deenadayalu *et al.* 2010). From figures 6.7 to 6.9, the values of excess molar volumes, V^{E}_{123} , decrease with an increase in the moles fraction of ionic liquid at fixed mole fraction of ethanol at each temperature of the system. From figures 6.7 to 6.9 V^{E}_{123} is negative for all ternary composition curves. The negative values of V^{E}_{123} for IL, ethanol and methyl acetate show that the effect due to the (ion- dipole) interactions between ethanol and methyl acetate and the IL and packing effect are dominating over the dipolar orders in ethanol and methyl acetate (Deenadayalu *et al.* 2008). The interactions between IL ions with ethanol and methyl acetate can occur through the cation of the IL and lone pair of electrons on the ethanol and methyl acetate as well as accommodation of smaller ethanol molecules into the interstices of the IL (Deenadayalu *et al.* 2008). Similar to the ($[MOA]^{+}[Tf_2N]^{-}$ + methanol + methyl acetate) ternary system.

Table 7.3 The V^{E}_{min} for the five binary systems at T = (298.15, 303.15, and 313.15) K from literature for the ([MOA]$^{+}$[Tf$_2$N]$^{-}$ + ethanol + methyl acetate or ethyl acetate) ternary systems

T/K	x_1	x_2	V^{E}_{min}/cm^3·mol^{-1}
	[MOA]$^{+}$[Tf$_2$N]$^{-}$ + ethanol		
298.15	0.0484	0.9516	-0.043[a]
303.15	0.0484	0.9515	-0.467[a]
313.15	0.1731	0.8269	-0.113[a]
	[MOA]$^{+}$[Tf$_2$N]$^{-}$ + methyl acetate		
298.15	0.5029	0.4971	-1.397[b]
303.15	0.6106	0.3894	-2.223[b]
313.15	0.6106	0.3894	-3.333[b]
	[MOA]$^{+}$[Tf$_2$N]$^{-}$ + ethyl acetate		
298.15	0.5450	0.4550	-1.579[b]
303.15	0.5450	0.4550	-1.551[b]
313.15	0.5450	0.4550	-1.834[b]
	Ethanol + methyl acetate		
298.15	0.7943	0.2057	0.034[c]
303.15	0.7898	0.2102	0.037[c]
	Ethanol + ethyl acetate		
298.15	0.7939	0.2061	0.025[c]
303.15	0.7894	0.2106	0.028[c]

[a] (Deenadayalu *et al.* 2008).

[b] (Deenadayalu *et al.* 2010).

[c] (González *et al.* 2007).

Table 7.4 The minimum excess molar volume, $V^{E}_{123\,min}$ for each ternary system ($[MOA]^+[Tf_2N]^-$ + ethanol + methyl acetate or ethyl acetate) at constant z values and at each temperature

x_1	x_2	x_3	z	$V^{E}_{123\,min}$/cm^3·mol^{-1}
		($[MOA]^+[Tf_2N]^-$ + ethanol + methyl acetate)		
		T = 298.15 K		
0.0765	0.2306	0.6929	9.00	-0.55
0.1364	0.3192	0.5444	4.00	-1.39
0.2715	0.3211	0.4073	1.50	-1.62
0.2868	0.4268	0.2864	1.00	-1.81
0.3879	0.4186	0.1935	0.50	-1.95
0.4298	0.4420	0.1282	0.20	-2.00
0.5834	0.3603	0.0562	0.10	-1.99
		T = 303.15 K		
0.0765	0.2306	0.6929	9.00	-0.72
0.1169	0.4168	0.4663	4.00	-1.21
0.3078	0.2305	0.4617	1.50	-2.04
0.3826	0.2354	0.3819	1.00	-2.16
0.4542	0.3194	0.2264	0.50	-2.24
0.4298	0.4420	0.1282	0.20	-2.25
0.5834	0.3603	0.0562	0.10	-2.32
		T = 313.15 K		
0.0765	0.2306	0.6929	9.00	-1.03
0.1538	0.2310	0.6152	4.00	-1.75
0.3078	0.2305	0.4617	1.50	-2.39
0.3826	0.2354	0.3819	1.00	-2.71
0.4542	0.3194	0.2264	0.50	-2.91
0.5290	0.3133	0.1576	0.20	-2.90
0.6689	0.2667	0.0644	0.10	-3.01
		($[MOA]^+[Tf_2N]^-$ + ethanol + methyl acetate)		
		T = 298.15 K		
0.0642	0.4497	0.4861	7.50	-2.61
0.1490	0.3499	0.5011	3.36	-2.24
0.2011	0.5454	0.2535	1.30	-1.87
0.3006	0.4468	0.2526	0.80	-1.67
0.3292	0.5326	0.1382	0.40	-1.59
0.4388	0.4513	0.1099	0.25	-1.28
0.5880	0.3644	0.0476	0.08	-0.93
		T = 303.15 K		
0.0642	0.4497	0.4861	7.50	-2.99
0.1490	0.3499	0.5011	3.36	-2.63
0.2011	0.5454	0.2535	1.30	-2.11
0.1567	0.7066	0.1339	0.80	-1.77
0.3292	0.5326	0.1382	0.40	-1.74
0.4388	0.4513	0.1099	0.25	-1.28
0.5880	0.3644	0.0476	0.08	-0.92
		T = 313.15 K		
0.0863	0.2603	0.6534	7.50	-3.43
0.1490	0.3499	0.5011	3.36	-2.92
0.2011	0.5454	0.2535	1.30	-2.35
0.3006	0.4468	0.2526	0.80	-1.87
0.3292	0.5326	0.1382	0.40	-1.74
0.4388	0.4513	0.1099	0.25	-1.29
0.5880	0.3644	0.0476	0.08	-0.80

Figures 6.22 to 6.24, are the ternary excess molar volume graphs obtained from using the Cibulka equation parameters for the system ($[MOA]^+[Tf_2N]^-$ + ethanol + methyl acetate) at the three temperature. At low mole fraction of ethanol the V_{123}^{E} values are positive as seen in the binary ($[MOA]^+[Tf_2N]^-$ + ethanol) system (Deenadayalu *et al.* 2008). The binary V_{m}^{E} for ($[MOA]^+[Tf_2N]^-$ + methyl acetate) and (ethanol + methyl acetate) is negative at all compositions and temperatures. From Figures 6.22 to 6.24, the negative V_{123}^{E} extends over most of the three component V_{123}^{E} region i.e. the region of low mole fraction of ethanol and it can also be seen that V_{123}^{E} decreases with an increase in the temperature.

7.1.4. ($[MOA]^+[Tf_2N]^-$ + ethanol + ethyl acetate)

For the system ($[MOA]^+[Tf_2N]^-$ + ethanol + ethyl acetate) the three binary systems are: ($[MOA]^+[Tf_2N]^-$ + ethanol), ($[MOA]^+[Tf_2N]^-$ + ethyl acetate), and (ethanol + ethyl acetate). The binary V_{m}^{E} data of ($[MOA]^+[Tf_2N]^-$ + ethyl acetate) at all temperatures, and at all mole fractions of ethyl acetate is negative due to the packing of small ethyl acetate molecules into the IL matrices. There is no correlation between V_{m}^{E} with the temperature for the system (Deenadayalu *et al.* 2010). From the Table 7.3, it can be observed that the system ($[MOA]^+[Tf_2N]^-$ + ethyl acetate) V_{min}^{E} decrease with an increase in the temperature except at T = 303.15 K (Deenadayalu *et al.* 2010). The binary V_{m}^{E} data of (ethanol + ethyl acetate) at T = (298.15, and 303.15) K, at all mole fractions of ethyl acetate is positive and opposite of that of (methanol + methyl acetate) and (methanol + ethyl acetate) due to the decrease in the ester chain length. The experimental V_{m}^{E} data are not available in the literature at T = 313.15 K. The V_{m}^{E} increase with an increase in the temperature of the system (González *et al.* 2007).

From Table 7.4, for the system ($[MOA]^+[Tf_2N]^-$ + ethanol + ethyl acetate) $V^{E}_{123\min}$ increases with a decrease in z values at each temperature except at z = 0.25, 0.08 at T = 303.15 K and at z = 0.40, 0.08 at T = 313.15 K. The values of $V^{E}_{123\,\min}$ -2.61, -2.99, and -3.43 $cm^3 \cdot mol^{-1}$ at each temperature is less than the ($[MOA]^+[Tf_2N]^-$ + ethyl acetate) binary system (Deenadayalu *et al.* 2010). From Figures 6.10 to 6.12, the values of excess molar volumes, V^{E}_{123} , decreases with a decrease in the mole fraction of ionic liquid at fixed mole fractions of ethanol at each temperature of the system. From Figures 6.10 to 6.12 V^{E}_{123} is negative for all ternary composition curves. The negative values of V^{E}_{123} for IL, ethanol and ethyl acetate show that the effect due to the (ion- dipole) interactions between ethanol and ethyl acetate and the IL and / or packing effect are dominating over the dipolar orders in ethanol and ethyl acetate (Deenadayalu *et al.* 2008). The interactions between IL ions with ethanol and ethyl acetate can occur through the cation of the IL and lone pair of electrons on the ethanol and ethyl acetate as well as accommodation of smaller ethanol molecules into the interstices of the IL (Deenadayalu *et al.* 2008).

Figures 6.25 to 6.27, is the ternary excess molar volume graphs obtained from using the Cibulka equation parameters for the system ($[MOA]^+[Tf_2N]^-$ + ethanol + ethyl acetate) at the three temperatures. The V^{E}_{123} values is more negative for ($[MOA]^+[Tf_2N]^-$ + ethanol + ethyl acetate) system than for ($[MOA]^+[Tf_2N]^-$ + ethanol + methyl acetate) system at all temperatures and also decreases with an increase in the temperature. The binary ($[MOA]^+[Tf_2N]^-$ + ethyl acetate) and (ethanol + ethyl acetate) is greater than ($[MOA]^+[Tf_2N]^-$ + ethanol) this indicates that there is a complex intermolecular interaction between these molecules.

7.1.5 ([BMIM]$^+$[MeSO$_4$]$^-$ + methanol or ethanol or 1-propanol + nitromethane)

For the ternary systems ([BMIM]$^+$[MeSO$_4$]$^-$ + methanol or ethanol or 1-propanol + nitromethane) the seven binary systems are: ([BMIM]$^+$[MeSO$_4$]$^-$ + methanol), ([BMIM]$^+$[MeSO$_4$]$^-$ + ethanol), ([BMIM]$^+$[MeSO$_4$]$^-$ + 1-propanol) (Deenadayalu *et al*. 2009), ([BMIM]$^+$[MeSO$_4$]$^-$ + nitromethane) (Iglesias *et al*. 2008), (methanol + nitromethane), (ethanol + nitromethane) (Nakanishi *et al.* 1970) and (1-propanol + nitromethane) (Cerdeirina *et al.* 1999). The binary excess molar volume for the systems ([BMIM]$^+$[MeSO$_4$]$^-$ + methanol or ethanol or 1-propanol) are negative for the entire composition range and at T = 298.15 K, which indicates that a more efficient packing and/or attractive interaction occurred when the ionic liquid and the alcohol were mixed (Deenadayalu *et al*. 2009). The excess molar volumes become less negative in the order methanol < ethanol < 1-propanol (Deenadayalu *et al*. 2009). Table 7.5 is a summary of V^{E}_{min} values for the binary systems related to the ([BMIM]$^+$[MeSO$_4$]$^-$ + methanol or ethanol or 1-propanol + nitromethane) ternary systems. From Table 7.5, it can be seen that for the systems ([BMIM]$^+$[MeSO$_4$]$^-$ + methanol or ethanol or 1- propanol) V^{E}_{min} values at T = 298.15 K are -1.100 cm^3·mol^{-1} at x_1 = 0.3228, -0.647 cm^3·mol^{-1} at x_1 = 0.4056 and -0.235 cm^3·mol^{-1} at x_1 = 0.4756, for methanol, ethanol or 1-propanol, respectively (Deenadayalu *et al*. 2009).

The V^{E}_{m} data of ([BMIM]$^+$[MeSO$_4$]$^-$ + nitromethane) at T = 298.15 K and at all mole fractions of [BMIM]$^+$[MeSO$_4$]$^-$ is negative due to the well packed molecules (Iglesias *et al.* 2008). From Table 7.5, it can be seen that for the system ([BMIM]$^+$[MeSO$_4$]$^-$ + nitromethane) V^{E}_{min} values at T = 298.15 K are -0.577 cm^3·mol^{-1} at x_1 = 0.2998 for nitromethane (Iglesias *et al.* 2008).

The V_m^E data of (methanol + nitromethane) at T = 298.15 K and at all mole fractions of methanol is negative due the geometrical fitting of the nitromethane into methanol structure (Nakanishi *et al.* 1970). From Table 7.5, it can be seen that the system (methanol + nitromethane) V_{min}^E values at T = 298.15 K is -0.185 $cm^3 \cdot mol^{-1}$ at x_1 = 0.5797 for nitromethane (Nakanishi *et al.* 1970; Cerdeirina *et al.* 1999).

The V_m^E data of (ethanol + nitromethane) at T = 298.15 K and at all mole fractions of ethanol is both positive and negative due to the break-up of the ethanol structure and geometrical fitting of the nitromethane into the ethanol structure (Nakanishi *et al.* 1970). From Table 7.1, it can be seen that the system (ethanol + nitromethane) V_{min}^E values at T = 298.15 K are -0.098 $cm^3 \cdot mol^{-1}$ at x_1 = 0.8039 for nitromethane (Nakanishi *et al.* 1970 *et al.* 1999).

The V_m^E data of (1-propanol + nitromethane) at T = 298.15 K and at all mole fractions of 1-propanol is positive due hydroden bond rupture and dispersive interactions between unlike molecules (Cerdeirina *et al.* 1999). From Table 7.5, it can be seen that the system (1-propanol + nitromethane) V_{min}^E values at T = 298.15 K are -0.0776 $cm^3 \cdot mol^{-1}$ at x_1 = 0.05041 for nitromethane (Cerdeirina *et al.* 1999).

Table 7.6, lists $V_{123\,min}^E$ for all ternary systems studied in this work for the $[BMIM]^+[MeSO_4]^-$ IL. From Table 7.6, it can be seen that for the systems ($[BMIM]^+[MeSO_4]^-$ + methanol or ethanol or 1- propanol + nitromethane) the minimum ternary excess molar volumes, $V_{123\,min}^E$, increase with a decrease in z values except at z = 4.21.

Table 7.5 The V^{E}_{min} for the seven binary systems at T = 298.15 K from literature for the ([BMIM]$^{+}$[MeSO$_4$]$^{-}$ + methanol or ethanol or 1- propanol + nitromethane) ternary systems

T/K	x_1	x_2	V^{E}_{min}/cm^3·mol^{-1}
	[BMIM]$^{+}$[MeSO$_4$]$^{-}$ + methanol		
298.15	0.3228	0.6772	-1.100[a]
	[BMIM]$^{+}$[MeSO$_4$]$^{-}$ + ethanol		
298.15	0.4056	0.5994	-0.647[a]
	[BMIM]$^{+}$[MeSO$_4$]$^{-}$ + 1-propanol		
298.15	0.4756	0.5244	-0.235[a]
	[BMIM]$^{+}$[MeSO$_4$]$^{-}$ + nitromethane		
298.15	0.2998	0.7002	-0.577[b]
	Methanol + nitromethane		
298.15	0.5797	0.4203	-0.185[c]
	Ethanol + nitromethane		
298.15	0.8093	0.1907	-0.098[c]
	1-Propanol + nitromethane		
298.15	0.05041	0.94959	0.0776[d]

[a] (Deenadayalu *et al.* 2009).

[b] (Iglesias *et al.* 2008).

[c] (Nakanishi *et al.* 1970).

[d] (Cerdeirina *et al.* 1999).

Table 7.6 The minimum excess molar volume, $V^{E}_{123\,min}$ for the ternary systems ($[BMIM]^+[MeSO_4]^-$ + methanol or ethanol or 1- propanol + nitromethane) at constant z values and at T = 298.15 K

x_1	x_2	x_3	z	$V^{E}_{123\,min}$/cm^3·mol^{-1}
		($[BMIM]^+[MeSO_4]^-$ + methanol + nitromethane)		
0.1452	0.2429	0.6120	4.21	-1.07
0.1332	0.6173	0.2494	1.87	-1.64
0.1591	0.7290	0.1118	0.70	-1.52
0.3706	0.5428	0.0866	0.23	-1.29
0.7200	0.2475	0.0325	0.04	-0.37
		($[BMIM]^+[MeSO_4]^-$ + ethanol + nitromethane)		
0.1263	0.3412	0.5325	4.21	-0.96
0.1640	0.5288	0.3071	1.87	-1.35
0.2045	0.6517	0.1438	0.70	-1.33
0.2942	0.6370	0.0688	0.23	-1.29
0.6796	0.2898	0.0306	0.04	-0.49
		($[BMIM]^+[MeSO_4]^-$ + 1-propanol + nitromethane)		
0.1372	0.2842	0.5785	4.21	-0.59
0.1454	0.5823	0.2723	1.87	-0.97
0.2412	0.5892	0.1696	0.70	-0.92
0.3456	0.5736	0.0808	0.23	-0.79
0.7289	0.2382	0.0329	0.04	-0.31

The values of $V^{E}_{123\,min}$ -1.64, -1.35 and -0.97 $cm^3 \cdot mol^{-1}$, respectively at T = 298.15 K is less than that for the ($[BMIM]^+[MeSO_4]^-$ + methanol or ethanol or 1- propanol) binary systems (Deenadayalu *et al.* 2009). From Figures 6.13 to 6.15 the values of excess molar volumes, V^{E}_{123} , in general decrease with an decrease in the moles fraction of ionic liquid at lower mole fractions of methanol or ethanol or 1-propanol at T = 298.15 K and is negative for all ternary composition curves. The negative values of V^{E}_{123} for ($[BMIM]^+[MeSO_4]^-$ +, methanol or ethanol or 1- propanol + nitromethane) show that there is strong attractive interactions between methanol or ethanol or 1- propanol and nitromethane with the IL.

The interactions between IL ions with methanol or ethanol or 1- propanol and nitromethane can occur through the cation of the IL and lone pair of electrons on the methanol or ethanol or 1- propanol and nitromethane as well as accommodation of smaller methanol or ethanol or 1-propanol molecules into the interstices of the IL (Deenadayalu *et al.* 2008). Hydrogen bonding between the alcohol and nitromethane can also contribute to association. Figure 6.28 to 6.30 is the ternary excess molar volume graphs obtained from using the Cibulka equation parameters for the system ($[BMIM]^+[MeSO_4]^-$ + methanol or ethanol or 1- propanol) at T = 298.15 K. The V^{E}_{123} values is more negative for ($[BMIM]^+[MeSO_4]^-$ + methanol + nitromethane) than for ($[BMIM]^+[MeSO_4]^-$ + ethanol + nitromethane) than for ($[BMIM]^+[MeSO_4]^-$ + 1-propanol + nitromethane) systems. At low mole fraction of nitromethane the V^{E}_{123} values are positive similar to the binary (ethanol + nitromethane) and (1-propanol + nitromethane) systems, respectively (Cerdeirina *et al.* 1999; Nakanishi *et al.* 1970).

From Figures 6.28 to 6.30, it can be seen that for the ternary systems the V^{E}_{123} increases with an increase in the alcohol chain length. The V^{E}_{123} is positive in IL-alcohol rich regions.

7.2 APPARENT MOLAR PROPERTIES

7.2.1 V_ϕ and κ_ϕ

7.2.1.1 ([MOA]$^+$[Tf$_2$N]$^-$ + methyl acetate or methanol) and (methanol + methyl acetate) binary systems

The apparent molar volume, V_ϕ, data for the binary systems ([MOA]$^+$[Tf$_2$N]$^-$ + methyl acetate or methanol) and (methanol + methyl acetate) at T = (298.15, 303.15, 308.15 and 313.15) K are listed in Tables 6.10, 6.12 and 6.14. In general the apparent molar volume data increase with an increase in temperature and the concentration of each binary system. Increasing V_ϕ with increasing molality have also been observed in the system (BMIMBr + methanol or ethanol) (Zafarani-Moattar *et al.* 2005) and for electrolytes in water (Sadeghi *et al.* 2009). For low molality of IL the ions are surrounded by solvent molecules indicating strong ion-solvent interaction and on increasing the IL concentration the ion-ion interaction increases resulting in large V_ϕ values.

The V_ϕ^0 , S_v and B_v values obtained from Redlich-Mayer type equation given in Table 6.18 indicate that for the (IL + methyl acetate) and (IL + methanol) binary system at infinite dilution, each IL ion is surrounded only by the methyl acetate or methanol molecules and is an infinitely large distance from the other ions. Therefore, V_ϕ^0 is unaffected by IL (ion-ion) interaction (Sadeghi *et al.* 2009) and V_ϕ^0 measures only the (ion- solvent) interaction i.e. (IL + methyl acetate) and (IL + methanol) interactions (Sadeghi *et al.* 2009). From Table 6.18 it can been seen that V_ϕ^0, increases with an increase in temperature for each binary system. This behaviour has also been observed for the system (1-alkyl-3-methylimidazolium bromide + water) (Sadeghi *et al.* 2009). For (IL + methyl acetate) the values of V_ϕ^0 is greater than for (IL + methanol) at all temperatures except T = 298.15 K indicating that the (ion + solvent)

interactions of (IL + methyl acetate) is stronger. For the (methanol + methyl acetate) binary system V_ϕ^0 is smaller indicating weaker (ion + solvent) interaction. The values of S_v obtained from the coefficient of the Redlich-Mayer type equation is positive for all binary mixtures and decrease with temperature for the systems (IL + methyl acetate) and (methanol + methyl acetate). The IL (ion-ion) interaction is stronger for (IL + methyl acetate) than for the (IL + methanol) except at T = 313.15 K. The ion-ion interaction decreases with an increase in temperature for the (IL + methyl acetate) system and for the (IL + methanol) system it has an opposite trend. For the (methanol + methyl acetate) system ion-solvent interaction is stronger than for the (IL + methanol) system. For the (IL + methanol) system S_v trend is similar to that of the system (1-butyl-3-methylimidazolium bromide + methanol) at different temperatures (Zafarani-Moattar *et al.* 2005). The effect of temperature on S_v values for the (IL + methanol) is less than that for (methanol + methyl acetate). B_v is generally negative except for hydrogen bonding interactions (Sadeghi *et al.* 2009). The negative B_v values imply for (IL + methyl acetate or methanol) systems a methanol or methyl acetate induced IL co-sphere over-lap effect (Sadeghi *et al.* 2009) i.e. increase of ion-ion interactions (Sadeghi *et al.* 2009) and the simultaneous release of methanol or methyl acetate to the bulk solvent (Sadeghi *et al.* 2009). For the (methanol + methyl acetate) system (solute-solute) interaction is the weakest. Table 6.18 shows B_v values increase with increasing temperature except for (IL + methanol) at T = 303.15 K indicating decreased ion-ion interactions. This trend was also observed for (1-hexyl-3- methylimidazolium bromide + methanol) for the T = (298.15 to 308.15) K (Sadeghi *et al.* 2009).

The E_ϕ^0 values of (IL + methanol or methyl acetate) for varying moles of IL and temperature given in Table 6.19 indicate that at each temperature E_ϕ^0 values for the binary systems (IL + methyl acetate or methanol) and (methanol + methyl acetate) have positive values and

decreases with an increase in temperature for the (IL+ methyl acetate or methanol) system due to the pure solvent, methyl acetate or methanol expanding more rapidly than the solution containing IL ions (Zafarani-Moattar *et al.* 2005). The E_{ϕ}^{0} values increases with temperature for the (methanol + methyl acetate) system indicating increase in thermal agitation increases with temperature resulting in methanol or methyl acetate molecules being released from the ion thereby increasing the solution volume more rapidly than for the pure solvent (Zafarani-Moattar *et al.* 2005). This behaviour has also been observed for the system (BMIMBr + water) (Zafarani-Moattar *et al.* 2005).

The speed of sound, isentropic compressibility and apparent molar isentropic compressibilities are given in Tables 6.20, 6.22 and 6.24. The speed of sound measurements decreases with an increase in temperature and concentration of the solute for the binary systems (IL + methyl acetate) and (methanol + methyl acetate). For the binary system (IL + methanol) the speed of sound decreases with an increase in temperature and increase with an increase the concentration of the solute. The isentropic compressibility is the sum of two contributions, κ_s (solvent intrinsic) and κ_s (solute intrinsic). The κ_s (solvent intrinsic) is the isentropic compressibility due to the compression of solvent: (methyl acetate or methanol) and κ_s (solute intrinsic) is compressibility due to the compression of the hydration shell of ions, or penetration of solvent molecules into the IL or methanol free volume (Sadeghi *et al.* 2009). κ_s values increase with an increase in temperature for each binary system at a fixed composition due to an increase in the thermal agitation resulting in the solvent molecules being released from the solute thereby increasing the solution volume making the solution more compressible.

For the binary system (IL + methanol) the isentropic compressibilities (κ_s) values decrease with an increase in concentration of the solute due to the combined effect of hydration of

ions and breaking the structure of methanol molecules because of κ_s (solute intrinsic) is dominant over the κ_s (solvent intrinsic) effect (Zafarani-Moattar *et al.* 2005). This behaviour has also been observed in the system BMIMBr in methanol (Zafarani-Moattar *et al.* 2005). At a particular temperature, the (IL + methanol) solution is more compressible than the (IL + methyl acetate) system. For the (IL + methyl acetate) and (methanol + methyl acetate) binary systems the κ_s value increase with an increase in concentration of methanol because κ_s (solvent intrinsic) effect is dominant over the κ_s (solute intrinsic) effect. To quantify the concentration at which κ_s isotherms converge, the temperature derivative of κ_s is needed. The isotherm converge when $d\kappa_s/dT = 0$, which implies that $d\kappa_s$(solvent intrinsic)/dT + $d\kappa_s$ (solute intrinsic)/dT = 0 (Zafarani-Moattar *et al.* 2005). When $d\kappa_s/dT = 0$, the intrinsic methyl acetate or methanol structure is completely broken and all the methyl acetate or methanol molecules are incorporated in the primary hydration shell of the ions. From figures 6.39, and 6.43, it can be see that for (IL + methyl acetate) and (methanol + methyl acetate) solutions, the κ_s versus *m* isotherms increase smoothly and do not converge within the experimental concentration due to $d\kappa_s$ (solute intrinsic)/$dT > 0$. For the (IL + methanol) solutions from fig. 6.41, it can be see that the κ_s versus *m* isotherms decrease smoothly with increasing concentration and do not converge within the experimental concentration. Therefore the concentration at which $d\kappa_s/dT = 0$, could not determined.

At a fixed temperature κ_ϕ values increases with an increase in concentration for all binary systems except for the system (methanol + methyl acetate) system at concentration *m* = 1.4044, 2.4424 and 3.8983 at $T = 298.15$ and $m = 2.4424$ and 3.8983 at $T = 303.15$ K. The κ_ϕ values decrease with an increase in temperature of each binary system except (IL + methanol) at higher concentration of IL at T = (303.15, 308.15 and 313.13) K. For all the system investigated κ_ϕ have both negative and positive values. The negative values of κ_ϕ are

attributed to the strong attractive interactions between the solute and solvent due to the solvation of the solute (Sadeghi *et al.* 2009). For all binary systems the (ion + solvent) interactions are weaker and methyl acetate or methanol molecules are released into the bulk solution, thereby making the solvent more compressible. As can be seen from Tables 6.20 and 6.22, the values of apparent molar isentropic compressibility of (IL + methyl acetate) is greater than those of (IL + methanol). This is because the (IL+ methanol) system (ion + solvent) interactions are stronger than the (IL + methyl acetate) system.

κ_ϕ^0 is the limiting apparent molar isentropic compressibilities. S_k , and B_k are empirical parameters. The values of κ_ϕ^0, S_k , and B_k obtained for each mixture at the experimental temperature are listed in Table 6.28. There are two factors that contribute to the κ_ϕ^0 : large organic ions could have some solvent intrinsic compressibility (positive effect) due to the intermolecular free space which makes the solution more compressible (Das *et al.* 2004) and also for large organic ions is the penetration (negative effect) of the solvent molecules into the intra-ionic free space due to the interaction of ions with the neighbouring solvent molecules methyl acetate or methanol. The solute intrinsic is essentially an electrostriction effect and causes constriction in the solution volumes, resulting in a more compact and, hence, a less compressible medium. The negative κ_ϕ^0 values of the IL or methanol can be interpreted in terms of loss of compressibility of the solvent methyl acetate or methanol. Negative limiting apparent molar isentropic compressibilities, κ_ϕ^0, for ($[MOA]^+$ $[Tf_2N]^-$ + methyl acetate or methanol), and (methanol + methyl acetate) can be attributed to the predominance of penetration effect of solvent molecules into the intra-ionic free space of IL or methanol ions over the effect of their solvent intrinsic compressibility. Negative limiting apparent molar isentropic compressibilities, κ_ϕ^0 , indicate that the solvent surrounding the IL or methanol would present greater resistance to compression than the bulk solvent. The κ_ϕ^0

values decrease with increasing the temperature. This behaviour has also been observed in the system BMIMBr in methanol and ethanol (Zafarani-Moattar *et al.* 2005). S_k and B_k have same meaning as S_v and B_v for apparent molar volume.

7.2.1.2 ([MOA]$^+$[Tf$_2$N]$^-$ + ethyl acetate or ethanol), (methanol + ethyl acetate) and (ethanol + methyl acetate or ethyl acetate) binary systems

The apparent molar volume, V_ϕ, data for the binary systems ([MOA]$^+$[Tf$_2$N]$^-$ + ethyl acetate or ethanol), (methanol + ethyl acetate) and (ethanol + methyl acetate or ethyl acetate) at T = (298.15, 303.15, 308.15 and 313.15) K are also listed in Tables 6.11, 6.13 and 6.15 to 6.17. The apparent molar volume increase with an increase in temperature of each binary system. In general the apparent molar volume increase with an increase the molality of the solute for the system ([MOA]$^+$ [Tf$_2$N]$^-$ + ethyl acetate), (methanol + ethyl acetate) and ethanol + methyl acetate). Increasing V_ϕ with increasing molality have also been observed in the system (BMIMBr + methanol or ethanol) (Zafarani-Moattar *et al.* 2005) and for electrolytes in water (Sadeghi *et al.* 2009). For low molality of IL, methanol and ethanol the ions are surrounded by solvent molecules indicating strong ion-solvent interaction and increasing the IL, methanol and ethanol concentration the ion-ion interaction increases resulting in large V_ϕ values. For the system (ethanol +ethyl acetate) decrease with an increase in molality of the solute and opposite to the systems ([MOA]$^+$[Tf$_2$N]$^-$ + ethyl acetate), (methanol +ethyl acetate) and (ethanol + methyl acetate) indicating increasing the ethanol concentration the ion-ion interaction decreases resulting in small values. For the ([MOA]$^+$[Tf$_2$N]$^-$ + ethanol) system is not systematic with molality.

The values of V_ϕ^0 values obtained from Redlich-Mayer type equation given in Table 6.18. For the IL binary system at infinite dilution, each IL ion is surrounded only by the ethyl

acetate or ethanol molecules and is an infinitely large distance from the other ions. Therefore, V_ϕ^0 is unaffected by IL (ion-ion) interaction (Sadeghi *et al.* 2009) and V_ϕ^0 measures only the (ion- solvent) interaction i.e. (IL + ethyl acetate) and (IL + ethanol) interactions (Sadeghi *et al.* 2009). From Table 6.18 it can been seen that the V_ϕ^0 increase with an increase in temperature for each binary system. This behaviour has also been observed for the system (1-alkyl-3-methylimidazolium bromide + water) at each temperature (Hasan *et al.* 2009). For (IL + ethyl acetate) the values of V_ϕ^0 is greater than for (IL + ethanol) at all temperatures except at T = (308.15, and 313.15) K indicating that the (ion + solvent) interactions of (IL + ethyl acetate) is stronger. For the (methanol + ethyl acetate) the values of V_ϕ^0 is smaller indicating weaker (ion + solvent) interaction of (methanol + ethyl acetate). For the system (ethanol + methyl acetate or ethyl acetate) the values of V_ϕ^0 for the system (ethanol + ethyl acetate) is greater than for (ethanol + methyl acetate) at all temperatures indicating that the (ion + solvent) interaction of (ethanol + ethyl acetate) is stronger than (ethanol + methyl acetate) system. The values of S_v and B_v together with the standard deviations of apparent molar volume, σ_v, are also given in Table 6.18. S_v is negative for the systems (IL + ethanol) and (ethanol + ethyl acetate) for all temperatures except T = 298.15 K for the system (IL + ethanol). S_v is positive for the system (IL + ethyl acetate), (methanol + ethyl acetate) and (ethanol + methyl acetate) and decreases with temperature for all the systems except at T = 313.15 K for the system (ethanol + methyl acetate) and (ethanol + ethyl acetate). The IL (ion-ion) interaction is stronger for (IL + ethyl acetate) than for the (IL + ethanol). The (ion-ion) interaction decreases with an increase in temperature for the (IL + ethyl acetate or ethanol) systems. For the (methanol + ethyl acetate) system ion-solvent interaction is stronger than for the (IL + ethyl acetate) system. For the (ethanol + methyl acetate or ethyl acetate) systems ion-solvent interaction is stronger than for the (methanol + ethyl acetate) system. The effect of temperature on S_v values for the (IL + ethanol) system is greater than for (ethanol +

methyl acetate) and (ethanol + ethyl acetate) systems. B_v is generally negative except for hydrogen bonding interaction shows that the interaction are weak and less complex ion formation takes place (Sadeghi *et al.* 2009). The negative B_v values imply for (IL + ethyl acetate), (methanol + ethyl acetate) and (ethanol + methyl acetate) systems methyl acetate or ethyl acetate induced IL or methanol or ethanol co-sphere over-lap effect (Hasan *et al.* 2009) i.e. increase of solute-solute interactions and the simultaneous release of methyl acetate or ethyl acetate to the bulk solvent (Sadeghi *et al.* 2009). The positive B_v values for the system (IL + ethanol) and (ethanol + ethyl acetate) at all temperatures indicate the strong ion-ion interaction. Table 6.18 shows B_v values increase with increasing temperature except for (ethanol + methyl acetate or ethyl acetate) at T = 313.15 K indicating the decreased solute-solute interactions. This trend was also observed for 1-hexyl-3- methylimidazolium bromide, with methanol for the temperature range of T = (298.15 to 308.15) K (Sadeghi *et al.* 2009).

The E_ϕ^0 values of (IL + ethanol or ethyl acetate), (methanol + ethyl acetate) and (ethanol + methyl acetate or ethyl acetate) for varying moles of IL, methanol and ethanol and temperature are given in Table 6.19 E_ϕ^0 values for the binary systems (IL + ethyl acetate or ethanol), (methanol + ethyl acetate) and (ethanol + methyl acetate or ethyl acetate) have positive values and decreases with an increase in temperature system due to the pure solvent, methyl acetate or ethyl acetate or ethanol expanding more rapidly than the solution containing ions (Zafarani-Moattar *et al.* 2005).

The speed of sounds, isentropic compressibilities and apparent isentropic compressibilities are given in Tables 6.21, 6.23 and 6.25 to 6.27. The speed of sound measurements in solution provides information about ion-ion, ion-solvent and solvent-solvent interactions. The speed of sound decrease with an increase in temperature for all binary systems. The speed of sound increase with increase in concentration of the solute for all the binary systems except (ethanol

+ methyl acetate or ethyl acetate) where it decrease. The isentropic compressibility is the sum of two contributions, κ_S (solvent intrinsic) and κ_S (solute intrinsic).The κ_S (solvent intrinsic) is the isentropic compressibility due to the compression of solvent: (methyl acetate, ethyl acetate and ethanol) and κ_S (solute intrinsic) is compressibility due to the compression of the hydration shell of ions or penetration of solvent molecules, into the IL or methanol or ethanol free volume (Sadeghi *et al.* 2009). κ_S values increases with an increase in temperature for each binary system at a fixed composition due to an increase in the thermal agitation resulting in the solvent molecules being released from the solute thereby increasing the solution volume making the solution more compressible .

For the binary system (IL + ethyl acetate or ethanol) and (methanol + ethyl acetate) κ_S values decrease with an increase in concentration of the solute due to the combined effect of hydration of ions and breaking the structure of the ethyl acetate or ethanol molecules because κ_S (solute intrinsic) is dominant over the κ_S (solvent intrinsic) effect (Zafarani-Moattar *et al.* 2005). This behaviour has also been observed in the system BMIMBr in methanol (Zafarani-Moattar *et al.* 2005). At a particular temperature, the (IL + ethanol) solution is more compressible than the (IL + ethyl acetate) system.

For the (ethanol + methyl acetate or ethyl acetate) binary system the κ_S value increase with an increase in concentration of solute κ_S (solvent intrinsic) dominant over the κ_S (solute intrinsic) effect.

From Figures 6.45 and 6.46, it can be see that for (ethanol + methyl acetate or ethyl acetate) solutions, the κ_S versus *m* isotherms increase smoothly and do not converge within the experimental concentration due to $d\kappa_S$ (solute intrinsic)/$dT > 0$. From Figures 6.40, 6.42 and 6.44 for the (IL + ethyl acetate or ethanol) and (methanol + ethyl acetate) solutions, it can be see that the κ_S versus *m* isotherms decrease smoothly with increasing concentration and do

not converge within the experimental concentration. Therefore the concentration at which $d\kappa_s/dT = 0$, could not determined. Similar behaviour has also been observed for system (BMIMBr + methanol) (Zafarani-Moattar *et al.* 2005).

The κ_ϕ values decrease with an increase in the concentration for all binary systems. The κ_ϕ values increase with an increase in temperature of all binary system. For all the system investigated κ_ϕ have positive values. The positive κ_ϕ values are attributed to the weak attractive interactions between solute and solvent due to the solvation of solute (Sadeghi *et al.* 2009). For all binary systems an increase in temperature, i.e, (ion + solvent) interactions are weaker and therefore some methyl acetate or ethyl acetate or ethanol molecules are released into the bulk, thereby making the medium more compressible. As can be seen from Tables 6.21 and 6.23, the values of apparent molar isentropic compressibility of (IL+ ethanol) are greater than those of (IL+ ethyl acetate). This is because the (IL+ ethyl acetate) system (ion + solvent) interactions are stronger than the (IL + ethanol) system. As can be seen from Tables 6.21, 6.23 and 6.25 to 6.27. The values of apparent molar isentropic compressibility of investigated (methanol + ethyl acetate), and (ethanol + methyl acetate or ethyl acetate) are larger than the (IL + ethyl acetate or ethanol). This is because the (methanol + ethyl acetate) and (ethanol + methyl acetate or ethyl acetate) system (ion + solvent) interactions are weaker than the (IL + ethyl acetate or ethanol) system.

The values of κ_ϕ^0, S_k, and B_k obtained for each mixture at the experimental temperature are listed in Table 6.28. The positive κ_ϕ^0 values of the IL or methanol or ethanol can be interpreted in terms of an increase in the compressibility of the solution compared to the pure solvent methyl acetate or ethyl acetate or ethanol. Positive limiting apparent molar isentropic compressibilities, κ_ϕ^0, for ($[MOA]^+ [Tf_2N]^-$ + ethyl acetate or ethanol), (methanol + ethyl acetate) and (ethanol + methyl acetate or ethyl acetate) can be attributed to the effect of

solvent intrinsic compressibility of these ions greater than the penetration effect. The κ_ϕ^0 values increase with an increase in the temperature. This behaviour has also been observed in the system BMIMBr in water (Zafarani-Moattar *et al.* 2005).

CHAPTER 8

CONCLUSION

In this chapter, the conclusion on the work done in this investigation is discussed.

The results obtained in this work for the densities and ternary excess molar volume for the systems ($[MOA]^+[Tf_2N]^-$ + methanol or ethanol + methyl acetate or ethyl acetate) at T = (298.15, 303.15 and 313.15) K and ($[BMIM]^+[MeSO_4]^-$ + methanol or ethanol or 1-propanol + nitromethane) at T = 298.15K over the entire composition range have been presented. For each ternary system that corresponding binary systems were obtained from the literature. The binary data was used for obtaining the Redlich-Kister parameters. The V_{123}^{E} data was correlated by the Cibulka equation. The results were discussed in terms of intermolecular interactions.

The apparent molar volumes and the apparent molar isentropic compressibility for the binary systems ($[MOA]^+[Tf_2N]^-$ + methanol or ethanol or methyl acetate or ethyl acetate), (methanol + methyl acetate or ethyl acetate) and (ethanol + methyl acetate or ethyl acetate) were obtained at T = (298.15, 303.15, 308.15 and 313.15) K. A Redlich-Mayer type equation was used for correlating the experimental apparent molar volume and apparent molar isentropic compressibility data. The results were discussed in terms of solute- solvent, solute-solute, and solvent-solvent interactions.

8.1 TERNARY EXCESS MOLAR VOLUMES

8.1.1 ($[MOA]^+[Tf_2N]^-$ + methanol or ethanol + methyl acetate or ethyl acetate)

The densities and V_{123}^{E} were reported for the systems ($[MOA]^+[Tf_2N]^-$ + methanol or ethanol + methyl acetate or ethyl acetate) at T = (298.15, 303.15, and 313.15) K.

The V_{123}^{E} values are negative for all compositions of IL. The smaller methanol or ethanol and methyl acetate or ethyl acetate molecules are probably incorporated into the vast IL matrix (a packing effect) which is further enhanced by intermolecular hydrogen bonding between the ethanol and methyl acetate or ethyl acetate molecules and ion–dipole interaction between the IL ions, methanol, ethanol, and methyl acetate or ethyl acetate molecules. The ternary excess molar volume of the (IL + methanol or ethanol + ethyl acetate) ternary system is more negative than the (IL + methanol or ethanol + methyl acetate) system because of the additional CH_2 group on the ethyl acetate molecule. The $V_{123\,\min}^{E}$ decrease with an increase in the temperature for all ternary systems. The Cibulka equation was used to correlate the ternary data and indicated that the ternary contribution (three-body effect) is dominant.

8.1.2 ($[BMIM]^+[MeSO_4]^-$ + methanol or ethanol or 1-propanol + nitromethane)

The densities and V_{123}^{E} were reported for the systems ($[BMIM]^+[MeSO_4]^-$ + methanol or ethanol or 1-propanol + nitromethane) at $T = 298.15$K. The V_{123}^{E} values are negative for all compositions of IL. The order of negative ternary excess molar volume of the ternary system (IL + 1-propanol + nitromethane) < (IL + ethanol + nitromethane) < (IL + methanol + nitromethane) because of the additional CH_2 group on the alcohol molecules. The Cibulka equation was used to correlate the ternary data and indicated that the ternary contribution (three-body effect) is dominant.

8.2 APPARENT MOLAR PROPERTIES

The apparent molar volumes and isentropic compressibilities of solutions of the ionic liquid, ($[MOA]^+[Tf_2N]^-$ + methyl acetate or ethyl acetate or methanol or ethanol), (methanol + methyl acetate or ethyl acetate) and (ethanol + methyl acetate or ethyl acetate) have been measured at T = (298.15, 303.15, 308.15 and 313.15) K and at atmospheric pressure. The limiting partial molar volume and limiting apparent molar isentropic compressibility data for the solutions at each temperature have been evaluated using the Redlich + Mayer type equations. The partial molar volume V_ϕ^0 values for the binary systems (IL + methyl acetate or ethyl acetate or methanol or ethanol) and (methanol + methyl acetate or ethyl acetate) and (ethanol + methyl acetate or ethyl acetate) are positive and increase with an increase in temperature. For the (methanol + methyl acetate or ethyl acetate) systems V_ϕ^0 values indicate that the (ion-solvent) interactions are weaker.

The partial molar isentropic compressibilities, κ_ϕ^0 is both positive and negative. Positive κ_ϕ^0, for ($[MOA]^+[Tf_2N]^-$ + ethyl acetate or ethanol), (methanol + ethyl acetate) and (ethanol + methyl acetate or ethyl acetate) can be attributed to the predominance of solvent intrinsic compressibility effect over the effect of penetration of ions of IL or methanol or ethanol. The positive κ_ϕ^0 values of the IL or methanol or ethanol can be interpreted in terms of increase in the compressibility of the solution compared to the pure solvent methyl acetate or ethyl acetate or ethanol. The κ_ϕ^0 values increase with an increase in temperature. Negative κ_ϕ^0, for ($[MOA]^+[Tf_2N]^-$ + methyl acetate or methanol), and (methanol + methyl acetate) can be attributed to the predominance of penetration effect of solvent molecules into the intra-ionic free space of IL or methanol ions over the effect of their solvent intrinsic compressibility. Negative κ_ϕ^0, indicate that the solvent surrounding the IL or methanol would present greater resistance to compression than the bulk solvent. The κ_ϕ^0 values decrease with increasing the

temperature. The infinite dilution apparent molar expansibility E_ϕ^0 values for the binary systems (IL + methyl acetate or ethyl acetate or methanol or ethanol) and (methanol + methyl acetate or ethyl acetate) and (ethanol + methyl acetate or ethyl acetate) have positive and decrease with an increase in temperature due to the pure solvent, methyl acetate or ethyl acetate or methanol or ethanol expanding more rapidly than the solution containing IL ions. For (IL + methyl acetate or ethyl acetate or methanol or ethanol) systems E_ϕ^0 indicates that the interaction between (IL+ methyl acetate) is stronger than that of the (IL + ethanol) than (IL + methanol) than (IL+ ethyl acetate) solution. For the (methanol + methyl acetate or ethyl acetate) systems E_ϕ^0 values indicate that the interactions are stronger than (IL+ ethyl acetate) system. For the (ethanol + methyl acetate or ethyl acetate) systems E_ϕ^0 values indicate that the interactions are weaker.

REFERENCES

Abdulagatov I M., Tekin A., Safarov J., Shahverdiyev A., Hassel E., *Int. J. Thermophys.*, **2008**, 29, 505-533.

Abrams D. S., Prausnitz J. M., *J. Amer. Chem. Soc*., **1975**, 21, 116.

Acevedo I. L., Postigo M. A., Katz M., *Can. J. Chem*., **1988**, 66 (3) 367.

Acree W. E. Jr., "Thermodynamic properties of Non-electrolyte Solutions", Academic Press, Inc., (London) Ltd., **1984**.

Aminabhavi T. M., Banerjee K., *J. Chem. Eng. Data*, **1998**, 43, 509 – 513.

Andreatta A. E., Arce A., Rodil E., Soto A., *J. Chem. Thermodyn*., **2009**, 41, 265-272.

Andreatta A. E., Arce A., Rodil E., Soto A., *J. Soln. Chem*., **2010**, 39, 371-383.

Anthony J. L., Maginn E. J., Brennecke J. F., *J. Phys. Chem. B*, **2001**, 105, 10942-10949.

Arce A., Rodil E., Soto A., *J. Chem. Eng. Data*, **2006**, 51, 1453-1457.

Armand M., Endres F., MacFarlane D. R., Ohno H., Scrosati B., *Nature Materials*., **2009**, 8, 621–629.

Armstrong J. P., Hurst C., Jones R. G., Licence P., Lovelock K. R. J., Satterley C. J., Villar-Garcia I., J. *Physical Chemistry Chemical Physics*., **2007**, 9, 982.

Arnett E. M., Mitchell E. J., Murty T. S. S. R., *J. Amer. Chem. Soc*., **1974**, 96, 3875.

Audrieth L. F., Long A., Edwards R. E., *J. Am. Chem. Soc.*, **1936**, 58, 428.

Auslander D., Onitiu L., *Acustica*, **1971**, 24, 205.

Azevedo R., Szydlowski J., *J. Chem. Thermodyn.*, **2004**, 36, 211-222.

Azevedo R., Esperanca J.M.S.S., Szydlowski J., *J. Chem. Thermodyn.*, **2005** (a), 37, 88-899.

Azevedo R.G., Esperanca J.M.S.S., Visak Z.P., Guedes H.J.R., *J. Chem. Eng. Data*, **2005** (b), 50, 997-1008.

Aziz R. A., Bowman D. H., Lim C. C., *Can. J. Phys*., **1972**, 50, 721.

Balescu R., Bull. Cl. Sci. Acad. Roy. Belg., **1955**, 41, 1242.

Baranyai K.J., Deacon G.B., McFarane D.R., *Aust. J. Chem*., **2004**, 57, 145-147.

Barrer R. M., *Trans. Faraday Soc.*, **1943**, 39, 59-67.

Battino R., *Chem. Rev*., **1971**, 71, 5.

Beath L.A., Ó Neil S.P., Williamson A.G., *J. Chem. Thermodyn*., **1969**, 1, 293.

Berthed A., Ruiz-Angel M. J., Carda-Broch S., *J. Chromatography A.*, **2008**, 1184, 6-18.

Bhujrajh P., Deenadayalu N., *J. Chem. Thermodyn*., **2006**, 38, 278-282.

Bhujrajh P., Deenadayalu N., *J. Soln. Chem*., **2007**, 36, 563-672.

Bhujrajh P., Deenadayalu N., *J. Chem. Eng, Data*, **2008**, 53, 1098-1102.

Blandamer M. J. *Introduction to Chemical Ultrasonics*, **1973**, 65-121.

Bottomly G.A., Scott R.L, *J. Chem. Thermodyn*., **1974**, 6, 973.

Boon J. A., Levinsky J. A., Pflug J. L., Wilkes J. S., *J. Org. Chem.*, **1986**, 51, 480.

Borra E. F., Seddiki O., Angel R., Eisenstein D., Hickson P., Seddon K. R., Worden S. P., *Nature*., **2007**, 447 (7147), 979–981.

Bravo R., Pintosh M., Amigo A., *J. Chem. Thermodyn*., **1991**, 23, 905;

Brennecke J.F., Maginn E.J., *ALChE J*, **2001**, 47, 2384-2389.

Bronsted J. N., Koefoed J., *Danske Vidensk. Selsk., Mat. Fys. Medd*., **1946**, 22, 1.

Brown I., Smith F., *J. Chem*. **1973**, 26, 705-721.

Calvar N., Gonzalenz B., Dominguenz A., Tojo J. *J. Chem. Eng. Data*, **2006**, 51, 696-701.

Cann M.C., Connelly M.E., Real World Cases in Green Chemistry, *American Chemical Society*, **2000**, 633-641.

Carmichael A.J., Seddon K.R. *J. Phys. Org. Chem*., **2000**, 13, 591-598.

Chakraborty M., Hans-Jörg B., *J. Thermodyn*., **2007**, 88, 43-49.

Chaturvedi C. V., Pratap S., *Acustica*, **1979**, 42, 260.

Chiu Y., Gaeta G., Heine T., Dressler R. A., Levandier D. J., 42nd AIAA/ASME/SAE/ASEE Joint Propulsion Con- ference and Exhibit, Sacramento, alifornia, July 9-12, **2006**, 2006–5010.

Chum H. L., Koch V. R., Miller L. L., Osteryoung R. A., *J. Amer. Chem. Soc*., **1975**, 97, 3264.

Cibulka I., *Coll. Czech. Chem. Comm.*, **1982**, 47, 1414.

Cohen Y., Volatile Organic Compounds in the Environment, **1996**, 7-32.

Colinet C., D. E. S., Fac. Des. Sci, Univ., Grenoble, France **1967**.

Cristina Silva Pereira., The 3rd International Congress on Ionic Liquids *Green Chemistry News*., **2009**.

Crosthwaite J. M., Muldoon M. J., Dixon J. K., Anderson J. L., Brennecke J. F., *J. Chem. Thermodyn.*, **2005**, 37, 559–568.

Dantzler E. M., Knoblem C. M., *J. Phys. Chem*., **1969**, 73, 1335.

Davis, J.H., Fox, P.A., *Chemm.Comm.,* **2003**, 11, 1209-1212.

Davis, Jr., the 3rd International Congress on Ionic Liquids *Green Chemistry News*, **2009**.

Deenadayalu N., Sen S., Sibiya P N., *J. Chem. Thermodyn*., **2009**, 41, 538-548.

Deenadayalu N., Bahadur I., Hofman T., *J. Chem. Thermodyn*., **2010** (a), 42, 726-733.

Deenadayalu N., Bahadur I., Hofman T., *J. Chem. Eng Data*, **2010** (b), online 10th May.

Derr E. L., Deal C. H., "Distillation **1969**", Sec. 3, p. 37, Brighton England Int., Conf. Distillation, Sept. **1969**.

Desmyter A., Van der Waals J. C., *Real. Trav. Chim. Prays-Bas*, **1958**, 77, 53.

Diaz Pena M., Martin F. F., *Annales Real Soc. Espan. Fis. Quim (Mandrid)*, **1963**, 59, 323.

Dolezalek F., Z. *Phys. Chem*., **1908**, 64, 727.

Domanska U. *Pure Appl. Chem*., **2005** (a), 77, 543-557.

Domanska U., *Thermochim. Acta*, **2006**, 448, 19-30.

Domanska U. Marciniak A., *J. Chem. Thermodyn*., **2005** (b), 37, 577-585.

Domanska U., Pobudkowska A., *J. Soln. Chem*. **2006** , 35, 311- 332.

Dupont, J., *J. Braz. Chem. Soc.*, **2004**, 15(3), 341-350.

Dupont J., de Souza R.F., Suarez P.A.Z., *Chem. Rev*., **2002**, 102, 3667-3692.

Earle M. J., Esperança J. M.S.S., Gilea M. A., Lopes J. N. C., Rebelo L. P.N., Magee J. W., Seddon K. R., Widegren J. A., *Nature*., **2006**, 439, 831.

Earle M. J., Esperancua J.M.S.S., Gilea M.A., The distillation and volatility of ionic liquids, **2006**, 831-834.

Esperanca J.M.S.S., Visak Z.P., Guedes H.J.R., Seddon K.R., Rebelo L.P.N., *J. Chem. Eng Data*, **2006**, 51, 2009-2015.

Ewing M. B., Marsh K. N., Stokes R. N., *J. Amer. Chem. Soc*., **1972**, 4, 637.

Ewing M. B., Marsk K. N., *J. Chem. Thermodyn*., **1974**, 6, 395.

Eyring H., *J. Chem. Phys*., **1936**, 4, 283.

Eyring H., Hirschfelder J. O., *J. Phys. Chem*., **1937**, 41, 249.

Fischer T., Sethi T., Welton T., Welton J., *Tetrahedron Lett*., **1999**, 40, 793-796.

Flory P. J., *J. Chem. Phys*., **1941,** 9, 660.

Flory P. J., *J. Chem. Phys*., **1942**, 10, 51.

Flory P. J., *J. Chem. Phys*., **1944**, 12, 425.

Flory P. J., *J. Amer. Chem. Soc*., **1965**, 87, 1833.

Flory P. J., Abe A., *J. Amer. Chem. Soc*., **1965**, 87, 1838.

Flory P. J., *Discuss Farady Soc*., **1970**, 49, 7.

Fowler R. H., Guggenheim E. A., "Statistical thermodynamics" Cambridge University Press **1939**.

Frank F., and Reid D.S., Water in Crystalline Hydrates Aqueous Solutions of Simple

Nonelectrolytes, **1973**, 2, 323-380.

Freemantle M., *Chem. Eng. News*, **1998**, 76, 32-37.

Fredenslund Aa., Gmehling J., Michelsen M. L., Rasmussen P., Prausnitz J. M., *Ind. Eng. Chem. Process Des. Dev*. **1977**, 16, 450.

Fredenslund Aa., Gmehling J., Rasmussen P., "Vapour-Liquid Equilibria Using UNIFAC" Elsevier, Amsterdam **1977**.

Fredenslund Aa., Jones R. L., Prausnitz J. M., *A. I. Ch. E. Journal*, **1975**, 21, 1086.

Fredlake C.P., Crosthwaite J.M., Hert D.G., Aki S.N.V, *J. Chem. Eng. Data*, **2004**, 49, 954-964.

Gabriel S., Weiner J., "Ueber einige Abkömmlinge des Propylamins". *Ber.* **1888**, 21 (2), 2669–2679.

Gale R. J., Osteryoung R. A., *Inorganic Chemistry*., **1979**, **18**, 1603.

Gao H., Qi F., Wang H., *J. Chem. Thermodyn*., **2009**, 41, 888-892.

Garcia M., Rey C., Perez Villar V., Rodriquez J. R., *J. Chem. Thermodyn*., **1984**, 16, 603.

Gardas R. L., Dagade D. H., Coutinho J. A. P., Patil K. J., *J. Phys. Chem.*., **2008**, 112, 3380–3389.

Gasdaska C., Faulkos P., Micro newton colloid thruster for ST7-DRS mission. AIAA paper, **2003**, 2003-4543.

Ge M-L., Zhao R-S., Yi Y-F., Zhang Q., Wang L-S., *J. Chem. Eng. Data*, **2008**, 53, 2408-2411.

Giridhar P., Venkatesan K.A., *Electrochimica Acta*, **2007**, 52, 3006-3012.

Gmehling J. G., Anderson T. F., Prausnitz J. M., *Ind. Eng. Chem. Fundam.* **1978**, 17, 269.

Gmehling J. G., Rasmussen P., Fredenslund Aa., *Ind. Eng. Chem. Process Des. Dev*., **1982**, 21, 118.

Golden A., Dabrowska K., Hofman T., *J. Chem. Eng. Data*, **2007**, 52, 1830-1837.

Gómez E., González B., *J. Chem. Eng. Data,* **2006**, 51, 2096-2102.

Gómez E., González B., Calver N., Dominguenz A., *J. Chem. Thermodyn*., **2008**, 40, 1208-1216.

González B., Calver N., Gómez E., Dominguenz A., *J. Chem. Thermodyn*., **2008**, 40, 1274-1281.

González E. J., Alonso A. Dominguenz A., *J. Chem. Eng. Data*, **2006**, 51, 1446-1452.

González E. J., González B., *J. Chem. Eng. Data*, **2007**, 52(5) 1641-1648.

Govindaswamy S., Andiappan A. N., Lakshmanan S. M., *J. Chem. Eng. Data*, **1976**, 21, 336.

Govindaswamy S., Andiappan A. N., Lakshmanan S. M., *J. Amer. Chem. Soc*., **1977**, 22, 264.

Govender U. P., Thermodynamics of liquid mixtures: experimental & theoretical studies on the thermo chemical & volumetric behavior of some liquid & liquid mixtures, PhD thesis, UKZN, Durban, **1996,** 2-6.

Greaves T.L., Weerwardena A., Fong C., Drummomd J.C., *J. Phys. Chem B*, **2006**, 110, 22479-22487.

Guggenheim E. A., "Mixtures" Oxford University Press, London **1952**.

Guggenheim E. A., *Proc. Roy. Soc.,* **1935**, A148, 304.

Gutuwki K.E., Broker G.A., Willauer H.D., *J. Amer. Chem. Soc*., **2003**, 125, 6632-6633.

Hamann S. D., Lambert J. A., *Aust. J. Chem*., **1954**, 1, 1.

Handa Y. P., Benson G. C., *Fluid Phase Equilibria*., **1979**, 3, 185.

Handa Y. S., Reeder J., Knobler C. M., Scott R. L., *J. Chem. Eng. Data*, **1977**, 22, 218.

Heil J. F., Prausnitz J. M., *A. I. Ch. E. Journal*, **1966**, 12, 678.

Heintz A., Lehman J.K., *J. Chem. Eng. Data*, **2003**, 48, 472-474.

Heintz A., Klasen D., Lehman J.K., *J. Sol. Chem*., **2002**, 31, 467-474.

Heintz A. *J. Chem. Thermodyn.,* **2005**, 37, 525-535.

Heitler W., *Ann. Physik*., **1926**, 80, 629.

Henderson D., *Ann. Rev. Phy. Chem*., **1974**, 25, 461.

Hermanutz F., Gähr F., Massonne K., Uerdingen E., oral presentation at the 45th Chemiefasertagung, Dornbirn, Austria, September **2006**, 20th – 22nd,

Higgins M. L., *J. Phys. Chem.,* **1941**, 9, 440.

Higgins M. L., *Ann. N. Y. Acad. Sci*., **1942**, 43, 1.

Hijmans J., Holleman Th., *Advan. Chem. Phys*., **1969**, 16, 223.

Hildebrand J. H., *J. Amer. Chem. Soc*., **1929**, 51, 66.

Hildebrand J. H., Scott R. L., "Solubilities of Non-electrolytes", Reinhold Publishing Corporation, New York **1950**.

Hirschfelder J. O., Stevenson D. P., Eyring H., *J. Phys. Chem*., **1937**, 5, 896.

Hofman T., Goldon A., Nevines A., Letcher T.M., *J. Chem. Thermodyn*., **2008**, 40, 580-591.

Holbrey J.D., Seddon K.R., *Clean Products and Processes*, **1999**, 1, 223-236.

Holder G. A., Whalley E., *Trans. Faraday Soc*., **1962**, 58, 2018.

Holleman Th., *Physica* **1953**, 29, 585.

Hutchings J. W., Fuller K. L., Heitz M. P., Hoffmann M, M., *Green Chemistry.,* **2005**, 7, 475-478.

Ignatiev N., the 3rd International Congress on Ionic Liquids *Green Chemistry News*, **2009**.

Izgorodina E., the 3rd International Congress on Ionic Liquids *Green Chemistry News*, **2009**.

Jacob K. T., Fitzner K., *Thermochim. Acta*, **1977**, 18, 197.

Jacobson B., *Acta. Chem. Scand*., **1951**, 5, 1214.

Jacobson B., *J. Amer. Chem. Soc*., **1952** (a), 6, 1485.

Jacobson B., *J. Chem. Phys*., **1952** (b), 20, 927.

James P. A., Christopher H., Robert G. J., Peter L., Kevin R. J. L., Christopher J. S., Ignacio J. V-G., *Physical Chemistry Chemical Physics* , **2007**, 9 (8): 982.

Jaquemin J., Husson P., Padua A. Major V., *Green Chem*., **2006**, 8, 172-180.

Jayakumar M., Venkatesan K.A., Srinivasan T.G., *Electrochimica Acta.*, **2007**, 52, 7121-7127.

Jeener J., *J. Chem. Phys*., **1956**, 25, 584.

Jork C., Kristen C., Pieraccini D., Stark A., Chiappe C., Beste Y. A., Arlt W., *J. Chem. Thermodyn*., **2005**, 37, 537–558..

Kaar J. L., Jesinowski A.M., Berberich J.A., Moulton R., *J. Am. Soc.,* **2003**, 125, 4125-4131.

Karkamkar, Aardahl C., Autrey T., *Material Matters*., **2007**, 2 (2), 6–9.

Kaulgud M. V., *Acustica*, **1960**, 10, 316.

Kaulgud M. V., *Indian J. Phys.*, **1962**, 36, 577.

Kaulgud M. V., *Z. Phys. Chem*. (NF), **1963**, 36, 365.

Kaulgud M. V., Tarsekar V. K., *Acustica*, **1971**, 25, 14.

Kehiaian, H. V., "Thermochemistry and thermodynamics" MTP International Review of Sciences, (Ed.) H. A. Skinner, Butter worths, London, **1972**, 121.

Kenneth R. S., Jason A. W., *Nature*, **2006**. 439, 831.

Keyes D. B., Hildebrand J.H., *J. Am. Soc.*, **1917**, 39, 2126.

Kihara T., *Rev. Mod. Phys*., **1953**, 25, 831.

Kincaid J. F., Eyring H., *J. Amer. Chem. Soc*., **1937**, 5, 587.

Kittel Ch., *J. Amer. Chem. Soc*., **1946**, 14, 614.

Kohler F., Monatsh, *Chem.*, **1960**, 91, 738.

Kolle, P.; Dronskowski, R., *Eur. J. Inorg. Chem.*, **2004**, *11*, 2313-2320.

Koo Y-M., the 3rd International Congress on Ionic Liquids *Green Chemistry News*, **2009**.

Kozlova S. A., Verevkin S. P., Heintz A., Peppel T., Kockerling M., *J. Chem. Thermodyn*., **2009**, 41, 330-333.

Krummen M, Wassersheid P., Gmehling J., *J. Chem Eng. Data*, **2002**, 47, 1411-1417.

Kumaran M.K., McGlashan M.L., *J. Chem. Thermodyn*., **1977**, 9, 259.

Kumelan J., Kamps A.P., Tuma D., Yokozeki A. Shiflett M.B., Maurer G., J. *Phys. Chem.B*., **2008**, 112, 3040-3047.

Lachwa J., Rebelo L.P.N., Seddon K.R., *J. Am. Soc.*, **2005**, 127, 6542-6543.

Lachwa J., Rebelo L.P.N., Seddon K.R., *Chem Comm.*, **2006**, 23, 2445-2447.

Lai T. T., Doan-Nguyen T. H., Vera J. H., Ratcliff G. A., *Can. J. Chem. Eng*., **1978,** 56, 358.

Lakhanpal M. L., Chaturvedi L. K., Sharma S.C., *Indian J. Chem*., **1975**, 13, 129.

Lakhanpal M. L., Chaturvedi L. K., Puri T., Sharma S.C., *J. Amer. Chem. Soc*., **1976**, 14A, 645.

Langeman R. T., Correy J. E., *J. Chem. Phys*., **1942**, 10, 759.

Leland T. W., Rowlinson J. S., Sather G. A., *Trans. Farady Soc*., **1968**, 64, 1447.

Leland T. W., Rowlinson J. S., Sather G. A., Watson I. D., *J. Amer. Chem. Soc*., **1969**, 65, 2034.

Lennard-Jones J. E., Devonshire A. F., *Proc. Roy. Soc*., **1937**, A163, 63.

Lennard-Jones J. E., Devonshire A. F., *J. Amer. Chem. Soc*., **1938**, A164, 1.

Letcher T.M., *Chemsa*, **1975**, 226.

Letcher T.M., Domanska U., Marciniak A., Marcianiak M., *J. Chem. Eng. Data*, **2005**, 50, 1294-1298.

Li X., Zhao D., Fei Z., Wang L., *Science in China*., **2006**, *B* 35, 181.

Liang K., Eying H., Marchi R. P., *Proc. Nat. Acad. Sci. (U. S.)*, **1964**, 52, 1107.

Linde C., Process and apparatus for attaining lowest temperatures for liquefying gases, and for mechanically separating gas mixtures, **1996**, 456-509.

Longuest-Higgins H. C., *Proc. Roy. Soc. (Lond*), **1951**, A205, 247.

Lopes J.N., Cordeiro T.C., Esperanca J.M.S.S., Guedes H.J.R., Huq S.,Rebelo L.P.N.,Seddon K.R., *J. Phys. Chem*., **2005**, 109, 3519-3525.

Lozano P., De Diego T., *J. of Molecular Catalysis A: Chemical*, **2004**, 214 113-119.

Lyubartsev A.P., Laaksonen A., *Applied Parallel Computing Large Scale Scientific and Industrial Problems*. Lecture Notes in Computer Science., **1998**, 1541.

Lyubartsev A.P., Laaksonen A., *Computer Physics Communications*., **2000**, 128, 565–589.

Ma S. M., Eying H., *J. Chem. Phys*., **1965**, 42, 1920.

MacFarlane D. R., Golding J., Forsyth S., Forsyth M., Deacon G. B., *Chem. Commun.*, **2001**, 1430.

Magzin *Chemical & Engineering news* **2009**, 27.

Maripuri V. C., Ratcliff G. A., *J. Amer. Chem. Soc*., **1971**, 49, 375.

Maripuri V. C., Ratcliff G. A., *J. Amer. Chem. Soc*., **1971**, 49, 506.

Marsh K.N., *Ann. Rep. RSC Sect C*, **1980**, 77, 101.

Marsh K.N., *Ann. Rep. RSC Sect C*, **1984**, 81, 209.

Marsh K.N., Boxall J.A., *Fluid Phase Equilib*., **2004**, 219, 93-98.

Mathieson A. R., *J. Chem. Soc*., **1958**, 4444.

Mathieson A. R., Thynne J. C. J., *J. Chem. Soc.* **1956** (a), 3708.

Mathieson A. R., Thynne J. C. J., *J. Chem. Soc.* **1956** (b), 3713.

Mathot V., Desmyter A., *J. Amer. Chem. Soc*., **1953**, 21, 782.

Mathot V., Staveley L. A. K., Young J. A., Parsonage N. G., *Trans. Farady Soc*., **1956**, 52, 1488.

Maurer G., Prausnitz J. M., *Fluid Phase Equilibria*, **1978**, 2, 91.

McGlashan, M. L., *Mol. Phys*., **1961**, 4, 87.

McGlashan M.L., *J. Chem. Thermodynamics*, **1979,** 1, 589.

McGlashan M. L., Morcom K. W., *Trans. Farady Soc*., **1961**, 57, 907.

Meindersma G. W., Podt A. J. G., de Haan A. B., Selection of ionic liquids for the extraction of aromatic hydrocarbons from aromatic/aliphatic mixtures. Fuel Process. Technol., **2005**, 87, 59–70.

Millero, F.J., *Chemical Reviews*, **1971**, 71, 147-176.

Millero, F. J., *American Chemical Society*, **1980**, 581-622.

Miner B. A. Eying H., *J. Amer. Chem. Soc*., **1965**, 53, 1227.

Moravkova L., Linek J., *J. Chem. Thermodyn*., **2008**, 40, 671-676.

Murthy A. S. N., Rao C. N. R., *Appl. Spectro. Rev*., **1968**, 69, 191.

Martyn J. E, José M.S.S. E., Manuela A. G., José N. C. L., Luís P.N. R., Joseph W. M.,

Nagata I., Z. Phys. Chem., **1973**, 107, 39.

Nagata I., *J. Chem. Eng. Data*, **1975**, 20, 110.

Nagata I., Katoh K., *Fluid Phase Equilibria*, **1980**, 5, 225.

Nagata I., *Thermochim. Acta*, **1988**, 127, 109.

Najdanovic-Visak V., Esperanca J.M.S.S., Rebelo L.P.N., *Phys. Chem*., **2002**, 4, 1701-1703.

Nevines J. A., Thermodynamics of nonelectrolytes liquid mixtures, PhD thesis, UKZN, Durban **1997**, 78-80.

Nguyen T. H., Ratcliff G. A., *J. Amer. Chem. Soc*., **1971**, 49, 120.

Nguyen T. H., Ratcliff G. A., *J. Amer. Chem. Soc*., **1971**, 49, 889.

Nguyen T. H., Ratcliff G. A., *J. Amer. Chem. Soc*., **1974**, 52, 641.

Nguyen T. H., Ratcliff G. A., *J. Chem. Eng. Data*, **1975**, 20, 256.

Nomoto O., *J. Amer. Chem. Soc*., **1956**, 11, 1146.

Nomoto O., *J. Phys. Soc. Japan*, **1958**, 13, 1528.

Nutsch-Kuhnkies *Acustica,* **1965**, 15, 383.

Ohta T., Koyabu J., Nagata I., *Fluid Phase Equilibria*, **1981**, 7, 1981.

Orey R. V., Prausnitz J. M., *Ind. Eng. Chem*., **1965**, 57, 18.

Oswal S. L., Oswal P., Modi P. S., Dave J. P., Gardas R. S., *Thermochimica Acta*, **2004**, 410, 1-14.

Pandey H. C., Jain R. P., Pandey J. D., *J. Amer. Chem. Soc*., **1975**, 34, 123.

Papageorgiou N., Athanassov Y., Armand M., Bonhˆote P., Pettersson H., Azam A., Gr¨atzel M., *J. Electrochem. Soc*., **1996**,143, 3099–3108.

Patterson D., Badin G. M., *J. Amer. Chem. Soc*., **1970**, 66, 321.

Paul Walden Bull. *Acad. Sci. St. Petersburg*, **1914**, 405-422.

Pereiro A. B., Rodriguez A., *J. Chem. Thermodyn*., **2006** (a), 38, 651-661.

Pereiro A.B., Rodriguez A., *J. Chem. Thermodyn*., **2006** (b), 39, 978-989.

Pereiro A. B., Rodriguez A., *J. Chem. Eng. Data*, **2007** (a), 52, 600-608.

Pereiro A. B., Rodriguez A., Verdia P., Tojo E., *J. Chem. Eng Data*, **2007** (b), 52, 337.

Pflug H. D., Benson G. C., *Can. J. Chem*., **1968**, 46, 287.

Pikkarainen L., *J. Chem. Thermodyn*., **1982**, 14, 503-507.

Pitzer K. S., *J. Am. Chem. Soc*., **1955**, 77, 3427.

Plechkova, N.V., Seddon, K.R., *Chem. Soc. Rev*., **2008**, 123.

Plechkova N.V., Seddon K.R, *Chem. Soc. Rev*., **2008**, 1-9**.**

Poole G. R., Aziz R. A., *J. Amer. Chem. Soc*., **1972**, 50, 646.

Poole C.F., *J. Chromatogr A*, **2004**, 1037, 49-82.

Porter A. W., *Trans. Farady Soc*., **1920**, 16, 336.

Prakash S., Prasad N., Singh R., Prakash O., *Acustica*, **1975**, 34, 121.

Prigogine I., Garikian G., *Physica*., **1950**, 16, 239.

Prigogine I., Mathot V., *J. Chem. Phys*., **1952**, 20, 49.

Prigogine I., Bellemans A., *J. Chem. Phys*., **1953**, 21, 561.

Prigogine I., Trappeniers N., Mathot V., *Discuss Farady Soc*., **1953**, 15, 93.

Prigogine I., (with the collaboration of Bellemans A., Mathot V., "The Molecular theory of solutions. North-Holland Publishing Co., Amsterdam **1957**.

Purification 2, Arnold Weissberger, 4th, New York, USA, **1986**, 565-662.

Qi F., Wang H., *J. Chem. Thermodyn*., **2009**, 41, 265-272.

Rao G.R. V., Venkataseshaiah V., Z. *Phys. Chem*., **1969**, 242, 193.

Rao M. V. P., Naidu P. R., *J. Amer. Chem. Soc*., **1974**, 6, 1195.

Rastogi R. P., *J. Sci. Ind. Res*., **1980**, 39, 480.

Rebelo L.P.N., Lopes J.N.C., Esperanca J.M.S.S., G*reen. Chem.* **2004**, 6, 369-381.

Rebelo L.P.N., Lopes J.N.C., Esperanca J.M.S.S., *J. Phys. Chem. B.* **2005**, 109, 6040-6043.

Reddy K. C., Subramanyam S. V., Bhimasenachar J., J. *Phys. Soc. Japan*, **1964**, 19, 559.

Redlich O., Kister A. T., *Ind. Eng. Chem*., **1948**, 16, 345.

Redlich O., Kister A. T., *Ind. Eng. Chem*., **1984**, 40, 345-348.

Redlich O., Mayer D. M., *Chem. Rev*. **1964**, 64, 221.

Redhi G.G., Thermodynamics of liquid mixtures containing carboxylic acids, PhD thesis, UKZN, Durban, **2003**, 6-16.

Riddick J. A., Bunger W. B., *Organic solvents Physical Properties and Methods of Purification 2*, Arnold Weissberger, 4th, New York, USA, **1986**, 565-662.

Rendall G. R., Proc. *Ind. Acad. Sci*., **1942**, 16A, 369.

Renon H., Prausnitz J. M., *J. Amer. Chem. Soc*., **1968**, 14, 135.

Robinson J., Osteryoung R. A., *J. Amer. Chem. Soc.*, **1979**, 101, 323.

Rogers R. D., Seddon K. R, Ionic liquids, ACS Symposium Series No. 818, *American Chemical Society., Washington, DC*, **2002**.

Rogers R. D., Seddon K. R., Ionic Liquids as Green Solvents, *American Chemical Society.*, **2003**, 2-5.

Rogers R.D, Swatloski R.P., Spear S.K., *J. of the American Chemical Society*, **2002**, 4974-4975.

Rowlinson J. S., Mathieson A. R., *J. Amer. Chem. Soc*., **1959**, 4129.

Rowlinson J S., "Liquid and liquid Mixture", *Butter worth & Co., London*, **1969**.

Rowlinson J. S., Watson I. D., *Chem. Eng. Sci*., **1969**, 24, 1565.

Rowlinson J. S., *Discuss Farady Soc*., **1970**, 49, 30.

Rowlinson J. S., Swinton F. L., " Liquid and Liquid Mixtures" *Butter worth & Co*., *London*, **1982**.

Sackmann H., Boczek A., *J. Physik. Chem.,* **1961**, 29, 329.

Sadeghi R., Shekari H., Hosseini R., *J. Chem. Thermodyn*., **2009**, 41, 273-289.

Samal K., Misra S.C., *J. Phys. Soc. Japan*. **1972**, 31, 1615.

Sanchez I. C., Lacombe R. H., *J. Phys. Chem*., **1976**, 80, 2352.

Sanchez I. C., Lacombe R. H., *J. Amer. Chem. Soc*., **1976**, 80, 2568.

Sayegh S. G., Ratcliff G. A., *J. Amer. Chem. Soc*., **1976**, 21, 71.

Scatchard G., *Chem. Rev*., **1931**, 8, 312.

Scatchard G., *Dan. Kemi*, **1932**, 13, 77.

Scatchard G., *J. Am. Chem. Soc*., **1934**, 56, 995.

Scatchard G., *Trans. Farady Soc*., **1937**, 33, 160.

Scatchard G., Ticknor L. B., Goates J. R., Mc Cartney E. R., *J. Am. Chem. Soc*., **1952**, 74, 3721.

Schaaffs W., Molekularakustik. Springer Verlag, Berlin-Gottingen Heidelberg, Chaps. XI and XII (1963); *Z. Physic*., **1940**, 115, 69.

Schaaffs W., Molekularakustik. Springer Verlag, Berlin-Gottingen Heidelberg, Chaps. XI and XII (1963); *Acustica*, **1974**, 30, 275.

Scott R. L., *J. Chem. Phys*., **1956**, 24, 193.

Scott R. L., Fenby D. V., Ann. *Rev. Phy. Chem*., **1969**, 16, 111.

Scurto A.M., Aki S.N.V.K., Brennecke J. *Phys. Chem. B*, **2004**, 108, 20355-20365.

Seddon K.R. *J. Chem. Tech. Biotechnol*., **1997**, 68, 351-356.

Seddon K.R., Stark A., Torres M., *Pure Appl. Chem*., **2000**, 72, 1391-1398.

Sen S., Proceedings of ACS-41st Annual Regional Meeting, San Diego, California, October **2007**.

Seshadri K., Reddy K. C., *J. Acoust. Soc. Ind*., **1973**, 4, 1951.

Seshadri K., Rao N., Reddy K. C., *Z. Phys. Chem. (NF*), **1974**, 89, 108.

Shana's M. Y., Canfield F. B., *Trans. Faraday Soc*., **1968**, 64, 2281.

Sheldon R., *Chem. Commun*., **2001**, 23, 2399-2407.

Sibiya P N., Deenadayalu N., *J. Chem. Thermodyn*., **2008**, 40, 1041-1045.

Sibiya P N., Deenadayalu N., *S. Afr. J. Chem*., **2009**, 62, 20-25.

Siman J. E., Vera J. H., Can. *J. Chem. Eng*., **1979**, 57, 355.

Singh R. P., Verma R. D., Meshri D. T., Shreeve J. M., Energetic
nitrogen-rich salts and ionic liquids. Angewandte Chemie, **2006** 45, 3584–3601.

Singh P. P., Nigam R. K., Sharma S. P., Aggarwal S., *Fluid Phase Equilibria*, **1984**, 18, 333.

Singh T., Kumar A., *J. Chem. Thermodyn*., **2008**, 40, 417-423.

Skjold-Joergensen S., Kolbe B., Gmehling J., Rasmussen P., Ind. Eng. Chem. Process Des. Dev., **1962**, 18, 714.

Skjold-Joergensen S., Rasmussen P., Fredenslund Aa., *Chem. Eng. Sci*. **1982**, 37, 99.

Smith G. P., Pagni R. M., *J. Am. Chem. Soc*., **1989**, 111 and 525.

Stokes R. H., Marsh K. N., Ann. *Rev. Phy. Chem*., **1972**, 23, 65.

Street W. B., Staveley L. A. K., *J. Amer. Chem. Soc*., **1967**, 47, 2449.

Swatloski R. P., Spear S. K., Holbrey J. D., Rogers R. D., *Journal of the American Chemical Society*., **2002**, 124/18, 4974–4975.

Tager A. A., Adamova L. V., *Russian Chem. Rev*., **1980**, 49, 325.

Tokuda H., Hayamizu K., Ishii K. Susan M., *J. Phys. Chem B*, **2004**, 108, 16593-16600.

Tokuda H., Hayamizu K., Ishii K. Susan M., *J. Phys. Chem B*, **2005**, 109, 6103-6110.

Tokuda H., Hayamizu K., Ishii K. Susan M., *J. Phys. Chem B*, **2006**, 110, 2833-2839.

Toop G. W., *Trans. TMS-AIME*, **1965**, 233, 850.

Tsao C.C., Smith J. M., "Applied Thermodynamics", Chem. Eng. Prog. Symp. No. 7, **1953**, 107.

Van Deal W., " Experimental thermodynamics" Vol. II, Thermodynamic Properties and the velocity of sound, Butterworths & Co., Pub. Ltd., London.

Van der Waals J. C., *Z. Physik. Chem*., **1890**, 5, 133.

Van Laar J. J., "Sechs Vortrage uber das thermodynamische Potential", Braunschweig, **1960**.

Van Laar J. J., Lorenz R., *Z. Anorg. Chem*., **1925**, 145, 239.

Verevkin S., the 3rd International Congress on Ionic Liquids *Green Chemistry News*, **2009**.

Visser P. J., Allaart K., Lenstra D., *Phys. Rev. E.,* **2002**, 65, 11.

Visser A.E., Swatloski R.P., Reichert W.M., Mayton R., Sheff S., Wierzbicki A., Davis Jr., Rogers R.D., *Envir. Sci. Technol*., **2002**, 36, 2523-2529.

Vonka P., Medlik V., Novak J. P., *Coll. Of Czech. Chem. Comm*., **1982**, 47, 1029.

Walas S., *Phase Equilibria in Chemical Engeneering*, Butterworths, Stoneham, MA, **1985**.

Walker A. J., Bruce N. C., *Chemical Communications*., **2004**, 2570.

Wang J., Tian Y.,Zhao Y., Zhuo K, Liu W., *Green Chem*., **2003**, 5, 618-622.

Wang J., Zhang S., Wang H., Pei Y., *J. Chem. Eng. Data*, **2009**, 54, 3252-3258.

Wasserscheid P., *Nature*., **2006**, 439, 797.

Welton T., *Chem. Rev*., **1999**, 99, 2071-2083.

Wenhsin Y., Yapens S., *Jing Young Kexae Xeubuo*, **1987**, 5, 131.

Widegren J.A., MageE J.W., *J. Chem. Eng. Data*, **2007**, 52, 2331-2338.

Williamson A. G., Scott R. L., *Trans. Farady Soc*., **1970**, 66, 335.

Wilkes J. S., Zaworotko M. J., *Chemical Communications*., **1992**, 965-967

Wilkes J.S., *Green Chem*., **2002**, 4, 73-80.

Wilkes J. S., Levisky J. A., Wilson R. A., Hussey C. L., *Inorg. Chem.*, **1982**, 21, 1263–1264.

Wilkes J. S., Levinsky J. A., Wilson R. A. Hussey C. A., *Inorg. Chem.*, **1982**, 21, 1263.

Wilkes J. S., Zaworotko M. J., *J. Chem. Soc., Chem. Commun.*, **1992**, 965.

Wilson G. M., *J. Amer. Chem. Soc*., **1964**, 86, 127.

Wilson G. M., Deal C. H., *Ind. Eng. Chem. Fundam*., **1962**, 1, 20.

Wishart J., the 3rd International Congress on Ionic Liquids *Green Chemistry News*, **2009**.

Wohl K., Trans, *Am. Inst. Chem. Eng*., **1946**, 42, 215.

Wohl K., *Errata Chem. Engr. Progress*, **1953**, 49, 218.

Wood S. E., *J. Amer. Chem. Soc*., **1957**, 79, 1782.

Wu B., Zhang Y. M., Wang H. P., *J. Chem. Eng. Data*, **2009**, 54, 1430-1434.

Wu C.T., Marsh K.N., *J. Chem Eng. Data*, **2003**, 48, 486-491.

Yang J., Lu X., Gui J., Xu W., *J. Chem. Thermodyn.*, **2005** (a), 37, 1250-1255.

Yang J., Lu X., Gui J., Xu W., *J. Chem. Thermodyn.*, **2005** (b), 37, 13-19.

Yang, Q., Dionysiou D.D., *Journal of Photochemistry and Photobiology, A: Chemistry*, **2004**, 165(1-3), 229-240.

Yates B., the 3rd International Congress on Ionic Liquids *Green Chemistry News*, **2009**.

Younglove B. V., *J. Acoust. Soc. Am*., **1965**, 38, 433.

Zafarani-Moattar M. T., Shekaari H., *J. Chem. Thermodyn.*, **2005** (a), 37, 1029-1035

Zafarani-Moattar M. T., Shekaari H., *J. Chem. Eng. Data*, **2005** (b), 50, 1694-1699.

Zafarani-Moattar M. T., Shekaari H., *J. Chem. Thermodyn.*, **2006**, 38, 1377-1384.

Zaitsau Dz. H. Kabo G.J., Strechan A.A., *J. Phys. Chem. A*., **2006**, 110, 7303-7306.

Zhang S., Sun N., He X., Lu X., Zhang X., *J.Phys. Chem. Ref. Data*, **2006**, 35, 1475-1516.

Zhong Y., Wang H., *J. Chem. Thermodyn*., **2007,** 39 291-296.

Ziemer J. K., Marrese-Reading C. M., Anderson M., Plett G., Polk J., Gamero-Castano M., Hruby V., Colloid thruster propellant stability after radiation exposure. AIAA paper, **2003**, 2003-4853.

APPENDIX 1

The Redlich-Kister parameters for the all binary systems used in this work at different temperature

T/K	A_0	A_1	A_2	A_3	A_4	σ/cm^3·mol^{-1}
			([MOA]$^+$[Tf$_2$N]$^-$ + methanol)			
298.15	3.01	-3.91	-0.68	- 4.54	-	0.03
303.15	5.05	-5.47	-6.58	-2.76	3.00	0.03
313.15	4.74	-3.75	0.31	-11.29	-	0.03
			([MOA]$^+$[Tf$_2$N]$^-$ + ethanol)			
298.15	1.32	-2.89	1.44	-0.63	-0.73	0.01
303.15	6.41	-9.59	-7.42	0.39	-2.20	0.07
313.15	2.36	- 4.92	-0.55	0.27	1.25	0.02
			([MOA]$^+$[Tf$_2$N]$^-$ + methyl acetate)			
298.15	-5.65	-0.17	-2.23	4.65	4.87	0.04
303.15	-8.37	-1.27	-	-	-	0.46
313.15	-11.30	-7.70	2.70	12.23	-	0.25
			([MOA]$^+$[Tf$_2$N]$^-$ + ethyl acetate)			
298.15	-6.00	1.64	-2.33	4.64	3.90	0.03
303.15	-6.01	1.30	-0.29	2.83	0.18	0.06
313.15	-7.25	0.99	-0.21	4.18	1.81	0.04
			(methanol + methyl acetate)			
298.15	-0.29	0.04	0.05	0.05	-	0.00
303.15	-0.27	0.02	0.06	0.05	-	0.00
			(methanol + ethyl acetate)			
298.15	-0.30	-0.04	-0.08	-	-	0.00
303.15	-0.27	-0.05	-0.07	-	-	0.00

			(ethanol + methyl acetate)			
298.15	0.77	0.02	0.14	-	-	0.00
303.15	0.84	0.07	0.15	-	-	0.00
			(ethanol + ethyl acetate)			
298.15	0.62	-0.11	-	-	-	0.00
303.15	0.69	-0.11	-	-	-	0.00
			($[BMIM]^+[MeSO4]^-$ + methanol)			
298.15	4.13	-2.63	0.16	-	-	
			($[BMIM]^+[MeSO4]^-$ + ethanol)			
298.15	2.50	-0.93	-0.08	-	-	
			($[BMIM]^+[MeSO4]^-$ + 1-propanol)			
298.15	0.95	-0.19	-	-	-	
			($[BMIM]^+[MeSO4]^-$ + nitromethane)			
298.15	-1.92	1.34	-0.47	1.58	-1.86	
			(methanol + nitromethane)			
298.15	-0.70	-0.40	-0.29	-	-	
			(ethanol + nitromethane)			
298.15	0.05	-0.57	-0.35	-0.59	-	
			(1-propanol + nitromethane)			
298.15	0.94	-0.26	0.15	-0.41	-	

APPENDIX 2

List of publications

1. Ternary excess molar volumes of {Methyltrioctylammonium Bis(trifluoromethylsulfonyl)imide + Ethanol + Methyl acetate, or Ethyl acetate} systems at T = (298.15, 303.15, and 313.15) K. (J. Chemical Thermodynamics 42, 2010, 726-733)

2. Ternary Excess Molar Volumes of {Methyltrioctylammonium Bis[(trifluoromethyl)sulfonyl]imide + Methanol + Methyl Acetate or Ethyl Acetate} Systems at (298.15, 303.15, and 313.15) K. (J. Chemical & Engineering Data 2010 Published online 10 May 2010)

3. Apparent Molar Volume and Isentropic Compressibility for Binary Systems {Methyltrioctylammonium Bis(trifluoromethylsulfonyl)imide + Methyl acetate or Methanol} and (Methanol + Methyl acetate) at 298.15, 303.15, 308.15 and 313.15 K and Atmospheric Pressure. (J. Solution Chemistry) Submitted.

4. Effect of Methyl acetate, Ethyl acetate and Ethanol on Partial Molar Volumes and Partial Molar Isentropic Compressibilities of Ionic liquid {Methyltrioctylammonium Bis(trifluoromethylsulfonyl)imide, Methanol and Ethanol at Different Temperatures: An Apparent Molar Volumes and Apparent Molar Isentropic Compressibility study. (J. Molecular liquid) in Preparation.

5. Physico-chemical Properties of Ternary mixtures of (1-Butyl-3-methylimidazolium methyl sulphate + Methanol or Ethanol or 1- Propanol + Nitro methane} at $T = 298.15$ K and Atmospheric Pressure. (J. Chemical & Engineering Data) in Preparation.